BASICS OF NUCLEAR PHYSICS AND OF RADIATION DETECTION AND MEASUREMENT

An open-access textbook for nuclear and radiochemistry students

Jukka Lehto

Laboratory of Radiochemistry
Department of Chemistry
University of Helsinki
Finland

2016

Contents

PREFACE

This book is written for nuclear and radiochemistry students to obtain basic knowledge in nuclear physics and in radiation detection and measurement. To obtain deeper knowledge on these areas more comprehensive books are needed. List of these books is given on the next page.

This book is called “open-access textbook”. The reason to this expression is that it is freely available in the internet. I will also deliver the book as word version to nuclear and radiochemistry, or any other field, teachers so that they can further modify it to better fit with their own teaching program. I would be happy to get copies of the modified versions.

This book was produced in the CINCH EU project 2013-2016 (Cooperation in education and training in nuclear chemistry) and it is delivered at the NucWik (https://nucwik.wikispaces.com/) pages developed in the project. The aim of the CINCH was to develop nuclear and radiochemistry (NRC) education in Europe. A major achievement of the project was the establishment of the NRC Network and NRC EuroMaster system for European universities offering NRC education.

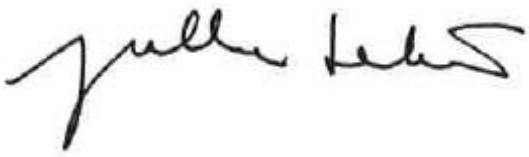

Jukka Lehto
Professor in radiochemistry
University of Helsinki, Finland

TEXTBOOKS FOR NUCLEAR AND RADIOCHEMISTRY

General radiochemistry:

Radiochemistry and Nuclear Chemistry, Fourth Edition, 2013, Elsevier, 852 pages
Gregory Choppin, Jan-Olov Liljenzin, Jan Rydberg, Christian Ekberg

Nuclear and Radiochemistry: Fundamentals and Applications,
3rd Edition, 2013, VCH-Wiley, 913 pages, Jens-Volker Kratz, Karl Heinrich Lieser

Nuclear- and Radiochemistry, Volume I - Introduction
De Gruyter, 2014, 450 pages, Frank Rosch

Nuclear- and Radiochemistry, Volume II – Modern applications
De Gruyter, 2016, 560 pages, Frank Rosch (Ed.)

Nuclear and Radiochemistry, 1st Edition, 2012, Elsevier, 432 pages, J.Konya and M.Nagy

Handbook of Nuclear Chemistry, 2nd Edition, 2012, Springer, 3049 pages
A. Vértes**,** S.Nagy**,** S.Klencsár**,** Z.Lovas**,** R.G.Rösch**,**

Detection and measurement of radiation:

Radiation Detection and Measurement, Fourth Edition, 2010, Wiley, 830 page, Glenn T. Knoll

Handbook of Radioactivity Analysis, 3rd Edition, 2012, Elsevier, 1329 pages, Michael L'Annunziata

Analytical radiochemistry / Radioanalytical chemistry:

Chemistry and Analysis of Radionuclides, 2011, Wiley-VCH, 406 pages, Jukka Lehto, Xiaolin Hou

Radioanalytical Chemistry, 2006, Springer, 473 pages, Bernd Kahn

I THE HISTORY OF THE RESEARCH OF RADIOACTIVITY

Content

The invention of radioactivity

Radioactivity was discovered by the French scientist Henri Becquerel in 1896 while he was investigating the radiation emitted from the uranium salts, which he noticed in the 1880s while preparing potassium uranyl sulfate. He began to investigate this phenomenon again upon the 1895 publication by K.W. Röntgen who reported about a new type of penetrable radiation (X-rays). Becquerel then experimented with possible formation of fluorescence and X-rays by UV-radiation of sunlight in uranium salts. He placed uranium salt in a package and exposed it to sunlight while it was on top of a photographic plate. The photographic plate was exposed, which he at first interpreted as fluorescence until the realization that the uranium salts exposed the plate without exposure to sunlight. Becquerel also noted that the radiation emitted by the uranium salts discharge electroscope charges and made the air conductive. Not too long after this Marie Curie, Becquerel's student, showed that not only potassium uranyl sulfate emits radiation but also other uranium salts and their solutions. In addition, the amount of the radiation in the samples was seen to be

proportional to the amount of uranium. Based on these observations it was clear that the emission of radiation was a property of uranium regardless of what compound it was present as. Marie Curie, along with her husband Pierre Curie, coined the term “radioactivity” to refer to the radiation emitted by uranium.

Discovering new radioactive elements– Thorium, Polonium, Radium

Marie Curie mapped out the ability of the elements, known then, to radiate and concluded that only thorium, in addition to uranium, was radioactive. She, however, noticed that the pitchblende mineral, from which uranium can be separated, had an even higher radioactivity level than pure uranium and concluded that it must also contain an even more active element than uranium. She dissolved pitchblende into acid and precipitated it into different fractions of which the radioactivity was measured. In order to measure the activity levels the Curies used the *electroscope*, which was designed by the University of Cambridge professor J.J. Thompson as a device for measuring the X-ray radiation. During her investigations, Marie Curie noticed that a new highly radioactive element coprecipitated along with bismuth, which she decided to name *polonium* in honor of her home country Poland. The amount of separated substance was, however, insufficient to determine the chemical properties and atomic weight. The same experiment also revealed that another element coprecipitated with barium and it was determined to be 900 times more radioactive than uranium. Due to this high level of radiation, Curie named the element *radium*.

Since pitchblende only contains a very small concentration of radium, the Curies decided to separate it in macro quantities from two tons of pitchblende. In 1902, after major efforts they extracted 0.1 g of radium chloride, allowing the determination of atomic weight. They determined the value to be 225, which we now know to be 226.0254. Later, in 1910, Marie Curie electrolytically separated radium as a pure metal as well. Together with her husband Pierre Curie and Henri Becquerel, she received the Nobel Prize for physics in 1903 and then in 1911 she was the sole recipient of the Nobel Prize for chemistry.

Characterization of radiation generated in radioactive decay

Soon after the first observations of radiations were made, the nature of radiation was examined. In 1898, Ernest Rutherford showed the presence of two types of radiation, *alpha* and *beta radiation*. A third type, *gamma radiation*, was detected in 1903 by Paul Villard. Both alpha and beta radiation

proved to bend in a magnetic field, though in opposite directions, and were therefore determined to be charged particles, with alpha radiation being positively and beta radiation negatively charged. Gamma radiation did not bend in a magnetic field and Rutherford demonstrated it to be an electromagnetic form of radiation with even shorter wavelengths than X-ray radiation. Research on the mass and charge of alpha and beta radiation showed alpha radiation to be helium ions and beta radiation to be electrons.

The finding of more radiating elements

The radiochemical separation of radium and polonium by Curie sparked a continuous finding of new radioactive elements in the 1910s. Precipitations were made of uranium and thorium salt solutions with various reagents and the activity levels of the resulting precipitates were measured. For example, Rutherford and his colleague precipitated a substance from a thorium solution, which they named thorium-X (later identified to be ^{224}Ra, $t_{1/2}$ 3.6 d). It lost its radioactivity in a month, while after the precipitation the activity of the remaining thorium solution increased from the lowered activity level back to the original level. At first, only small quantities of new radioactive substances were collected so neither their atomic weight nor optical spectrum could be measured. They were identifiable only by the type of radiation they emitted, alpha and/or beta radiation, and the rate at which their radiation levels diminished. For these reasons the new radiating substances could not be named and were referred to be based on their parent nuclide, for example U-X, Ac-D, or Ra-F. These new substances were shown to belong to three decay series, which began with uranium and thorium. Around 1910 a total of 40 new radiating substances were known, all of which ended up as the stable nuclides Ra-G, Th-D, and Ac-D, later identified to different isotopes of lead. The formation of alpha particle emitting radioactive gases, called emanation and later identified as radon gas, occurred in all of the decay series.

What is radioactive decay?

Rutherford and Soddy had already hypothesized in 1902 that observed phenomena were explainable by the spontaneous decay of radioactive elements into other elements, and that the rate of decay was exponential. The concept of the atom as the smallest indivisible particle began to break down. In 1913, both Kasimir Fajans and Frederick Soddy independently concluded that radioactive decay series starting with uranium and thorium always resulted in elements with an atomic number two units lower in alpha decay and one unit higher in beta decay. Many radioactive substances found in

radioactive decay series were, however, found to be chemically identical to each other in spite of their atomic weights. Fajans and Soddy determined that elements could occur as different forms with differing masses, which Soddy named *isotopes.* Thus, for example, it was possible to identify the uranium series member formerly known as ionium to thorium and thus an isotope to previously known element thorium. The 40 members of the natural radioactive decay series could now be categorized using the isotope concept into eleven elements and their different isotopes. The full understanding of the isotope concept, however, still required the discovery of neutrons.

Understanding of the structure of atoms is established

In 1911, when examining the passage of alpha radiation through a thin metallic foil, Rutherford found that most of the alpha particles passed through the foil without changing direction. Some of the particles, however, changed direction, a few up to 180 degrees. From this, Rutherford concluded that atoms are mostly sparse, particle-permeable space and they have a small positively charged nucleus from which the alpha particles scatter. From the angle of the scattering alpha particles, he calculated that the diameter of the nucleus is approximately one-hundred-thousandth of the diameter of the whole atom.

Soon after this, Niels Bohr presented his theory of atomic structure. According to him, atoms have a small, positively charged nucleus around which the negatively charged electrons orbit. Electrons, however, do not orbit the nucleus randomly, but in predefined shells with a specified energy: the closer to the nucleus the higher the energy and lower in the outermost shells. The number of electrons in the atom is equal to the charge of the nucleus, and is the same as the atomic number of the element in the periodic table. The nuclear charge was, however, not yet able to be directly measured. The values were then determined by Henry Mosely and his group bombarding elements with electrons, which led to removal of the shell electrons from their orbits and formation of X-ray radiation as the electron holes were filled with electrons from upper shells. Characteristic X-ray spectra were obtained for each element. From these, it was found that the frequencies (n) of the emitted X-rays correlated with the systematics n = constant × $(Z-1)^2$ in relation to the atomic number (Z) of the elements, from which all elements' atomic numbers could be calculated. For example, the atomic number of uranium was able to be determined as 92.

In 1920, the first artificial nuclear reaction was triggered by Rutherford. He targeted nitrogen with alpha particles and determined that hydrogen nuclei were emitted from the nitrogen atoms, which

he called protons. Until 1932, it was expected that atoms consisted of positively charged protons in the nucleus and orbiting electrons. James Chadwick then identified previously discovered penetrating radiation to neutrons, particles with the same mass as protons but no charge. With this knowledge, Bohr's atomic model could be completed: the nucleus contains the atomic number of positively charged protons as well as a variable number of neutrons. Elements with nuclei containing a different amount of neutrons, and therefore having a different atomic weight, are isotopes of these elements.

Accelerators – artificial radioactivity

The first particle accelerators were developed during the 1930s and in 1932 the first accelerated particle(proton)-induced nuclear reaction, $^{1}H + {}^{7}Li \rightarrow 2\,{}^{4}He$, was accomplished. Also in 1932, the husband and wife team, Frederic and Irene Joliot-Curie, accomplished creating the first artificial radioactive nucleus by bombarding boron, aluminum, and magnesium with alpha particles. Bombarding aluminum produced ^{30}P, which decayed by positron emission with a 10 minute half-life. Positrons, particles with the same mass as an electron but an opposite charge, were identified two years earlier.

The consequences of fission and transuranic elements

Already in the first half of the 1930s, following the discovery of accelerators attempts were made to make heavier elements by bombarding uranium with neutrons. Otto Hahn, Lise Meitner, and Fritz Strassman also attempted this, but in 1938, they found that uranium nuclei split into lighter elements when bombarded with thermal neutrons. This process was proven to release an extremely large amount of energy. At the beginning of the Second World War, when it was demonstrated that the harnessing of this energy could be used by the armed forces, the US government began developing a nuclear weapon. The venture was called the Manhattan Project and was headed by Robert Oppenheimer. In the first stage, Enrico Fermi and his team started the first nuclear reactor in Chicago in 1942, which was used as the basis for the building of reactors in the subsequent years for plutonium weapon production. Within the nuclear reactor, a controlled chain reaction of uranium fission by neutrons is generated. At the same time, it was proven that the thermal neutrons do not arise from the fission of the prominent uranium isotope ^{238}U, but from the fission ^{235}U. The latter isotope only accounts for 0.7% of naturally occurring uranium. In order to provide enough ^{235}U for nuclear weapons an isotope enriching plant was built in Oak Ridge, Tennessee, in which

the enrichment process was based on the different diffusion rate of the hexafluoride molecules of the two uranium isotopes.

In addition to uranium, the Manhattan Project also used a new, heavier element that undergoes fission more sensitively than ^{235}U, plutonium, for the development of nuclear weapons. In the mid-1930s, Meitner, Hahn, and Strassman had already suspected that there were elements heavier than uranium when they verified that ^{239}U, which they got by bombarding ^{238}U with neutrons, decayed by beta emission. They knew that the decay produced element 93, but were unable to prove it. At Berkeley University, Edwin McMillian and his team confirmed its existence and named the element neptunium. In 1941, they were also able to confirm the existence of element 94, ultimately called plutonium, which then began to be produced in Hanford, Washington as a material for weapons. Plutonium was separated from uranium, irradiated in a nuclear reactor, by the PUREX method, which is still used at the nuclear fuel reprocessing plants. In this method, the spent fuel is dissolved in nitric acid and extracted by tributyl phosphate allowing uranium and plutonium to transfer into the organic phase while other substances remain in the acid. When plutonium is reduced to trivalent state, it can be extracted from uranium back to the aqueous phase and further reduced to metal. The Manhattan Project also developed a large number of other radiochemical separation methods for the separation of radionuclides, some of which are still in use.

The sad conclusion of the Manhattan Project occurred in the summer of 1945, first with the test explosion in New Mexico and then with the annihilation of Hiroshima and Nagasaki in August.

The race to find new elements continues

Synthesis of new, heavier than uranium elements did not end with the development of plutonium. At first, they were produced in Berkeley in Lawrence Livermore Laboratory under the direction of Glenn T. Seaborg. In the 1940s and early-1950s they found americium (element 95), curium (96), berkelium (97), californium (98), einsteinium (99), fermium (100), and mendelevium (101). Later other nuclear centers, particularly Dubna in Russia and Darmstadt in Germany, joined the race. So far, the heaviest element that has been identified is number 116. All of these super heavy elements are very short-lived.

Utilization of radioactivity

Until the development of nuclear weapons, radioactive research was at the level of basic research. As early as 1912, however, de Hevesy and Paneth used ^{210}Pb (RaD) to determine the solubility of lead chromate. De Hevesy was also responsible for the first biological radionuclide experiment: in 1923, using the ^{212}Pb tracer he studied the uptake and distribution of lead in bean plants. The invention of accelerators, and its use in the production of artificial radionuclides, brought researchers new opportunities to use radionuclides in investigations. Until the introduction of nuclear reactors, however, large-scale production of radionuclides was not possible. Already in 1946, the Oak Ridge nuclear center sold radionuclides, which began to be more widely used in research towards the end of the 1940s.

The nuclear energy era begins

After the war, the nuclear reactors that were originally built for production of nuclear weapons were also used for production of electricity. The first nuclear reactors producing electricity were introduced in the Soviet Union in 1954 and in England in 1956. The output of the aforementioned reactors were 5 MV and 45 MV, while modern reactors run at a capacity of 500-1500 MV. Presently (2014), there are a total of 437 electricity producing nuclear power plants in 31 countries. In a few countries, France, Belgium, Hungary and Slovakia, over half of the electricity is nuclear energy.

The development of radiation measurement

As previously stated, Bequerel, like many other early investigators, used *photographic plates* for the detection of radiation. The second radiation detection device of that time was the *electroscope*, which had a metal rod with two metal plates hanging from it inside a glass ball. An electrical charge was applied to the plates, pushing them apart. When the radiation ionized the air within the glass ball and made it conductive, the charge between the plates was discharged and the shortening of the distance between the two plates was proportional to the amount of radiation hitting the ball. In 1903, William Crookes took a device called a spinthariscope into use, which for the first time utilized the *scintillation effect*. In this device, the alpha radiation hit the screen of the zinc sulfide layer, which caused excitation and the formation of light upon relaxation. The light had to be detected visually. In the late 1940s, a photomultiplier tube was invented, allowing the light to be

transformed into an electrical pulse able to be counted electronically. Scintillation crystals (e.g. NaI(Tl)) and liquid scintillation counting are now common radiation measurement methods. Before the Second World War the most prominent radiation measuring devices were the Geiger- Müller counter and the Wilson cloud chamber. The Geiger-Müller counter, which prototype H. Geiger and W. Müller developed in 1908, is based on the ability of radiation to penetrate a very thin window (previously enamel, presently beryllium) to a gas filled metal cylinder, which is connected to the voltage between the anode wire in the center of the cylinder and the metallic cylinder wall as a cathode. Radiation particles or rays ionize gas within the tube and cause an ion/electron cascade that can be detected and counted as electrical pulses in an external electric circuit. The Geiger- Müller counter is still used as a dosimeter in radiation protection and also in beta counting. In the Wilson cloud chamber, radiation is directed through a window into an enclosed space filled with water vapor. When the volume of the chamber is suddenly extended with a piston, the steam cools and the chamber becomes supersaturated. The radiation ionizes the gas and the generated ions act as the water vapor condensation centers. The phenomenon lasts for a couple of seconds and can be detected by the track of the water droplets along the glass wall, which can be photographed.

Geiger counters were the most common tool for radiation measurements still in the 1950s. Later, they were replaced in most cases by liquid scintillation counting in beta detection, as well as the scintillation and semiconductor detectors for the counting and spectrometry of alpha particles and gamma radiation. Scintillation crystals and the photomultiplier tubes used for their pulse amplification were developed in the late 1940s; the semiconductor detector was only developed in the early 1960s. Development of multichannel analyzers has also been important step in the radiation measurements.

II THE STRUCTURE OF ATOM AND NUCLEUS - NUCLIDES, ISOTOPES, ISOBARS – NUCLIDE CHARTS AND TABLES

Content

Atom and nucleus – protons and neutrons
Electrons
Nuclide
Isotope
Isobar
Nuclide charts and tables

Atom and nucleus – protons and neutrons

The atom consists of a small nucleus and of electrons surrounding it. The diameter of the nucleus ranges between $1.5 \cdot 10^{-15}$ m and $10 \cdot 10^{-15}$ m or 1.5-10 fm (femtometers) whereas the diameter of whole atom is $1\text{-}5 \cdot 10^{-10}$ m or 1-5 Å (angstrom) or in SI-units 0.1-0.5 nm (nanometers). Great majority of the mass, however, is in the nucleus. Compared to density of an atom the density of nucleus is huge at 10^{17} kg/m^3.

Atomic nucleus consists of protons (p) and neutrons (p), together these nuclear particles are called nucleons. Protons are positively charged, having a charge of one unit (+1) while neutrons are neutral having no charge. The number of protons determines the chemical nature of atoms, i.e. of what elements they are. The number of protons (Z) is called the atomic number and it is characteristic for each element. The number of neutrons is designated by letter N and the sum of protons and neutrons is called the mass number (A). Thus A (mass number) = Z (proton number) + N (neutron number).

In the nucleus the force that binds the protons and neutrons is the nuclear force that is far stronger force than any other known force (gravitation, electric, electromagnetic and weak interaction forces). The range of the nuclear force is very short; the space where it acts is approximately same as the volume of the nucleus. The nuclear force is charge-independent, so the n-n, p-p and n-p

attraction forces are of same strengths, and short range means that nucleons sense only their nearest neighbors. Figure II.1. shows the potential diagram of a nucleus, i.e. the potential energy as a function of the radius of the nucleus. In the figure, the range of nuclear force can be seen as potential well outside of which there is a positive electric layer, potential wall, due to positive charges of protons in the nucleus. Any positively charged particles entering the nucleus have to surpass or pass this potential wall. For a neutron, with no charge, it is easier to enter the nucleus since it does sense the potential wall.

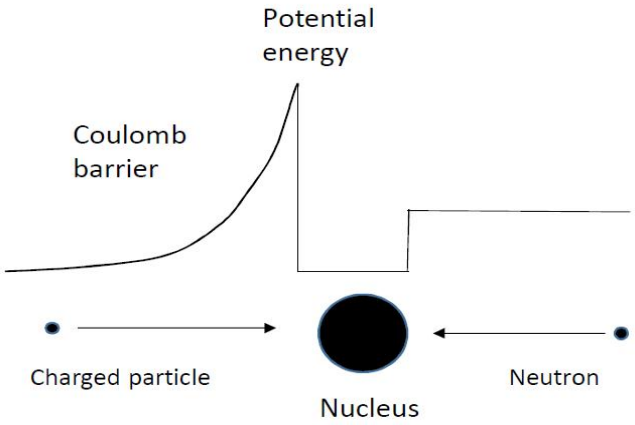

Figure II.1. Potential diagram of an atomic nucleus.

Electrons

Electrons (symbol e or e^-) surrounding the nucleus are located in shells (Figure II.2.). Electrons closest to the nucleus are located on the K shell and they have the highest binding energy, which decreases gradually on outer shell L, M, N and O. The charge of the electron is equal but opposite to that of proton, one negative unit (-1). To preserve its electrical neutrality the atom has as many electrons as there are protons.

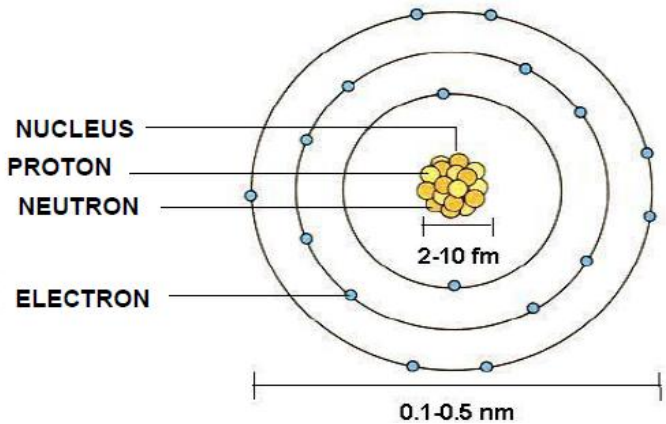

Figure II.2. Atomic nucleus and the electron shells.

Nuclide

Nuclide is defined as an atomic nucleus with a fixed number of protons (Z) and a fixed number of neutrons (N). Thus, also the mass number (A) is fixed for a certain nuclide. Nuclides are presented as elemental symbols having the atomic number (Z) on the lower left corner and the mass number (A) on the upper left corner.

$^{12}_{6}C$ (carbon-12) $^{18}_{8}O$ (oxygen-18) $^{35}_{16}S$ (sulphur-35)

Since the atomic number is already known from the elemental symbol, it is usually left away and the nuclides are presented as follows ^{12}C, ^{18}O and ^{35}S. Sometimes, especially in the older literature, the nuclides are marked in the following way C-12, O-18 and S-35.

With respect to stability, the nuclides can be divided into two categories:

- stable nuclides
- unstable, radioactive nuclides, shortly radionuclides

Isotope

Isotopes are defined as nuclides of the same element having different number of neutrons. Thus the mass number of isotopes varies according to the number neutrons present. For example, ^{12}C and ^{13}C are isotopes of carbon, the former having six neutrons and the latter seven. These two are the stable isotopes of carbon with the natural abundances of 98.9% and 1.10%, respectively. In addition to these carbon has several radioactive isotopes, radioisotopes, with mass number of ^{9}C ¾ ^{11}C and ^{14}C ¾ ^{20}C, of which the best known and most important is ^{14}C.

Radioisotope and radionuclide terms are often incorrectly used as their synonyms. Radionuclide, however, is a general term for all radioactive nuclides. We may, for example, say that ^{14}C, ^{18}O and ^{35}S are radionuclides, but we not should say ^{14}C, ^{18}O and ^{35}S are radioisotopes since radioisotope always refers to radioactive nuclides of a certain element. So, we may say, for example, that ^{14}C, ^{15}C and ^{16}C are radioisotopes of carbon. The two heavier isotopes of hydrogen ^{2}H and ^{3}H are most often called by their trivial names deuterium and tritium, designated as D and T.

Isobar

Isobar, as will be seen later in context of beta decay, is an important term also. Isobars are defined as a nuclide having a specific mass number, such as ^{35}Ar, ^{35}Cl, ^{35}S and ^{35}P are isobars.

Nuclide charts and tables

A graphical presentation, where all nuclides are presented with neutron number as x-axis and proton number as y-axis (or the other way round), is called a nuclide chart (Figure I.3.). Stable nuclides in the middle part are often marked with black color. The radioactive nuclides are located on both sides of the stable nuclides, neutron rich on right side and proton-rich on the left. In this kind of presentation, the elements are listed on vertical direction while the isotopes for each element are on horizontal lines. The isobars, in turn, can be seen as diagonals of the chart. For each nuclide, some important nuclear information, such as half-life, is given in the boxes. More detailed nuclear information can be found in nuclide databases, some of which are freely available in the internet, such as http://ie.lbl.gov/toi/.

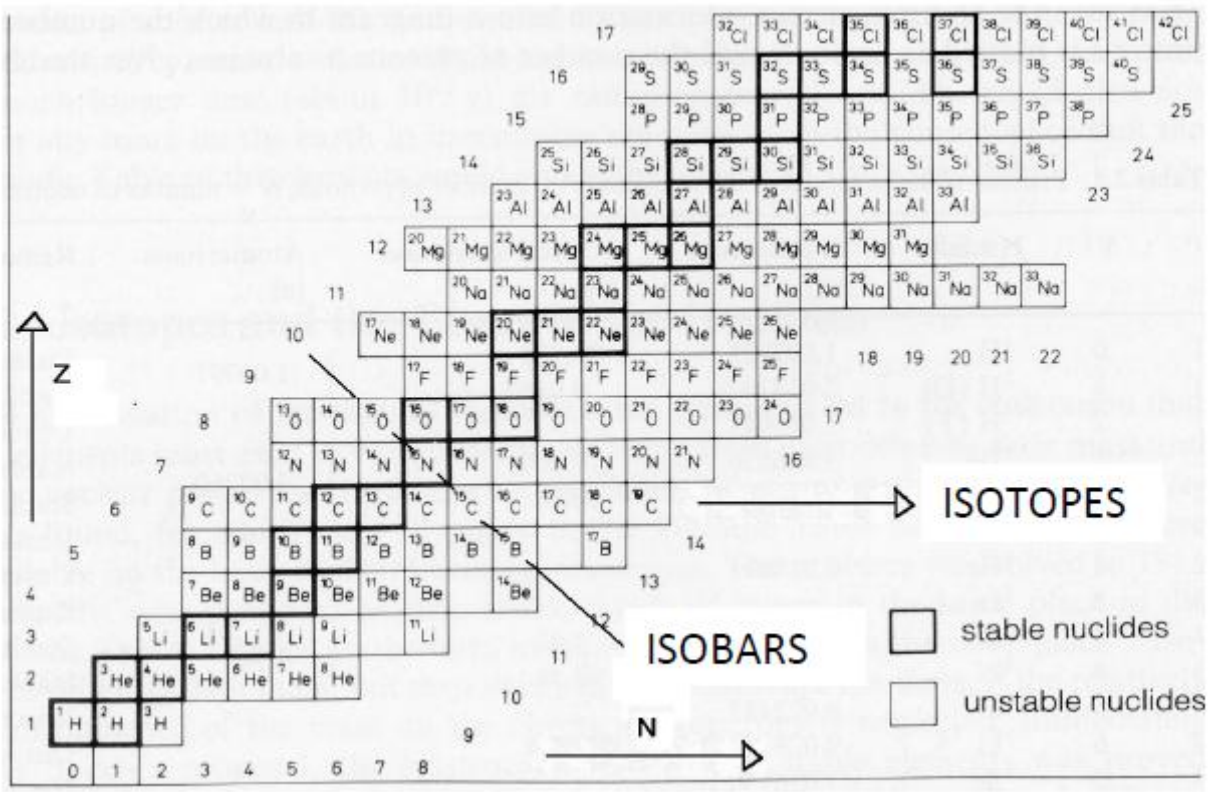

Figure II.3. Part of a nuclide chart.

III STABILITY OF NUCLEI

Content

Stable nuclides – parity of nucleons
Neutron to proton ratio in nuclei
Masses of nuclei and nucleons
Mass defect - binding energy
Binding energies per nucleon
Energy valley
Fusion and fission
Semi-empirical equation of nuclear mass
Magical nuclides

Stable nuclides – parity of nucleons

In the nature there are 92 elements and these have altogether 275 stable nuclides. Of these nuclides, 60% have both even number of protons and neutrons. They are called even-even nuclides. About 40% of nuclides have either even number of protons or neutrons. If the proton number is even and neutron number is odd the nuclide is called even-odd nuclide and in the opposite case and odd-even nuclide. Odd-odd nuclides where both proton and neutron numbers are odd are very rare. In fact, there are only four of them: ^{2}H, ^{6}Li, ^{10}B and ^{14}N.

Based on what was told above it is obvious that nuclei prefer nucleon parity and in the way that protons favor parity with other protons and neutrons with other neutrons. Single proton and single neutron do not form a pair with each other, which can be seen as the small number odd-odd nuclides. When looking at the nuclide chart, one can see that the elements with an even atomic number have considerably more stable isotopes than those having odd atomic number. For example $_{32}$Ge has five stable isotopes, of which four have also an even number of neutrons, while $_{33}$As has only one stable isotope and $_{31}$Ga two.

Neutron to proton ratio in nuclei

Another important factor affecting stability of nuclei is the neutron to proton ratio (n/p). There are two forces affecting the stability of nucleus and they work in opposite directions. The nuclear force is binding the nucleons together, while the electric repulsion force due to protons' positive charges is pushing the protons away from each other. The stable isotopes of the lightest elements have the same, or close to same number of protons and neutrons. As the atomic number of the elements is increasing the repulsion force due to increasing number of protons increases. To keep the nucleus as one piece heavier elements have increasing number of neutrons compared to protons. In the heaviest stable element, bismuth, the n/p ratio is around 1.5, while the heaviest naturally occurring element, uranium, has 92 protons and 143 (^{235}U) or 146 (^{238}U) neutrons, the n/p ratio thus being 1.6. Figure III.1 (left side) shows all nuclides as a nuclide chart where the neutron number is on x-axis and the proton number of y-axis. The stable nuclides are seen as black boxes and one can see that they are not on the diagonal line (n/p=1), except in case of the lightest elements, but on a bended curve due to systematically increasing n/p ratio. The nuclides above the stable nuclides are proton-rich radionuclides and those below neutron-rich radionuclides. As seen from the right side of the Figure III.1 the n/p ratio remains close to unity up to atomic number 20 (Ca) where after clear and increasing excess of neutrons appear.

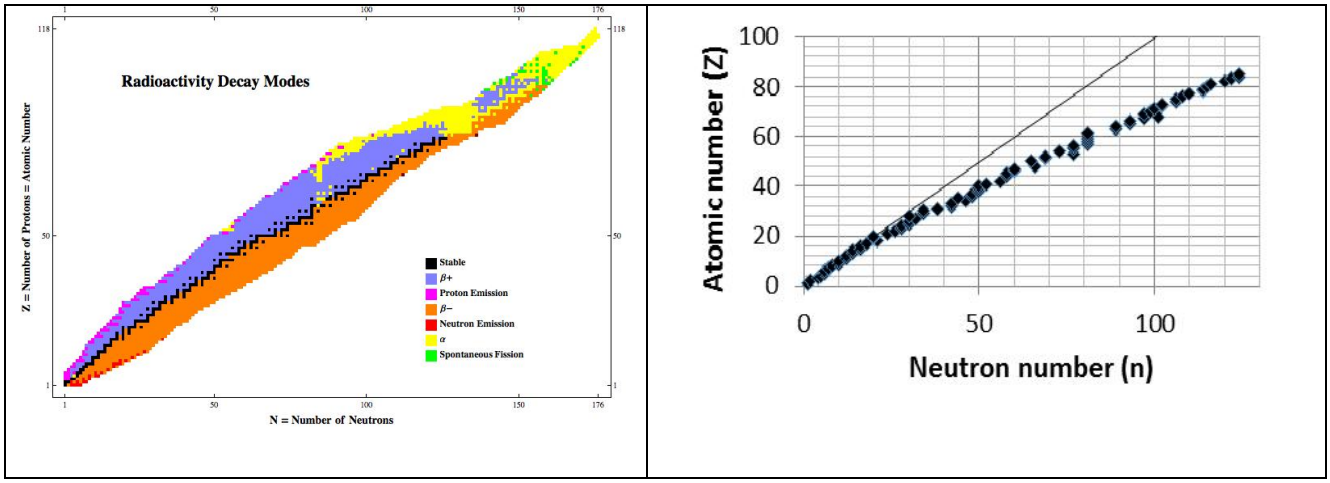

Figure III.1 Nuclide chart (left) (http://oscar6echo.blogspot.fi/2012/11/nuclide-chart.html). Neutron numbers of the most abundant isotopes of the stable elements as a function of atomic number (right).

Masses of nuclei and nucleons

The masses of atoms, nuclei and nucleons are not presented in grams due to their very small numbers but instead in relative atomic mass units (amu). Atomic mass unit is defined as a twelfth part of the mass of ^{12}C isotope in which there are six protons and six neutrons. The mass of ^{12}C is 12 amu and amu presented in grams

$$1 \text{ amu} = (12 \text{ g}/ 12) / N = 1\text{g} / N = 1.66 \cdot 10^{-24} \text{ g} \qquad \text{[III.I]}$$

where N is the Avogadro number $6.023 \cdot 10^{23}$ mol^{-1}. The mass of a proton is 1.00728 amu and that of neutron 1.00867 amu. The mass of an electron is only one 2000th part of the masses of nucleons, 0.000548597 amu. The masses in amu units are presented with the capital M while those in grams are presented as lower case m.

Mass defect - binding energy

At first sight, it would look logical that the mass of a nucleus (M_A) is the sum of masses of neutrons and protons.

$$M_A(calculated) = Z \times M_p + N \times M_n \qquad \text{[III.II]}$$

For example the mass of deuteron would thus be 1.007825 amu + 1.008665 amu = 2.016490 amu. The measured mass, however, is 2.014102 amu, being 0.002388 amu smaller than the calculated mass. This mass difference is called the mass defect ΔM and its general equation is:

$$\Delta M_A = M_A(measured) - M_A(calculated) \qquad \text{[III.III]}$$

Mass defect is the mass a nucleus loses when it is “constructed” from individual nucleons.

Mass (m) and energy (E) are interrelated and converted to each other by the Einstein equation $E = m \times c^2$ (c = speed of light). Thus, the mass defect can be converted to energy and one amu corresponds to 931.5 MeV of energy. In radioactive decay and nuclear reaction processes, the energies are presented as electron volts (eV) which is the energy needed to move an electron over 1 V potential difference. Electron volts are used as energy unit instead of joules (J) since the latter would yield very low numbers and the formers are thus more convenient to use. In joules one electron volt is as low as $1.602 \cdot 10^{-19}$ J. The mass defect of deuteron 0.002388 amu corresponds an energy of 2.224 MeV. This energy is released when one proton combines with one neutron to form

a deuteron nucleus. Accordingly, at least this much of energy is needed to break deuteron nucleus to a single proton and a neutron. This mass defect, presented as energy, is thus the binding energy (E_B) of the nucleus.

$$E_B \text{ (MeV)} = -931.5\ \Delta M_A \text{ (amu)} \qquad \text{[III.IV]}$$

Binding energies per nucleon

Table III.I. gives the mass defects and binding energies to some elements. As seen, the total binding energy systematically increases with the mass of the nuclide, being already 1800 MeV in uranium In addition, binding energies are given per nucleon (E_B/A) in Table III.II. This value is also presented for a number on elements as a function of their mass numbers in Figure III.2.

Table III.II. Atomic masses (M_A), mass defects (ΔM_A), binding energies (E_B) and binding energies per nucleon (E_B/A) for some elements.

Element	Z	N	A	M_A (amu)	ΔM_A (amu)	E_B (MeV)	E_B/A (MeV)
H	1	0	1	1.007825	0	-	-
H(D)	1	1	2	2.014102	-0.002388	2.22	1.11
Li	3	3	6	6.015121	-0.034348	32.00	5.33
B	5	5	10	10.012937	-0.069513	64.75	6.48
C	6	6	12	12.000000	-0.098940	92.16	7.68
Mg	12	12	24	23.985042	-0.212837	198.3	8.26
Zr	40	54	94	93.906315	-0.874591	814.7	8.67
Hg	80	119	199	198.96825	-1.688872	1573.2	7.91
U	92	146	238	238.05078	-1.934195	1801.7	7.57

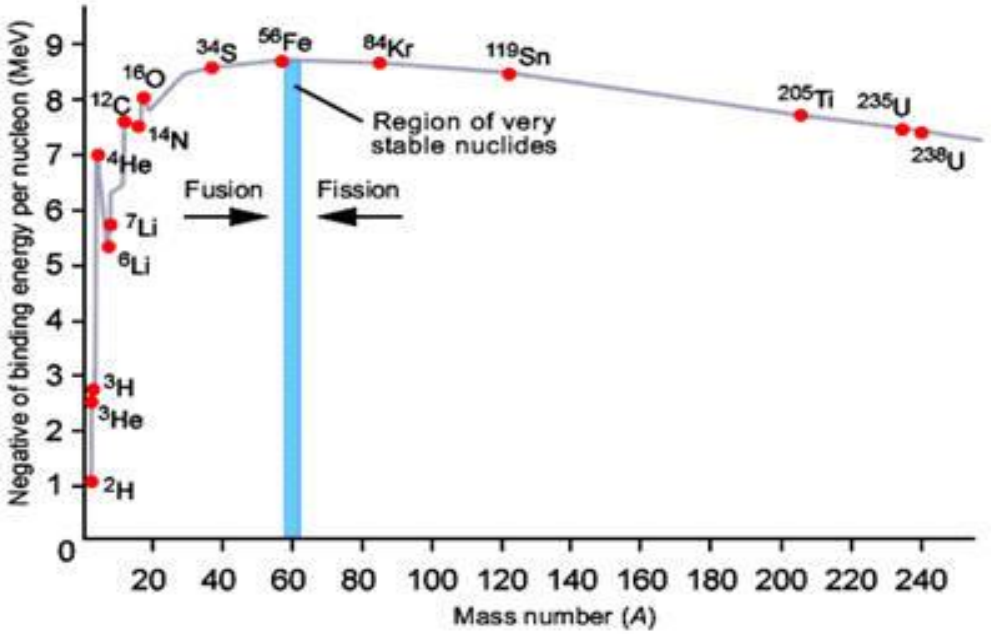

Figure III.2. Binding energy per nucleon E_B/A (MeV/A) of elements as a function of their mass number (http://www.daviddarling.info/encyclopedia/B/binding_energy.html).

The Figure III.2 shows that the binding energy per nucleon increases dramatically from the lightest elements to mass numbers between 50 and 60. As the E_B/A value for tritium is 1.11 MeV, it is at 8.8. MeV for iron (A=55). Thereafter E_B/A slowly decreases, being for example 8.02 MeV for thallium and 7.57 MeV for uranium. Thus, the intermediate-weight elements, such as iron, cobalt and nickel are the most stable. At certain mass numbers, or strictly speaking at certain proton and neutron numbers, the lighter nuclides have exceptionally higher binding energy than their neighbors do as seen in Figure III.2 and these nuclides are also exceptionally stable. For example, for ^{4}He the E_B/A value is as high as 7.07 MeV whereas for the next heavier nuclide ^{6}Li it is only 5.33 MeV. The high stability of ^{4}He makes it understandable why in alpha decay they are emitted from heavy nuclides.

Energy valley

When the lighter nuclides (Z<25) are presented in a three-dimensional coordinate system where the axes are mass excess (mass defect with positive sign), atomic number (Z) and neutron number (N), we see a picture presented in Figure III.3. The figure shows a formation of the so-called energy valley where the stable nuclides are at the valley bottom while the proton-rich radionuclides are at the left edge and neutron-rich radionuclides at the right edge. As will be later described the radionuclides decay by beta decay on diagonal isobaric lines from the edges to the bottom.

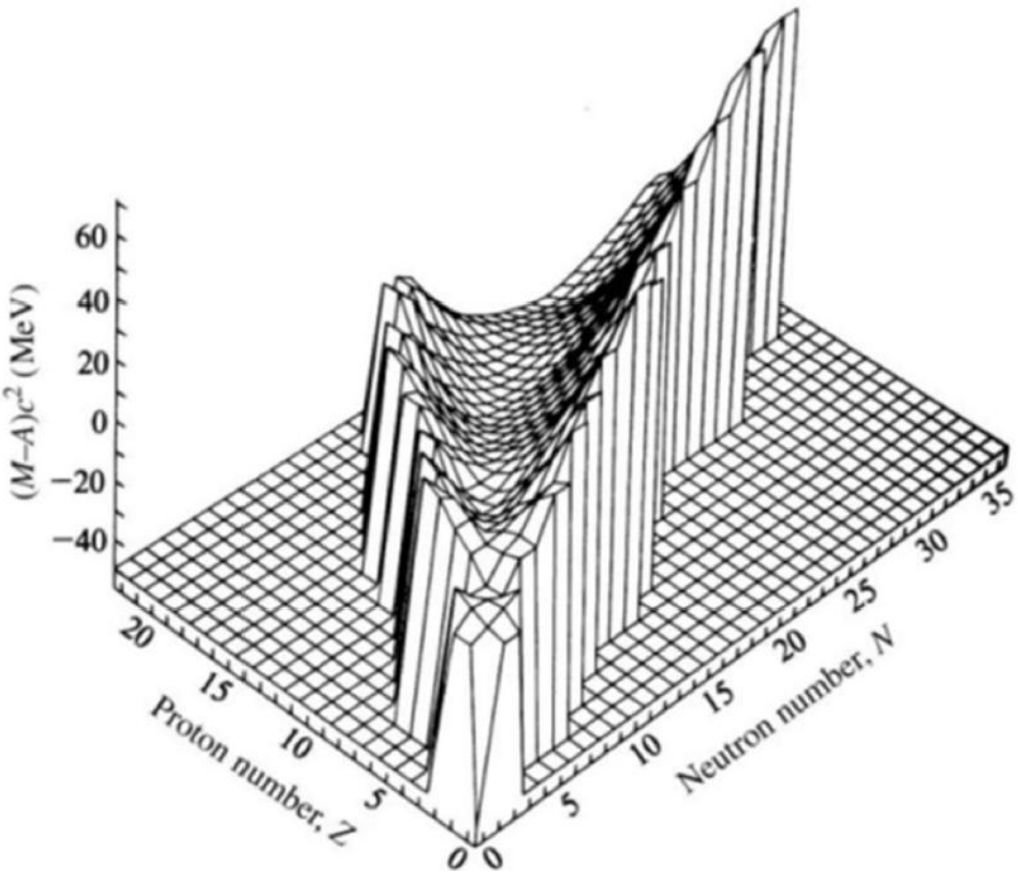

Figure III.3. Energy valley, i.e. mass excess as a function of neutron and proton numbers of lighter elements (Z = 1-25) (http://slideplayer.com/slide/1589163/)

Fusion and fission

One can see from Figure III.2. that when two light nuclides (A<30) combine into a heavier nuclide energy is released. For example, combination of two ^{20}Ne nuclides into ^{40}Ca nuclide releases 24 MeV of binding energy. The E_B/A value for ^{20}Ne is 8.0 MeV and the total binding energy of two ^{20}Ne nuclides is 2×20×8.0 MeV = 320 MeV, whereas the total binding energy of ^{40}Ca is 24 MeV higher (40×8.6 MeV = 344 MeV). Combination of two light elements to give a heavier and energetically more stable element is called fusion. Fusion has been exploited in fusion bombs, also called hydrogen bombs, in which fusion of deuterium and tritium creates huge amounts of energy. For energy production, fusion reactors are still being developed where the biggest problem is how to obtain high enough temperature to induce and maintain the fusion process. In fusion reactors, this is accomplished by using plasma but it cannot be done in energetically or economically profitable way yet. In fusion bombs, the high temperature is obtained by exploding a U or Pu fission bomb, covering the fusionable material.

An opposite reaction to fusion is fission where heavy elements split into two lighter, usually intermediate-sized, elements. For example, in the following fission reaction:

$$^{236}U \;\; ® \;\; ^{140}Xe + {}^{93}Sr + 3n \qquad \text{[III.V]}$$

191.5 MeV energy is released since the binding energy of ^{236}U per nucleon is 7.6 MeV and the total binding energy 236×7.6 MeV = 1793.6 MeV. The binding energies per nucleon for ^{140}Xe and ^{93}Sr are 8.4 MeV and 8.7 MeV, respectively, and their total binding energies 1176 MeV and 809.1 MeV. Thus the energy released in this reaction is 1176 MeV + 809.1 MeV – 1793.6 MeV = 191.5 MeV. Of the naturally occurring elements uranium partly (0.005%) decays by spontaneous fission. A more common way to obtain fission is the induced fission in which the heavy elements are bombarded by neutrons. For example, the ^{236}U in equation III.V is obtained by exposing ^{235}U to a neutron flux. After neutron absorption the forming ^{236}U nucleus is excited which results in fission reaction. There are two terms for fissioning nuclide, fissionable and fissile. Fissionable is a general term for any nuclide able to undergo a fission while fissile means that a nuclide undergos fission with thermal neutrons. Fissile nuclei, the most important of which are ^{235}U and ^{239}Pu, have even proton number but odd neutron number. When a thermal neutron enters the nucleus of a fissile element the nucleus goes to an excited energy state due to paring of nucleons. Fission, as fusion, was first utilized in bombs in 1940s but from 1950s on the main exploitation field has been nuclear energy production.

Semi-empirical equation of nuclear mass

Based on the liquid droplet model of nucleus in which nucleons are taken as incompressible droplets that have a binding interaction with only their closest neighbors, an equation has been derived to calculate the binding energies of nuclei. This equation is semi-empirical since some of its parameters have been obtained from experimental data.

$$E_B\,(\text{MeV}) = a_v \times A - a_a \times (N-Z)^2/A - a_c \times Z^2/A^{1/3} - a_s \times A^{2/3} \pm a_d/A^{3/4} \qquad \text{[III.VI]}$$

where A is the mass number, Z the atomic number, N the neutron number and a_v, a_a, a_c, a_s and a_s are experimentally obtained coefficients, the values of which are $a_v = 15.5$, $a_a = 23$, $a_c = 0.72$, $a_s = 16.8$ and $a_d = 34$. The basic starting point in the equation is that the total binding energy is directly

proportional to the number of nucleons which is taken into in the equation by the term $a_v \times A$. This "volume energy" decreases by factors that are taken into account by the three further terms in the equation. The last term either increases or decreases the energy or has no effect on it. The second term $a_a \times (N-Z)^2/A$ takes into account the variance in neutron to proton ratio and is called asymmetry energy, the third term $a_c \times Z^2/A^{1/3}$ takes into account the coulombic repulsion between the protons and the fourth term $a_s \times A^{2/3}$ takes into account the energies on the surface of a nucleus which differ from those in its bulk. The fifth term $a_d/A^{3/4}$ takes into account the parity of nucleons: in case of an even-even nuclide the term has a positive value while for odd-odd it is negative. For even-odd and odd-even nuclides term has a value of zero.

When N in the equation is substituted by A-Z we get an equation where the binding energy is presented as a function of atomic number Z:

$$E_B = a Z^2 + b Z + c \pm d/A^{3/4} \qquad \text{[III.VII]}$$

where the coefficients a, b and c are dependent only on the mass number A. At a fixed mass number, i.e. isobaric line, the equation has a form of a parabel. Figure III.4 shows an example of such parabels which are important in understanding the beta decay modes decribed in chapter IV. In beta decay processes the decay takes place on isobaric lines, a neutron is transformed into a proton or vice versa and thus no change in the mass number is taken takes place. The curves in Figure III.4 present the nuclides in beta decay chains. The nuclide, or nuclides, on the bottom are stable while nuclides on the edges are radioactive stepwisely decaying towards the stable nuclide(s), neutron-rich radionuclides on left side by β^- decay and proton-rich nuclides on the right side by β^+/EC decay. Identical parabel is obtained when taking a cut in the energy valley (Figure III.3) along an isobaric line. The third term in equation III.VI, $\pm d/A^{3/4}$, explains why there is only one parabel on the left side of the Figure III.4 and two overlying parabels on the right side. When the mass number in the isobar is odd the $\pm d/A^{3/4}$ term has value of zero and all the transformations occur from odd-even to even-odd or vice versa. In the other case, when the mass number is even, the transformations are from odd-odd to even-even (or vice versa) and correspondingly the term $\pm d/A^{3/4}$ changes its sign in each transformation which results in the formation of two parabels. The upper parabel is for the less stable nuclide, that is the odd-odd nuclide, whereas the lower parabel for the even-even nuclides.

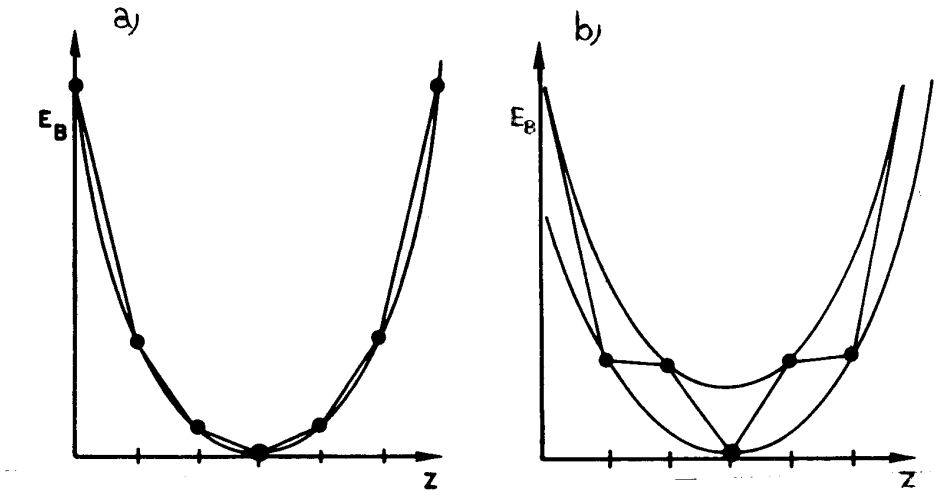

Figure III.4. Parabels derived from semiempiral equation of nuclear mass for a fixed mass number. a) odd mass number, b) even mass number. Points on the parabels represent nuclides and the lines between them beta decay processes.

Magical nuclides

Droplet model, on which the semiempirical equation of nuclear mass is based, widely but not completely explains the nuclear mass and systematics of energy changes in nuclear transformations. However, as can also be seen in Figure III.2, there are some exceptions which cannot be described with the equation. For example, ^{4}H, ^{16}O, ^{40}Ca, ^{48}Ca and ^{208}Pb have exceptionally high stabilities. From this it has been concluded that certain neutron and proton numbers create higher stabilities. These numbers, called magical numbers, are 2, 8, 20, 28, 50, 82 for both protons and neutrons and 126 for neutrons. These cannot be described with the droplet model but instead a nuclear shell model has been applied to explain the nature of magical numbers. This shell model is analogous to atomic electron shell model: nucleons are located on certain shells which have sites for only a certain number of nucleons on and those nuclides having full shells are more stable than the others. Droplet model and shell model are not exlusive, they rather complement each other.

With superheavy elements the magical neutron and proton number are no more identical. After element with atomic number of 82 the magical proton numbers are 114, 126, 164, 228 while the corresponding values for neutrons above N=126 are 184, 196, 228 and 272.

IV RADIONUCLIDES

Content

Radionuclides can be divided into four categories based on their origin:

- Primordial naturally occurring radionuclides
- Secondary naturally occurring radionuclides
- Cosmogenic naturally occurring radionuclides
- Artificial radionuclides

Primordial radionuclides

Primordial (primary) radionuclides, as well as other elements, were formed in the nuclear reactions following the creation of the universe and they have been present in the earth ever since of its birth some 4.5 billion years ago. Due to the high flux of energetic protons and alpha particles, a great number of heavy elements were created in these nuclear reactions. Those elements and nuclides with considerably shorter half-life than the age of the Earth have already decayed away and only those with half-lives comparable with the age of the Earth still exist. These primordial radionuclides can be classified into two cathegories:

- parent nuclides of natural decay chains, ^{238}U, ^{235}U and ^{232}Th
- individual radionuclides of elements lighter than bismuth (Table IV.I.)

Table IV.I Lighter primordial naturally occurring radionuclides

Nuclide	Isotopic abundance	Decay mode	Half-life
^{40}K	0.0117%	β^-	$1.26 \cdot 10^9$ a
^{87}Rb	27.83	β^-	$4.88 \cdot 10^{10}$ a
^{123}Te	0.905	EC	$1.3 \cdot 10^{13}$ a
^{144}Nd	23.80	α	$2.1 \cdot 10^{15}$ a
^{174}Hf	0.162	α	$2 \cdot 10^{15}$ a

Many of these very long-lived radionuclides were earlier considered as stable ones but as the measurement techniques have developed, their radioactive nature has become apparent. The isotopic abundances to these radionuclides are also presented, as in Table IV.I, because their fractions of the total element do not change in human observation time period. Considering radiation dose to humans the most important of these radionuclides is the ^{40}K having a very long half-life of $1.26 \cdot 10^9$ years and an isotopic abundance of 0.0117%. Since humans have a practically constant potassium concentration in their bodies, their ^{40}K concentration is also constant, below 100 Bq/kg. ^{41}K contributes to several percentages (5% for Finns) of their total radiation dose.

Secondary natural radionuclides - decay chains

The three primordial radionuclides ^{238}U, ^{235}U and ^{232}Th are parent nuclides in decay chains, which end up through several alpha and beta decays to stable lead isotopes. In between there are a number radionuclides of twelve elements. The half-life of ^{238}U is $4.5 \cdot 10^9$ y and it starts a series with 17 radionuclides and the ^{206}Pb isotope is the terminal product (Figure IV.1.) This decay chain is called uranium series and as the mass numbers of the product are divided by four the balance is two.

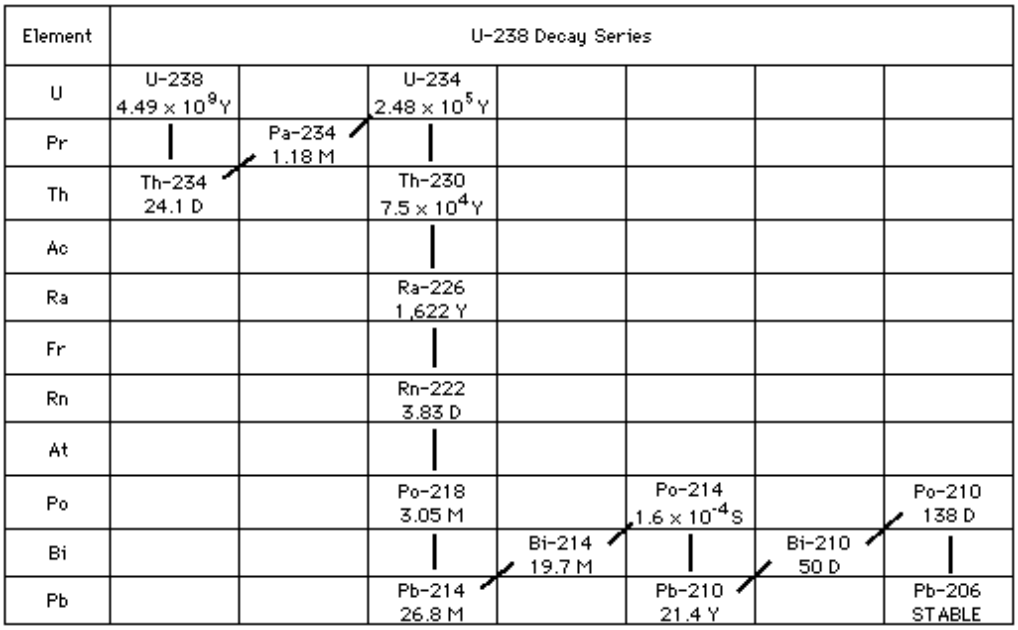

Figure IV.1. The uranium decay chain, A = 4n+2 (http://www2.ocean.washington.edu/oc540/lec01-17/).

From ^{235}U, having a half-life of $7 \cdot 10^8$ y, starts the A=4n+3 decay chain, called actinium series. There are altogether 15 radionuclides between ^{235}U and the terminal product, the stable ^{207}Pb isotope.

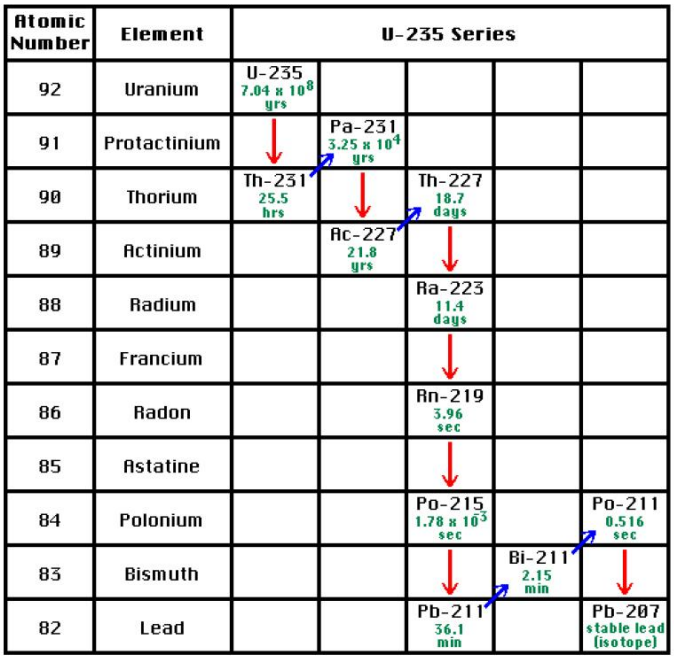

Figure IV.2. The actinium decay chain, A = 4n+3 (http://eesc.columbia.edu/courses/ees/lithosphere/labs/lab12/U_decay.gif).

The third decay chain starts from ^{232}Th, with the half-life of $1.4 \cdot 10^{10}$ y. This A = 4n chain is called thorium series and it has ten radionuclides between ^{232}Th and the terminal product ^{208}Pb.

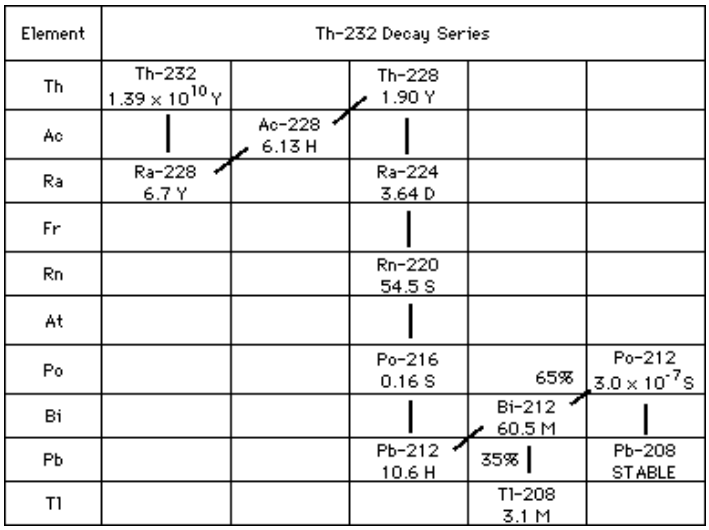

Figure IV.3. The thorium decay chain, A = 4n (http://www2.ocean.washington.edu/oc540/lec01-17/).

The uranium series has some important radionuclides with respect to radiation dose to humans. Most important of these is ^{222}Rn with a half-life of 3.8 days. Part of the radon formed in the ground emanates into the atmosphere and also to indoor air. When inhaling radon-bearing air the solid alpha-emitting daughter nuclides ^{218}Po, ^{214}Bi and ^{214}Pb may attach to lung surfaces and give a radiation dose. In fact, radon in indoor air causes largest fraction of radiation dose to humans, for example, more than half in Finland. Other important radionuclides in the uranium series are ^{238}U, ^{226}Ra, ^{210}Pb and ^{210}Po, which cause radiation dose to humans via ingestion of food and drinking water.

In nature, there has also been a fourth decay chain, starting from ^{237}Np, but due to its relatively short half-life of $2.1 \cdot 10^6$ y, more than three orders of magnitude shorter than the age of the Earth, it has decayed away long time ago. This chain consisted of seven radionuclides between ^{237}Np and the end product ^{209}Bi.

Cosmogenic radionuclides

Cosmogenic radionuclides generate in the atmosphere through nuclear reactions induced by cosmic radiation. The main components of cosmic radiation are highly energetic protons and alpha particles. In the primary reactions of particles with atoms of the atmosphere, neutrons are also formed and these can induce further nuclear reactions. Altogether about forty cosmogenic radionuclides are known and some of them are listed in Table IV.II. These are formed in nuclear reactions of air gas molecules, especially oxygen, nitrogen and argon. The most important from the radiochemistry point of view are radiocarbon ^{14}C and tritium ^{3}H that are formed in the following reactions:

$$^{14}N + n \rightarrow {}^{14}C + p \qquad [IV.I]$$

$$^{14}N + n \rightarrow {}^{12}C + {}^{3}H \qquad [IV.II]$$

Table IV.II. Important cosmogenic radionuclides.

Nuclide	Half-life	Nuclide	Half-life
^{3}H	12.3 a	^{7}Be	53 d
^{10}Be	$2.5 \cdot 10^{6}$ a	^{14}C	5730 a
^{22}Na	2.62 a	^{26}Al	$7.4 \cdot 10^{5}$ a
^{32}Si	710 a	^{32}P	14.3 d
^{33}P	24.4 d	^{35}S	88 d
^{36}Cl	$3.1 \cdot 10^{5}$ a	^{39}Ar	269 a

Since the intensity of cosmic radiation is in the long-term constant, the production of the cosmogenic radionuclides is rather constant. There is, however, great variation at different heights of the atmosphere and at different latitudes. Most energetic particles lose their energy already in the upper parts of the atmosphere. Gaseous cosmogenic radionuclides, such as ^{14}C (CO_2) and ^{39}Ar, remain in the atmosphere while solid products attach to aerosol particles and deposit on the ground, especially with precipitation.

The most important cosmogenic radionuclide is ^{14}C that is taken up by plants as CO_2 in photosynthesis. It is widely used in age determination of carbonaceous materials. Furthermore, measurement of some other cosmogenic radionuclides has been utilized in evaluation of transfer and mixing processes in the atmosphere and in the oceans.

Artificial radionuclides

During the last 70 years, more than 2000 artificial radionuclides have been produced. These have been obtained in the following ways:

- in nuclear weapon production and explosions
- in nuclear power production
- in production of radionuclides with reactors and accelerators

Nuclear explosions create a wide variety of fission products, transuranium elements and activation products, which are essentially the same as formed in nuclear power reactors. Most important of these are the fission products ^{90}Sr and ^{137}Cs and isotopes of transuranium elements Pu, Am and

Cm. Underground nuclear weapons tests leave the radioactivity mostly underground but in the atmospheric tests the radioactivity first spreads in the atmosphere and eventually deposits on the ground. In the 1950's to 1980's more than four hundred nuclear weapons tests were carried out by the USA, Soviet Union, China, France and the UK. These tests resulted in a heavy local and regional contamination. The explosion clouds of the most powerful tests entered the upper part of the atmosphere, the stratosphere, from where the radioactive pollutants have deposited on a global scale. The highest radiation dose to humans have so far has resulted from radioactive cesium nuclide ^{137}Cs but in the long-term the largest contribution to the radiation dose comes from ^{14}C created from atmospheric nitrogen by neutron activation.

In *nuclear weapon production,* a source of radionuclides is plutonium production, which is done by irradiating ^{235}U-enriched uranium in a nuclear reactor. In uranium weapon material production no new radionuclides are formed since only ^{235}U is enriched with respect to ^{238}U. The radionuclides formed in plutonium production are essentially the same as in nuclear explosions and in nuclear power reactors. After radiochemical separation of plutonium for weapons material the rest, the high-active waste solution, contains the fission products and other radionuclides than Pu and U. These waste solutions are stored in tanks in the USA and they still wait to be treated before final disposal. In the Soviet Union, only part of the waste solutions are in tanks while a large fraction was discharged into the environment at the Majak site, first to Techa river and later to Karachai lake. This has resulted in a huge contamination of the area. In nuclear weapons production, there has been two major accidents leading to large environmental contamination. The first occurred in 1957 in Sellafield in the UK where a plutonium production reactor caught fire and released large amounts of radioactivity, especially radioactive iodine. In the same year, a high-active waste tank exploded at the Majak site in Russia and large areas, fortunately mostly inhabited, were contaminated with radionuclides.

The 99.99% of the radioactivity created in *nuclear power production* is in spent nuclear fuel of which 96% is uranium dioxide, 3% is fission products and 1% is transuranic elements, mainly plutonium. Spent nuclear fuel will be disposed of either after reprocessing or as such into geological formations. In reprocessing the nuclear fuel is dissolved in nitric acid and uranium and plutonium is separated for further use as a fuel while the rest, fission products and minor actinides, remain in the high-active waste solution which is vitrified for final disposal. In addition to fission products (^{135}Cs, ^{129}I, ^{99}Tc, ^{79}Se etc.) and transuranium elements the spent nuclear fuel contains long-lived activation products, such as ^{14}C, ^{36}Cl, ^{59}Ni, ^{93}Mo, ^{93}Zr and ^{94}Nb, formed in impurities in the nuclear fuel and

in the metal parts surrounding the fuel. In addition to radionuclides in spent fuel, also activation and corrosion products, such as ^{60}Co, ^{63}Ni, ^{65}Zn, ^{54}Mn, are formed in nuclear power plants in steel of their pressure vessel and impurities in the primary coolant. These end up in the low and medium active waste and are disposed of in repositories constructed for them. Nuclear power plants also release rather small amounts of liquid and gaseous radionuclide-containing discharges into the environment. Liquid releases contain same radionuclides as found in low and medium active waste while air releases contain gaseous radionuclides, such as ^{14}C and ^{85}Kr. From the final disposal of nuclear waste, the radiation dose to humans will be very small.

There have been, however, three *major accidents in nuclear power plants* resulting in a large release of radionuclides into the environment. The first one occurred in 1979 in Harrisburg, USA, but only noble gases and other gaseous radionuclides were released from the damaged reactor and no long-term contamination of the surrounding area took place. The second and the largest accident took place in Chernobyl, Ukraine, where a power reactor exploded and caught fire in 1986. This accident caused a severe environmental contamination, not only in Ukraine, Belorussia and Russia, but also in many other countries in Europe. In 2011, several reactors damaged due to tsunami in Fukushima in Japan. Large radioactive releases, about one tenth of that from the Chernobyl accident, ended up to the Pacific Ocean and also to a large area inlands northwest of the plant.

A wide range of *radionuclides for research and medical use* are being produced in reactors and accelerators. After use, they are mainly either aged or released into the environment. Some of the most important radionuclides used in medical and biosciences and in clinical use are listed in Table IV.III.

Table IV.III. Some important radionuclides used in bio and medical sciences.

Nuclide	Radiation	Half-life	Nuclide	Radiation	Half-life
^{3}H	beta	12.3 a	^{14}C	beta	5730 a
^{18}F	beta	1.8 h	^{32}P	beta	14.3 d
^{35}S	beta	87 d	^{45}Ca	beta	165 d
^{82}Br	beta/gamma	36 h	^{99m}Tc	gamma	6 h
^{125}I	gamma	57 d	^{131}I	beta/gamma	8 d

V MODES OF RADIOACTIVE DECAY

Content

There are four basic modes of radioactive decay:

- spontaneous fission
- alpha decay
- beta decay
- internal transition

FISSION

In addition to spontaneous fission, which is one of the radioactive decay modes, induced fission is also shortly discussed here. The reason for the spontaneous fission is that the nucleus is too heavy and it is typical only for the heaviest elements (heavier than uranium). In fission, the nucleus splits into two nuclei of lighter elements, for example:

$$^{238}U \rightarrow {}^{145}Ba + {}^{90}Kr + 3\,^{1}n + 200MeV \qquad [V.I]$$

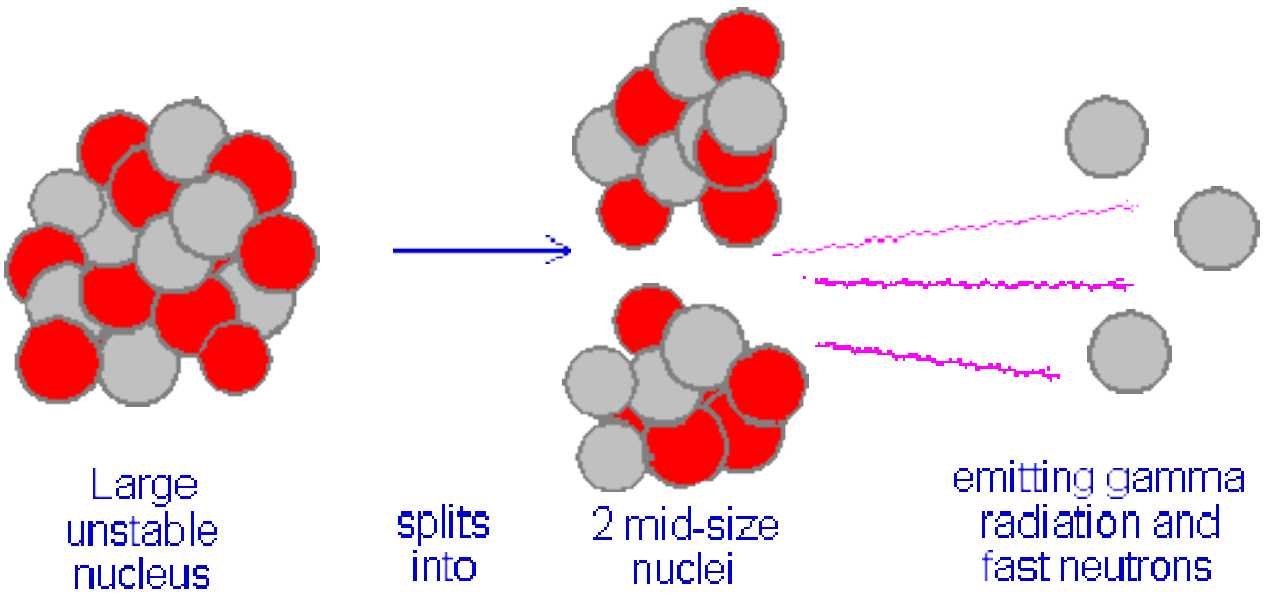

Figure V.1. Spontaneous fission of a heavy nucleus into two nuclei of lighter elements (http://physics.nayland.school.nz/VisualPhysics/NZP-physics%20HTML/17_NuclearEnergy/Chapter17a.html).

In an induced fission a nucleus is bombarded with a particle, such as a neutron, which results in fission, such as

$$^{235}U + n \rightarrow {}^{236}U \rightarrow {}^{141}Ba + {}^{92}Kr + 3\,^{1}n + 200MeV \qquad [V.II]$$

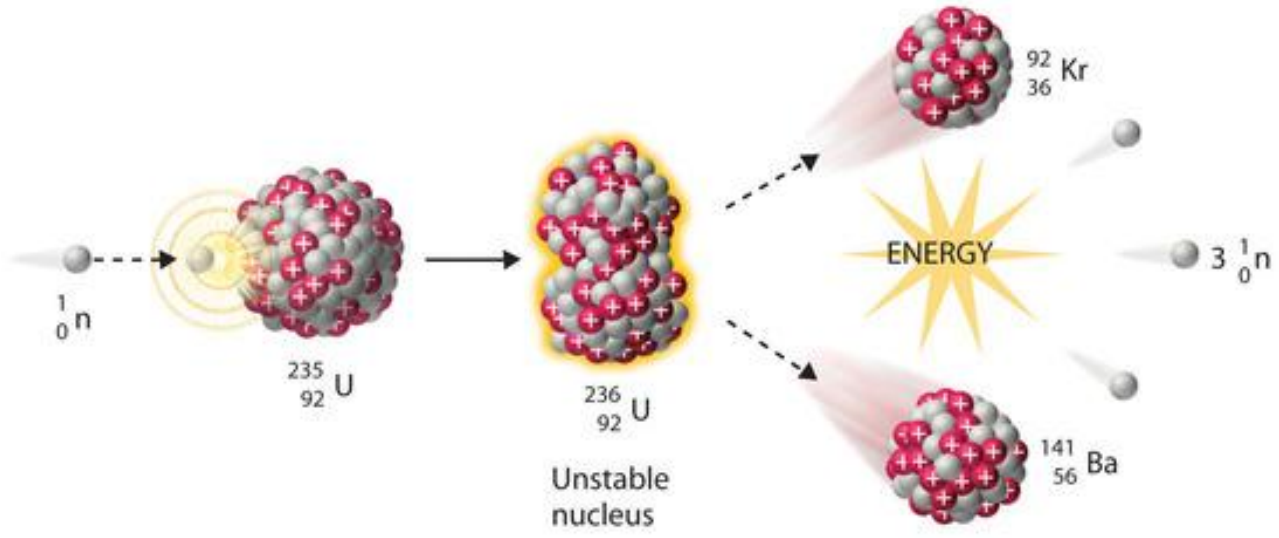

Figure V.2. Induced fission of a heavy nucleus into two nuclei of lighter elements (http://chemwiki.ucdavis.edu/Physical_Chemistry/Nuclear_Chemistry/Nuclear_Reactions).

In addition to the lighter elements, called fission products, fission yields into emission of 2-3 neutrons and a large amount of energy, the distribution of which is shown in Table V.I.

Table V.I. Distribution of the 200 MeV energy in the fission of ^{235}U.

Kinetic energy of the fission products	165 MeV
Kinetic energy of neutrons	5 MeV
Energy of the instantaneously released gamma rays	7 MeV
Kinetic energy of the beta particles of fission products	7 MeV
Kinetic energy of the gamma rays of fission products	6 MeV
Kinetic energy of neutrinos from beta decays	10 MeV

In the nature, there is only one nuclide, ^{238}U that decays spontaneously by fission. Fission is, however, not the only decay mode of ^{238}U and in fact only 0.005% of it undergoes this decay mode while the rest decays by alpha decay. Spontaneous fission of uranium has its own specific decay half-life which is $8 \cdot 10^{15}$ a. With transuranium and superheavy elements, spontaneous fission is more common but as with uranium, spontaneous fission is mostly a minor decay mode. For example, all plutonium isotopes with a mass number between 235 and 244 partly decay by spontaneous fission. There are, however, some heavy radionuclides, such as ^{256}Cf and ^{250}No, which decay solely by spontaneous fission.

Fission products, the lighter nuclides formed in fission, are radioactive. The heavy elements, such as uranium, have higher neutron to proton ratios compared to elements formed in fission. In the fission, however, only 2-3 neutrons are released and therefore the fission products have too many neutrons for stability. For example, barium isotopes formed in fission have approximately the same neutron to proton ratio as ^{238}U, 1.59. The stable barium isotopes, however, have neutron to proton ratio in the range of 1.32-1.46. To obtain stability, the fission products gradually correct their neutron to proton ratio by decaying with β^- decay mode, i.e. they transform excess neutrons to protons until the nuclide has neutron to proton ratio that enables stability. An example of such decay chain is shown in Figure V.3.

Nuclide	Half-life	n/p ratio
^{137}Te	3.5 s	1.63
↓		
^{137}I	24.5 s	1.58
↓		
^{137}Xe	3.8 min	1.54
↓		
^{137}Cs	30 a	1.49
↓		
^{137}Ba	stable	1.48

Figure V.3. A fission product decay chain ending in stable ^{137}Ba.

There is a large number of fission daughter products. They are, however, not evenly formed at various mass numbers. Instead, they are concentrated to two mass number ranges with mass numbers between 90-105 and 130-140. Graphical presentation of the fission product yields, the percentage of fissions leading to specified mass number, as a function of mass number results in the formation of a double hump curve given in Figure V.4. The upper mass range is independent of the fissioning nuclide while the lower mass range shifts into higher mass numbers as the mass of the fissioning nuclide increases.

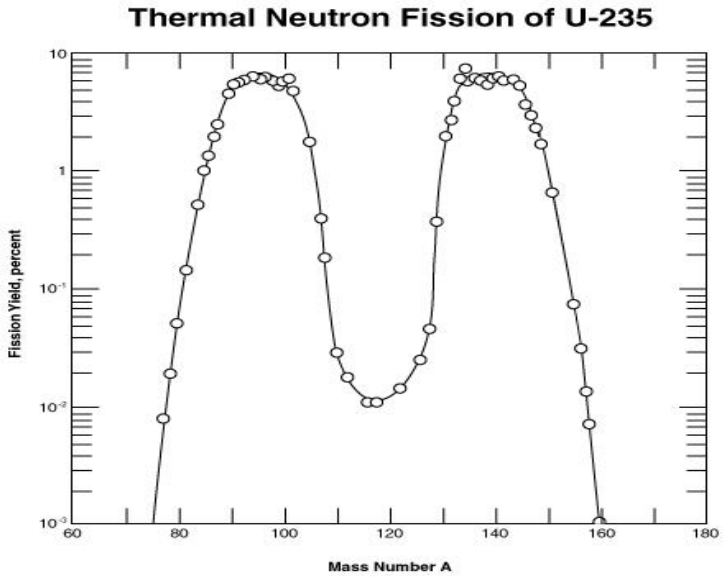

Figure V.4. Distribution of fission products of ^{235}U (http://www.science.uwaterloo.ca/~cchieh/cact/nuctek/fissionyield.html).

Most fission products have short half-lives and they decay rapidly. In a relatively short term, tens to hundreds of years after fission of uranium or plutonium material, the most-prevailing components are the fission products ^{90}Sr and ^{137}Cs, the half-lives of which are 28 y and 30 y, respectively. In the very long term, the long-lived fission products dominate the mixture, first ^{99}Tc with a half-life of 210.000 years, then ^{135}Cs with a half-life of 2.300.000 years and, finally, ^{129}I with a half-life of 16.000.000 years.

ALPHA DECAY

The reason for alpha decay is the same as for fission, the nucleus is too heavy. Alpha decay is, however, typical for somewhat lighter elements than fission. In alpha decay, an excess of mass is released by the emission of a helium nucleus, called an alpha (α) particle:

$$^{226}Ra \rightarrow {}^{222}Rn + {}^{4}He\ (\alpha) \qquad [V.II]$$

Helium nucleus has two protons and two neutrons and thus in alpha decay the mass number decreases by four units while the atomic number decreases by two. Alpha decay is the most typical mode for elements heavier than lead, especially in case of proton-rich nuclides. Also at intermediate mass region, many proton-rich nuclides decay by alpha decay. Alpha decay seldom takes place to only ground energy state of the daughter nuclide but in most cases also to its excited states. As will be later discussed with internal transition, these excited states relax either by emission of gamma rays or by internal conversion. Below in the Figure V.5 are shown examples of the two cases: a decay purely to the daughter's ground state (^{212}Po) and a decay to both ground state and excited states (^{211}Po). With the heaviest elements, alpha decay can result in emission of a number of alpha particles of different energy and even a greater number of gamma rays.

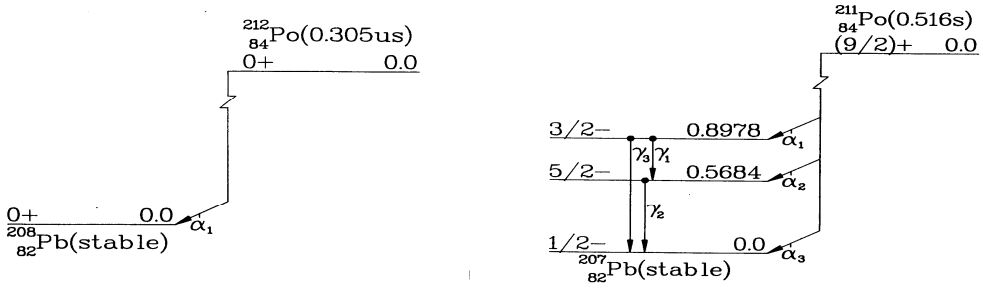

Figure V.5. Decay schemes of ^{212}Po and ^{211}Po (Radionuclide Transformations, Annals of the ICRP, ICRP Publication 38, Pergamon Press, 1983).

Many alpha decay processes compete with beta decay so that part of the nuclides decays by alpha decay and the rest with beta decay. Two examples of such cases are given in Figure V.6. On the left side is the case of ^{218}Po where 99.98% of the decays go through alpha emission while a small fraction of 0.02% through beta emission. On the right side is the case of ^{211}At of which 41.9% decay by alpha decay and the rest 58.1% by electron capture mode. In some cases, such as in case of ^{226}Ac, all these three processes take place.

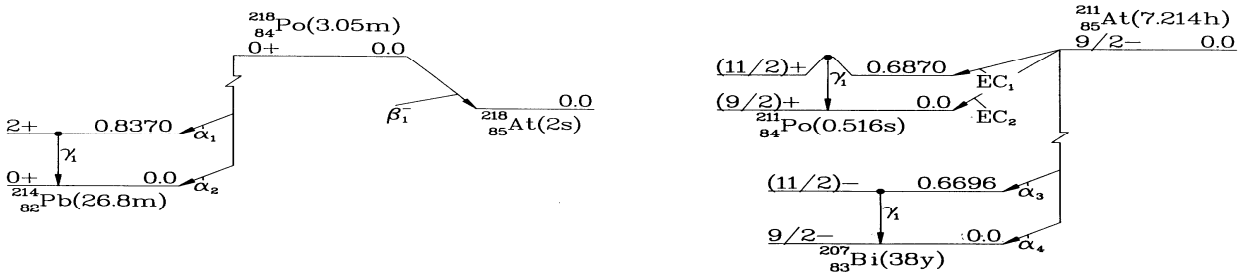

Figure V.6. Decay schemes of ^{218}Po and ^{211}At (Radionuclide Transformations, Annals of the ICRP, ICRP Publication 38, Pergamon Press, 1983).

The decay energy in the alpha decay Q_α, which is the energy/mass difference between the ground states of the parent and daughter nuclides, can be calculated in the following way. As already mentioned, one atomic mass unit corresponds to 931.5 MeV energy. As M_Z is the mass of the parent nucleus and the masses of the daughter and alpha particle are M_{Z-2} and M_{He}, the decay energy is

$$Q_\alpha = -931.5 \text{ MeV } (M_{Z-2} + M_{He} - M_Z) \qquad \text{[V.II]}$$

For example, when ^{238}U decays by alpha emission to ^{234}Th the decay energy is:

$$Q_\alpha = -931.5 \text{ MeV/amu } (234.043594 + 4.002603 - 238.0507785)$$
$$= -931.5 \text{ MeV/amu } (-0.0045815 \text{ amu}) = 4.274 \text{ MeV} \qquad [V.III]$$

Where 234.043594, 4.002603 and 238.0507785 are the atomic masses of ^{238}U, helium and ^{234}Th. Atomic masses are used instead of nucleus masses since the masses of electrons are the same on both sides of the reaction and balance each other. Thus, in the decay above a mass of 0.0045815 amu transforms into energy of 4.274 MeV. This energy divides into two parts, into the kinetic energy of the alpha particle (E_α) and into recoil energy of the daughter nuclide (E_{Z-2}). In the decay process both the energy $Q_\alpha = E_\alpha + E_{Z-2}$ and the moment are preserved and we can calculate the kinetic energy of the alpha particle by $E_\alpha = Q_\alpha (M_{Z-2}/M_Z)$ and that of the daughter nuclide by $E_{Z-2} = Q_\alpha (M_\alpha/M_Z)$. For the case presented above, we get for the kinetic energy 4.202 MeV for the alpha and for the recoil energy 0.072 MeV for ^{234}Th. Even though the recoil fraction of the energy is less than 2% it is still 10.000 times higher than the energies of chemical bonds. Thus, the recoil always results in the breaking of the chemical bond between the daughter nuclide and the compound where the parent initially was. Energies of alpha particles are always high. The lowest observed energy 1.38 MeV is that of ^{144}Nd and the highest 11.7 MeV that of ^{212}Pb, while typically the energies range from 4 MeV to 8 MeV.

Emitting alpha particles have definite energies, since the transition from the ground state of the parent to the ground and excited states of the daughter occur between definite quantum states. Thus, the alpha particles are monoenergetic, as are the gamma rays of the transitions from the excited states of the daughter nuclide. Due to the monoenergetic nature of the alpha particles, their spectrum is called line spectrum. In Figure V.7 on left, there is the line spectrum of alpha particles emitted in the decay of ^{241}Am, where five peaks of the following alpha particles are seen 5.389 MeV (1.3%), 5.443 MeV (12.8%), 5.486 MeV (85.2%), 5.512 MeV (0.2%) and 5.544 (0.3%). Due to the limited energy resolution of the spectrometer, i.e. limited capability to respond to alpha particles of same energy in the same manner, the observed alpha spectrum gives only one observable peak.

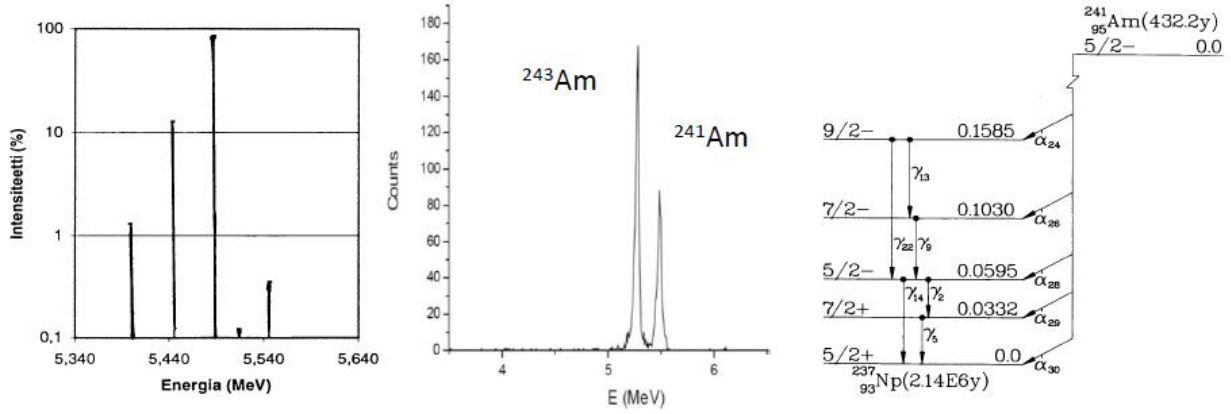

Figure V.7. Distribution of alpha particle energies (left), observed alpha spectrum with ^{243}Am tracer (middle) and the decay scheme (right, (Radionuclide Transformations, Annals of the ICRP, ICRP Publication 38, Pergamon Press, 1983) of ^{241}Am.

As mentioned, the reason for alpha decay of nuclides is their too heavy mass. Theoretically, all nuclides with mass number larger than 150 are unstable and should decay by alpha decay. As seen from Figure II.1, representing the potential diagram of nuclei, the nucleus has a high positive potential wall that an alpha particle has to go over to leave the nucleus. For nuclei with a mass number between 150 and 200, the energies of alpha particles are not high enough to do this. Even for heavier nuclei, the potential wall is higher than the energies of the alpha particles but nevertheless many of them decay by alpha emission. For example, for ^{238}U the height of the potential wall is about 9 MeV while the energy of the emitting alpha particle is only 4.2 MeV, which has been explained by the tunneling phenomenon assuming a certain probability of alpha particles crossing the potential wall.

BETA DECAY PROCESSES

The reason for beta decay is an unsuitable neutron to proton ratio. There are three different types of beta decay processes:

- b^- decay
- positron decay or b^+ decay
- electron capture

of which the first is characteristic for neutron-rich nuclides and the two latter for proton-rich nuclides.

For all beta decay processes the mass number does not change since a neutron in the nucleus transforms into a proton in b^- decay and vice versa in positron decay and electron capture. All beta decay processes take place on isobaric lines towards stable nuclides in the middle:

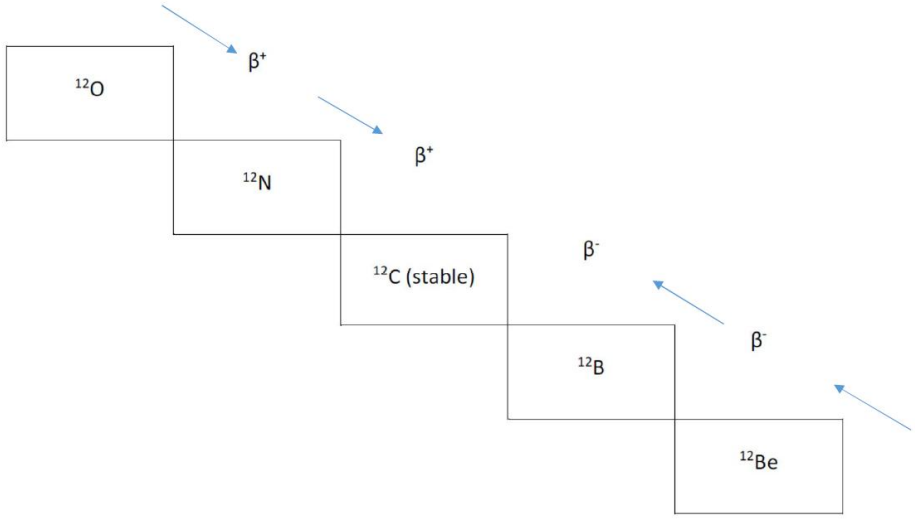

Figure V.8. Beta decays on isobaric line A=12.

b^- decay

In b^- decay, later called beta minus decay, the nuclide has too many neutrons for stability, i.e. the nucleus is neutron-rich. This kind of nuclides are formed in fission of heavy elements, such as uranium and plutonium, and in neutron-induced nuclear reactions. In beta minus decay, an excessive neutron in the nucleus transforms into a proton and a beta particle (β^-) is emitted. Thus, the atomic number of the daughter nuclide is one unit higher than that of the parent.

$$(n) \rightarrow (p^+) + \beta^- \qquad [V.IV]$$

where parentheses refer to particles within the nucleus. The emitting beta particle is physically identical to an electron and is also called negatron.

As already mentioned when alpha decay was discussed, nuclear transformations between the parent and the daughter always occur between defined quantum (energy) states. The observed spectrum of

the beta particles is, however, not a line spectrum but a continuous one, ranging from zero to a maximum energy (E_{max}) characteristic for each radionuclide (Figure V.9). The conflict between the defined energy states of the parent and the daughter from one side and the continuous beta spectrum on the other is explained by the fact that not only beta particles are emitted in beta minus decay but also antineutrinos ($\bar{u}$). They have practically no mass and thus beta detectors do not detect them. In each beta decay process the total kinetic energy of beta particle plus antineutrino is the same as the maximum energy (E_{max}) but their energy fractions varies in the 0-100% range. When, for example, the other gets 35% of the energy the other gets 65%. The complete beta minus decay reaction is thus:

$$(n) \rightarrow (p^{+}) + \beta^{-} + \bar{u} \qquad [V.V]$$

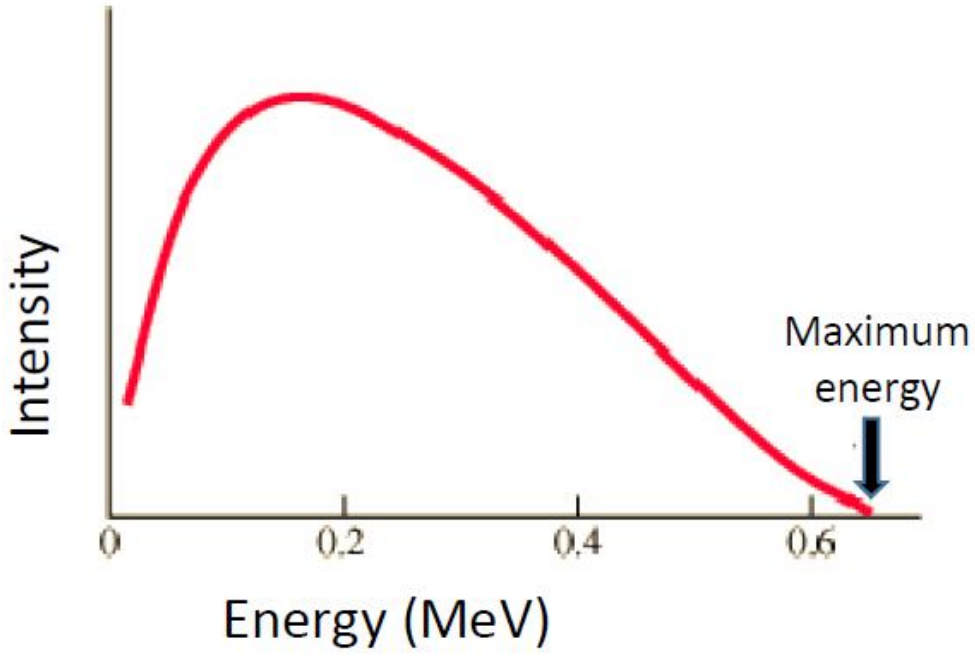

Figure V.9. A beta spectrum.

As seen in Figure V.9 the kinetic energy does not divide identically to beta particle and antineutrino. Instead, the average energy of beta particles is approximately one third of the maximum energy.

The decay energy in beta decay does not go only to the kinetic energies of beta particle and antineutrino but also to the recoil energy of the daughter nuclide. Due to the small mass of emitting beta and antineutrino particles, the recoil energy is much smaller than in alpha decay. Recoil energies of daughter nuclides are discussed later for all three beta decay processes.

The energies of beta particles vary in a very wide range (Table V.II).

Table V.II. Average energies (E) and maximum energies ($E_{max)}$ of some beta emitters. E » 0.3×E_{max}.

Nuclide	E (MeV)	E_{Max} (MeV)	Nuclide	E (MeV)	E_{max} (MeV)
^{3}H	0.0057	0.018	^{14}C	0.0495	0.180
^{32}P	0.695	1.71	^{90}Y	0.935	2.30

Beta decays lead often to excited states of the daughter nuclide and these excited states relax with internal transition, which will be discussed later. Some beta emitters, such as ^{3}H, ^{14}C, ^{32}P, ^{35}S and ^{63}Ni, are, however, pure beta emitters as the beta transitions occur from the ground state of the parent to the ground state of the daughter. Figure V.10 shows examples of both cases: a decay only to ground state (^{39}Ar) and a decay both to ground state and to exited states (^{41}Ar).

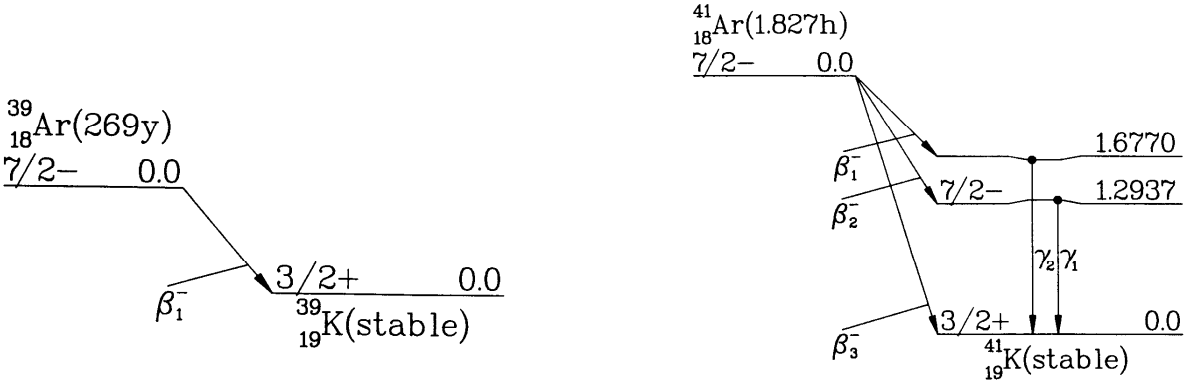

Figure V.10. Decay schemes of ^{39}Ar and ^{41}Ar (Radionuclide Transformations, Annals of the ICRP, ICRP Publication 38, Pergamon Press, 1983).

In β^- decays, the decay energy is simply calculated from the difference between the atomic masses of the daughter nuclide and the parent nuclide:

$$Q_{\beta^-} = -931.5 \text{ MeV/amu } (M_{Z+1} - M_Z) \quad [V.VI]$$

The mass of emitting beta particles (electrons) does not need to be taken into account since the atomic number of the daughter nuclide is one unit higher and it needs an extra electron to become electrically neutral. Daughter nuclides are initially ionized, having a charge of one positive unit, but these immediately take an electron from the surroundings to regain electroneutrality. The taken electron is of course any electron from the surrounding matter but we can imagine that it is the emitted beta particle to rationalize the Equation V.VI.

Positron decay and electron capture

Positron decay and electron capture are opposite reactions to β^- decay. They occur with proton-rich nuclides and in them a proton within a nucleus transforms into a neutron. Proton-rich nuclides are generated in accelerators, especially in cyclotrons, by bombarding target nuclei with proton-bearing particles, such as protons and alpha particles.

Positron decay

In positron decay, a proton turns into a neutron and a positron particle (β^+) is emitted. Thus, in positron decay the atomic number decreases by one unit.

$$(p^+) \rightarrow (n) + \beta^+ \quad [V.VII]$$

Positron particle is a counter particle of electron. It has the same mass as electron but its charge is plus one unit. In the beta minus decay, an antineutrino is emitted along with the beta particle and similarly to this a neutrino is emitted with positron particle in positron decay. Thus the complete reaction is:

$$(p^+) \rightarrow (n) + \beta^+ + \upsilon \quad [V.VIII]$$

As in beta minus decay, also positron decay often takes place via the excited states of the daughter nuclide and the excitation energy is relaxed by internal transition. There are, however, some

radionuclides, particularly within light positron emitters, that decay solely to ground state. Examples of pure positron emitter nuclides are ^{11}C, ^{13}N, ^{15}O, ^{18}F. Figure V.9 shows examples of both: a pure positron emitter (^{18}F) and a nuclide with excited states (^{22}Na).

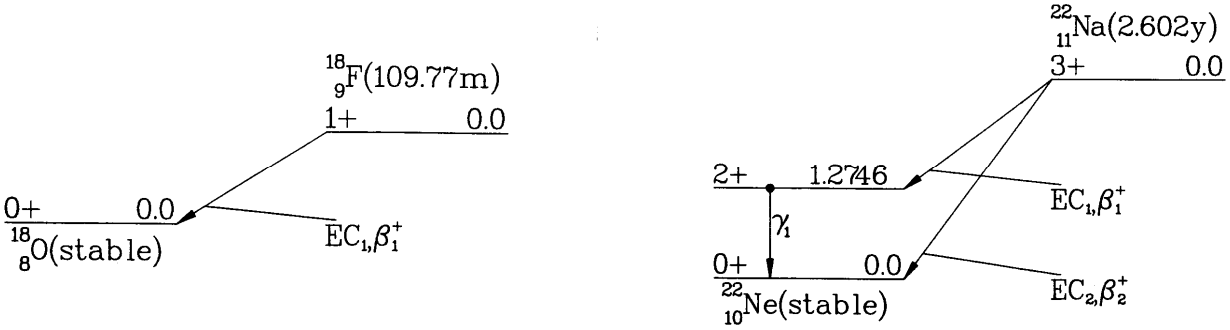

Figure V.11. Decay schemes of ^{18}F and ^{22}Na (Radionuclide Transformations, Annals of the ICRP, ICRP Publication 38, Pergamon Press, 1983).

Opposite to beta minus decay, the masses of the emitting positron and one electron need to be taken into account when calculating the decay energy. Since the daughter nuclide has one unit lower atomic number an electron needs to leave the atom. Another electron mass is lost with the emitting positron. Thus the decay energy is:

$$Q_{\beta+} = -931.5 \text{ MeV/amu } (M_{Z-1} + 2M_e - M_Z) \qquad [V.IX]$$

The positron particle created in positron decay is unstable and, after losing its kinetic energy, it annihilates, i.e. it combines with its counter particle, electron. In the annihilation process, the masses of the two particles turn into kinetic energy of two gamma quanta. These gamma quanta emit to opposite directions and their energy is 0.511 MeV which corresponds to the mass of an electron. These gamma rays are used to measure activities of positron emitters since their measurement is easier than measurement through detection of positron particles.

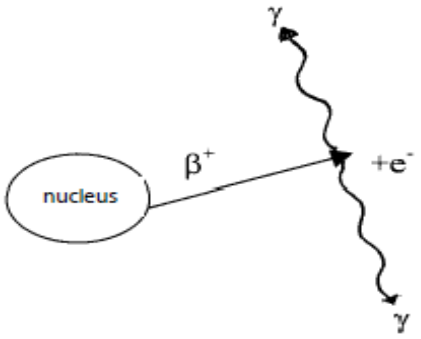

Figure V.12. Positron emission and positron annihilation.

Due to neutrino emission, the spectrum of positron particles is continuous. The distribution of positron energies is, however, somewhat different from that of beta particles (V.9). The average energy of positron particles is somewhat higher, at about $0.4E_{max}$, than with beta particles for which it is round $0.3E_{max.}$

Electron capture

As mentioned, electron capture (EC) is a competing process for positron decay. It is a prevalent process for heavier (Z>80) proton-rich nuclides while positron decay is that for lighter (Z<30) nuclides. In between (Z=30-80) both processes take place concurrently.

In electron capture, a proton within a nucleus transforms into a neutron by capturing an electron from the atom's electron shell:

$$(P^+) + e^- \text{ ®} (n) + \upsilon \qquad [V.X]$$

As in positron decay, the atomic number of the daughter is one unit lower than that of the parent. Most typically, the captured electron comes from the inner K shell, but also from the L shell while capture from upper shells is very rare.

When calculating the decay energy the mass of the captured electron can be omitted since the atomic number of the daughter is one unit lower and thus needs an electron less than the parent needs. The decay energy is simply the mass difference of the daughter and the parent.

$$Q_{EC} = -931.5\,(M_{Z-1} - M_Z) \qquad [V.XI]$$

As seen from Equation V.X there are neutrinos emitted in electron capture. In fact, all decay energy goes to the kinetic energy of emitted neutrinos. Thus, no detectable radiation is emitted in the primary decay process. In many cases the electron capture, however, leads to excited states of the daughter. These excited states relax by internal transition and the gamma rays emitted in this process can be used to measure the activities of such EC nuclides, such as ^{85}Sr. There are, however, also EC nuclides without any daughter nuclide's excitation states. Measurement of these nuclides is based on the secondary radiations created in all EC processes. As the hole of the captured electron is filled by an electron from upper shells, X-rays are emitted and the energy of these rays is the energy difference between the shells (Figure V.13 left). Thus, these rays are characteristic X-rays of the daughter nuclide and they can be measured by an X-ray detector to determine the activity of the parent (Figure V.13 right). An example of a pure EC nuclide is ^{55}Fe for which the decay scheme is given in Figure V.14. Another way to determine the activity of pure EC nuclides is to measure Auger electrons by liquid scintillation counting. Auger electrons are created when the energy of the X-rays is transferred to shell electrons, which are thereby emitted. These electrons are mono-energetic having energy of the X-ray minus the binding energy of the electron.

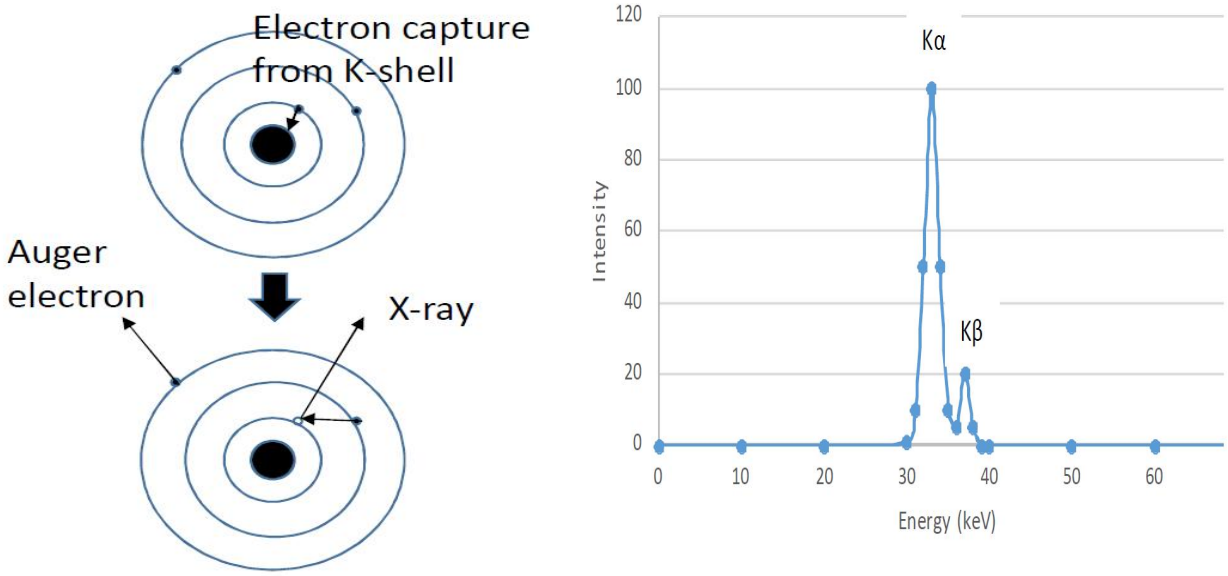

Figure V.13. Electron capture, formation of Auger electrons and characteristic X-rays and the ensuing X-ray spectrum.

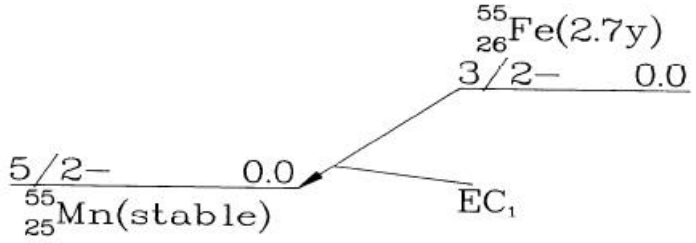

Figure V.14. Decay scheme of ^{55}Fe (Radionuclide Transformations, Annals of the ICRP, ICRP Publication 38, Pergamon Press, 1983).

Odd-even-problem

As mentioned in chapter III the plot of the semi empirical equation of nuclear mass for defined mass number is parabola. The beta decaying nuclides lay on the edges of the parabola, β^- nuclide on the left edge and β^+/EC nuclide on the right while stable nuclide/s locate at the bottom. These parabolas are cross-sections of the energy valley presented in Figure III.3. Depending on the mass number, there are either one or two parabolas: one for odd nuclides and two for even nuclides. For odd mass numbers, there is only one stable nuclide at the bottom while for even numbers there are two or three. For even mass numbers, the nuclides on the upper parabola have both odd atomic number and odd neutron number and thus these nuclides are odd-odd nuclides. In turn the nuclides on the lower parabola the both numbers are even and these nuclides are thus even-even nuclides.

Beta decay at odd mass numbers. Figure V.15 shows an isobaric cross-section for the mass number 145. Since the mass number is odd, there is only one parabola. b^- decays occur on the left edge of the parabola: $^{145}_{58}Ce$ decays to $^{145}_{59}Pr$ and this further to stable $^{145}_{60}Nd$. b^+ and EC decays occur on the right edge: $^{145}_{62}Sm$ decays to $^{145}_{61}Pm$ and this further stable $^{145}_{60}Nd$. The nuclide at the bottom of the parabola $^{145}_{60}Nd$ has the lowest mass, which means that it is the most stable of these nuclides. In this case, it has an even atomic number and an odd neutron number and is thus an even-odd nuclide. There are 105 of this kind of isobaric cross-sections (parabolas) and the number of stable nuclides in them is obviously the same.

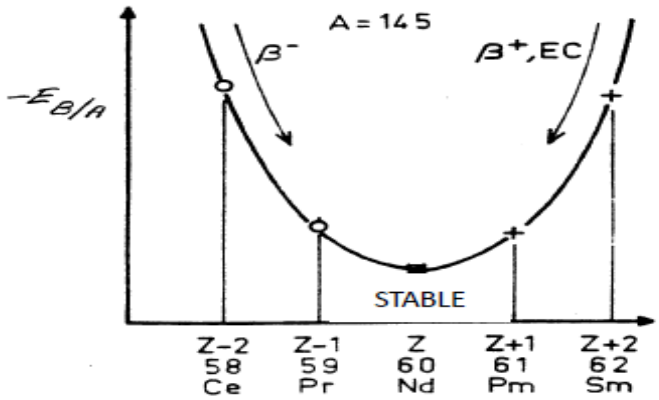

Figure V.15. Beta decays with a mass number of 145.

Beta decays at even mass numbers. Isobaric cross-sections with even mass numbers have two parabolas, the upper for odd-odd nuclides and the lower for even-even nuclides. As with odd mass numbers and also with even mass numbers, the beta decays occur along the edges of the parabolas, but in this case the decay takes place from one parabola to another since in each decay the nuclide changes from even-even nuclide to odd-odd nuclide or vice versa. The rarest case in this kind of beta decay processes end up to the bottom of the upper parabola where the nuclide has an odd-odd nature. There are only four such cases and all are among the lightest elements, ^{2}H, ^{6}Li, ^{10}B and ^{14}N. Heavier odd-odd nuclides are unstable due to their imparity of both protons and neutrons. An example of these with the mass number 142 is presented in Figure V.14. Here the bottom nuclide of the upper parabola is $^{142}_{59}\mathrm{Pr}$, being an odd-odd nuclide, is heavier than the adjacent nuclides on the lower parabola, $^{142}_{58}Ce$ and $^{142}_{60}Nd$. Therefore $^{142}_{59}\mathrm{Pr}$ decays to both directions, though the beta minus decay is clearly prevalent by 99.98%. Another example of these is ^{64}Cu (Figure V.17) for which 61% of decays take place with β^+ and EC and the rest (39%) with β^- decay. In the isobaric cross-section with mass number 142 (Figure V.16) we also see that $^{142}_{58}Ce$ is heavier than $^{142}_{60}Nd$ and thus the decay to this lighter nuclide should take place. This would, however, require that the decay process goes through a heavier $^{142}_{59}\mathrm{Pr}$ nuclide, which is impossible. The only possibility is double beta decay and this kind of decay has indeed been observed. An example of this is the decay of ^{82}Se to ^{82}Kr where two beta particles are emitted and the atomic number increases by two units. The decay is, however, very slow, the half-life for it being as long as 1.7×10^{20} years.

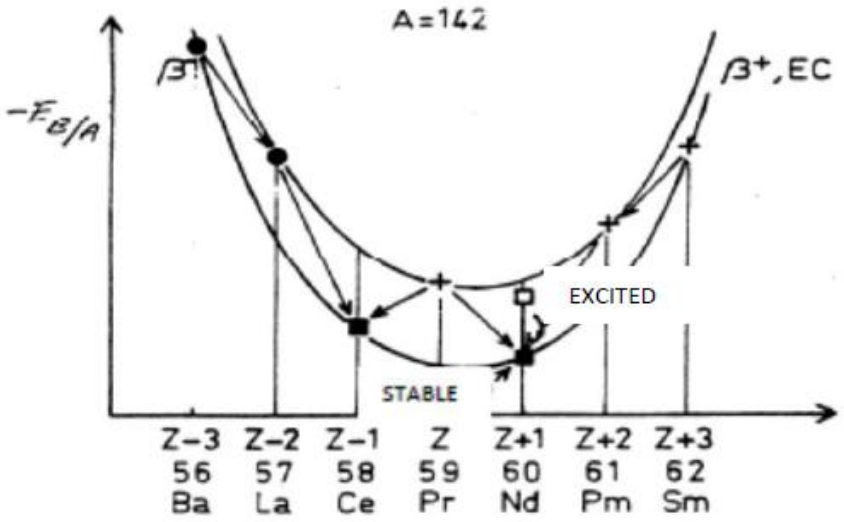

Figure V.16. Beta decay at the isobaric cross-section A=142. Two stable nuclides, both even-even nuclides.

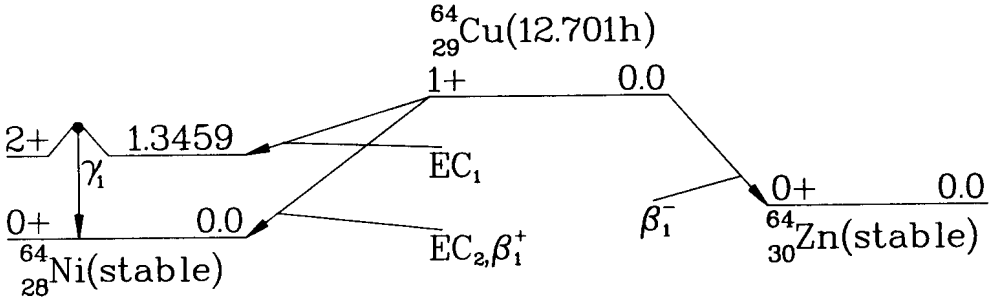

Figure V.17. Decay scheme of ^{64}Cu (Radionuclide Transformations, Annals of the ICRP, ICRP Publication 38, Pergamon Press, 1983).

Below in Figure V.18 there are plots for the other cases of even mass numbers. On the left hand side there is the case with only one stable nuclide and on the right a case with three stable nuclides. The former is a typical case and there are altogether 78 of them. The latter, however, is rare and only three cases are known, for example at mass number 96 there are three stable nuclides ^{124}Xe, ^{124}Te and ^{124}Sn.

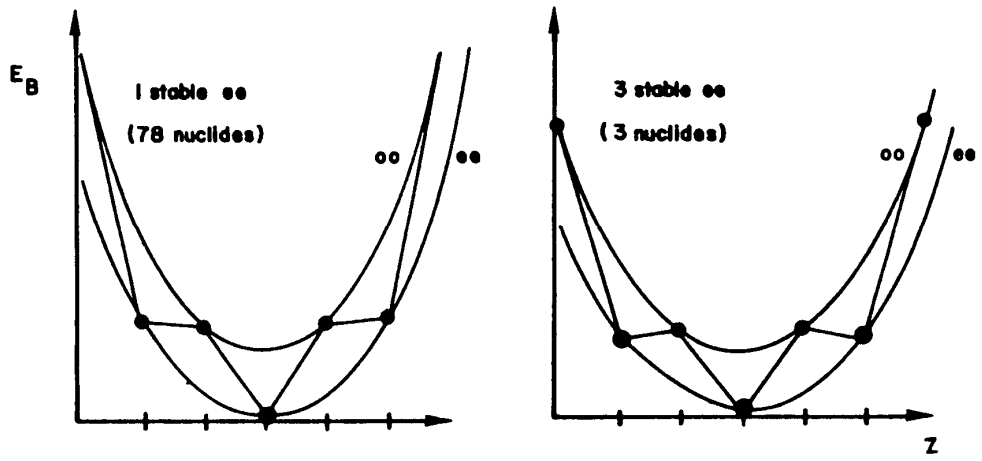

Figure V.18. Beta decay processes at even mass numbers. Left: one stable nuclide. Right: three stable nuclides.

Recoil of the daughter in beta decay processes

The direction where neutrinos are emitted is not known, since we do observe them, but if it emits to opposite direction to beta particle the recoil energy of the daughter atom is zero. In case they both are emitted to same direction the recoil energy is its maximum (E_d). Decay energy in this case is

$$Q = E_d + E_{max} \qquad [V.XII]$$

where E_{max} is the maximum energy of the beta particle. As already mentioned the recoil energies in beta decay processes are small due to the small mass of electron/positron. Thus, Q and E_{max} are practically identical. For example, in the beta decay of ^{14}C where E_{max} is 156 keV, E_d is only 7 eV (0.004%). Compared to energies of chemical bonds, this recoil energy is, however, considerable and therefore the beta decay recoil often results in breaking chemical bonds.

Consequences of beta decay processes

Beta decay processes result in the formation of beta particles, positrons and neutrinos/antineutrinos as primary emissions. After primary processes, there are secondary processes, which lead to additional emission of radiation. These are:

- Beta decay often occurs to the excited states of the daughter nuclide. Relaxation of the excitation occurs by internal transition (described in next section) and emission of gamma rays and conversion electrons.
- As the positrons annihilate with electrons 0.511 MeV gamma rays are formed.
- In electron capture, X-rays are formed as the hole in the electron shell is filled with an electron from the upper shells. The X-rays are characteristic of the daughter atom and their energies correspond to the energy differences between the shells.

· Auger electrons are formed as a consequence of electron capture as the X-rays, formed as explained above, transfer their energy to electrons in the upper electron shells and these electrons are emitted. These Auger electrons are mono-energetic and their energies are fairly low, at most a few tens of electron volts.

INTERNAL TRANSITION - GAMMA DECAY AND INTERNAL CONVERSION

As mentioned, beta and alpha decays in most cases do not lead only to the ground state of the daughter but also to its excited states. These excitations are relaxed by two ways:

· gamma decay

· internal conversion

These two processes together are called internal transition (IT).

Gamma decay

In gamma decay, the daughter nuclide releases its excitation energy by emitting electromagnetic gamma radiation (γ). When, for example, ^{232}Th decays (Figure V.19) by alpha mode to ^{228}Ra only a fraction (76.8%) of alpha particles receive the maximum energy of 4.011 MeV, the rest being decayed by emission of 3.952 MeV alpha particles (23.0%) and 3.828 MeV alpha particles (0.2%). These latter alpha energies are a cause of decay to excited states of ^{228}Ra. The energies of gamma rays emitted in the de-excitation can be calculated from the energy differences of the alpha particles, for example, 4.011 MeV - 3.952 MeV = 0.059 MeV. There are also gamma transitions from one excitation state to another, for example, 0.126 MeV gamma rays are emitted from this kind of transition in case of ^{232}Th decay.

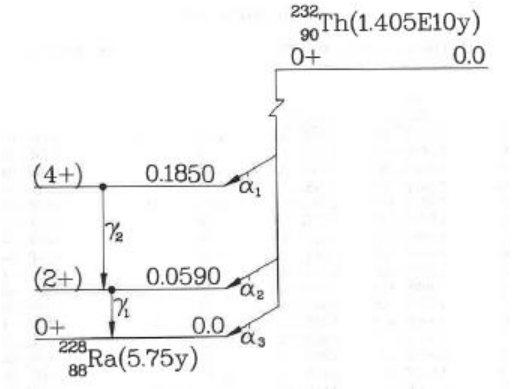

Figure V.19. Decay scheme of ^{232}Th (Radionuclide Transformations, Annals of the ICRP, ICRP Publication 38, Pergamon Press, 1983).

Typically, gamma decays take place very rapidly, in less than 10^{-12} seconds, i.e. practically at the same time as the alpha and beta emissions. Sometimes, the gamma decays are delayed and if their life-times are so long that they can be measured, the excited states are considered as individual nuclides, isomeric states of the daughter. These nuclides are marked with "m" with the mass number. The life-times for the isomers are expressed as half-lives since their rate of decay behaves in an identical manner with other radionuclides. For example, when ^{137}Cs decays to stable ^{137}Ba, there is in between an isomer of barium ^{137m}Ba which has a half-life of 2.6 minutes. The half-lives of isomeric radionuclides vary in a wide range and the longest half-life of 900 years is known for ^{192m}Ir.

As mentioned already, the gamma decays occur from excited states to ground state or between the excited states. Since all these states have defined energy levels, the gamma rays have defined energies. Thus, also the spectrum obtained is a line spectrum. Figure V.20 shows the decay scheme and the gamma spectrum of ^{241}Am. As seen, all three gamma transitions are seen in the spectrum. The heights of the peaks depend on the intensity of each transition. Intensities are the fractions of each transitions from total decay events. For example, the intensities of the three gamma transition in the case of ^{198}Au are 96% for γ_1 (412 keV), 0.8% for γ_2 (676 keV) and 0.2% for γ_3 (1088 keV). The sum of the intensities is not 100% because part of de-excitations takes place by internal conversion, as described later.

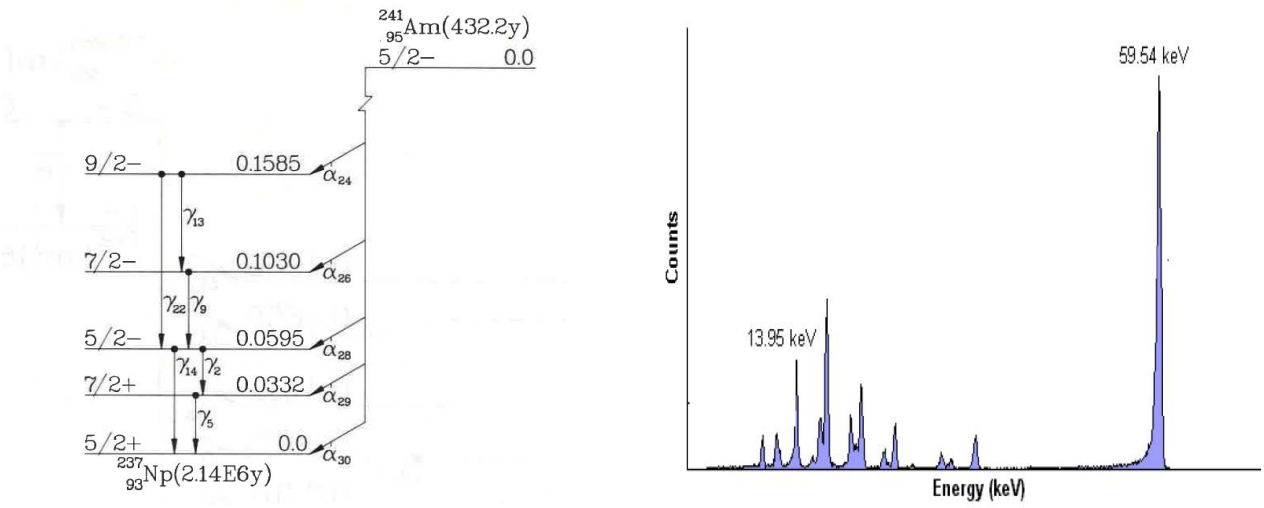

Figure V.20. Decay scheme (Radionuclide Transformations, Annals of the ICRP, ICRP Publication 38, Pergamon Press, 1983) and gamma spectrum ^{241}Am (http://www.amptek.com/products/x-123-cdte-complete-x-ray-gamma-ray-spectrometer-with-cdte-detector/).

Gamma-emitting radionuclides are not only constituted of the beta and alpha-decaying radionuclides with excitation states of the daughter. They can also be obtained by activation of a nuclei by electromagnetic and particles bombardments, for example with neutrons. In fission, gamma rays are also emitted as primary emission, i.e. instantly during the fission process.

The recoil energy of the daughter in gamma decay is very small, being only less than 0.1% of the energy of the gamma ray. Thus, practically all decay energy goes to gamma radiation.

Internal conversion

As mentioned above, a competing process to gamma decay is internal conversion (IC). In it, excitation energy is not released by gamma ray emission but transferred to a shell electron, which is then emitted. The phenomenon is analogous to formation of Auger electrons, which are emitted by the action of energy released from electron transitions from upper to lower shells. The electrons emitted in internal transitions are called conversion electrons. They are monoenergetic and their energy is the excitation energy minus the binding energy of the emitted electron. Most conversion electrons come from the inner K-shell since it has a strongest interaction with the nucleus. For example, in the decay of ^{137m}Ba the conversion electrons come five times more from K shell than from the L shell. In a continuous beta spectrum, the conversion electrons are seen as peaks. An example is given in Figure V.21 where the beta spectrum of ^{137}Cs is shown. The conversion electrons, from both K and L shells, are seen as individual peaks at higher energies.

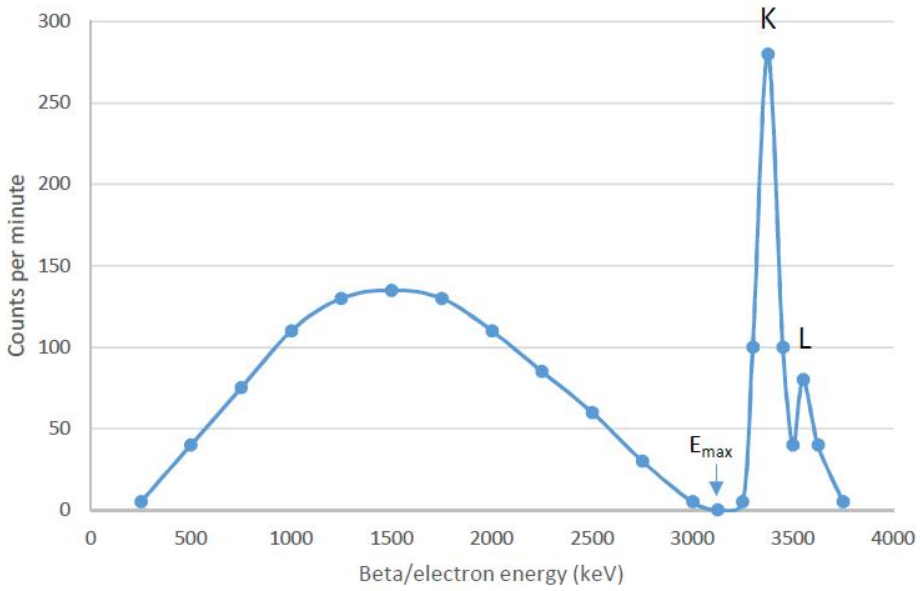

Figure V.21. Beta and conversion electron spectrum of ^{137}Cs.

The ratio of the intensity of internal conversion to that of gamma decay is called conversion coefficient (a_{IC})

$$a_{IC} = I_{IC}/I_g \qquad [V.XIII]$$

Figure V.22 shows the decay scheme of ^{137}Cs. 94.6% of the beta transitions go through the 662 keV excitation state of ^{137}Ba. This excitation state relaxes by emission of 662 keV gamma rays with an intensity of 89.8% (85.1% intensity of all decay events) and the rest 10.2% (9.6%) by internal conversion. Thus the conversion coefficient is 89.8/10.2 = 0.11.

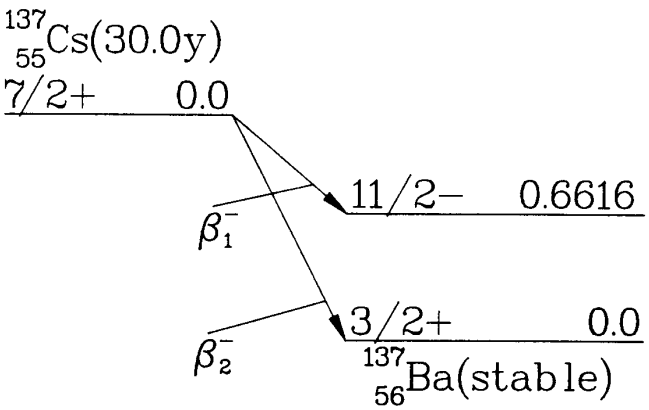

Figure V.22. Decay scheme of ^{137}Cs (Radionuclide Transformations, Annals of the ICRP, ICRP Publication 38, Pergamon Press, 1983).

PARTICLES AND RAYS IN RADIOACTIVE DECAY PROCESSES

Table V.III. Primary and secondary particles and rays present in radioactive decay processes.

Particle/quant	*Symbol*	*Mass (amu)*	*Charge*
proton	p	1.007277	+1
neutron	n	1.008665	0
electron, negatron, beta particle	e, e^-, β^-	0.00054859	-1
positron	β^+	0.00054859	+1
neutrino	υ	~0	0
antineutrino	$\bar{u}$	~0	0
gamma ray	γ		
X-ray	rtg, X		

VI RATE OF RADIOACTIVE DECAY

Content

Decay law – activity - decay rate

Half-life

Activity unit

Specific activity - activity concentration

The relation between the activity and the mass

Determination of half-lives

Activity equilibria of consecutive decays

- Secular equilibrium
- Transient equilibrium
- No-equilibrium
- Equilibria in natural decay chains

Decay law – activity - decay rate

The rate of radioactive decay is a characteristic feature for each radionuclide. Decay rate, also called activity, is the number of nuclear transformations (decays) (dN) at a defined time difference (unit time) (dt) and it is referred to as A (activity):

$$A = \left| - \, dN/dt \, \right| \qquad \text{[VI.I]}$$

Radioactive decay is a stochastic phenomenon and we cannot know when a single nucleus will decay or what is the exact number of decays in unit time. If a fairly large number of radioactive nuclei are considered we can, however, know what fraction of nuclei will probably decay in unit time. This fraction, the probability of radioactive decay events, is characteristic for each radionuclide and it is called decay constant (λ). If, for example, the decay constant is 0.0001 s^{-1} it means that among 100000 radioactive nuclei probably 10 nuclei will decay in one second and accordingly among 1000000 nuclei probably 100 nuclei. Thus radioactive decay rate is directly proportional to the number of radioactive nuclei.

$$A = \left| - dN/dt \right| = \lambda \times N \qquad \text{[VI.II]}$$

where N is the number of radioactive nuclei.

In the following we will see what is the number of radioactive nuclei (N) at defined time point (t) when their initial number (N_0) is known at time point t_0. From the equation VI.II we get $\frac{dN}{N} = -\lambda \times dt$ and its integration $\int \frac{dN}{N} = \int -\lambda \times dt$ yields $\ln N = -\lambda \times t + C$. When considering time t = 0, when $N = N_0$, the constant C gets a value $\ln N_0$ and inserting this into the equation $\ln N = -\lambda \times t + C$ yields $\ln N - \ln N_0 = -\lambda \times t$ and further $\ln \frac{N}{N_0} = -\lambda \times t$. Taking antilogarithm from both sides yields $\frac{N}{N_0} = e^{-\lambda \times t}$ and further

$$N = N_0 \times e^{-\lambda \times t} \qquad \text{[VI.III]},$$

which equation answers the question what is the number of radioactive nuclei (N) at certain time point (t) when we know the initial number on nuclei (N_0) at time point t_0. Thus, to calculate this only the value of the decay constant (λ) is to be known.

The number of radioactive nuclei is not usually known and their number is also difficult to directly determine. Usually we are, however, more interested in development of activities with time. As seen from Equation VI.II the activity is directly proportional to the number of decaying nuclei, thus we can transform Equation VI.III to calculate activity (A) at a time point (t) just by replacing N with A:

$$A = A_0 \times e^{-\lambda \times t} \qquad \text{[VI.IV]}$$

Half-life

Decay constants are known for all radionuclides and they are tabulated in various textbooks and databases. They are, however, not used in calculations of activities but instead half-lives ($t_{½}$) are used for this purpose. Half-life is defined as the time in which half of the initial radioactive nuclei have decayed. Since the activity is directly proportional to the number of radioactive nuclei this

means that also activity decreases to half within the time of half-life. In the following, the relation between the decay constant and the half-life will be shown. In addition, an equation by which activities can be calculated at desired time points using half-lives will be derived.

Do not use upper-case T½ for half-life, use lower lower-case t½. *T refers to temperature, t to time.*

We consider a time difference equal to a half-life t = t½, during which time the number of radioactive nuclei decays to half, i.e. $N = N_0/2$. Inserting $t = t_{1/2}$ and N = N0/2 to Equation VI.III $N = N_0 \times e^{-\lambda t}$ yields $N_0/2 = N_0 \times e^{-\lambda \times t_{1/2}}$ and further $e^{\lambda \times t_{1/2}} = 2$. Taking logarithms from both sides gives $\lambda \times t_{1/2} = \ln 2$ and further $\lambda = \frac{\ln 2}{t_{1/2}}$. Replacing λ in equations $N = N_0 \times e^{-\lambda t}$, $A = A_0 \times e^{-\lambda t}$ with ln2/t½ yields

$$N = N_0 \times 2^{-\frac{t}{t_{1/2}}} \qquad \text{[VI.V]} \quad \text{and} \qquad A = A_0 \times 2^{-\frac{t}{t_{1/2}}} \qquad \text{[VI.VI]}$$

With the latter equation we can calculate activities using half-lives at any time points when we know the initial activity. When we want to calculate the initial activity at an earlier time point we use the inverse equation

$$A_0 = A \times 2^{\frac{t}{t_{1/2}}} \qquad \text{[VI.VII]}$$

Activity unit

The official SI unit of activity is Becquerel (Bq) and it means one decay in SI unit time, i.e. one second:

$$1 \text{ Bq} = 1 \text{ decay s}^{-1} \qquad \text{[VI.VIII]}$$

Earlier Curie (Ci) was used as the activity unit. One Curie is 3.7×10^{10} decays in second and thus

$$1 \text{ Ci} = 3.7 \times 10^{10} \text{ s}^{-1} = 3.7 \times 10^{10} \text{ Bq} \qquad \text{[VI.IX]}$$

Curie unit was derived as the number of decays taking place in one gram of ^{226}Ra in one second using half-life of 1580 years (today it is known to be 1600 years).

Sometimes activities are expressed as a dps unit, meaning disintegrations per second which are equal to activities presented as Bequerels. In some instances, for example in liquid scintillation counting, activity is also presented as dpm units (disintegrations per minute). One dpm is 1/60 dps or 16.7 mBq.

Specific activity - activity concentration

Specific activity is often used as a synonym to activity concentration, but strictly speaking they have different meanings. Specific activity refers to concentration of a radionuclide with respect to the total amount of the same element as the radionuclide. Thus, specific activity is its concentration in a unit mass or mole of the same element, for example, 5 kBq of ^{137}Cs per 1 g of Cs or 0.038 kBq of ^{137}Cs per 1 mole of Cs.

Activity concentration in turn is the concentration of a radionuclide in a unit mass or volume of any matter in question, for example, 5 kBq of ^{137}Cs per 1 kg of soil or 5 kBq of ^{137}Cs per 1 litre of water.

The relation between the activity and the mass

Conversion of activities to masses or vice versa is based on the radioactive decay law

$$A = \lambda \times N \qquad \text{[VI.X]}$$

which shows the direct dependence of the activity on the number of decaying nuclei. Replacing λ by $\ln 2/t_{1/2}$ and N by $(m/M)\times N_A$ (where m is the mass in grams, M the molar mass of the element and N_A the Avogadro number) yields

$$A = \frac{\ln 2 \cdot m \cdot N_A}{t_{1/2} \cdot M} \qquad \text{[VI.XI]}$$

or the other way round

$$m = \frac{A' \cdot M' \cdot t_{1/2}}{\ln 2' \cdot N_A} \qquad \text{[VI.XII]}$$

which can be used to convert activities to masses or vice versa.

Determination of half-lives

The determination of half-lives can be accomplished in two ways:

1) For radionuclides decaying with such a fast rate that we can observe the decrease in a reasonable time the half-lives can be determined from their activities as a function of time as shown below in Fig. VI.1.

When representing graphically the equation $A = A_0 \cdot 2^{-\frac{t}{t_{1/2}}}$ we get an exponential curve (Figure VI.1, left side). Taking logarithms from both sides yields the equation $\ln A = -\frac{\ln 2}{t_{1/2}} \cdot t + \ln A_0$, the graphical representation of which is line with a slope of $-\frac{\ln 2}{t_{1/2}}$ and the y-axis intersection is $\ln A_0$, i.e. activity at time t_0 (Figure VI.1, right side). The half-life is obtained by fitting a line to the logarithms of observed activity values and calculating the half-life from the slope. If, for example, in Figure VI.1 time were in years, the half-life of the nuclide would result by solving the equation $-0.693 = -\frac{\ln 2}{t_{1/2}}$ into 1 year.

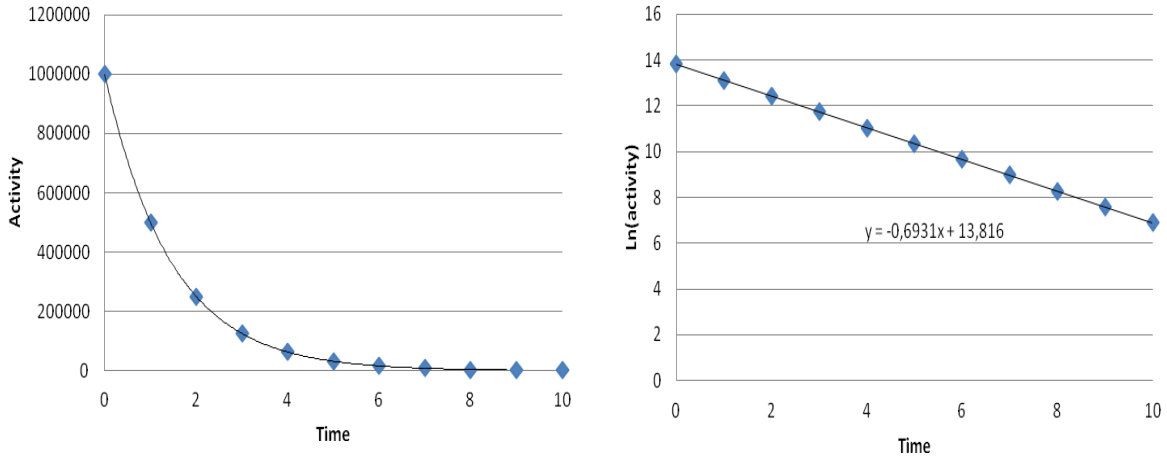

Figure VI.1. Activity (A) as a function of time (t). Left side presents activity in linear scale and right side in logarithmic scale.

The method described above in Fig. VI.1 can also be used to determine half-lives of two coexisting radionuclides supposing that they differ enough from each other. Figure VI.2 shows the total activity curve of two radionuclides as a function of time both in a linear and a logarithmic activity scale. In the first phase, when there are still both radionuclides present, the logarithmic curve shape resembles an exponential one. As the shorter-lived radionuclide has decayed the curve turns into a line. This line represents the decay of the longer-lived radionuclide and its half-life can be calculated from the slope of this line. To calculate the half-life of the shorter-lived radionuclide the line is extrapolated to time point zero and the extrapolated activity values of the line are subtracted from total activity curve. This yields another line representing the decay of the shorter-lived radionuclide for which the half-life is calculated from its slope.

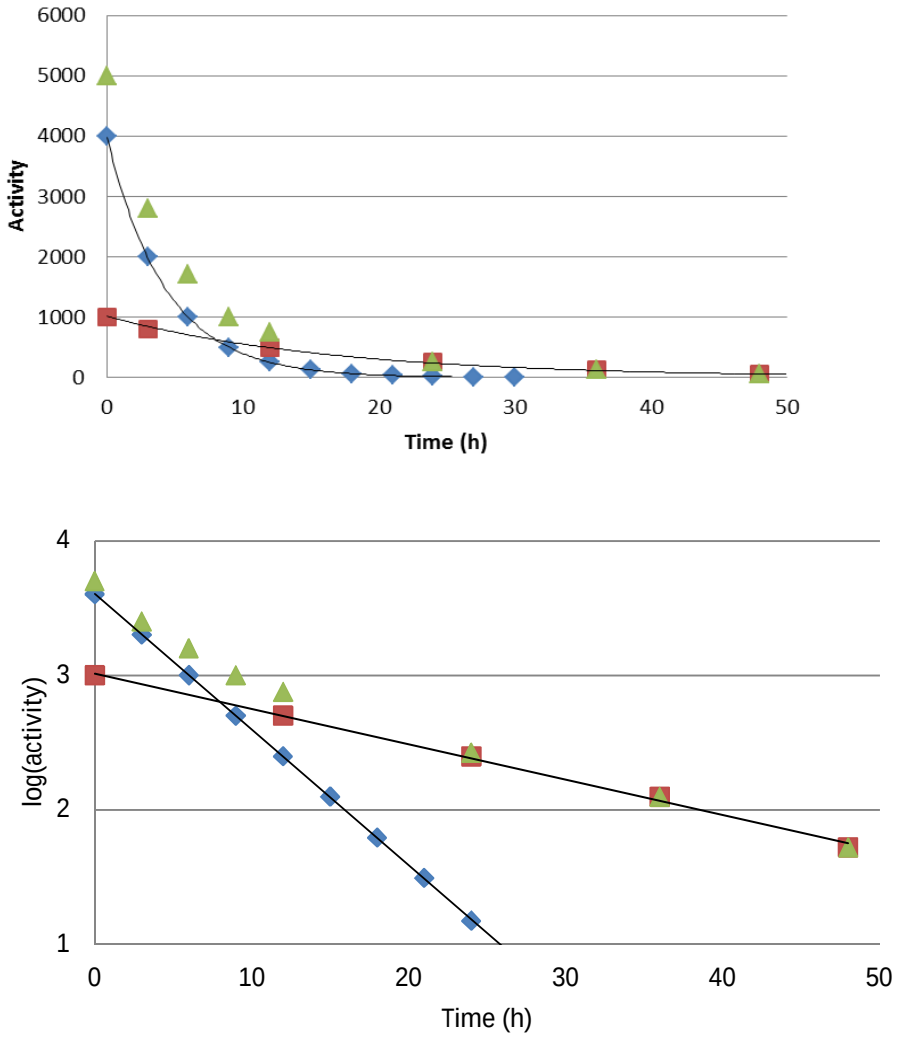

Figure VI.2. Individual and total activities of two coexisting radionuclides as a function of time. Top: activity in linear scale. Bottom: activity in logarithmic scale. Diamond (t): Radionuclide with a half-life of 3 hours. Square (n): radionuclide with a half-life of 12 hours. Triangle (p): total activity.

2) For long-lived radionuclides for which the activity decreases so slowly that we cannot observe its decrease the half-life is determined by measuring both the activity and the mass of the radionuclide and calculating half-life from the equation $t_{1/2} = \frac{\ln 2 \cdot m \cdot N_A}{A \cdot M}$. For example, when the half-life is 10^6 years the activity decreases by 0.00007% in one year. Small differences in activity like this cannot be measured. To determine the half-life of long-lived radionuclides we need to measure the mass (m) of the radionuclide and count rate (R) obtained from the activity measurement. In addition, we also need to accurately know the counting efficiency (E) of the measurement system. If, for example, we have 1.27 mg of ^{232}Th and the count rate obtained from its measurement is 2.65 cps and counting efficiency of the measurement system is 51.5% (0.515) the activity of the sample is A= R/E = 2.65 s^{-1}/0.515 = 5.15 Bq. The number of thorium atoms in the sample is $1.27 \cdot 10^{-3}$ g × $6.023 \cdot 10^{23}$ atoms/mole /232.0 g/mole = $3.295 \cdot 10^{18}$. Now the half-life can be calculated from the equation $t_{1/2} = \frac{\ln 2}{A} \times N$ = 0.693 × $3.295 \cdot 10^{18}$ /5.15 s^{-1} = $4.44 \cdot 10^{17}$ s = $1.41 \cdot 10^{10}$ a. This method can also in principle be used to measure half-lives of shorter lived radionuclides but in their case the accurate measurement of the mass may either completely exclude the use of this method or at least results in inaccurate value.

Activity equilibria of consecutive decays

In the following we discuss two consecutive decay processes and their activity equilibria. Equilibrium means that the activities of the parent and daughter nuclides are the same. Consecutive decays and their equilibria are especially important in natural decay chains of uranium and thorium and in beta decays chains following fissions. In these chains there are typically more than two radionuclides present at the same time. Their equilibrium calculations are rather complicated and require computer programs. An example of such calculation is given at the end of the chapter. Here we, however, focus on equilibrium between two radionuclides, the parent nuclide and the daughter nuclide. When considering two consecutive decays the number of the parent nuclei (N_1) depends only on its characteristic decay rate, i.e. decay constant (λ_1). The number of the daughter nuclei (N_2) in turn is dependent both on its own decay rate (λ_2) and on the parent's decay rate (λ_1). The former determines the decay (decrease) of the daughter nuclides while the latter determines the ingrowth from the parent (increase). Thus the number of daughter nuclei is

$$dN_2/dt = \lambda_1 N_1 - \lambda_2 N_2 \qquad \text{[VI.XIII]}$$

The solution of this equation with respect to N_2 is

$$N_2 = [\lambda_1/(\lambda_2 - \lambda_1)]N_1^0\left(e^{-\lambda_1 t} - e^{-\lambda_2 t}\right) + N_2^0 e^{-\lambda_2 t} \qquad \text{[VI.XIV]}$$

where N_1^0 and N_2^0 are the numbers of parent and daughter, respectively, at time point zero (t=0). The first term in the equation presents the number of daughter nuclei due to ingrowth and the decay of ingrown nuclei while the second term represents decay of those daughter nuclei that were present at time point zero. Figure VI.3 gives a graphical presentation of the Eq. VI.XIV for a case where the half-life of the daughter is clearly shorter than that of the parent nuclide, i.e. its shows the ingrowth of the daughter nuclide activity as a function of the number half-lives of the daughter nuclide. Activity is here presented as the percentage of the maximum activity obtainable.

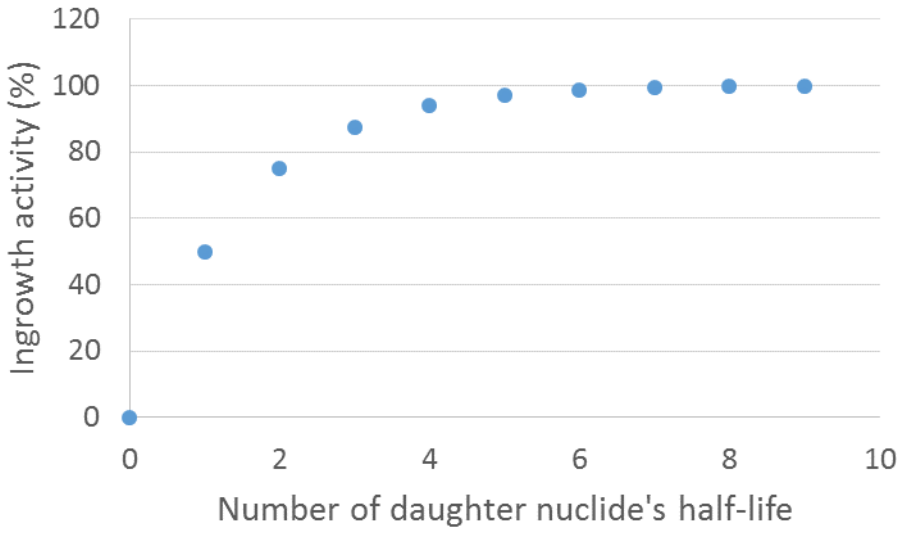

Figure VI.3. Activity (percentage of the maximum activity) of the daughter nuclide as a function of the number of daughter nuclide's half-life. The half-life of the daughter is clearly shorter than that of the parent nuclide. No daughter nuclides present at time 0.

In the following we will examine how the equilibrium develops in cases where we have initially only the parent nuclide and daughter nuclide grows in with time. There are three alternatives depending on the ratio of the half-lives of the two nuclides:

- secular equilibrium, in which the half-life of the parent nuclide is very long and the half-life of the daughter nuclide is considerably shorter than that of the parent
- transient equilibrium, in which the half-life of the parent is so short that we observe decrease in its activity in a reasonable time and the half-life of the daughter nuclide is shorter than that of the parent
- no-equilibrium, in which the half-life of the parent nuclide is shorter than that of the daughter

Secular equilibrium

An example of a secular equilibrium is a case where the parent nuclide is the fission product ^{137}Cs which decays by beta decay process to ^{137m}Ba which in turn decays by internal transition process to stable ^{137}Ba. The half-life of ^{137}Cs is 30 years while the half-life of ^{137}Ba is only 2.6 minutes. Figure VI.4 shows the development of activities in a case when ^{137m}Ba has been chemically separated from its parent ^{137}Cs with $BaSO_4$ precipitation and both ^{137m}Ba-bearing precipitate and remaining solution containing only ^{137}Cs are measured for their ^{137}Cs and ^{137m}Ba activities immediately after chemical separation and measurements are repeated as a function of time. ^{137m}Ba in precipitate decays following its half-life on 2.6 minutes (squares). The activity of ^{137}Cs in the solution phase (diamonds) remains practically constant since observation time (30 min) is extremely short compared to the half-life of ^{137}Cs (30 years). ^{137m}Ba in the solution (triangels) starts immediately after chemical separation to grow in and attains equilibrium with ^{137}Cs in about ten half-lives of the daughter, i.e. half an hour. Since the activities of ^{137m}Ba and ^{137}Cs are the same the total activity (curve 4) is twice the parent nuclide.

Secular does not mean eternal. Looking at a very long-term all secular equilibria are transient. How long-term we need to look depends on the half-life of the parent. For example, if we looked the example describe above for a hundred years period the equilibrium would appear as transient equilibrium. For ^{230}Th ($t_{1/2}$ = 75000 y), for example, the transient equilibrium period with ^{226}Ra would be hundreds of thousands of years.

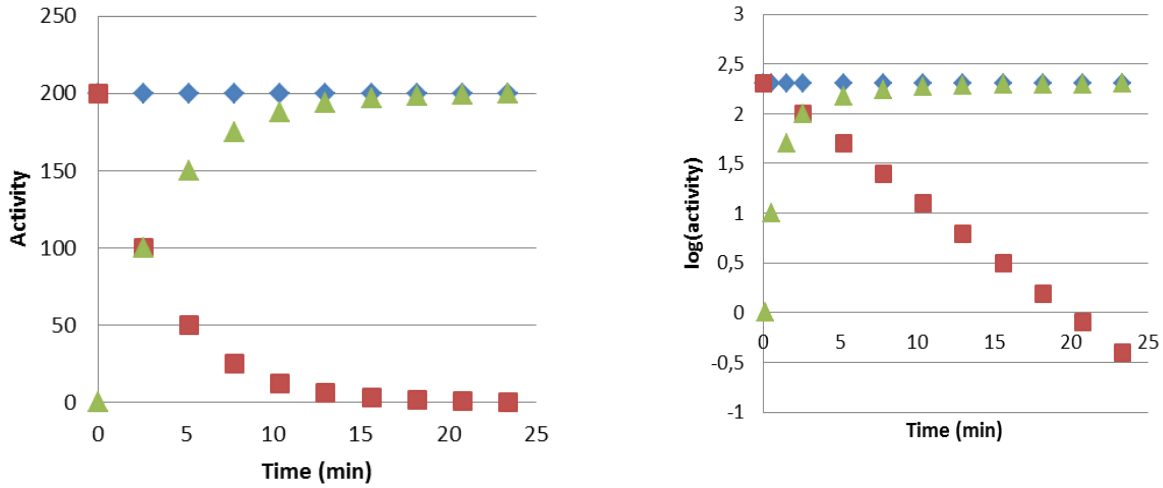

Figure VI.4. Development of a secular radioactive equilibrium in which the half-life of the parent nuclide is very long and the half-life on the daughter nuclide (^{137m}Ba, $t_{½}$ = 2.6 min) is considerably shorter than that of the parent (^{137}Cs, $t_{½}$ = 30 a). Left: activity on linear scale. Right: activity on logarithmic scale. Diamond (t): ^{137}Cs. Square (n) ^{137m}Ba if separated from ^{137}Cs. Triangle (p): ingrowth of ^{137m}Ba after its separation from ^{137}Cs.

Transient equilibrium

An example of transient equilibrium is a beta decay chain where ^{140}Ba decays to ^{140}La and the latter to stable ^{140}Ce.

^{140}Ba (β^-, 12.8 d) à ^{140}La (β^-, 40.2 h) à ^{140}Ce (stable) [VI.XV]

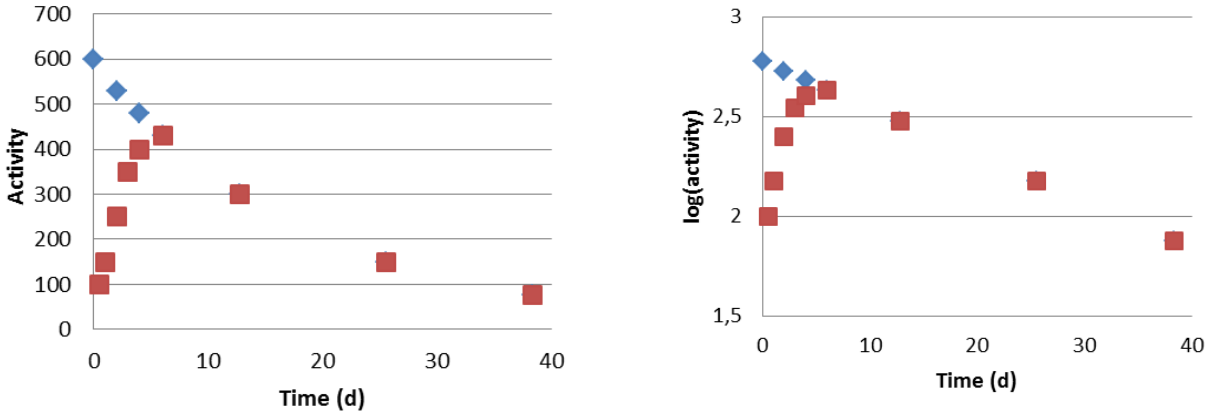

Figure VI.5. Development of a transient radioactive equilibrium in which the half-life of the parent (^{140}La, $t_{½}$ = 40.2 d) is so short that we observe decrease in its activity in a reasonable time and the half-life on the daughter nuclide (^{140}Ba, $t_{½}$ = 12.8 d) is shorter than that of the parent. Left: activity on linear scale. Right: activity on logarithmic scale. Diamond (t): ^{140}La. Square (n): ^{140}Ba.

The transient equilibrium is otherwise identical with the secular equilibrium except that the parent nuclide decays with such a short rate that we observe decrease in its activity in a reasonable time. After attaining the equilibrium in about ten half-lives of the daughter, about two weeks in case of Fig. VI.5, both parent and the daughter decay at the rate of the parent nuclide. Furthermore, after attaining the equilibrium the total activity is twice the activity of the parent nuclide.

No-equilibrium

An example of no-equilibrium case is the alpha decay pair ^{218}Po ($t_{½}$ = 3 min) à ^{214}Pb ($t_{½}$ = 26.8 min), where the half-life of the parent is shorter than that of the daughter. No equilibrium develops since the parent decays before the daughter.

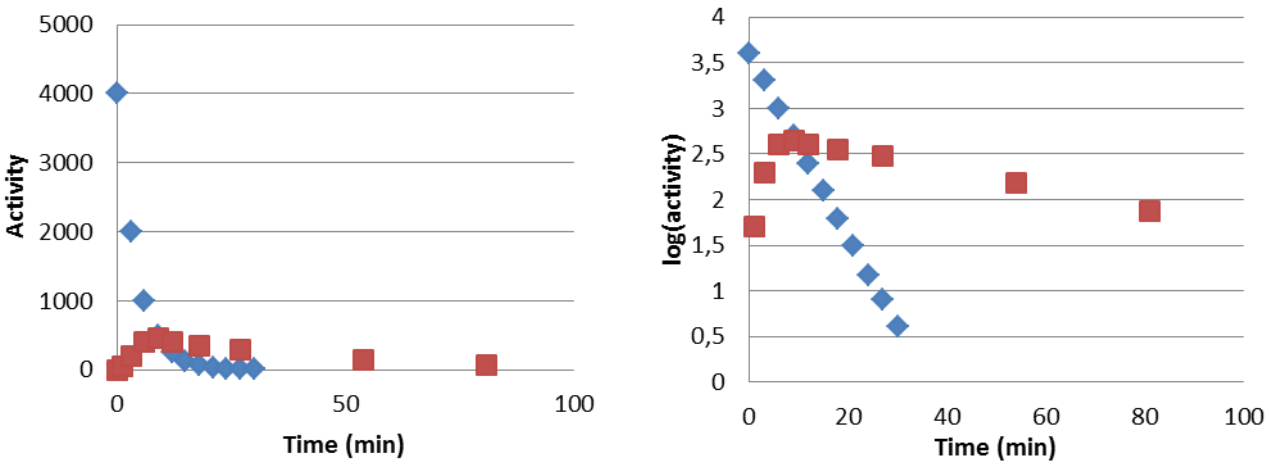

Figure VI.6. Development of activities in case of no radioactive equilibrium, in which the half-life of the parent nuclide (^{218}Po, $t_{½}$ = 3 min) is shorter than that of the daughter (^{214}Pb, $t_{½}$ = 26.8 min). Left: activity on linear scale. Right: activity on logarithmic scale. Diamond (t): ^{218}Po . Square (n): ^{214}Pb.

Equilibria in natural decay chains

In natural uranium and thorium decay chains there are individual pairs in which there would not be any equilibrium if they were present separately. An example of such pairs in the ^{238}U decay chain is ^{234}Pa parent ($t_{½}$ = 6.7 h) and ^{234}U daughter ($t_{½}$ = 245000 y). They are, however, typically in equilibrium since the grandparent of ^{234}Pa, ^{238}U ($t_{½}$ = 4.4 × 10^{9} y), feeds continually new ^{234}Pa and they are in equilibrium with each other. ^{238}U has the longest half-life in the whole chain and

therefore the activities of all subsequent radionuclides in the chain have the same activity as ^{238}U supposing that the system has been closed millions of years. In the nature there are chemical processes, such as dissolution into groundwater, that remove some component of the chains which causes disequilibria in the chains.

In the geosphere in the natural decay chains beginning from ^{238}U, ^{235}U and ^{232}Th the activities of all members are the same in each series, identical with those of ^{238}U, ^{235}U and ^{232}Th, in systems which have been preserved without disturbances long enough. In such case the series is in equilibrium state. If some component of the series is removed, by dissolution for example, the equilibrium is disturbed and a disequilibrium state is created. If for example uranium is dissolved from a primary uranium-bearing mineral by oxidation the remaining radionuclides in the series will be supported by its most long-lived radionuclide which is ^{230}Th in case of ^{238}U series. If the dissolved uranium will then be precipitated somewhere out of the system a new equilibrium will start to develop. The time required to attain the equilibrium is governed by the most long-lived daughter radionuclide in the series, ^{230}Th in case of ^{238}U series. The half-life of ^{230}Th is 75000 years and this time is required to attain 50% of the equilibrium, 150000 years for 75% equilibrium, 225000 years for 87.5% equilibrium and eight half-lives, 600000 years, for 99.6% equilibrium. The disequilibria can be utilized in dating geological events. If for example, the $^{230}Th/^{238}U$ ratio is 0.5 in a uranium mineral we may calculate that this uranium mineral was precipitated 75000 years ago.

To calculate activities of all members in a series manually is a cumbersome task. Computer programs for this purpose have been fortunately developed. One of them is the Decservis-2 program developed at the Laboratory of Radiochemistry, University of Helsinki, Finland. An example of such calculation carried out by Decservis-2 is shown in Figure VI.6. Here, we assume separation of ^{226}Ra (1 Bq) from the system and development of equilibrium between ^{226}Ra and its progeny in 10000 years. We have to assume that the gaseous ^{222}Rn, the daughter of ^{226}Ra, is not escaped from the system. In the first phase, up to about a month, the equilibrium is attained with ^{222}Rn, ^{218}Po, ^{214}Pb, ^{214}Bi and ^{214}Po and the time required for equilibrium is governed by the most long-lived member of these, ^{222}Rn with a half-life of 3.8 days. In the second phase, up to about 200 years, the equilibrium is attained with ^{210}Pb, ^{210}Bi and ^{210}Po and the time required for equilibrium is governed by the most long-lived member of these, ^{210}Pb with a half-life of 22 years. The half-life of ^{226}Ra is 1600 years and decrease in its activity and correspondingly activities of its progeny can be seen after about 1000 years.

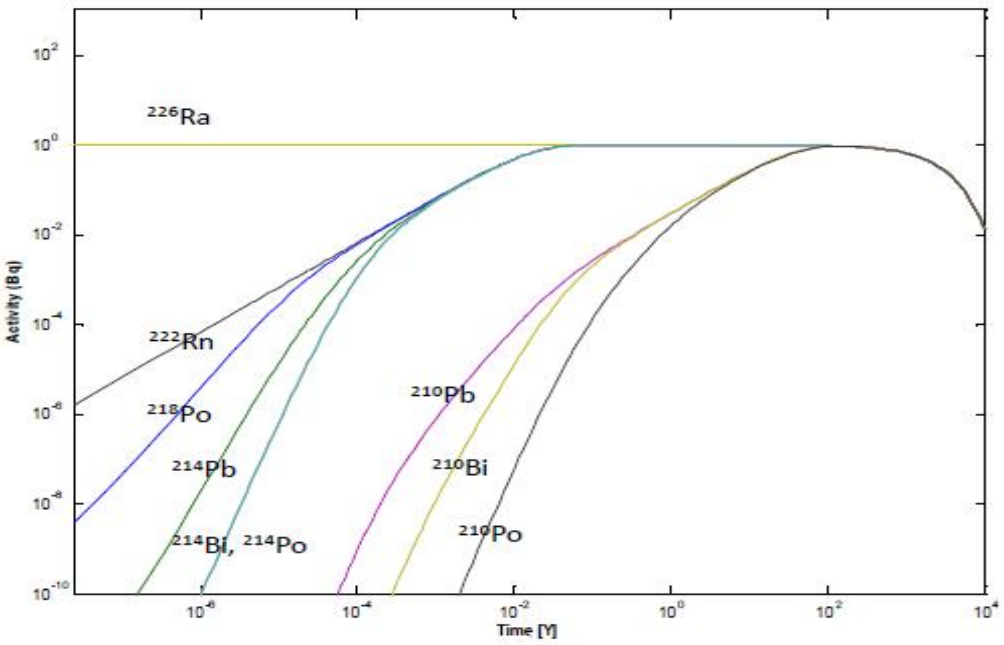

Figure VI.7. Attainment of radioactive equilibrium of ^{226}Ra progeny.

VII INTERACTION OF RADIATION WITH MATTER

Content

Absorption curve and range

Absorption of alpha radiation

Absorption of beta radiation

Absorption of gamma radiation

Summary

This chapter will address the immediate physical effects in medium arising from radiation resulting from radioactive decay and from other ionizing radiation. Later, in chapter XV we discuss on nuclear reactions, which also are a form of radiation interaction process in medium. The main focus in nuclear reactions will be production of radionuclides by intensive, high-energy particle beams from various accelerators and neutron-induced reactions in reactors. The chemical effects, such as the breaking of chemical bonds caused by radiation and formation of new ones, which fall within the scope of the radiation chemistry, are not dealt with.

Physical radiation interactions in the medium are important for many reasons:

- radiation cannot be detected and measured directly, but through the interactions of radiation with detector materials
- they are the primary cause of harmful effects of radiation on humans
- they are the basis for radiation protection measures
- they are the foundation of the radiation exploitation, such as production of radionuclides or autoradiography

The primary interaction mechanisms of radiation with medium are:

- ionization
- scattering from the nucleus or electron shell
- excitation of nuclei or atoms
- formation of electromagnetic radiation (bremsstrahlung, Cherenkov radiation)
- absorption into the nucleus – nuclear reaction

Radiation other than the neutron radiation has a much greater possibility of interacting with the electron cloud than with the nucleus due to the much larger size of the electron cloud compared to nucleus. The removal of electrons from the electron shells of the medium atoms by ionization is the central pattern by which all radiation except neutrons loses their energy when moving in the medium. While the cross section of the ionization by protons or alpha particles can be several hundreds of thousands of barns (for definition, see Chapter XV) it is only under ten for nuclear scattering and still considerably less for nuclear transformations. Radiation, which causes ionization, is called ionizing radiation. The primary result in ionization is the formation of ion pair, electron and positive ion. In most cases, the emitting electrons are so high in energy that they can cause further ionization, secondary ionization, which can be an even a larger portion of the overall ionization than the primary ionization. The radiation energies generated by radioactive decay are typically at least in the keV range. These are high energies compared to energies of atom ionization, which are usually less than 15 eV and those of chemical bonding, which are even lower at 1-5 eV. It is therefore understandable that electrons arising from primary ionization have such a high kinetic energy to cause secondary ionization. Similarly, it is understandable that the primary high energy of a particle or gamma ray does not lose its energy in only one collision with an electron, but several.

Absorption curve and range

The ranges, length of passage, of different types of radiation in different type of media have been studied by determining absorption curves. Different thickness absorption plates are placed between a radioactive point source and a detector and the decrease in count rate in the detector is recorded as a function absorber thickness (Figure VII.1). All other factors than the absorber thickness, affecting the counting efficiency should be equal during the measurements. A graph of the count rate is then drawn as a function of absorber thickness, yielding an absorption curve of the radiation in the used absorber medium (Figure VII.2).

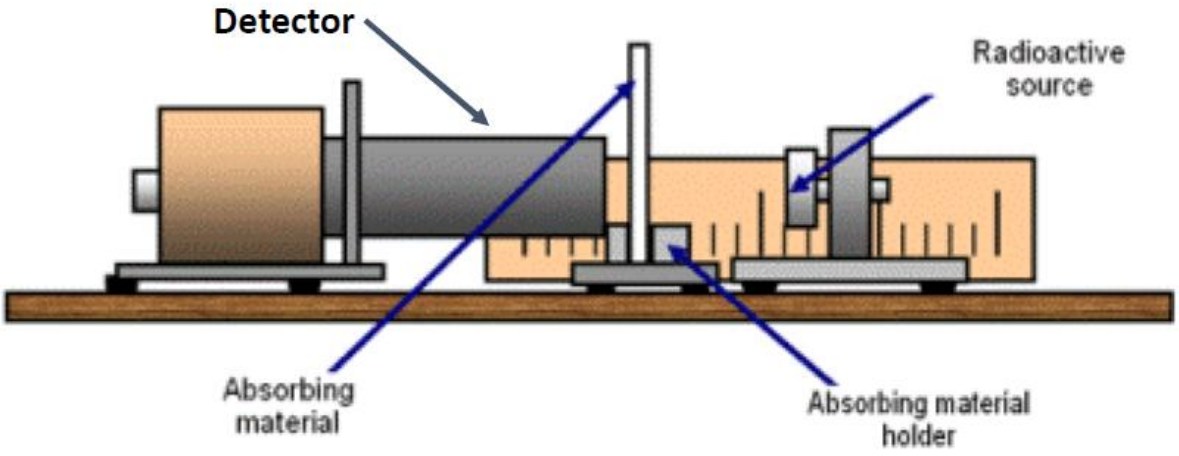

Figure VII.1 Radiation absorption curve determination system (modified from https://tap.iop.org/atoms/radioactivity/511/page_47096.html).

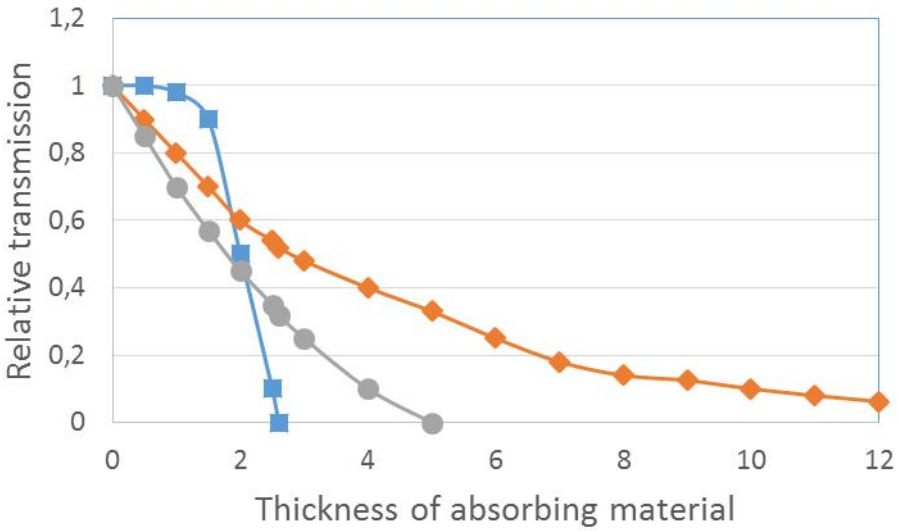

Figure VII.2. Absorption curves of alpha (square), beta (ball) and gamma/neutron radiation (diamond).

The absorption curves can be used to calculate the specific ranges of different radiation types. Range, for example, can be reported as the medium range, *i.e.* absorber thickness, in which the radiation intensity (counting rate) has dropped to half its original. Another way is to represent the maximum range, *i.e.* absorber thickness, wherein the radiation intensity has dropped to zero. Maximum range is a reasonable term for charged particle radiation, since indeed their intensity drops to zero. For gamma radiation and neutrons, as seen from Figure VII.2, however, it is not a suitable term since the decrease of gamma and neutron intensity decreases in an exponential manner

and, in principle, no zero is reached. The range can be expressed in terms of absorption plate thickness, but it is more commonly represented as surface density (F), which is absorption plate thickness (d) multiplied by absorption material density (s), in other words F = d×s. Surface density is used instead of absorber thickness to obtain a quantity which is independent of the nature of the absorber material. When using different types of absorber materials varying amount of electrons are present in the same thickness, less in case of low density material and vice versa. This is essential since the electrons are mainly responsible for radiation absorption. The number of electrons per unit mass (g) is, however, approximately the same for all elements at about 2.9×10^{23}. Thus, when we express the absorber thickness as the surface density the radiation meets the same amount of electrons in its path in media at same surface density values, no matter what is the nature of the material. The most commonly used surface density unit is mg/cm^2.

Absorption of alpha radiation

In comparison to other radiation types from radioactive decay, alpha radiation is characterized by the fact that the alpha particles are large and their energies are always high, usually between 4-9 MeV. Due to this, alpha particles do not readily scatter from medium atoms, rather their range is short and path is direct (Figure VII.3). For example, the 4.8 MeV alpha particles of ^{226}Ra have a maximum range of 3.3 cm in air and only 0.0033 cm in water. Alpha radiation causes very intense ionization, for example, when traveling in air a 7.7 MeV alpha particle causes 3200 ion pairs/cm. The ion pairs generated in unit length is called specific ionization. Figure VII.4 shows specific ionization of alpha radiation (and of protons and electrons) as a function of particle energy. First specific ionization somewhat increases, but at energies higher than 1 MeV specific ionization decreases systematically. The specific ionization of alpha particles is clearly higher than that of protons, let alone electrons. This is due to their larger size and higher electric charge. Most of the electrons produced in primary ionization have a high energy, on average 100 eV, but some even higher than 3 keV and thus they cause strong secondary ionization.

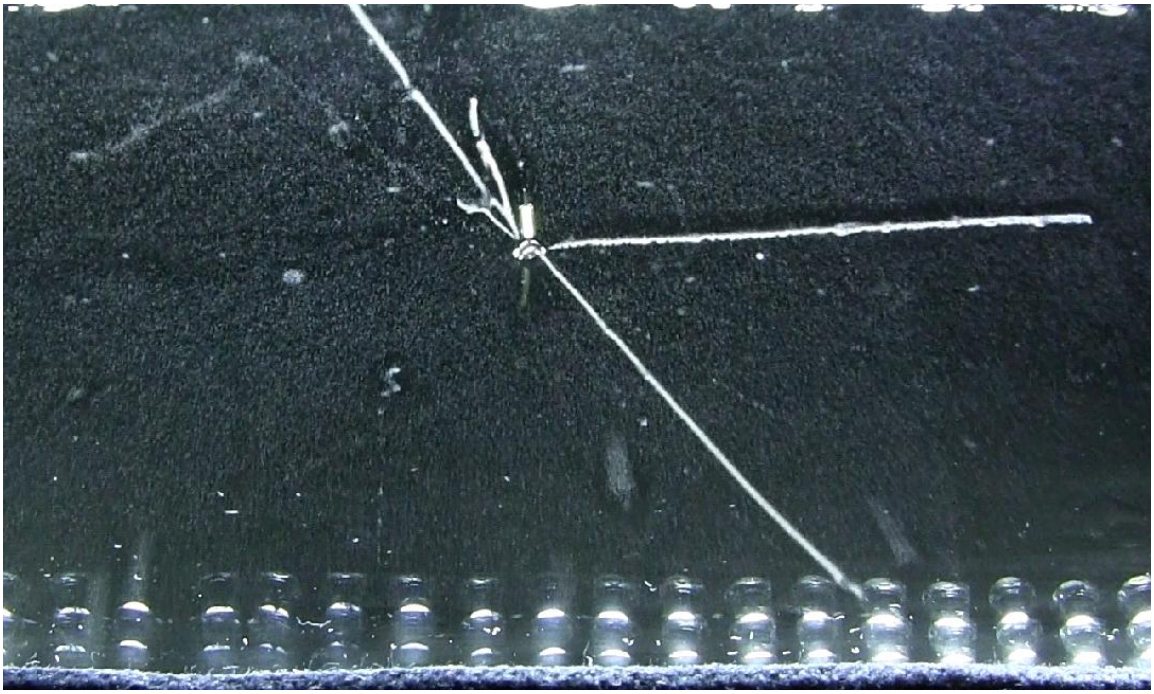

Figure VII.3. Alpha radiation tracks of a ^{226}Ra source imaged in a cloud chamber. (https://simple.wikipedia.org/wiki/Cloud_chamber).

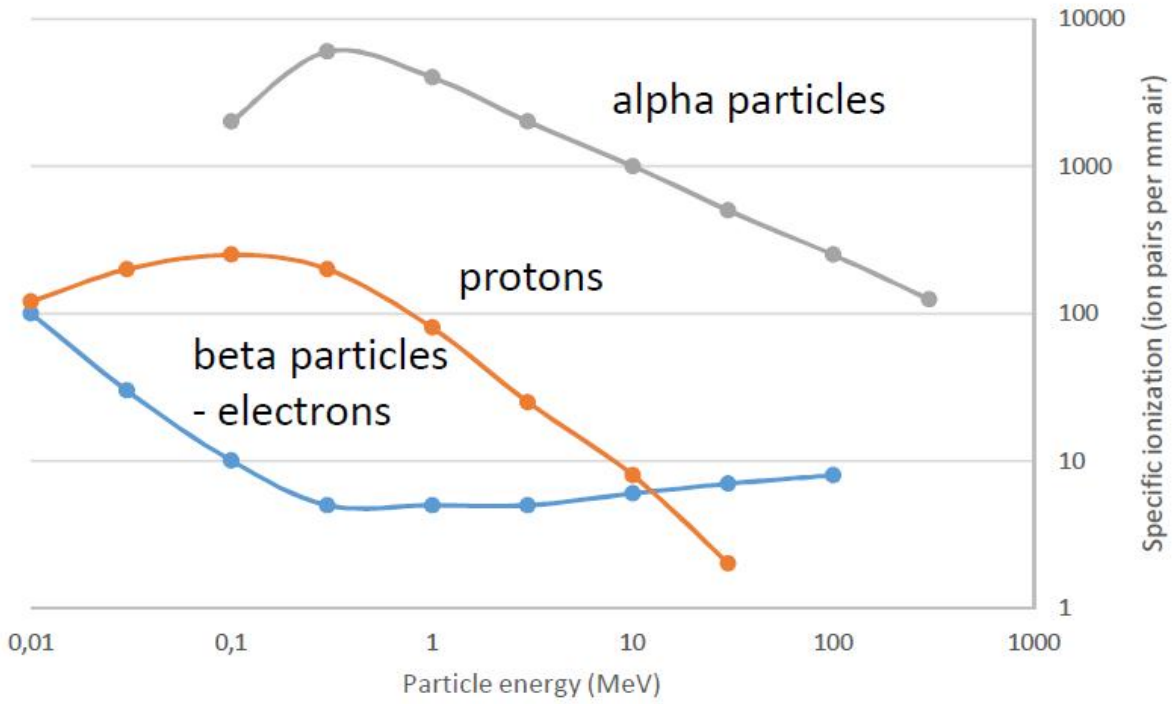

Figure VII.4. The specific ionization of alpha particles, protons, and electrons (ion pair/mm) in the air as a function of particle energy.

Specific ionization is not uniform along the entire path traveled by the alpha particle. Ionization increases as the particle slows and reaches its maximum before it completely loses its energy and its positive charge (Figure VII.5).

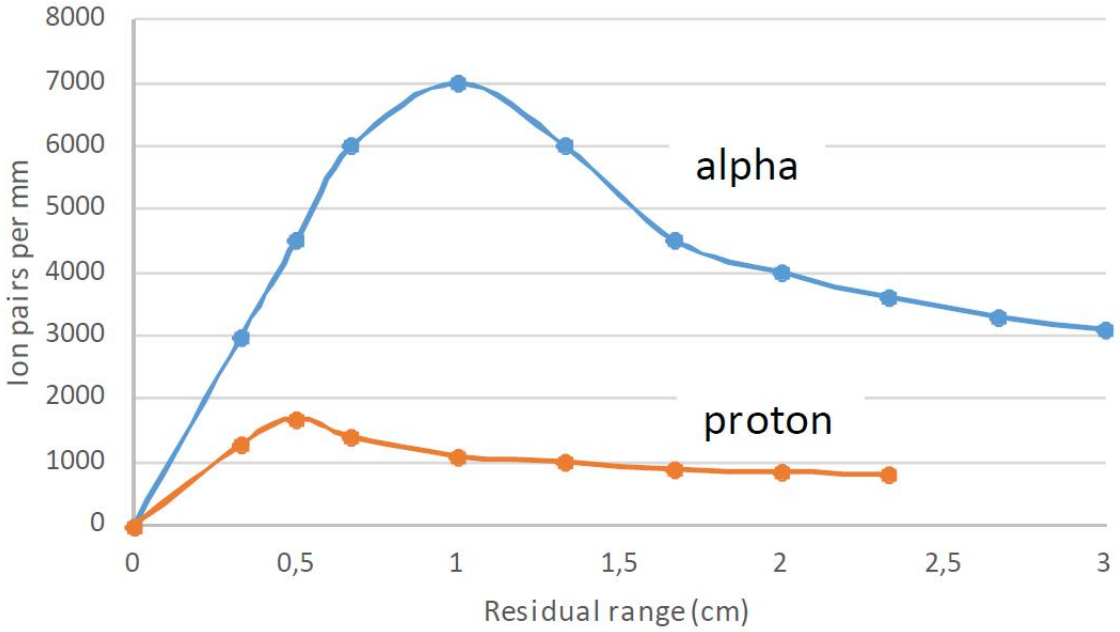

Figure VII.5. Specific ionization of alpha particles and protons as a function of their residual range.

Absorption of beta radiation

In principle, beta radiation loses energy by the same processes as alpha radiation: ionization and excitation of medium atoms, but the essential difference is that the beta radiation range is much larger than that of alpha radiation and the track is not straightforward but quite winding. This is due to the fact that the beta particle size is much smaller than the alpha particle and hence, the probability of collision per unit length is lower. The small mass of the beta particle also means that the velocities are much greater than those of alpha particles. When the energies of the particles are the same, their velocities are proportional to their masses in accordance to the formula $E = m \times v^2$. As noted earlier, the maximum range of the 4.8 MeV alpha radiation is 3.3 cm in the air and only 0.0033 cm in water. Electrons with equivalent energy have maximum ranges that are far greater, *e.g.* 17 meters in the air. For alpha radiation, each particle travels approximately the same distance. In beta radiation, however, the track varies very much from one particle to another. The attenuation of a beta particle flux means that as the beta radiation flux travels further in an absorbing medium it loses a growing number of its individual particles.

Since the size and mass of beta particles and electrons in atoms are identical, the beta particles may lose a large fraction of their kinetic energy in individual collisions. In addition, their travel direction may change a lot, scattering can even occur in the completely opposite direction. The relative energy loss and change of path depend on both beta particle energy and the collision angle. The two identical particles, the beta particle and the shell electron, behave like billiard balls when one hits the other. The smaller the collision angle the greater is the change in residual path. As the beta particle hits the electron directly to its middle point, the ionized electron travels to the initial direction of the beta particle while the beta particle goes to opposite direction. The relative energy loss is higher for low energy beta particles. High energy beta particle paths are straightforward, for example even at energies of 0.2 MeV the path is straight. Beta particles with high energy will eventually slow down and their paths will become winding. The path of a beta particle beam is also affected by secondary electrons created by ionization, which cannot be distinguished physically from the original β^--particles, emitting in varying directions and causing further ionization. In fact, 70-80% of total ionization is caused by secondary ionization. Since the range of beta radiation is longer than alpha radiation, the specific ionization it causes is of a significantly lower magnitude (Figure VII.4).

Due to the above factors, as well as the fact that the beta particle energies are not constant, but vary between 0 and E_{max}, their absorption curve resemble an exponential curve (Figure VII.2). The absorption curve of a monoenergetic electron beam has a different shape, but if their energy is the same as the maximum energy of beta radiation, both cases yield approximately the same maximum range.

Figure VII.6. shows the five processes involved in beta radiation absorption:

- ionization
- excitation
- bremsstrahlung
- positron annihilation
- Cherenkov radiation

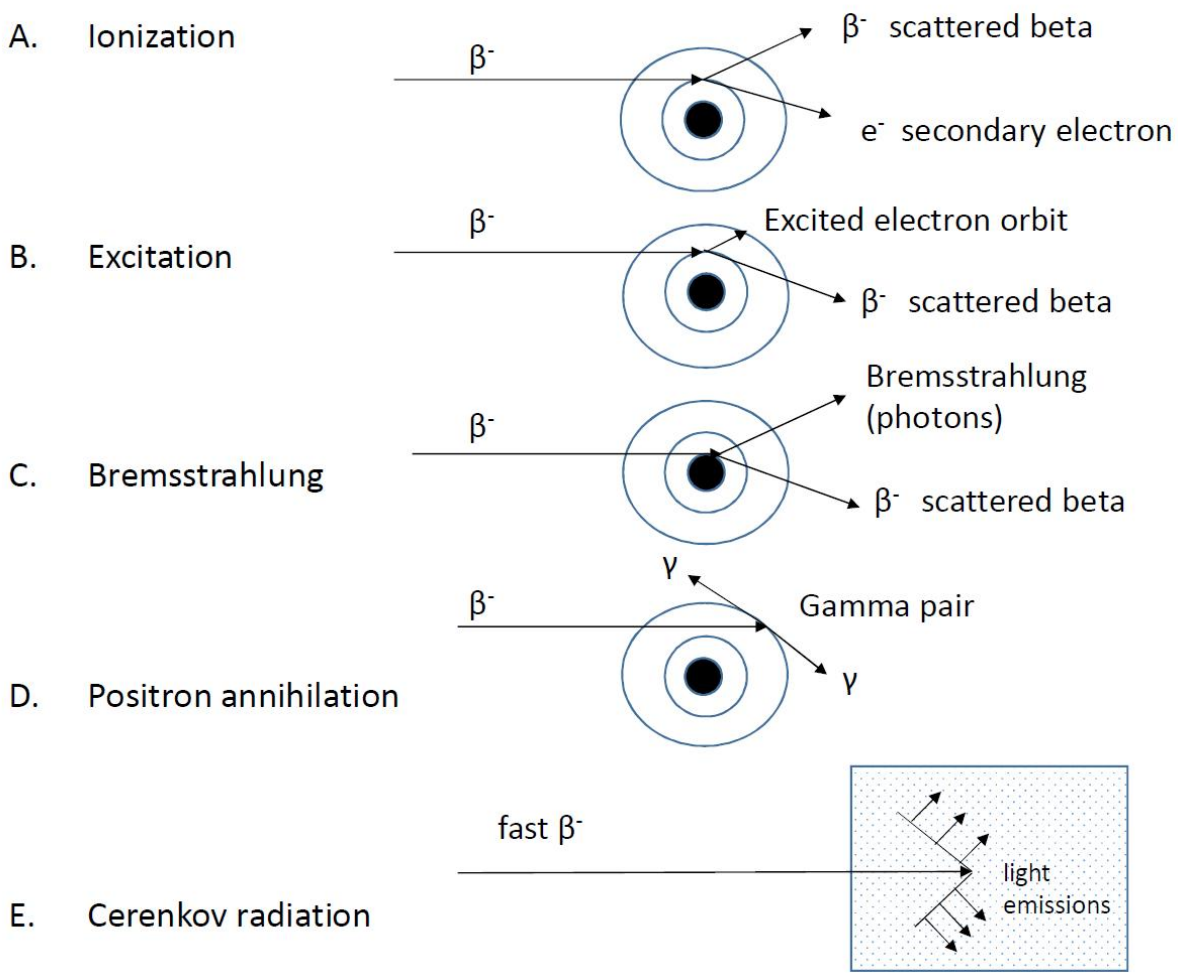

Figure VII.5. Beta radiation absorption processes

As already stated, the beta radiation created in radioactive decay loses its energy in media by essentially two mechanisms: ionizing and excitation. Both processes cause approximately the same fraction of energy loss. In ionization a beta particle collides with a media electron, removes it from its orbit and proceeds with lower energy and to a direction different from that before the collision. In excitation, collision energy of beta particle is not enough for electron removal from an atom, but rather moves the electron to a higher energy level, i.e. yields electron excitation. The result of both processes is the emission of electromagnetic radiation, when an electron hole is filled by an electron from an upper electron shell or when an excitation level relaxes.

Bremsstrahlung is the electromagnetic energy that is generated when an electron interacts with the electric field of an atomic nucleus. The beta particle energy decreases by the amount of energy of the generated photon. The proportion of energy loss of beta radiation caused by bremsstrahlung is, however, very small. For example, only 1% of the energy of the 1 MeV beta particles is absorbed

in aluminum by bremsstrahlung and the remaining almost exclusively by ionization and excitation. At higher beta energies the proportion of energy loss by bremsstrahlung increases. In addition, formation of bremsstrahlung is affected by the atomic number of the radiation absorbing material: the higher it is the more bremsstrahlung. For example, in lead already 10% of the energy of 1 MeV energy beta radiation is absorbed by formation of bremsstrahlung. Since the electromagnetic radiation of bremsstrahlung is noticeably more penetrating than beta radiation it is sensible to use a lower atomic number than lead as a protective material. One centimeter thick Plexiglas, for example, prevents penetration of high energy beta particles without the fundamental formation of bremsstrahlung like with lead.

When determining the absorption curve for beta radiation, a curve in accordance to Figure VII.6 is obtained by drawing an absorption layer thickness as a function of gross count rate measured from a beta source. After a specific absorber thickness is achieved the count rate levels off. This flat proportion is due to both the background radiation and the bremsstrahlung generated in the absorber. When their contribution is deducted from the total curve the beta radiation decrease due to the absorber and its maximum range are obtained (In Fig. VII.6 at 300 mg/cm^2).

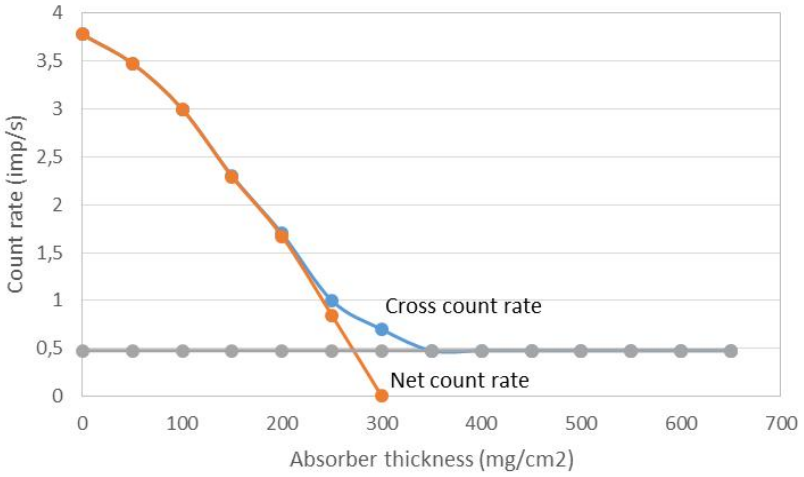

VII.6. Beta radiation absorption curve, background radiation and bremsstrahlung subtraction, as well as maximum range determination.

Positron particles experience the same interactions in the media as b^- particles. When a positron has lost its kinetic energy, it combines with its antiparticle electron and they both disappear, annihilate.

$$e^- + b^+ \rightarrow 2\gamma \qquad [VII.I]$$

The result is the development of two gamma photons emitting in opposite directions, at the same energy of 0.511 MeV. This energy is equivalent to the electron rest mass of 0.000548597 amu: 0.000548597 amu × 931.5 MeV/amu = 0.511 MeV. Upon the filling of the electron shells also X-ray radiation is generated.

Cherenkov radiation is blue light, which is created when a beta particle travels through the medium faster than light. In water the beta particle energy must be at least 263 keV to exceed the speed of light. In the absorption of beta radiation energy the formation of Cherenkov radiation forms only a small fraction, less than 0.1%. Cherenkov radiation may, however, be used to measure high energy (E_{max} >700 keV) beta radiation with liquid scintillation counter: this involves direct measurement of the light intensity of Cherenkov radiation without using liquid scintillator agents.

Absorption of gamma radiation

Since gamma radiation is weightless and uncharged, it rarely interacts in media. That is why it is penetratable and has a long range. Specific ionization of gamma radiation is small compared to beta radiation, let alone alpha radiation. For example, a 1 MeV gamma photon causes only one ion pair per centimeter in the air, compared to many tens by beta radiation and several tens of thousands by alpha radiation.

Gamma rays do not have an exact range. An individual gamma photon can lose its energy partly or completely in one or a few collisions with target atoms. When looking at a large number of gamma photons, or a flux, the attenuation, that is the flux density decrease, occurs exponentially according to the following formula:

$$f = f_0 \cdot e^{-\mu x} \qquad \text{[VII.II]}$$

in which f_0 is the initial flux density, f the flux density, when gamma radiation has traveled through the absorption layer with a thickness of X, and μ is the absorption material's total attenuation coefficient. Since attenuation is exponential, exact numerical range value cannot be obtained with gamma radiation. Instead, for example, each of the absorber material layer thicknesses, in which the flux density is reduced by *e.g.* half or one-tenth of the original, can be used as range values:

$$X_{½} = \ln 2/\mu \quad \text{and} \quad X_{1/10} = \ln 10/\mu \qquad \text{[VII.III]}$$

The total attenuation coefficient contains all of the interaction processes affecting gamma radiation attenuation. Overall, there are five interaction processes:

- coherent scattering
- photoelectric effect
- Compton scattering
- pair formation
- photonuclear reactions

Figure VII.7 shows the first four of these interaction processes. The fifth, photonuclear reaction, which has a very small role in the overall attenuation, is covered in the chapter dealing with nuclear reactions. Coherent scattering, where the media atom absorbs the gamma photon and emits it again, also has little effect in energy loss of gamma radiation. The direction of the photon changes during scattering, but the energy is only reduced by the portion belonging to the recoil energy of the scattering atom. As the mass of the atom is large compared to the relativistic mass of the gamma photon ($E = m \times v^2$), its recoil energy is very small.

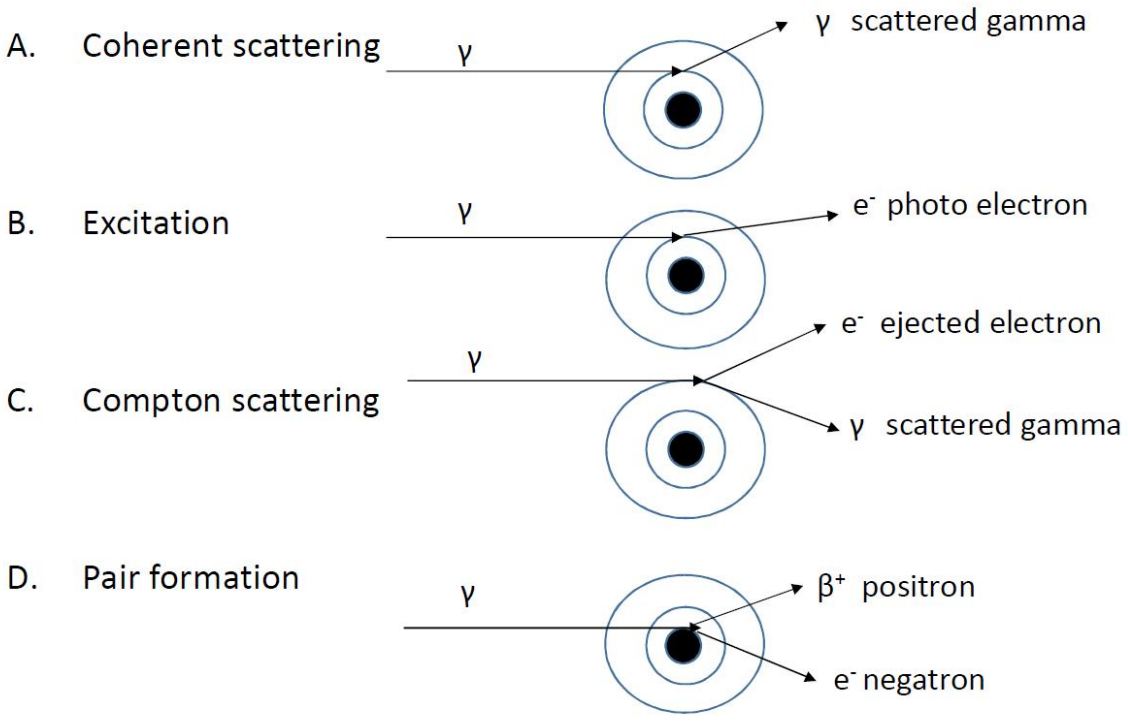

Figure VII.7. Attenuation mechanisms of gamma radiation in media.

The three other interaction processes, photoelectric effect, Compton scattering, and the pair formation, however, all have a large impact on the gamma radiation absorption.

In the photoelectric effect the gamma photon interacts with an individual orbital electron to which all of its energy is transferred and it is emitted from the atom. The kinetic energy of the emitted electron equals the kinetic energy of a gamma photon minus the electron binding energy. Generally, in the photoelectric effect the electron released is from the inner orbit. The filling of the vacant electron hole by higher energy orbit electrons causes formation of X-ray radiation and Auger electrons.

In Compton scattering, only part of the gamma photon energy transfers to the emitting electron. Gamma photon energy decreases by the electron binding energy and kinetic energy of the emitted electron. The scattered gamma photon continues traveling with less energy and change of direction. This scattered photon can still cause new Compton electron emissions.

In pair formation, the gamma photon is transformed by the action of nuclear electric field to an electron-positron pair. The phenomenon is the opposite of positron annihilation. Since the rest masses of electron and positron both correspond to energy of 0.511 MeV, the energy of the gamma photon has to be at least 1.022 MeV in order to form a pair. The rest of the photon energy will be shared equally as kinetic energy of the electron and positron:

$$E_{\gamma} = 1.02\ \text{MeV} + E_{e^-} + E_{e^+} \qquad \text{[VII.IV]}$$

The generated electron is absorbed by the media, as described in beta radiation absorption, and upon loss of its kinetic energy the positron is annihilated.

The fractions of these three interaction mechanisms in gamma radiation attenuation depend on two factors: gamma photon energy and media density (atomic number) (Figure VII.8). The photoelectric effect is prevalent at the lower gamma energies, the Compton scattering at the intermediate energy levels, and pair formation at high gamma energy levels. The increase of the atomic number of the absorber increases the fraction of photoelectric effect, as well as the probability of pair formation. The effect of the atomic number on Compton scattering is opposite, namely the probability decreases as the atomic number increases.

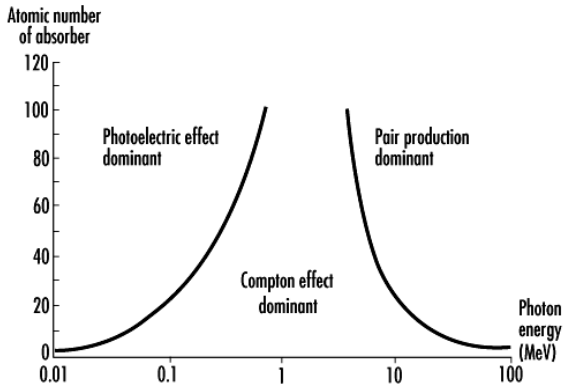

Figure VII.8. The effect of the gamma photon energy and atomic number of the absorber material on the gamma absorption by photoelectric effect, Compton scattering, and pair formation (http://www.ilocis.org/documents/chpt48e.htm).

Summary

Type of radiation	*Specific ionization in air (ion pair/cm)*	*Range in the air*	*Interaction process*
Alfa radiation	tens of thousands	a few centimeters	· ionization · excitation
Beta radiation	tens to hundreds	a few meters	· ionization · excitation · bremsstrahlung formation · positron annihilation · Cherenkov radiation
Gamma radiation	few	exponential attenuation, "range" meters, tens of meters	· coherent scattering · photoelectric effect · Compton scattering · pair formation · photonuclear reaction

VIII MEASUREMENT OF RADIONUCLIDES

Content

Count rate and factors affecting on it

Pulse counting vs. energy spectrometry

Basic components of radiation measurement equipment systems

Energy resolution

Radiation detectors and their suitability for the measurement of various types of radiation

Measurement of radionuclides with mass spectrometry

There are two principal means to measure radionuclide activities: radiometric and mass spectrometric. Radiometric methods are based on detection and measurement of radiation emitted by radionuclides whereas in mass spectrometric methods number of atoms are counted. The results of these methods, activity (A) in case of radiometry and number of radioactive atoms (N) in mass spectrometry, can be can be converted to each other by the radioactive decay law equation $A = N \times \ln 2/t_{½}$ where $t_{½}$ is the half-life of the radionuclide. This chapter mostly discusses the basic principles of radiometric methods and at the end mass spectrometric methods are shortly described.

Detection and measurement of radiation are based on atomic scale interactions of particles and rays, emitted in radioactive decay, with detector materials. There are many types of interaction processes, as was discussed in previous chapter, but radiation detection and measurements make use of two of these processes, ionization and excitation. The electrons obtained in ionization are amplified to observe pulses representing individual decay processes. In the case of excitation light is formed in de-excitation process. These light photons are transformed into electrons which are further amplified to detectable electric pulses. In both cases the pulse rate is proportional to the decay rate and typically the pulse height to the energy of the detected particle or ray. Thus, each pulse obtained from the radiation measurement system represents individual radioactive decay event and the pulse height the energy of detected particle or ray.

Count rate and factors affecting on it

Radiation measurement system counts electric pulses resulting from primary interactions of radiation with the detector material, ionization and excitation. The primary result observed in radiation measurements is the number of pulses (X) which divided by the measurement time (t) gives the count rate (R) which in turn is proportional to the activity (A) of the source measured:

$$X\ (imp) / t\ (s) = R\ (imp/s) = E \bullet A\ (Bq) \qquad [VIII.I]$$

where E is the counting efficiency, i.e. the factor giving the fraction of particles or rays emitted in decay that were transformed into electric pulses in the measurement system. This counting efficiency depends on a number factors, coefficients (c) which except one decrease the count rate with respect to the activity:

$$E = c_{se} \bullet c_{ge} \bullet c_{dt} \bullet c_{bc} \bullet c_{ab} \bullet c_{sa} \qquad [VIII.II]$$

where

- c_{se} is the sensitivity coefficient representing the fraction of particles or rays, hitting the detector, which the detector is able to transform into electric pulses. Sensitivity factor is not only dependent on the detector material but also on type of radiation. All detector materials are more sensitive to alpha and beta radiation than to gamma radiation since large part of gamma radiation penetrates the detector. For example, in gas ionization detectors practically all beta and alpha particles entering the detector are transformed into electric pulses while only a few percent of gamma radiation.

- c_{ge} is the geometry coefficient which is relevant to all types of radiation in the same manner. In radioactive decay particles and rays emit randomly to all directions but only those hitting the detector can be detected. Considering a radioactive point source which is at a distance of *h* from a round-shaped detector with a diameter of *r* only those particles or rays emitted in the space angle *G* (= 2π (1-sinα)) can be detected (Fig. VIII.1). In this case the geometry factor is:

$$c_{ge} = \frac{G}{4\rho} = \frac{1}{2}(1 - \sin\alpha) = \frac{1}{2}\left(1 - \frac{h}{\sqrt{h^2 + r^2}}\right) \qquad [VIII.III]$$

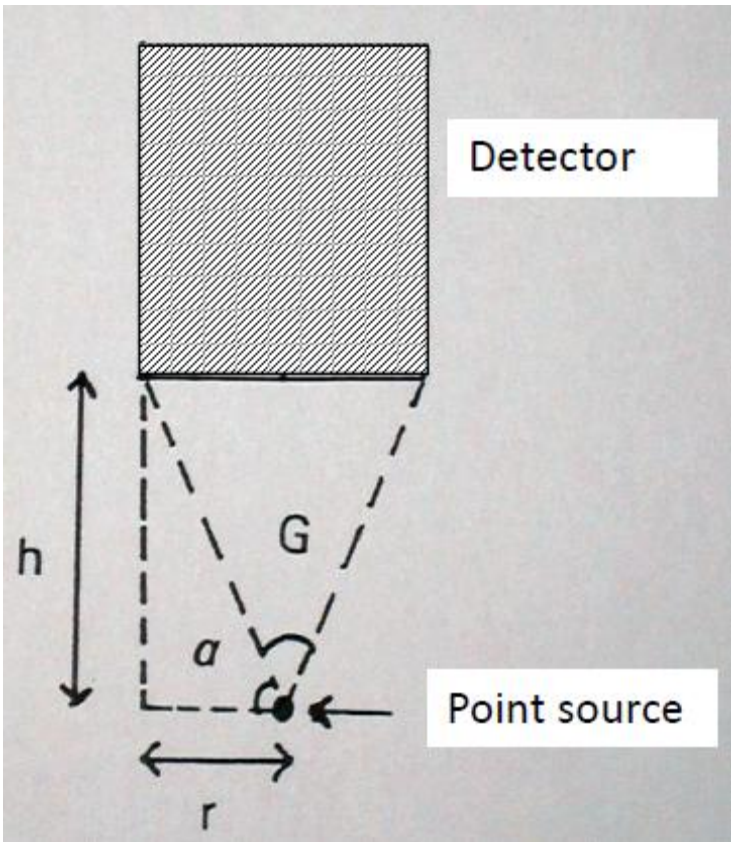

Figure VIII.1. Effect of counting geometry on radiation detection of a point source.

In practice the situation is more complicated since the sources are seldom point sources. As a rule the geometry factor is the higher the closer is the source to the detector. To improve geometry in gamma spectrometry well-type detectors, instead of planar, are used. In these the source is placed inside a hole in the detector and a larger fraction of gamma rays are thus detected. The best geometry in obtained in liquid scintillation counting where the radionuclide is uniformly distributed in liquid scintillation cocktail and in principal all beta and alpha particles can lead to formation of light pulses when exciting scintillator molecules are surrounding them in all directions.

- c_{dt} is the dead-time coefficient. Dead-time is the time when the detector is unable to process a new pulse as the processing of the former pulse is still ongoing. Thus, the dead-time is the minimum time that the detector needs to separate two radiation events and thus to be recorded as two separate pulses. The dead-time is measured from the equation:

$$R_o = R/(1-R\times\tau) \qquad \text{[VIII.IV]}$$

where R is the observed count rate, τ the dead-time and R_o the count rate corrected for dead-time. The dead-time is the higher and the smaller is c_{dt} the higher is the activity of the source measured which is visualized in Figure VIII.2. At high count rates the observed count rate is radically affected by dead-time and therefore should be taken into account.

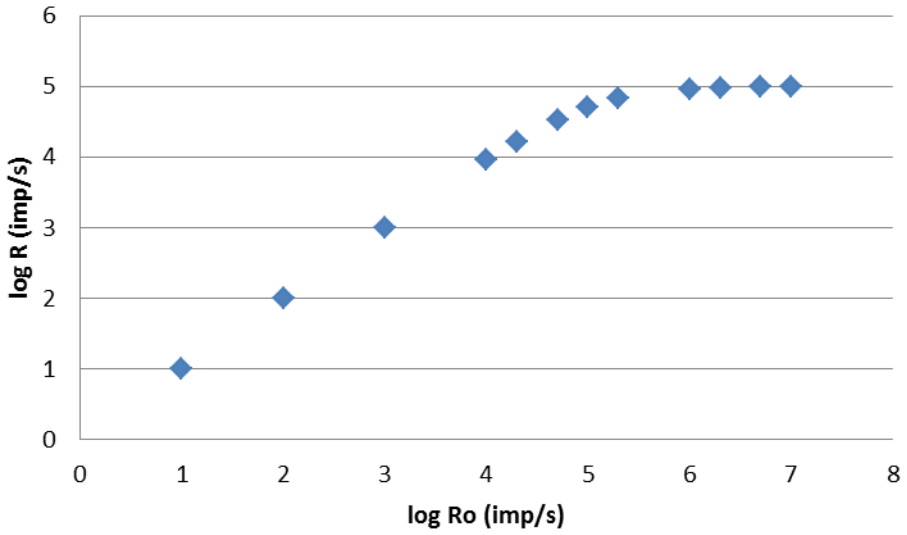

Figure VIII.2. Observed count rate (R) as a function of count rate taking into account 10 µs dead-time of the detector.

- c_{bc} is the backscattering coefficient relevant for beta particles. When scattering from atoms of surrounding matter beta particles considerably change their path direction and can be scattered even to opposite direction of their initial path. Some of the beta particles, not initially emitted towards the detector, may scatter from the surrounding material, such as a lead shield, and go to detector. Thus backscattering can increase the observed count rate and it is the only factor in Eq. VIII.II that has a value higher than one. Backscattering is dependent on the backscattering material: the higher its atomic number is the more efficiently it scatters. Backscattering is also dependent on the structure of the measurement system: the closer to detector and source there is scattering material the higher is backscattering. Backscattering is relevant when measuring beta radiation with gas ionization detectors and semiconductor detectors but not when measurement is done with liquid scintillation counting. Gamma radiation and particularly alpha radiation do not scatter that much that it would be important in their measurement.

- c_{ab} is the absorption coefficient which counts for absorption of radiation between the source and the detector. It is dependent on the type and thickness of the matter between the source and the

detector as well as on the type of radiation. The thicker the absorbing material and the higher is its density the larger fraction of radiation is absorbed in this material. Absorption is most relevant for alpha radiation since its range is short and it effectively absorbs even in air. Therefore, alpha measurements are done in vacuum. Measuring gamma radiation is least troublesome with respect to absorption since its range is long and it is readily penetrating radiation. The problem with beta radiation is between those of alpha and gamma radiation. When a beta measurement is done with liquid scintillation counting, part of the beta particle energies can be absorbed before they result in excitation with a scintillator molecule. When, in turn, beta measurement is done with a gas ionization detector beta particles can absorb in air between the source and the detector and especially in the window on the detector. With the high energy beta emitters, such as ^{32}P (E_{max} = 1.7 MeV), this is not a problem but with low energy beta emitters, such as tritium (0.018 MeV), the absorption is already so high that gas ionization detectors are ruled out.

- c_{sa} is the self-absorption coefficient which is due to absorption of radiation into the sample itself. This factor is most important for alpha radiation and least important for gamma radiation while the importance for beta radiation is in between the two former. Since the range of alpha radiation is very short the counting sources in alpha spectrometry using semiconductor detectors are prepared as "massless" which means that the mass of the counting source should be as small as possible. The greater the mass of the source is the broader the peaks become, deteriorating energy resolution, and the lower the intensity of detected pulses is. Smallest mass is obtained by electrodeposition of alpha emitters on metal discs. Preparing counting sources by microcoprecipitation and counting the alpha spectrum from the resulting very small amount of precipitate on a filter somewhat deteriorates energy resolution but most often yields into a sufficient result. When measuring alpha radiation with liquid scintillation counting self-absorption is of no importance since alpha emitters are dissolved in the scintillation cocktail and practically all alpha particles yield formation of an electric pulse, i.e. the counting efficiency is nearly 100%. Gamma radiation is highly penetrating and for gamma rays of at least a few hundred keV energy self-absorption is of minor importance. For gamma rays of lower energy self-absorption has to be carefully taken into account. When measuring aqueous solutions self-absorption can be easily accounted for by measuring aqueous standard samples in same geometry as the unknown samples. For solid samples the standardization with respect to self-absorption, efficiency calibration, is not that simple since there is no comprehensive set of standards having various radionuclides in solid matrices identical or close to the composition of

the unknown sample. Self-absorption in solid samples is dependent on many factors, most important of which are the elemental composition, density and thickness of the sample and the energy of gamma rays. When measuring beta radiation with liquid scintillation counting self-absorption is not a problem since the sample is usually dissolved in liquid scintillation cocktail. Only when measuring solid samples by liquid scintillation, self-absorption needs to be taken into account. However, when beta radiation is measured with gas ionization detectors self-absorption needs a careful consideration, especially when beta emitters with lower beta energies are measured and, therefore, the counting sources are prepared in a similar manner as in alpha spectrometry with semiconductor detectors, by electrodeposition or microcoprecipitation.

As seen, there are a number of factors affecting the counting efficiency. All of them have effect on the observed count rate. This, however, does not mean that the values of the coefficients would need to be determined in each activity measurement. Usually when the activity of an unknown sample (A_x) is to be determined its count rate (R_x) is measured and compared to the count rate obtained of a standard (R_{st}) with a known activity (A_{st}) and the activity of the unknown sample can be calculated as follows:

$$A_x = A_{st} (R_x/R_{st}) \qquad \text{[VIII.V]}$$

This method, however, applies only when both the unknown sample and the standard are measured in identical conditions which guarantees same counting efficiency for both measurements. When measuring aqueous samples by gamma spectrometry it is enough that both the standard and the unknown sample are measured in the same geometry, i.e. the sample sizes are identical and the distance from the detector is the same. For solid samples, as already mentioned, this is usually not enough, since self-absorption needs to be taken into account either by using a standard with the same, or nearly the same composition, or by computational methods requiring knowledge on the chemical composition of the unknown sample. In liquid scintillation counting direct comparison of the count rate of the unknown sample to that of the standard is not used but the counting efficiency is determined for each individual sample. This, however, also needs standardization which is described in the chapter on liquid scintillation counting.

Pulse counting vs. energy spectrometry

In measuring radiation there are two modes:

- Pulse counting which means that pulses from a radioactive source are counted irrespective of their energy. Either pulses generated by all particles or rays are counted or they are counted at a defined energy range. Thus, in the pulse counting mode no multichannel analyzer is used.
- Energy spectrometry in which the energies of each particle or ray are determined and sorted to corresponding channels of a multichannel analyzer. As a result the number of pulses (or count rate when divided by measurement time) in each channel is obtained, i.e. an energy spectrum is obtained. Figure VIII.3 shows a simple example, the energy spectrum of ^{137}Cs measured with a solid scintillation detector. The peak at the right corner represents pulses from the 662 keV gamma transition in the decay of ^{137}Cs.

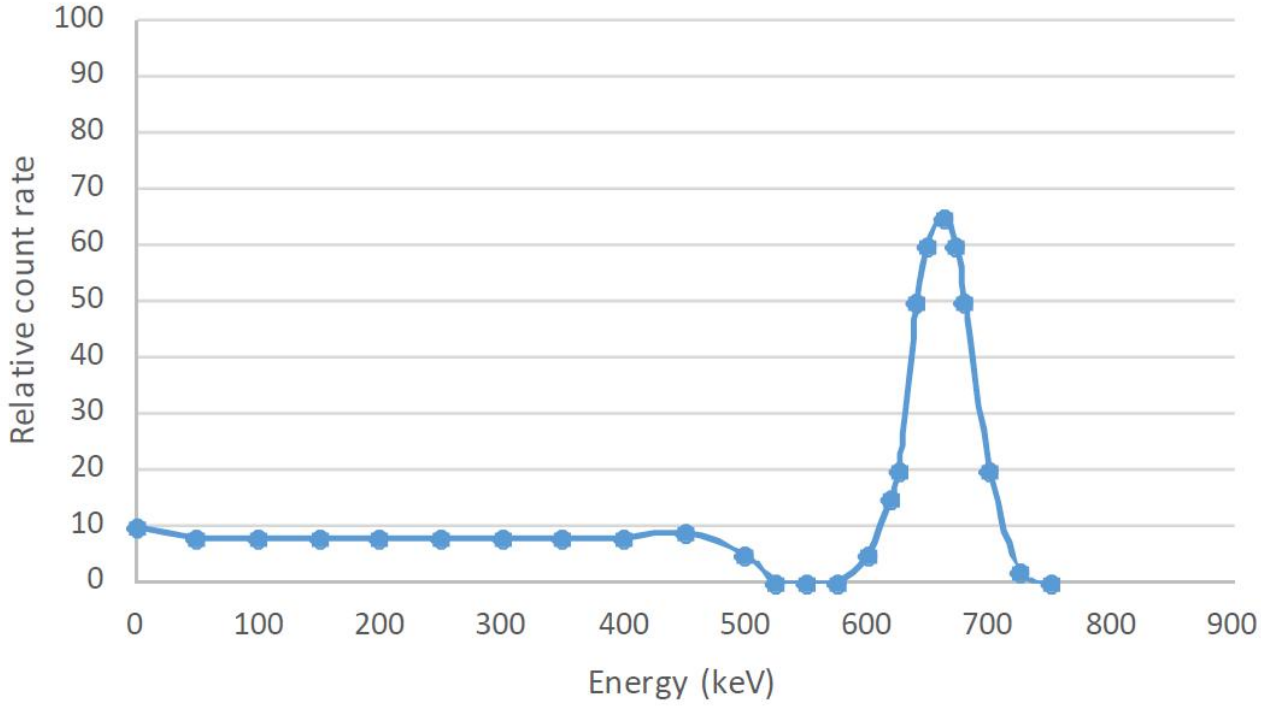

Figure VIII.3. Gamma spectrum of ^{137}Cs measured with a solid scintillation detector.

Pulse counting is used to measure gross alpha and gross beta activities in environmental samples. In these no information is obtained on the radionuclide composition, which however, may in typical situations be approximately known. Pulse counting is also used in laboratory experiments with added tracers, for example when studying sorption of a certain radionuclide on a mineral in

controlled conditions. In these, typically known amount of a single radionuclide is added to the system and its activity is measured after the experiments, for example in the solution phase in the above-mentioned sorption experiments. Since there are no interfering radionuclides present no energy spectrometry is needed. The activity of the tracer is measured by determination of pulses in the energy area (channel range) representing energies of the tracer. This type of measurements are typically carried out with gamma-emitting tracers using solid scintillation detectors. For example, to measure the activity of ^{137}Cs tracer only peaks representing its photopeak are measured. This is done by setting discriminators to the pulses: the lower discriminator reject pulses with lower pulse size than set while the upper one reject those of higher than set. Thus amount of pulses from the set energy range is obtained and this can be converted to count rate by dividing with counting time. A third example of pulse counting mode is the measurement of beta radiation with GM-tubes. All beta particles entering the interior of the tube cause a pulse of same height. Thus no spectrometric data can be obtained.

If the sample contains several radionuclides and their individual activities are to be measured energy spectrometry is needed. Gamma spectrometers with semiconductor detectors, having very good energy resolution, can differentiate tens of radionuclides from the same sample and their activities are measured from the areas of specific peaks belonging to each nuclide. Solid scintillation detectors can also be used for energy spectrometry but are seldom used for that due to their limited energy resolution. Gamma spectrometry is also used for radionuclide identification in which positions of peaks and their relative intensities are made use of. Alpha spectrometry with semiconductor detectors is used to measure both activities of alpha emitters and their isotopic ratios, the latter bringing often valuable information, for example, on the source or origin of the alpha emitter. Alpha measurements, however, require radiochemical separations and typically only one element is measured at a time. Beta spectrometry is most often carried out by using a liquid scintillation counter, but also with proportional counter. Due to continuous nature of beta spectra, however, only one beta emitter is measured at a time. Sometimes it is possible to measure two beta emitters from the same samples if the energy difference of the two beta emissions is high enough.

Basic components of radiation measurement equipment systems

Radiation measurement equipment systems consist of the following components (Figure VIII.4):

- Detector, the function of which is to transform the energy of radiation into an electric pulse (gas ionization detectors and semiconductor detectors) or to a light pulse (scintillation detectors). Various detectors are discussed in later chapters in more detail.
- Voltage source which collects the initial electric pulses into electrodes.
- Preamplifier which amplifies the weak pulses coming from semiconductor detectors to enable the pulse transfer through cables into the main amplifier.
- Main amplifier is called linear amplifier since its function is not only to increase the pulse height to a measureable one but also preserve the energy information. This is done by amplifying each initial pulse with the same factor so that the observed pulse heights are linearly related to the heights of the initial pulses coming from the detector and the preamplifier.
- In scintillation detectors there is, instead of preamplifier and linear amplifier, a photomultiplier tube (PMT) which converts the light pulse into an electric pulse and amplifies the initial pulse into a measureable electric pulse.

After this there are two options depending on whether the equipment is used as a multichannel analyzer or as a single-channel analyzer. The former is used in energy spectrometry and the latter in pulse counting.

- A multichannel analyzer (MCA) sorts the pulses into various channels depending on their pulse height which is proportional to the energy of the particle or ray. For example 1 mV pulse goes to channel 1, 12 mV pulse to channel 12 and 715 mV pulse to channel 715. This results in the formation of an energy spectrum. A multichannel analyzer may have even thousands of channels. Prior to sorting the pulses into channels the analog-to-digital converter (ADC) transforms the analogical pulses into digital form.
- A single channel analyzer (SCA) counts only pulses at a defined height range. As described above, selection of pulse height range is accomplished with voltage discriminators, lower and upper. In addition, there is a pulse counter that sums all pulses coming to the discriminator window. For example, single channel can be set to count only pulses with heights between 50 mV and 150 mV, i.e. pulses that would go channels 50-150 in the multichannel analyzer,

presuming same settings. Single-channel analyzer is used to measure only one radionuclide at the time. The discriminators are set by measuring the spectrum of the desired radionuclide by using a narrow discriminator window at increasing mV range. Plotting the counts at increasing mV results in the formation of an energy spectrum. The measurement window is set by measuring the spectrum of the desired radionuclide and selecting from the spectrum the lower and upper discriminator voltage values so that the pulses from the photopeak is between them. Single channel mode is typically used in gamma counters with solid scintillation detectors.

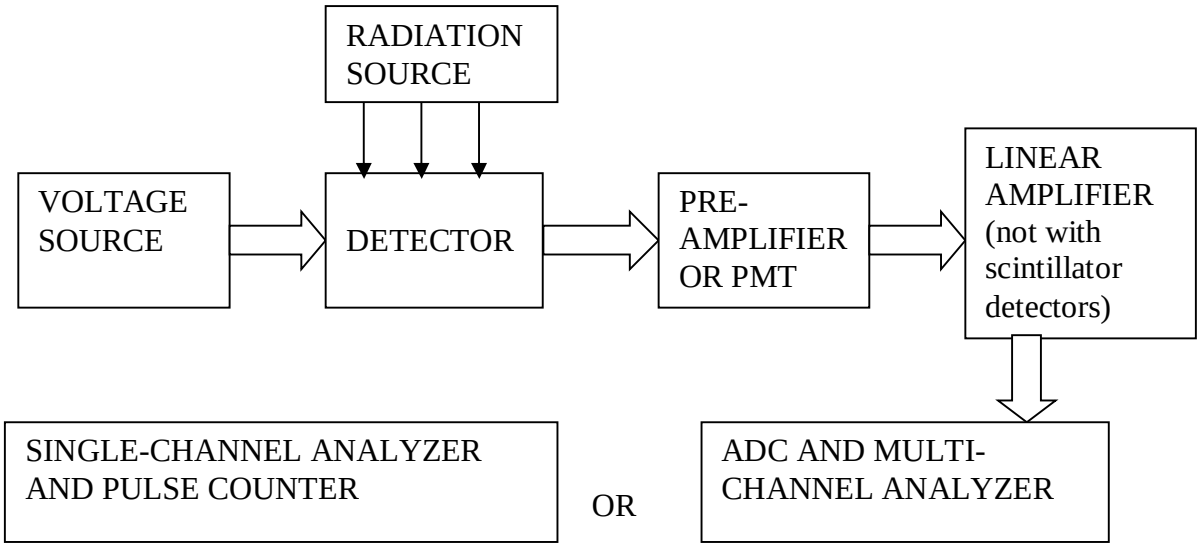

Figure VIII.4. Components and scheme of radiation measurement equipment systems. PMT is photomultiplier tube.

Energy resolution

In energy spectrometry it is essential that the measurement system can differentiate different particle or ray energies as efficiently as possible. This is mostly dependent on the type of detector. The better the energy resolution the better the system can differentiate energies close to each other and the narrower are the observed peaks in a spectrum. Resolution (R) is expressed as the peak width at half of the height of peak maximum (FWHM = full width at half maximum) (Figure VIII.5). Instead of the absolute value the energy resolution can also expressed as the relative value ($\Delta E/E$)×100%, where E is the energy of the peak maximum and ΔE is FWHM. For example, for ^{137}Cs the energy resolution of the 662 keV peak is typically 60 keV and the relative resolution value (60/662)×100% = 9%. For semiconductor gamma detectors, which are superior with respect to

energy resolution compared to solid scintillation detectors the energy resolution is often expressed as the FWHM of the ^{60}Co peak at 1332 keV. The energy resolution of semiconductor gamma detectors is clearly below 2 keV. Energy resolution is also dependent on the energy, the absolute values being better for low energy gamma rays, and therefore the resolution value should always refer to the energy for which is given. The energy resolution for 2 MeV gamma rays of germanium semiconductors is below 2 keV (0.1%), below 1.5 keV (0.15%) for 1 MeV rays and below 1 keV (0.2%) for 0.5 MeV rays. For NaI(Tl) solid scintillation detector the corresponding values are about 100 keV (5%) for 2 MeV rays, 70 keV (7%) for 1 MeV rays and about 50 keV (10%) for 0.5 MeV rays. Thus the germanium detectors have about 50-times better resolution compared to the NaI(Tl) detectors. Silicon semiconductor alpha detectors have resolutions between 20-30 keV (0.4-0.6% for typical alpha energies of 4-7 MeV) which are about ten times lower than values obtainable with liquid scintillation counters.

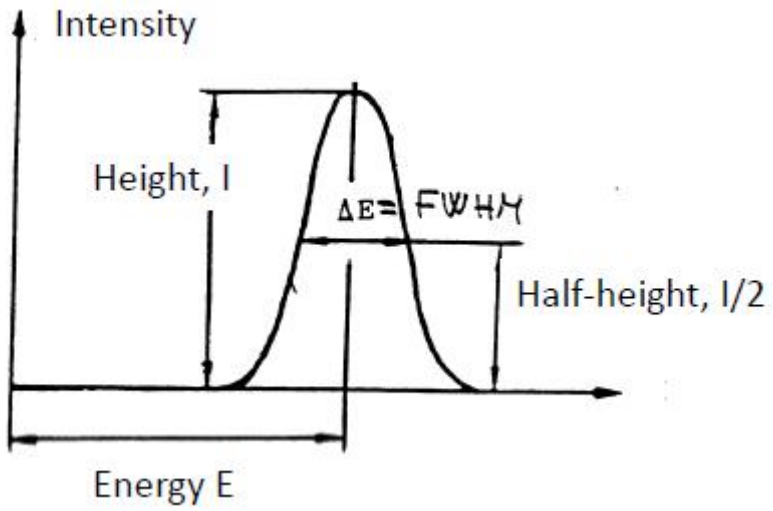

Figure VIII.5. Energy resolution of spectrum peak.

Radiation detectors and their suitability for the measurement of various types of radiation

Most typical radiation detectors discussed in following chapters can be divided into three groups:

1. Gas ionization detectors

· Ionisation chamber

· Proportional counter

· Geiger-Muller (GM) tube

2. Scintillation detectors

· Liquid scintillation

· Solid scintillation detectors

3. Semiconductor detectors

Alpha radiation is most accurately measured with semiconductor detectors. Their background pulses are very low and their energy resolution is good, at 5 MeV energies even 15 keV. The energy resolution of liquid scintillation counting, another choice to measure alpha radiation, is about ten times poorer than that of semiconductor detectors. Sample preparation for liquid scintillation counting is, however, clearly less difficult since the sample is just dissolved in the liquid scintillation cocktail for measurement while for semiconductor detectors counting sources need to be prepared by electrodeposition or microcoprecipitation. Another benefit of liquid scintillation counting is a very good, practically 100%, counting efficiency. In liquid scintillation counting the beta emitters present can cause problems by creating extra pulses to alpha peaks. In modern liquid scintillation counters this is overcome by alpha-beta discrimination system that differentiates alpha and beta pulses from each other and count them separately. Due to the poor energy resolution liquid scintillation counting is not a proper method to determine the isotopic ratios of alpha emitters. For this purpose semiconductor detectors need to be used.

For **beta radiation** the most often used method is liquid scintillation counting. It yields into high counting efficiencies and is suitable also for low energy beta radiation. Liquid scintillation counting also enables determination of beta spectra. Usually, however, due to the continuous nature of beta spectra, only one beta emitter can be measured at a time. Other options to measure beta radiation are the gas ionization detectors, GM tube and proportional counters, the latter of which can also produce beta spectra. The drawbacks of gas ionization detectors are more laborious counting source preparation, lower counting efficiency and the fact they cannot be easily used in measurement of beta emitters with the lowest energies, such as tritium. The benefit of gas ionization detectors is their clearly lower background compared to liquid scintillation counting and thus much lower detection limits are obtained.

For the measurement of **gamma radiation** solid scintillation and semiconductor detectors are used. The benefit of solid scintillation detectors is their higher counting efficiency as the detectors can be produced in large sizes and they are often of well-type in which the sample is inside the detector.

Solid scintillation detectors are usually utilized for gamma counting in single-channel mode. The benefit of semiconductor detectors is their superior energy resolution compared to solid scintillators and therefore they are typically used for gamma spectrometric measurements in radionuclide identifications and measurement of radionuclide activities from samples having several gamma-emitting nuclides.

In a well-equipped radionuclide laboratory, measuring a range of radionuclides, there are the following radiation measurement apparatus:

- semiconductor detector(s) for gamma spectrometry for the determination of radionuclides from environmental and radioactive waste samples, for example
- gamma counter(s) having a solid scintillation detector and a sample changer for the measurement of tracer gamma emitters used in model experiments
- liquid scintillation counter(s) with alpha-beta discrimination for the measurement of tracer beta and alpha emitters as well as beta and alpha emitters separated from various samples
- low background liquid scintillation counter(s) for the measurement of low beta activities
- semiconductor alpha detector(s) for the measurement of alpha emitters separated from various samples
- gas ionization detector(s) to measure low activity beta emitters separated from various samples

Measurement of radionuclides with mass spectrometry

An alternative for radiometric methods for the determination of radionuclide activities is mass spectrometry. Most often inductively-coupled mass spectrometry (ICP-MS) is today used for this purpose. As mentioned, mass spectrometer counts atoms instead of radiation. This makes mass spectrometry particularly suitable for the measurement of long-lived radionuclides for which the detection limit of mass spectrometry is below those obtained by radiometric methods. For example, for ^{99}Tc ($t_{½}$ = 211000 y) the detection limit is at best 1 mBq for a gas ionization detector and clearly higher in liquid scintillation counting. 1 mBq means that there are about four decays in an hour but this activity of ^{99}Tc corresponds to about 100 million atoms. This amount of atoms can be easily detected and counted by mass spectrometry and even as low as a 0.001 mBq detection limit can be achieved by ICP-MS. In principle all radionuclides with half-lives longer than 100 years can be

measured by ICP-MS. However, for the radionuclides with half-lives round this limit, radiometric methods are still more sensitive and provide with more accurate results.

The components of an ICP-MS are presented in Figure VIII.6. The sample solution is introduced into the system by a nebulizer which turns the solution into a fine mist (aerosol). This is transferred with argon flow into the torch where plasma is created with the help of radiofrequency. Plasma atomizes the sample, ionizes the atoms and the ions are directed into a mass analyzer for the separation of ions based on their mass to charge ratio (m/z).

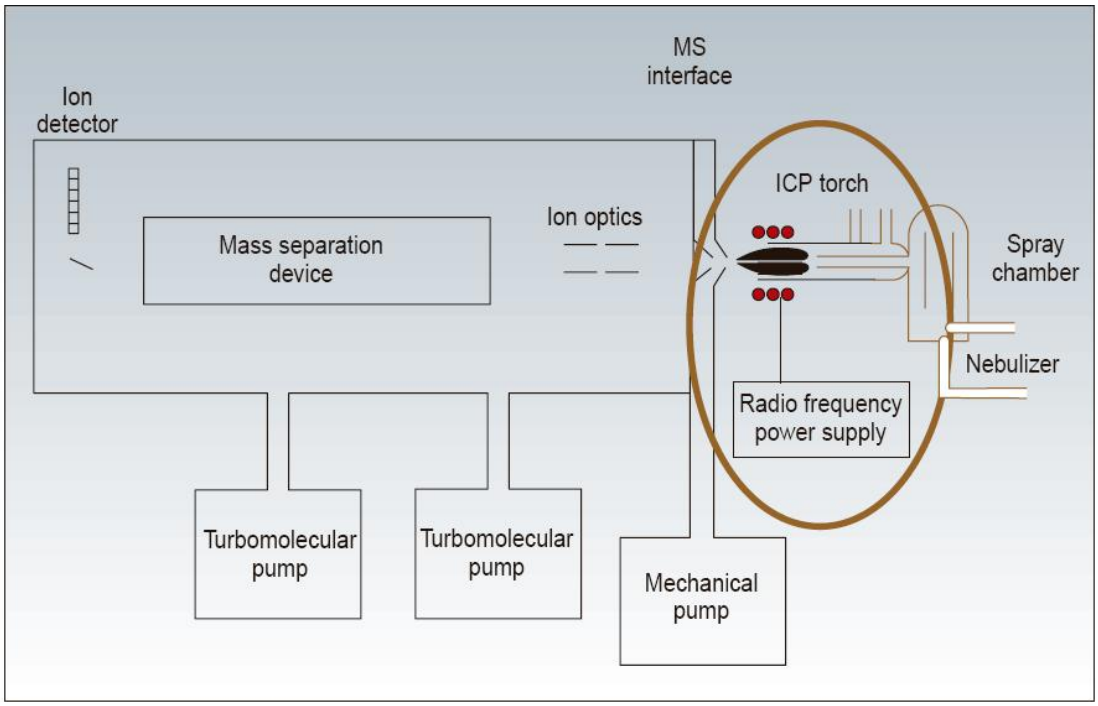

Figure VIII.6. Components of an ICP-MS system
(http://www.people.fas.harvard.edu/~langmuir/SN-ICP-MS.html).

The mass analyzer is either quadrupole or double focusing system. The former is smaller, cheaper and easier to operate. The latter, however, is much more sensitive yielding to lower detection limits and to more accurate isotopic ratios. A quadrupole consists of four metallic rods aligned in a parallel diamond pattern. By placing a direct current field on one pair of opposite rods and a radio frequency field on the other pair, an ion of a selected mass and charge ratio (*m/z*) is allowed to pass through the rods to the detector while the others are forced out of this path. By varying the combinations of voltages and frequency, an array of different m/z ratio ions can be scanned in a

very short time. The high-resolution double focusing system in turn consists of an electromagnet and an electrostatic analyzer in series. After mass separation the ions are detected and counted.

Some radionuclides, such as uranium, can be measured from natural waters directly with ICP-MS without chemical separation of interfering elements. Most radionuclides, however, need to be separated into a pure form prior to measurement. The separation requirements may essentially differ from those used in radiochemical separations for radiometric measurements. For example, if plutonium is measured by alpha spectrometry 1% of uranium activity in the counting source does not result in a large error. In mass, however, this 1% activity means about 2000-times excess of ^{238}U compared to ^{239}Pu which would prevent the measurement of plutonium. In mass spectrometry there are three types of interferences that need to be taken into account when measuring radionuclides. First, the isobars with approximately same mass cause interference, for example ^{129}Xe in ^{129}I measurement and ^{135}Ba in ^{135}Cs measurement. Second, in the plasma there are not only single atoms formed but also polyatomic ions such as $^{204}Hg^{35}Cl$ or ^{238}UH which interfere with the measurement of ^{239}Pu having approximately the same mass. Even though only a small fraction of the total elemental concentrations forms these polyatomic ions $^{204}Hg^{35}Cl$ or ^{238}UH their concentrations are nevertheless much higher than that of plutonium due to the greater abundances of the polyatomic ion forming elements, in this case Hg, Cl and U. Therefore, chemical separations are needed to enable measurement of radionuclides at very low concentrations. Third type of interference comes from broadening the neighbor mass peaks at higher concentration. Due to this, for example, ^{238}U at much higher concentrations compared to plutonium causes extra counts to the mass peak of ^{239}Pu.

ICP-MS is increasingly used for the measurement of long-lived radionuclides, especially actinides. For neptunium it is clearly superior to radiometric methods due to its low specific activity. In plutonium measurement, mass spectrometry also offers a change to measure individually ^{239}Pu and ^{240}Pu which cannot be separated from each other in alpha spectrometry. In turn, ^{238}Pu cannot be measured by mass spectrometry due to interference of uranium. Thus, to determine all relevant plutonium isotopes both mass and alpha spectrometry are needed.

The most sensitive mass spectrometric method, even more sensitive than high-resolution ICP-MS, is accelerator mass spectrometry (AMS) which consists of two electromagnet mass analyzer and a tandem accelerator in between (Fig. VIII.7). AMS is very suitable for the measurement of long-lived radionuclides, such as ^{14}C, ^{36}Cl, ^{41}Ca, ^{59}Ni, ^{129}I and actinide isotopes. For ^{14}C measurement in

carbon dating it has become a standard method. All radionuclide measurements with AMS require chemical separation of the target nuclide into a pure form.

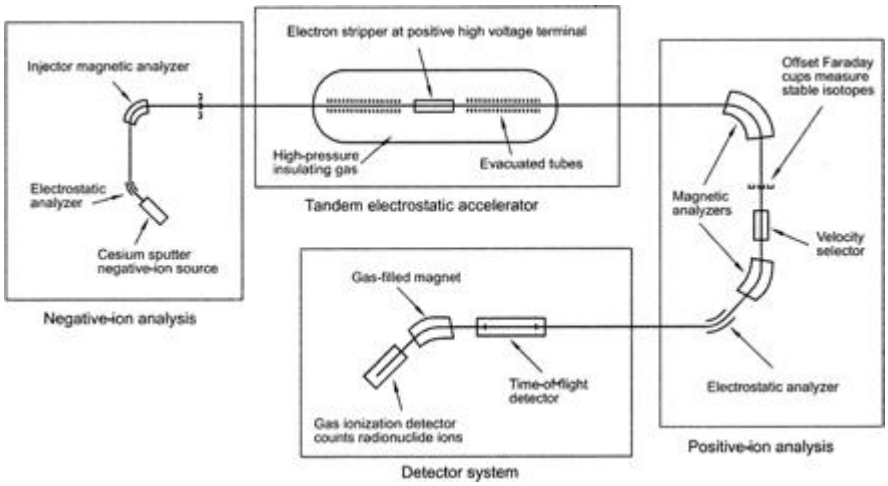

Figure VIII.7. Components of accelerator mass spectrometry (AMS) (http://gsabulletin.gsapubs.org/content/115/6/643/F1.expansion.html).

The direct determination of radionuclides from solid samples can be accomplished in two ways: laser ablation ICP-MS and secondary ion mass spectrometry (SIMS). In laser ablation the solid sample is exposed to a laser beam and the elements thus evaporated from the surface are directed into ICP-MS for mass analysis. In SIMS the surface is sputtered with Cs^+ ions and the elements released from the surface are directed into a mass analyzer.

IX GAMMA DETECTORS AND SPECTROMETRY

Content

Solid scintillators

Semiconductor detectors

Energy calibration

Efficiency calibration

Interpretation of gamma spectra

Subtraction of background

Sample preparation for gamma spectrometric measurement

For the detection and measurement of gamma radiation basically two types of detectors are used: semiconductors and solid scintillators (also called phosphors). The primary physical process in both detector types is ionization of the detector material Here, first the two detector types and then energy and efficiency calibrations, and finally the formation of various peaks in gamma spectra and subtraction of background are described.

Solid scintillators

In solid scintillators the detection process is based on the same principle as in liquid scintillation counting (LSC), described in a later chapter: radiation excites the detector material atoms (molecules in case of LSC) to a higher energy state and as the excitation state is relaxed visible light is emitted and further the light pulses are transformed into electric pulses with the aid of a photomultiplier tube. Liquid scintillators are not applicable for gamma radiation due to their low density and thus low gamma radiation stopping power and instead solid materials with higher density are used. Scintillation process was used for the radiation detection and measurement already in the beginning of the 20th century as ZnS was used to detect and count alpha radiation. There are a number of solid scintillation detector materials of which NaI is the most extensively used and discussed here in more detail. Some other materials and their benefits over NaI are discussed at the end of the section.

NaI is an effective material for gamma ray measurement since it can be manufactured in large crystals that can absorb readily penetrating gamma rays. The larger the crystal the higher is the

counting efficiency. NaI as such is, however, not capable of forming light. It needs an activation by adding Tl^+ ions into the crystal framework and therefore the crystal material is denoted as NaI(Tl). Tallium ions act as luminescent centers in the NaI crystal. Typically 0.001 mol-% of tallium is added to NaI. The light formation process in NaI(Tl) takes place in the following way:

- gamma radiation primarily results in the formation of electrons (e^-) and holes (h^+) in ionization of the detector atoms: $\gamma \rightarrow e^- + h^+$
- the electrons interact with tallium ions to form tallium atoms $e^- + Tl^+ \rightarrow Tl^0$ while the holes interact with tallium ions to form divalent tallium ions $h^+ + Tl^+ \rightarrow Tl^{2+}$
- then tallium atoms interact with holes to form excited tallium ions $h^+ + Tl^0 \rightarrow (Tl^+)^*$ and divalent tallium ions interact with electrons also forming excited tallium ions $e^- + Tl^{2+} \rightarrow (Tl^+)^*$
- finally the excitation state of tallium is relaxed and the excitation energy is emitted as visible light $(Tl^+)^* \rightarrow Tl^+ + h\nu$ (335,420 nm)

Since the excitation energy level of $(Tl^+)^*$ is lower than that of NaI the crystal does not absorb the formed light photons.

The light photons, more than 10000 for each MeV energy absorbed in the NaI(Tl) crystal, are transformed into electric pulses with a photomultiplier tube (PMT) (Figure IX.1). The number of light photons is directly proportional to the energy of gamma rays absorbed in the crystal. The light photons first hit the photocathode at the PMT end facing the NaI(Tl) crystal. Photocathode material is typically made of Cs_3Sb, which releases electrons when light photons hit it. The number of released electrons is directly proportional to the number of photons hitting the photocathode. PMT multiplies the number of electrons to a countable electric pulse with the aid of successive dynodes, also made of Cs_3Sb, the number of which is typically 10-14. Electric voltage is applied between each pair of dynodes which results in the increase of electron energies between the dynodes increasing release on electrons from dynodes. The high voltage through the whole PMT is 1000-2000V and the multiplication factor of electrons across the PMT is about 10^6. This multiplication factor is the same for all events and thus the initial number of electrons released from the photocathode is always multiplied in the PMT by the same factor. Thus, the energy information of a gamma ray absorbed in the crystal remains in all steps: formation of electrons as the primary process, formation of light photons in the crystal, formation on electrons in the photocathode and multiplication of electrons in PMT. Thus the height of the electric pulse is directly proportional to the energy of the detected gamma ray. This is, however, an ideal picture and the response varies

from event to another and, instead of lines, broader peaks in the spectra are observed. The maximum of each peak, however, represents the energy of a detected gamma ray.

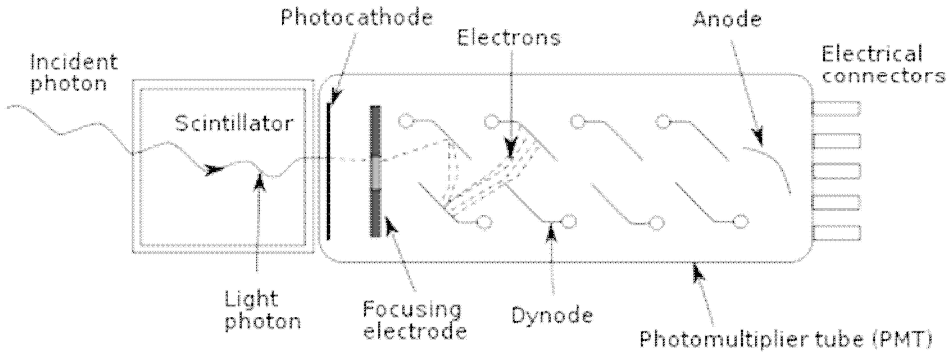

Figure IX.1. Photomultiplier tube (PMT) attached to a solid scintillation detector (http://chemwiki.ucdavis.edu/Analytical_Chemistry/Instrumental_Analysis/Spectrometer/Detectors/Detectors).

Since NaI(Tl) can be produced as large crystals they have good gamma ray detection efficiency, much better than what is obtained with semiconductor detectors. They can also be produced as well-type crystals in which a cylindrical whole is drilled in the middle of crystal. The sample to be counted is placed in the hole, which considerably increases counting efficiency compared to planar crystals. The drawback of solid scintillators in comparison with semiconductor detectors is their poor energy resolution. The energy resolution of NaI(Tl) detector is approximately 50-100 keV for gamma rays of energy between 2 - 0.5 MeV while with semiconductor detectors the resolution is about 50-times better (Figure IX.2). Therefore, due to overlapping peaks solid scintillators cannot be used for identification of radionuclides from samples having a large number of radionuclides. Solid scintillators are used in gamma spectrometry only when high detection efficiency is needed and when the sample does not have a large number of radionuclides. More usually, solid scintillators are used in counting of single radionuclides in a single channel mode. In this, only the pulses of the photopeak, representing the energy of the most intensive gamma transition, are counted. This is accomplished by use of voltage discriminators: the lower discriminator rejects pulses of smaller height than the set value while the upper discriminator rejects pulses of greater height than the set value.

In addition to NaI(Tl) detectors there are other types of solid scintillators, such as CsI(Tl), $Bi_4Ge_3O_{12}$ and $LaBr_3(Ce)$. In developing solid scintillators two objectives have been sought: to improve counting efficiency and to improve energy resolution. An example of the former is

$Bi_4Ge_3O_{12}$, also called BGO, which has a better counting efficiency compared to NaI(Tl) due its higher density of 7.1 g/cm^3 compared to 3.7 g/cm^3 of NaI(Tl). The Ce-activated lanthanum chloride $LaBr_3$(Ce) in turn has a much better energy resolution than NaI(Tl), 3% vs. 8% for 662 keV gamma rays. The BGO detector, however, has a lower energy resolution than NaI(Tl). Thus the choice of the detector should be done on the basis of what property is most needed, efficiency or energy resolution.

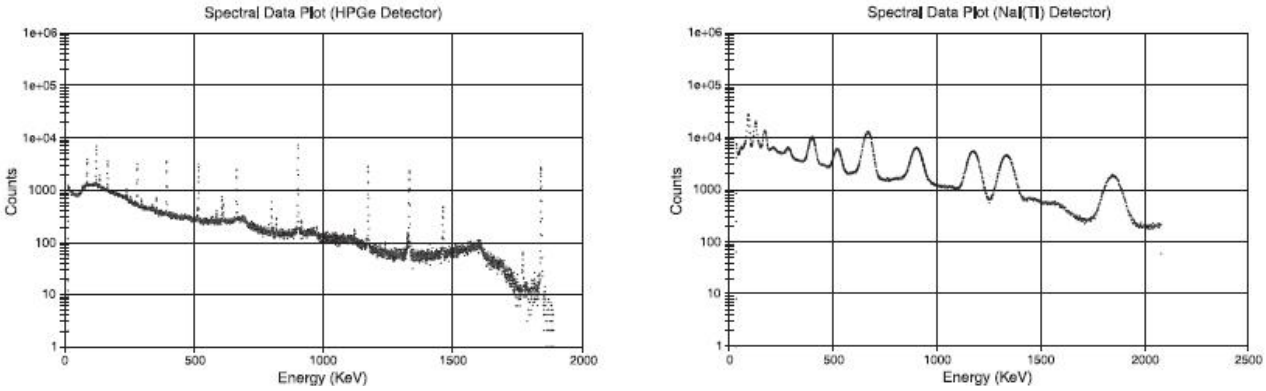

Figure IX.2. Gamma spectra collected from the same source by a semiconductor detector (left) and by a scintillation detector (right) (http://www.canberra.com/ literature/fundamental-principles/).

Semiconductor detectors

Semiconductor detectors are diodes produced either of silicon or germanium, the former being used for alpha and X-ray detection and the latter for gamma detection. Germanium is more suitable to gamma detection than silicon due to its higher atomic number Z=32, and thus density, which increase the stopping power compared to silicon, the atomic number of which is only Z=14. The formation of photoelectric effect is proportional to the atomic number of the element absorbing gamma rays. Thus, for example, 0.1 MeV gamma rays are absorbed 40-times more efficiently in germanium than in silicon. The detector consists of two parts (Figure IX.3). The other part is pure Si/Ge, having four electrons in the outer shell, doped with atoms having five electrons in the outer shell, such as phosphorus. This type of semiconductor is called n-type and it acts as an electron donor. The other part, p-type, is also pure Si/Ge but now doped with atoms with three electrons in the outer shell, such as boron. This part acts as an electron acceptor with electron holes surrounding boron atoms. When these two parts are attached to each other electrons from n-type move to p-type and a narrow layer at interface, junction, becomes free of electrons and holes. This layer is called depletion layer. When now electrodes are attached to the other sides of n-type and p-type

semiconductors, anode to n-type and cathode to p-type and a reverse bias voltage is applied across the system the electrons in the n-type move towards the cathode and the holes towards the anode. This results in a broadening of the depletion layer. To observe maximal depletion layer thickness very high voltages, even up to 5000 V, are used. When a gamma ray or an alpha particle hits this depletion layer it becomes conducting and an electric pulse is recorded in the external electric circuit. This pulse is amplified with a preamplifier and linear amplifier, transformed into a digital form with ADC and counted with multichannel analyzer. Since the energy to create an electron-hole pair is constant to each detector material (about 3 eV for germanium), the electric pulse is directly proportional to the energy of gamma ray or alpha particle. Thus they can be used for energy spectrometry. The semiconductor detectors act similarly to gas ionization detectors (ionization chamber and proportional counter), but the advantage of semiconductor detectors is that the formation time of an electric pulse is much shorter than in the gas ionization detectors. In addition, semiconductor detectors produce about ten times higher number of electrons (and holes) per unit energy absorbed in the detector. To be efficient for gamma ray detection the germanium detector has to be large and the depletion layer should be several centimeters wide. To observe thick depletion layer the germanium used has to be very pure, the fraction of foreign atoms being one atom per 10^{10} germanium atoms. These kinds of detectors are called High-purity germanium detectors (HPGe). In the early phases on germanium detector development, beginning from the 1950's, such pure germanium was not available but contained so high amounts of acceptor atoms that only a few millimeter thick depletion zones were obtainable. This naturally decreased the counting efficiency. To compensate the effect acceptor impurities Li^+ ions were added to germanium crystals, called lithium-drifted germanium detectors (Ge(Li)). Lithium ions compensated the charges of acceptors and made them thus immobile. Li-drifted germanium crystals needed to be kept at liquid nitrogen temperature (-200 ^oC) all the time; room temperature would destroy them due to high mobility of lithium ions at higher temperatures. In the case of alpha detection the n-type facing to the source need to be very thin in order to enable penetration of alpha particles into depletion layer, which is also very thin, less than one micrometer. Alpha detectors and spectrometry are described in more detail in chapter XI.

As already mentioned, the energy resolution of germanium detector is 50-times better than that of NaI(Tl) detector and absolute resolution is about 2 keV (0.1%) for gamma rays with energies of 2 MeV, about 1.5 keV (0.15%) at 1 MeV, about 1 keV (0.2%) at 0.5 MeV and about 0.5 keV (0.5%) at 0.1 MeV. Thus germanium detectors can be used to identify gamma-emitting radionuclides from a mixture of a number of radionuclides, for example, from environmental and nuclear waste

samples. Modern gamma spectrometers are provided with advanced programs, with a memory-stored library of peaks and their intensities of most gamma emitters, and thus the radionuclide identification is done automatically. Quantitative analysis of radionuclides is based on measurement of net areas of the representative peaks and using pre-determined efficiency calibration, the latter being described later in this chapter.

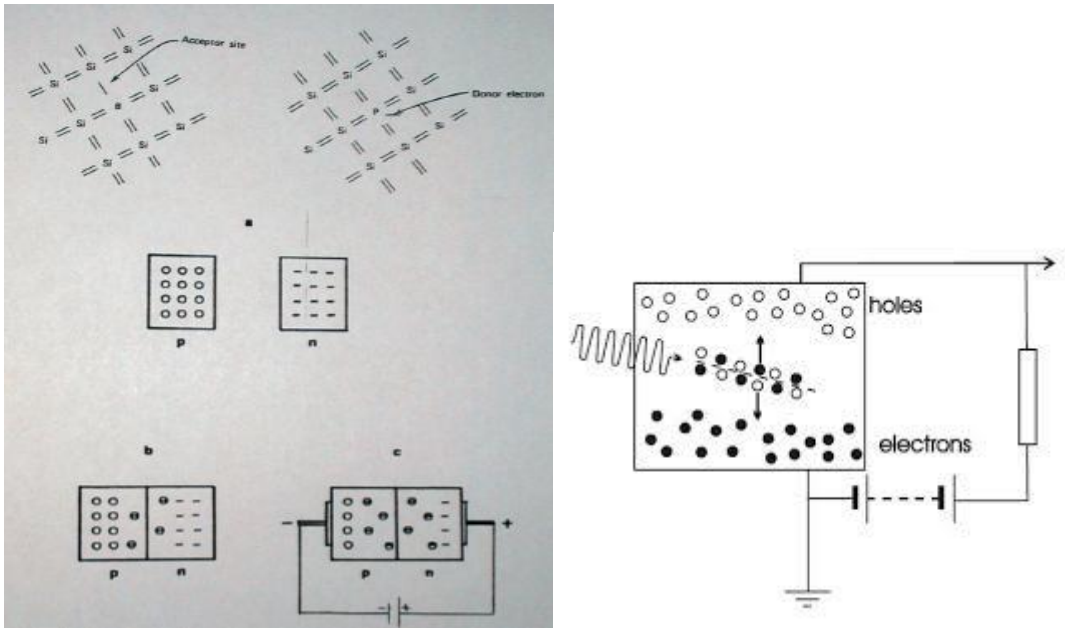

Figure IX.3. Structure and function of a semiconductor detector.

The detection efficiency of germanium detectors is dependent on the size of the detector: the larger the detector the higher the efficiency. Efficiency depends also on the gamma energy (Figure IX.4). At higher gamma energies the efficiency decreases due to penetration of gamma rays without interactions with the detector. At energies higher than about 150 keV the efficiency decreases more or less linearly when both energy and efficiency are presented on logarithmic scales. Ordinary germanium detectors are covered with an aluminum shield, which effectively absorbs low energy gamma rays. This can be seen in Figure IX.4 as a dramatic drop in efficiency of gamma ray energies below 100 keV. To overcome this and to enable also measurement of low energy gamma rays broad energy (BEGe) and low energy (LEGe) germanium detectors have been developed. These have, instead of aluminum, very thin window, made of either beryllium or carbon composite, between the source and the detector. This allows efficient detection of low energy gamma emitters, such as ^{210}Pb (46.5 keV) and ^{241}Am (59.5 keV) supposing their activities are high enough. Energies down to 3 keV can be measured with BEGe/LEGe detectors and even below 1 keV with ultra-low energy detectors.

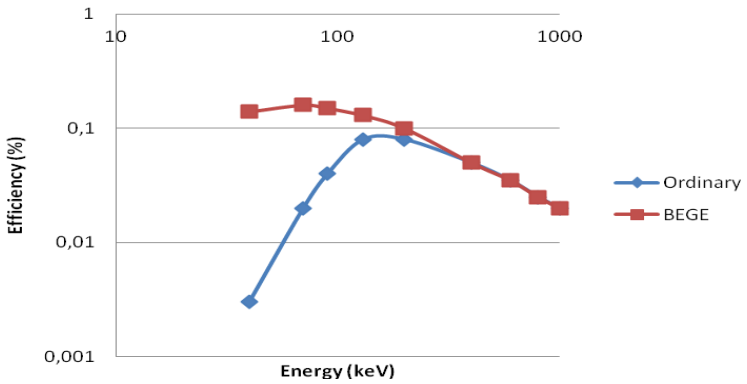

Figure IX.4. Efficiencies of an aluminum-covered ordinary and broad energy (BEGE) germanium detectors with same relative efficiency as a function of gamma ray energy.

When used the germanium detectors need to be cooled to about -200 ºC with liquid nitrogen cryostat (Fig. IX.5) or electrically to reduce electric noice which would considerably increase the background. Modern high purity germanium detectors (HPGE) can be let to warm when not in use but the earlier generation Li-drifted germanium detectors would destroy when letting them to warm up.

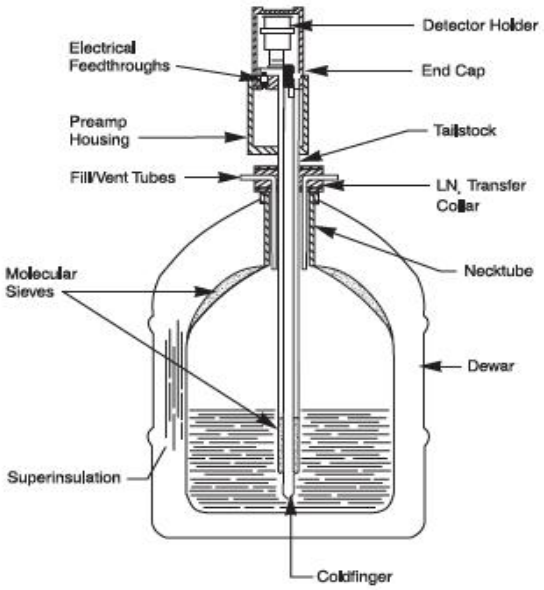

Figure IX.5. Liquid nitrogen cryostat for cooling germanium detectors (http://www.canberra.com/products/detectors/germanium-detectors.asp).

Germanium detectors have three types of shapes: planar, coaxial and well (Figure IX.6). Low-energy (LRGe) and broad energy-detectors (BEGe) are planar. The detector size in this construction mode is small and therefore these detectors are not able to efficiently detect high-energy gamma rays. In the coaxial mode the depletion layer is much thicker and therefore they are suitable in the

detection of high-energy gamma rays. In the well-type the sample in placed inside the hole bored in the detector which considerably improves the counting efficiency.

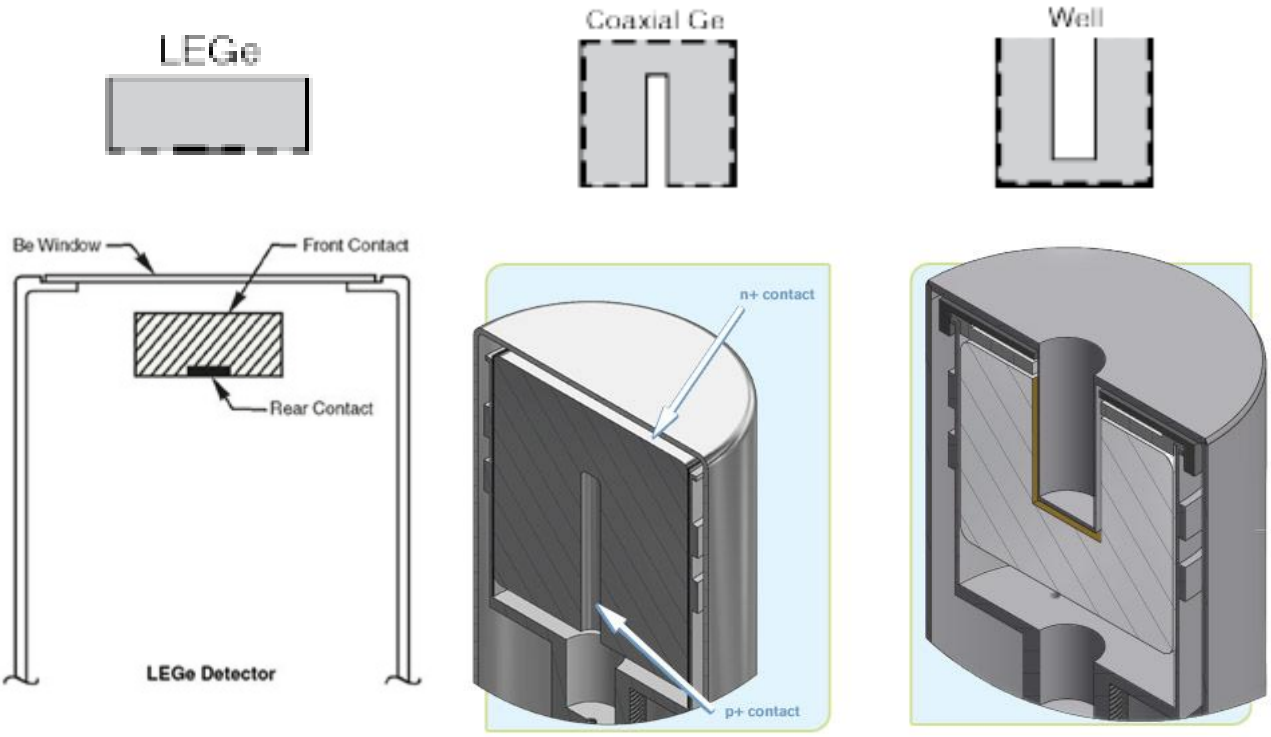

Figure IX.6. Germanium detectors used for gamma spectrometry. Left: planar detector, middle: coaxial detector, right: well-type detector (http://www.canberra.com/products/detectors/germanium-detectors.asp).

The counting efficiency of the detectors is the fraction of gamma rays resulting in the formation of electric pulse of the total gamma ray number hitting the detector. The efficiency varies with detector type and the gamma ray energy as was shown in Figure IX.4. To compare efficiencies of various detectors this absolute efficiency is, however, not typically used but instead the efficiency is expressed in a relative manner by comparing the detector efficiency at 1332 keV photo-peak of ^{60}Co to that of a Na(I) detector of size 3×3 inches at detector to source distance of 25 cm. This relative efficiency varies typically between 10% and 100%, the highest values obtained with larger detectors.

Energy calibration

Multichannel analyzer sorts the pulses according to their heights, which are proportional to the energy of the gamma rays. To know what channel represents what energy the system needs to be

calibrated. This is done by measuring standards of known energies depicted in Figure IX.7. In the figure the channel number are on the x-axis and the energies of the radionuclides on the y-axis. Here, three radionuclides with the following gamma energies are used:

Nuclide	Energy
^{57}Co	122 keV
^{137}Cs	662 keV
^{60}Co	1173 keV and 1332 keV

By plotting a curve of the peak energy versus the channel where the mid point of the peak appears a calibration curve is obtained. This curve is linear since the initial pulses from detector, proportional to the energy of gamma rays, are amplified in a linear manner. For example, if the maximum of the 662 keV peak of ^{137}Cs were in the channel 950, the maximum of the 122 keV peak of ^{57}Co would be in the channel 175 (=950×122/662) and accordingly the 1173 keV and 1332 keV peaks of ^{60}Co in channels 1683 (=950×1173/662) and 1911 (=950×1332/662). This linear calibration can now be used to identify unknown peaks in the spectrum. If, for example, a peak maximum of an unkonown sample was found in the channel 1198, one could see from the line that this channel corresponds to 835 keV energy. By examining spectrum library this energy could be shown to belong to ^{54}Mn. Modern gamma spectrometers both store the calibration curve in their memory and also have a spectrum library and do the identification analysis automatically. They utilize not only gamma energies of each radionuclides but also relative intensities in case the nuclide has several gamma transitions.

One needs to bear in mind that the channels where each peaks go to depends on the settings of the amplifier: the higher the amplification the higher is the channel where peaks go. For example, when amplifier gain is doubled, the 662 keV peak of ^{137}Cs would be found in the above mentioned case in which the channel is 1900 instead of 950.

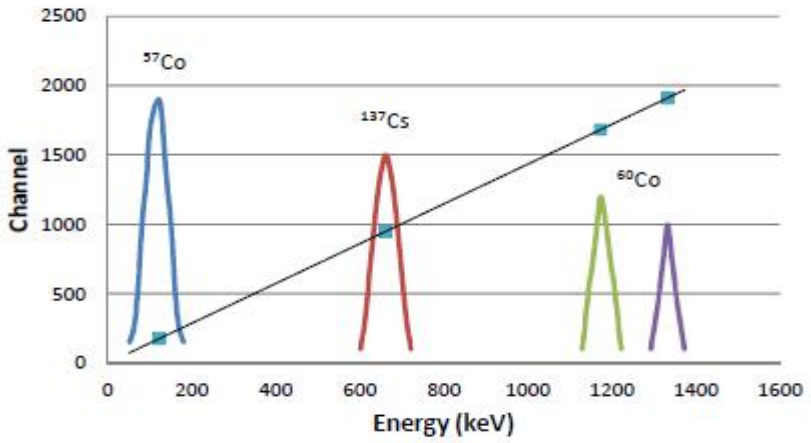

Figure IX.7. Energy calibration in gamma spectrometry.

Efficiency calibration

As is seen from Figure IX.4 the detector efficiency as a function of gamma ray energy is not constant but varies considerably. This must be taken into account by carrying out an efficiency calibration. The system is calibrated by measuring a mixture of radionuclides with a wide range of gamma photopeak energies. The activities of radionuclides should naturally be known and their values should be certified. Such radionuclide mixtures with certified activities are commercially available for efficiency calibration. At least seven radionuclides with varying energy should be used in the mixture. More radionuclides are needed for energy range below about 200 keV since the efficiency here varies in a more complex manner than at higher energies where an approximately linear relationship is obtained between energy and efficiency when presented in logarithmic scales. An example of composition of such standards with energy range from 60 keV to 1836 keV is presented in Table IX.I. This standard is meant for high accuracy calibration and consists of twelve nuclides. The standard is measured sufficiently long time to get at least 10000 counts to every photopeak and their net count rates are calculated by subtracting the background. Net count rates are then compared with activities to calculate the efficiencies and curve is fitted for the efficiencies as a function of gamma energy, i.e. efficiency calibration curve is plotted (Figure IX.8). This calibration curve can then be used to calculate the counting efficiency of photopeaks in actual sample measurements. Software of modern gamma spectrometers do this automatically based on the calibration curve stored in their memory.

Table IX.I. Composition of a standard for efficiency calibration of gamma spectrometer (NIST).

Nuclide	Photopeak energy (keV)	Nuclide	Photopeak energy (keV)
^{241}Am	59.5	^{85}Sr	514.0
^{109}Cd	88.0	^{137}Cs	661.7
^{57}Co	122.1	^{54}Mn	834.8
^{139}Ce	165.9	^{65}Zn	1115.5
^{203}Hg	279.2	^{60}Co	1173.2 and 1332.5
^{113}Sn	391.7	^{88}Y	1836.1

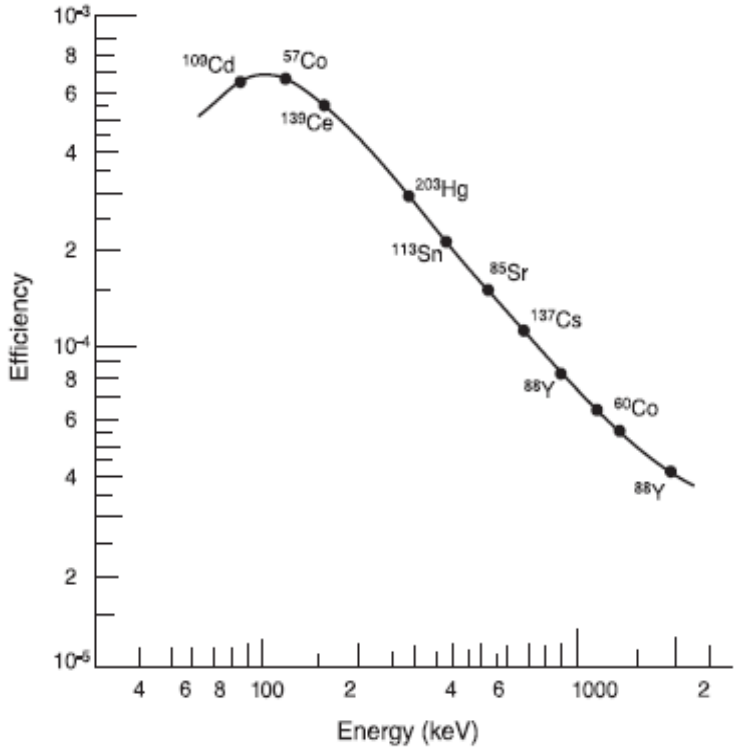

Figure IX.8. Efficiency calibration curve (http://www.canberra.com/literature /fundamental-principles/).

Efficiency calibrations are typically done in pure water solutions with the density of approximately 1 g/ml. Calibration curves are determined for all geometries used in actual sample measurements, i.e. for different sample vials, volumes and distances from the detector. When a liquid sample has an essentially different density than that of water, for example, in the case of solutions with high salt concentrations, self-absorption of gamma rays in the sample creates an additional challenge. This is more important with low energy gamma rays. For this kind of samples additional

calibrations are needed to account for the density. Even more challenging is the calibration of solid samples due to the lack of proper solid standards with certified radionuclide activities. One can prepare own solid standards by mixing radionuclide standard solution with the solid matrix, sediment for example, and evaporating the solution. When using these kinds of in-house standards the composition of the actual samples should not essentially vary from that of the standard. Another way to do the efficiency calibration for solid samples is to use computational methods, for example by using Monte Carlo computer models. In these, the self-absorption is calculated by taking into account the density and elemental composition of the sample.

Interpretation of gamma spectra

In the interpretation of gamma spectra all three major atomic scale interaction processes of gamma rays with detector material need to be taken into account. These are photoelectric effect, Compton effect and pair formation (Figure IX.9).

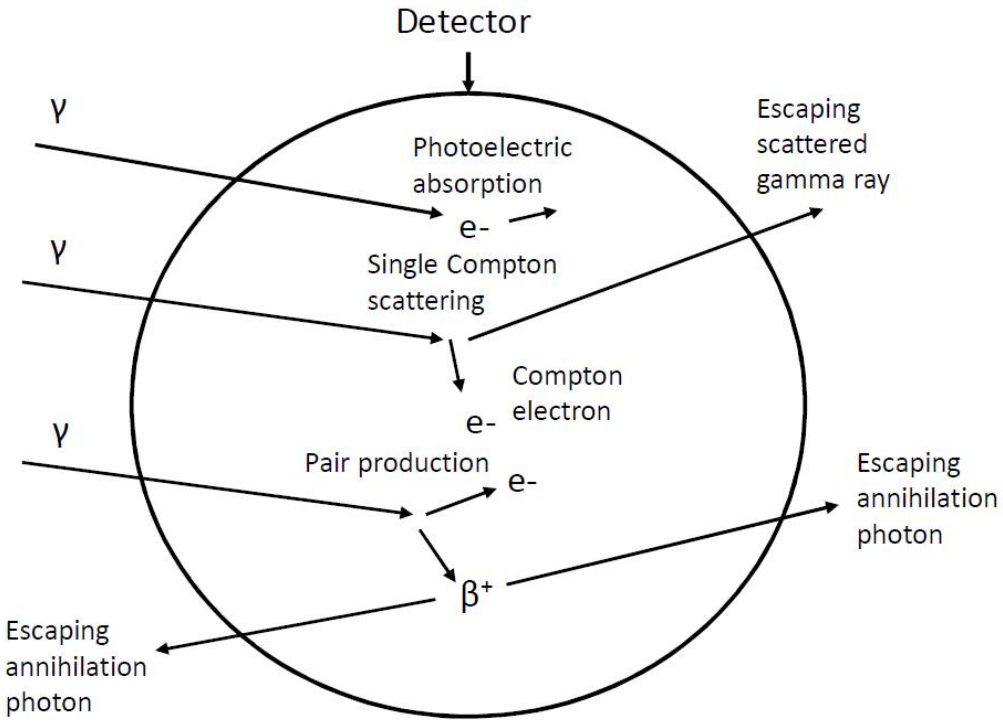

Figure IX.9. Photoelectric effect, Compton effect and pair formation in a gamma detector (circle) and escape of gamma rays from the detector.

In the photoelectric effect a gamma ray loses its energy to a shell electron and these electrons create electric pulses of approximately same height. These can be seen as a peak in the gamma spectrum

(IX.9, left side). Another area in the spectrum (IX.9, middle) is the Compton continuum, which is created when gamma ray loses only part of its energy to an electron and the scattered gamma ray escapes the detector. If Compton-scattered gamma ray will not escape the detector but loses its residual energy in a further photoelectron event the created total electric pulse will go to the photopeak area. Varying proportion of the gamma energy is lost to Compton electrons and therefore a continuum is seen. Compton electrons do not, however, have continuous energy between zero and the photopeak energy (E_γ) but their spectrum ends at about 200 keV less than the E_γ. This is due to fact that the maximum energy that the gamma ray can lose is when it is scattered to opposite direction to its initial path and the maximum energy of the scattered gamma ray in this case is about 200 keV less than its initial energy, more or less irrespective of the initial energy. Thus a valley is created between the Compton continuum and the photopeak. As seen from the right side of the Figure IX.10 there are, however, pulses in this valley. These are due to simultaneously occurring multiple Compton events and summation of the ensuing electric peaks. At part of such summation pulses go to the photopeak area and they need to be subtracted in the way later described.

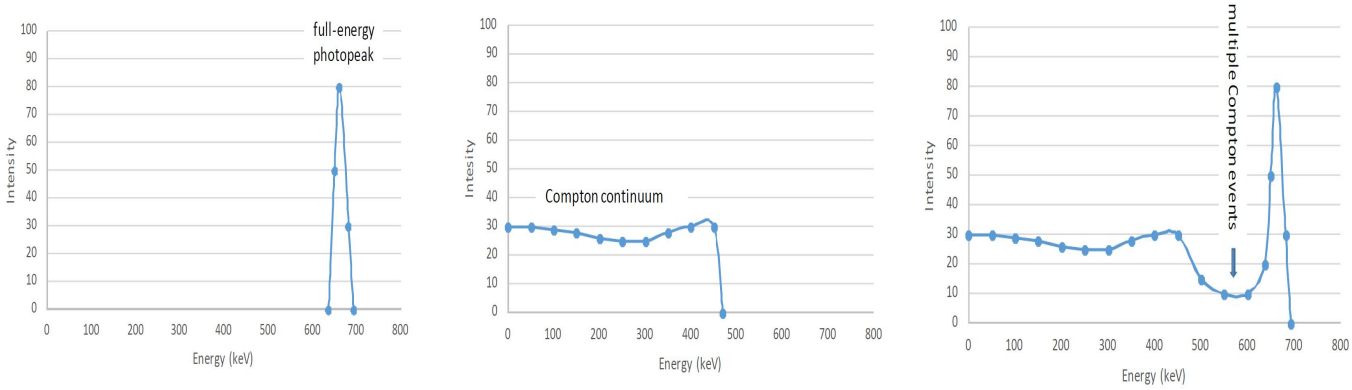

Figure IX.10. Photopeak, Compton continuum and their combination in a gamma spectra.

Gamma rays with energies higher than 1.022 MeV may undergo pair formation, i.e. turn into an electron and a positron. If they both lose their energy in the detector an electric pulse goes to the photopeak area. However, since the positron is not stable but annihilates after losing its kinetic energy with an electron to form two gamma rays of 0.511 MeV energy. In the case where one of these escapes the detector, a peak at E_γ - 0.511 MeV is created and correspondingly a peak at E_γ - 1.022 MeV when both annihilation gamma rays escape (Figure IX.11).

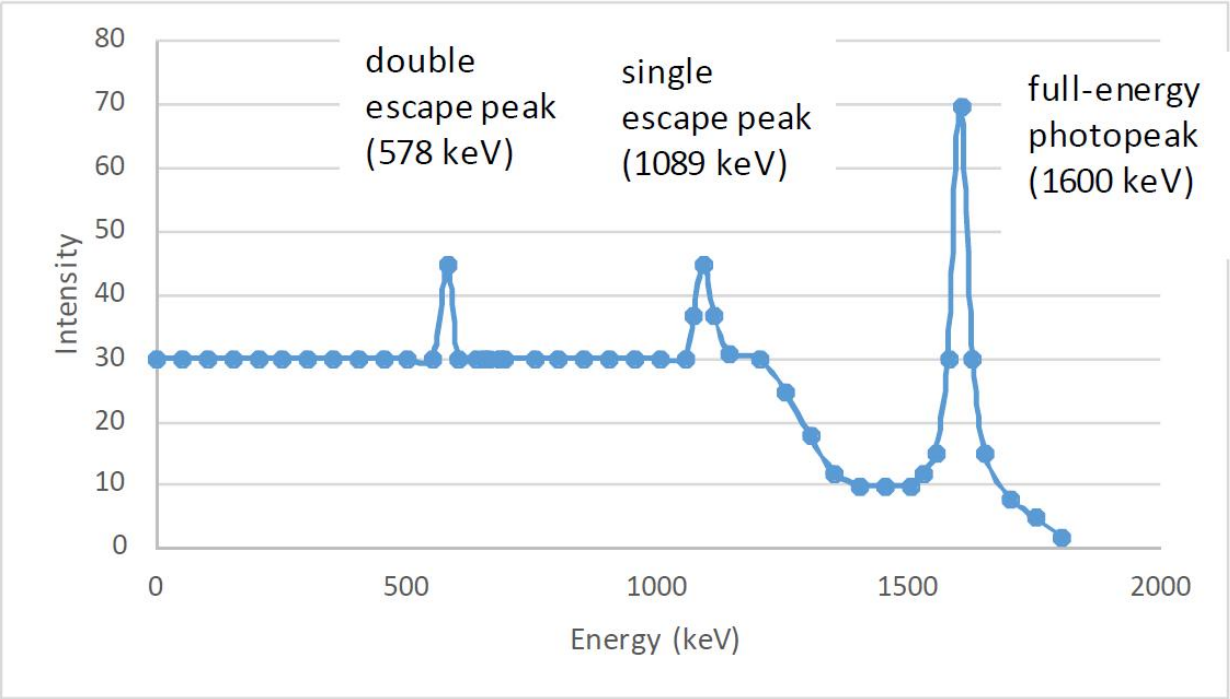

Figure IX.11. Peaks appearing in a gamma spectrum due to pair formation and escape of annihilation gamma rays from the detector.

Still there may be additional peaks in gamma spectra. If two gamma rays simultaneously lose their energy in the detector a sum peak will be formed which is called coincidence summing. Furthermore, X-rays formed after electron capture, internal conversion and formation of Auger electrons may appear at the low energy region, but only when broad energy detector (BEGE) is used. In summary, gamma spectra are complicated, especially when several radionuclides are measured from same sample. Fortunately, there are computer programs, such as the SAMPO program, that take care of the peak analysis.

Subtraction of background

From gamma spectra radioactivities are determined from net peak areas of the photopeaks. In total peaks there are background counts created by external radiation, electric noise, Compton background of the radionuclides, if any, with higher photopeak energy and from multiple Compton events of the measured radionuclide. To get the net peak area the Compton background pulses are subtracted in the way presented in Figure IX.12. In addition, the pulses coming from external

sources are subtracted from net peak area based on a separate background measurement but only if there is a peak, corresponding to the measured photopeak, in the background spectrum.

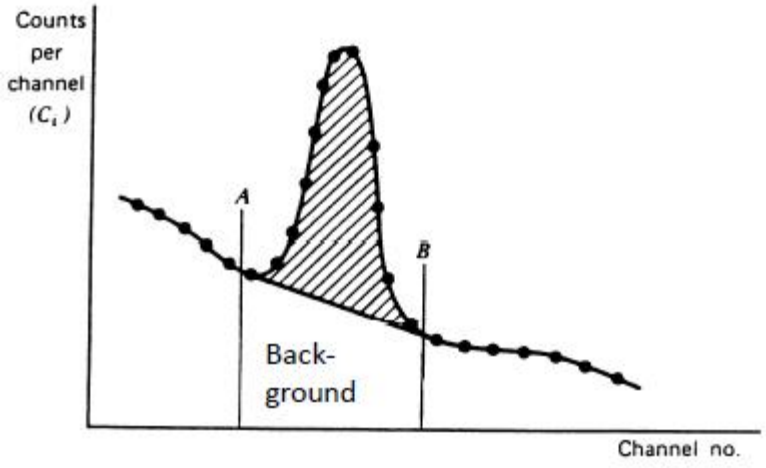

Figure IX.12. Subtraction of Compton background from gross photopeak area.

Sample preparation for gamma spectrometric measurement

Typically gamma spectrum is measured from samples without pretreatment by packing the sample into vial used in efficiency calibration. Also, the sample volume needs to correspond to a calibrated volume. Sometimes, however, pretreatment of samples is necessary. In cases where the activity concentration is so low that the activity of the target nuclide cannot be determined in a reasonable time, preconcentration is needed. For example, ^{137}Cs concentration in natural waters is usually so low that even measuring one-liter samples does not allow its detection in a reasonable time. Thus ^{137}Cs is preconcentrated by evaporation into a smaller volume or is chemically separated, for example, by precipitation with ammonium phosphomolybdate. The latter method also separates efficiently ^{137}Cs from interfering radionuclides and thus gives a more accurate result.

X GAS IONIZATION DETECTORS

Content

Ionisation chamber

Proportional counter

Geiger-Műller counter

Dead-time

Use of Geiger-Műller and proportional counters

Photons and particles emitted in radioactive decay ionize gas molecules which phenomenon is utilized in detection and measurement of radiation. In detectors based on the gas ionization, the ionizable gas is inside a metal chamber, which has typically a cylinder shape and is called tube. A voltage is applied to the tube so that the metal wall acts as cathode and a metal wire in the middle of the tube as anode (Figure X.1).

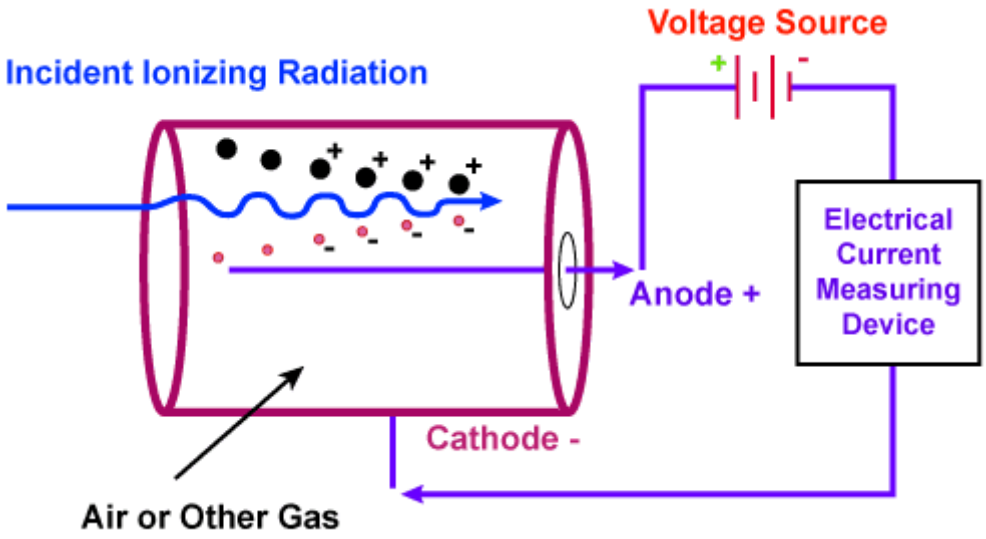

Figure X.1. Gas ionization detector (http://www.equipcoservices.com/support/tutorials/introduction-to-radiation-monitors/).

Gamma radiation penetrates the tube wall and ionizes the filling gas whereas beta and alpha radiations are not able to penetrate the wall. For the detection of alpha and beta active sources they either need to be placed inside the tube or the tube needs to have a penetrable window made of glass, mica or plastic. For the detection of external alpha radiation the window thickness should be

very small. The filling gas is typically noble gas, such as argon, that the radiation ionizes to Ar^+ ions. Due to electric field applied between the electrodes these argon cations transfer towards the cathode, the tube wall, while the electrons transfer towards the anode, the metal wire in the middle of the tube. From the anode wire the electrons are transported through an external circuit to the tube wall where they neutralize Ar^+ ions back to Ar atoms. The electrons going through the external circuit are registered as an electric pulse representing an individual radiation absorption event. Thus the number of electric pulses corresponds to the number of radiation absorptions in the tube which in turn corresponds to the number particles or photons hitting the tube, i.e. the number of pulses corresponds to the activity of the source detected. As will be explained below the height of a pulse corresponds to the energy of a particle or a photon being absorbed in the tube in the case of two modes of gas ionization detectors (ionization chamber and proportional counter) but not in the third mode (Geiger-Műller counter). Depending on the voltage applied across the tube there are three types of gas ionization detectors (Figure X.2).

- Ionization chamber
- Proportional counter
- Geiger-Műller counter

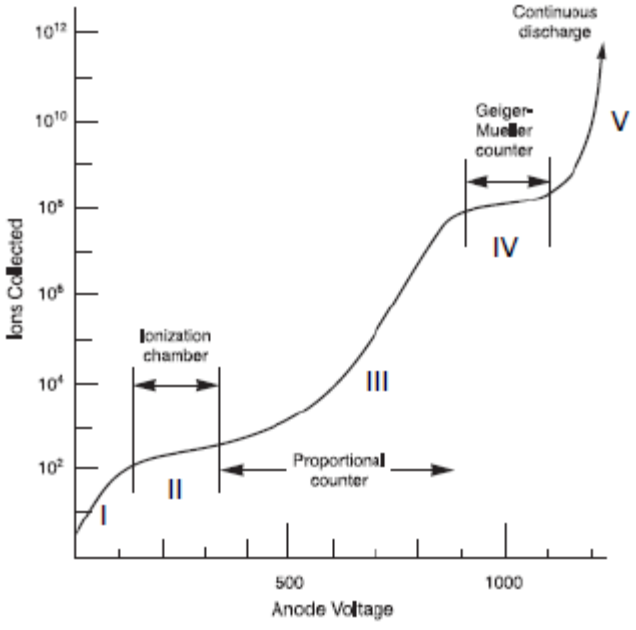

Figure X.2. Operation ranges of three gas ionization detectors as a function of high voltage applied across the tube (http://www.canberra.com/literature/fundamental-principles/).

Ionization chamber

In the low voltage region, below about 50 V in Figure X.2, the velocities of the electrons and the Ar^+ ion, induced by radiation absorption, towards the electrodes are so low that part of them are recombined back to Ar atoms before reaching the electrodes. This area (I in Figure X.2) is called recombination area. As the voltage is high enough to prevent recombination, all electrons and cations are collected to the electrodes. This area (II) is seen in Figure X.2 as about a 200 V wide area in the range of 130-330 V. In this range the number of ions (or electrons) collected on the electrodes is independent of the voltage applied. Gas ionization detectors operating at this voltage area are called ionization chambers. Since all ions and electrons are collected on the electrodes the height of the electric pulse recorded is proportional to the energy of the particle losing its kinetic energy in the filling gas. The higher is the initial energy the more there is ionization in the chamber and consequently the higher is the electric pulse recorded. Alpha particles have typically very high energies and they also cause very high specific ionization. Therefore, the pulses observed from alpha particles are much higher than those from beta particles. Ionization chambers are typically used for the detection of alpha radiation, for the measurement of absolute activities of radioactive sources and in radiation monitoring and dosimetry. In typical radionuclide laboratories, however, ionization chambers are very seldom used for activity measurements.

Proportional counter

As the voltage is further increased from ionization chamber operation range the electrons have such a high energy that they cause additional, secondary ionization. In this range (III) the height of the electric pulse is dependent on the voltage applied. A gas ionization detector working in this range is called proportional counter since the height of the electric pulse, at constant voltage, is proportional to the energy of the photon or particle losing its energy in the filling gas by ionizations. This is because the amplification of the electrons due to secondary ionizations is constant providing that the voltage remains the same. Thus, as in case of ionization chamber the proportional counter can be used in nuclear spectrometry, i.e. in determination of alpha and beta particle energies. As seen in Figure X.2 the amplification factor of electrons in proportional counters is up to about 10^5. Since the pulse height is highly dependent on the voltage proportional counters need very stable high voltage sources. The advantage of proportional counter compared to ionization chamber is that the observed pulse is much higher and thus easier to detect.

Geiger-Műller counter

As the voltage is further increased from the proportional counter area all individual particles or photons cause complete ionization of the filling gas (area IV). This means that the observed electric pulses have the same heigth and are thus independent of the energy of the particle or photon losing its energy in the tube. Thus Geiger-Műller counter cannot be used in nuclear spectrometry but only in pulse counting, i.e. determination of activities or radiation intensities. The amplification of electrons in a Geiger-Műller tube is in the range 10^6-10^7. Thus the pulses are in the volt range and no amplifiers are needed unlike in ionization chambers and proportional counters. As seen in Figure XI.2 the number of electrons (pulse height) is more or less constant in about 200 V wide voltage range. Since the plateau has not exactly a constant value the high voltage source needs to be stable. In good Geiger-Műller tubes the slope of the plateau is below 1%. As the voltage is still increased from the Geiger-Műller voltage range there will be a continuous electric discharge (area V) which can destroy the tube rather quickly.

In addition to argon (or neon) the filling gas in GM tubes contains about 10% of halogen or organic gas, such as ethyl alcohol, which act as quenching gases. As the argon ions approach the cathode or when they hit it they may cause additional ionization which in turn causes additional erroneous pulses. As the ionization potentials of halogens and ethyl alcohol are lower than that of argon, Ar^+ ions transfer their positive charges to them when hitting them. These in turn do not cause additional ionization and their positive charge is neutralized on the surface of the cathode.

Dead-time

When recording high pulse rates in GM tubes and in proportional counter (as also in most other radiation detectors) one needs to take into account the dead-time. As the argon gas ionizes, the induced electrons travel very fast to the anode while the positive argon ions travel much slower which causes a very low electric field near the anode (Figure X.3). The detector is then unable to record pulses that are caused from new radiation absorption events due to the travel of argon ions towards the cathode and recovery of the filling gas back to argon atoms. The time when the detector cannot record new pulses is called dead-time and it is marked with τ.

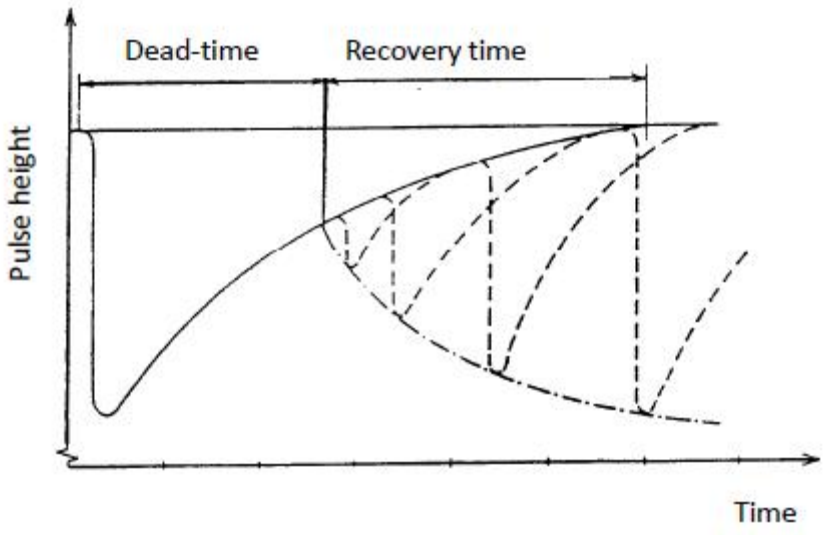

Figure X.3. Pulse shape in proportional and Geiger-Műller counters.

When so high count rates are measured that the dead-time becomes important the observed count rates need to be corrected for dead-time τ (unit s). For that we mark observed count rate by R (imp/s) and the true count rate by R_0 (imp/s) that would be observed if there was no dead-time. Because of the dead-time, R_0 - R impulses in each second remain unrecorded. On the other in each second the tube is unable to record impulses a time $R \times \tau$ during which $R_0 \times R \times \tau$ photons or particles hit the detector. Thus

$$R_0 - R = R_0 \times R \times \tau, \text{ from which we solve } R_0 \qquad [X.I]$$

$$R_0 = R/(1-R\times\tau) \qquad [X.II]$$

This equation can be used to correct the observed count rate to true count rate as far as the dead-time of the tube is known. For example, if the observed count rate is 1000 imp/s and the dead-time is 0.2 ms the true count rate is $1000/(1-1000\times0.0002) = 1250$ imp/s or 25% higher than the observed one. At ten times lower count rate 100 imp/s the true count rate is only 2% higher.

In GM tubes the dead-time is 0.1-0.4 ms while in proportional counters it is much shorter, only a few microseconds. Therefore, a proportional counter can be used to measure a hundred times higher count rates without the essential effect of dead-time. If proportional counter is used not only for pulse counting but also for nuclear spectrometry the highest count rates should, however, be avoided since the tube has, in addition to dead-time, also a recovery time (Figure X.3). If a new

particle is recorded during the recovery time the pulse height response of the tube is higher than when each particle is recorded completely individually without overlap. The total recovery time in proportional counters is much higher than the dead-time, around 0.1 ms.

Use of Geiger-Műller and proportional counters

Still in the 1950's GM tubes were the most typical detectors for radiation measurements. For the activity measurements of individual radionuclides they needed to be first chemically separated from other radionuclides. Development of solid scintillation and semiconductor detectors have almost completely made chemical separation of gamma-emitting radionuclides unnecessary and thus also replaced gas ionization tubes in their measurements. Furthermore, liquid scintillation counting has mostly replaced measurement of beta-emitting radionuclides with gas ionization detectors. The gas ionization detectors are, however, still in extensive use, especially in radiation protection for the measurement or radiation doses and dose rates as well as in detection of surface contamination. In addition, GM tubes can be used in teaching since they are cheap and easy to operate and instead of more sophisticated equipment they can be used to demonstrate some basic features in radiation measurements. Basically GM tubes can be used to measure all types of radiation. Gamma radiation is readily penetrating and counting efficiencies are only 1-2%. Thus GM tubes are used only for gamma dose and dose rate measurements. All beta and alpha particles entering the tube create electric pulse. However, to enter a tube the alpha and beta sources either need to be placed inside the tube or the window between the source and the tube should be very thin. For alpha radiation the thin window is made of plastics and these types of tubes are used to detect alpha contamination from various surfaces. For beta radiation the thin (0.1 mm) windows are made of mica, glass or beryllium but even these are too thick to allow measurement of the lowest beta energies, such 18 keV beta energies of tritium. Even though scintillation counting today is a standard method for beta counting, a gas ionization detector has one important advantage over it: the background is much lower which enables measurement of lower activities. An example of such equipment is the Risö Beta Counter (Figure X.4) which is a rather simple equipment and easy to operate. It has five sample positions for sources prepared after chemical separation and individual GM-tubes for each sample position. The samples are shielded against external radiation by lead shield and a guard counter that detects external radiation passing through the lead shield and subtracts the count rate observed in the guard detector from the total observed count rate. With this equipment the background count rate is typically only 0.2 cpm compared to at least ten times higher background observed with liquid scintillation counting.

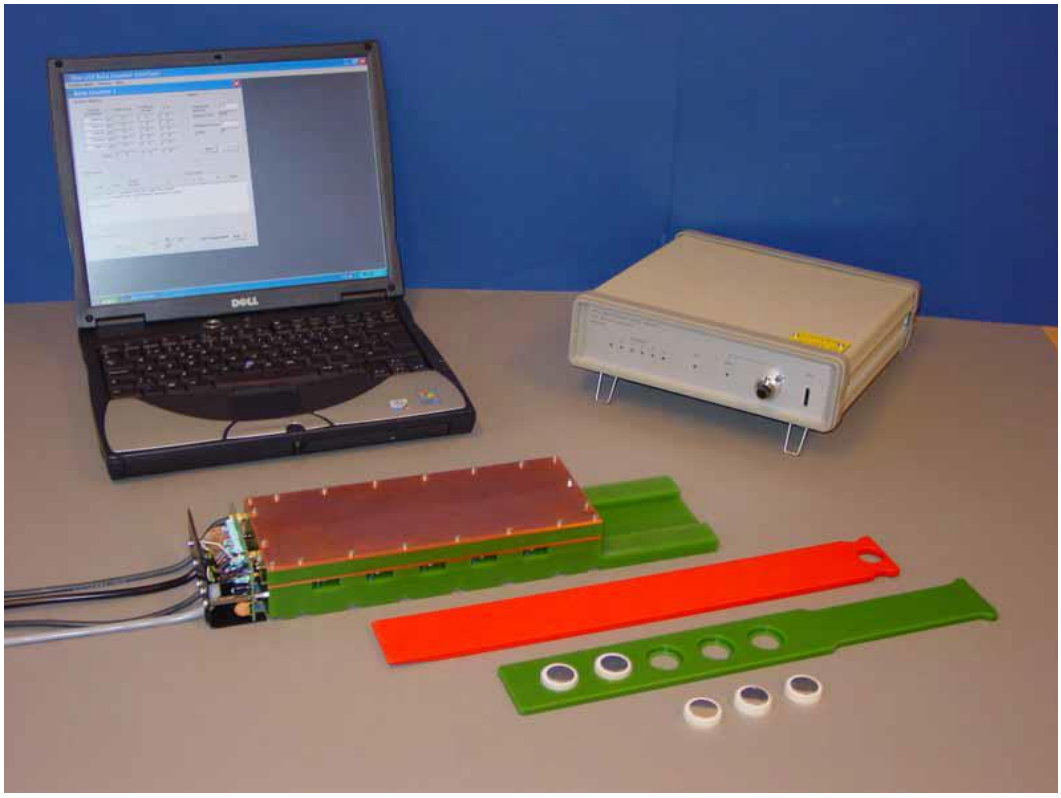

Figure X.4. Risö Beta Counter (http://www.nutech.dtu.dk/english/Products-and-Services/Dosimetry/Radiation-Measurement-Instruments/GM_multicounter).

Neutrons as neutral particles do not cause any ionization in gas ionization detectors. To detect neutrons the tube is filled with BF_3 gas where boron is enriched with respect to ^{10}B isotope. In this gas the neutrons cause the following nuclear reaction:

$$^{10}B + n \rightarrow {}^{7}Li + {}^{4}He \qquad [X.III]$$

and the emitted alpha particles and the recoiled lithium atoms cause ionization of the gas which makes the neutron detection and counting possible.

XI ALPHA DETECTORS AND SPECTROMETRY

Content

Semiconductor detectors for alpha spectroscopy

Alpha spectrometry

Sample preparation for alpha spectrometry

In an ordinary radiochemical laboratory the alpha-emitting radionuclides studied are those listed in Table XI.I. Of these Po, Ra, Th and U isotopes are naturally occurring radionuclides while Pu and Am isotopes are artificial transuranium nuclides. The natural alpha-emitting radionuclides belong to the decay series beginning from ^{238}U, ^{235}U and ^{232}Th. The sources of the transuranium elements are the the nuclear weapons tests in the 1950' and 1960's and of the Chernobyl accident in 1986 as well as the nuclear waste, especially the spent nuclear fuel. Some of these radionuclides, such as ^{235}U, ^{226}Ra and ^{241}Am emit gamma radiation, which can in some cases be used for their measurement. The intensities and/or gamma ray energies are, however, typically so low that the gamma spectrometric measurement does not yield accurate results. Moreover, gamma spectrometry does not allow determination of isotopic composition of uranium, which is important information in many studies. Accurate measurements, enabling also determination of isotopic compositions, are obtained either by alpha spectrometry of by mass spectrometry. The former is discussed here in this chapter.

Table XI.I. Most typical alpha-emitting radionuclides studied in radiochemical laboratories.

Nuclide	Half-life (y)	Alpha energies (MeV) - Intensities (%) in parenthesis
^{210}Po	0.38	5.310 (100)
^{226}Ra	1600	4.784 (94.4), 4.601 (5.6)
^{228}Th	1.91	5.520 (71.1), 5.436 (28.2)
^{230}Th	75400	4.770 (76.3), 4.702 (23.4)
^{232}Th	1.4×10^{10}	4.083 (77.9), 4.019 (22.1)
^{234}U	245000	4.859 (71.4), 4.796 (28.4)
^{235}U	7.0×10^{8}	4.474 (57.2), 4.441 (18.8), 4.288 (6.0), 4.676 (4.7), 4.635 (3.9) etc.
^{238}U	4.5×10^{9}	4.270 (79.0), 4.221 (20.9)
^{238}Pu	88	5.499 (70.9), 5.456 (29.0)
^{239}Pu	24100	5.157 (70.8), 5.144 (15.1), 5.105 (11.5)
^{240}Pu	6560	5.168 (72.8), 5.124 (27.1)
^{241}Am	433	5.486 (84), 5.443 (13)

Semiconductor detectors for alpha spectroscopy

Semiconductor detectors were discussed already in chapter IX where gamma spectrometry was described. In gamma spectrometry the detector material is germanium whereas in alpha spectrometry the material is silicon. The principal idea in both is the same. They are both diodes composing of an n-type Si/Ge, having an electron donor additive, such as phosphorus, P(V), and a p-type Si/Ge, having an electron acceptor additive, such as boron, B(III). When these are attached to each other a depletion zone is developed around the interface due to combination of electrons and holes on the interface. When a reverse bias voltage is applied across the crystal this depletion zone widens. These are transferred close to electrodes due to the voltage applied. The thickness of the zone is dependent on the voltage applied being typically only 40-60 V in silicon alpha detectors. For the detection of gamma rays the depletion zone needs to be thick, several centimeters, in order to absorb the readily penetrating gamma rays. This is accomplished by using a larger crystal made of very pure germanium and by using a high voltage up to 5000 V. In the case of alpha detection with Si-detectors the depletion zone should be very thin due to the short range on alpha particles in silicon, only 30 μm. Typically the depletion zone in silicon detectors used in alpha spectrometry is 100-200 μm. There are two types of silicon detectors in production (Figure XI.1): surface barrier

detectors (SBB) and passivated ion-implanted detectors (PIPS) the latter being a more modern construction mode.

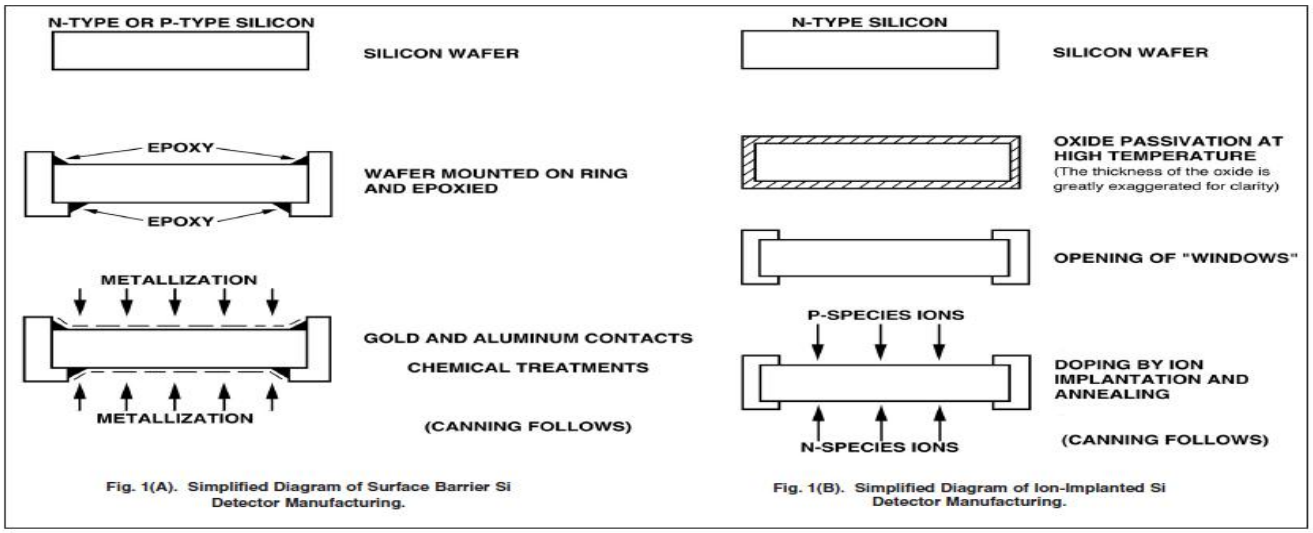

Figure XI.1. Production of silicon detectors for alpha spectrometry. Left: surface barrier detectors. Right: Passivated ion-implanted detector. (http://www.ortec-online.com/Products-Solutions/RadiationDetectors/silicon-charged-particle-detectors.aspx).

To produce a detector, the edges of a silicon wafer, with thickness less than 500 µm, are first insulated from each other to prevent continuous current across the wafer. In SBB detectors the insulation is done with epoxy resin and a ring mounted around the wafer. In PIPS detectors the surface of the wafer is first passivated by heating which results in the formation of about 50 nm thick non-conducting SiO_2 layer. This layer is removed from the middle of both sides of the wafer. To transform the silicon wafer into a diode the other side is treated with acceptor atoms producing p-type layer and the other side with donor atoms to produce n-type layer. In the SBB detectors this is accomplished by forming a thin, 100-200 nm, layer of Au on the other side (n-type) and a layer of Al on the other (p-type). In PIPS detectors this is done by ion-implantation technique by bombarding high energy atoms on the sides. The PIPS detectors have several advantages over SSB detectors:

- The surface layer is mechanically and chemically more resistant and can be cleaned with alcohol, for example. In SBB detectors the gold surface is very sensitive and cannot be touched at all.
- The “window”, the passive layer on the surface is somewhat thinner resulting in a better energy resolution.

The detectors are rather small in size (Figure XI.2.) Their diameters are only 2 to 4 centimeters and thickness less than 500 µm (about 1 cm including the metallic cover). Table XI.II. shows properties of alpha detectors available from Canberra. As seen from the table the resolution is very good, 20-40 keV. Resolution is here determined for ^{241}Am 5.486 MeV alpha particles. Thus the relative resolution is 4-8%. The resolution is better for the smallest detectors, being about two-times better for the smallest detector in Table XI.II compared to the largest. The background in alpha detectors is very low, only 4-16 counts per day being directly proportional to the surface area of the detector. The background is almost solely caused by cosmic radiation. It is evident that the counting efficiency is better for the larger crystals. Thus one needs to make a compromise with respect to resolution on the one hand and to counting efficiency on the other when selecting a detector. The selection depends naturally on what is needed, high resolution or high efficiency. When measuring alpha activities in environmental and biological samples the activity levels are typically very low requiring very long counting times. In this case a larger detector would be desirable. On the other hand, the background pulses increase with detector size and the overall performance is also dependent on the sample size in comparison with the detector size. In some cases highest possible resolution is a priority. For example, typically ^{239}Pu and ^{240}Pu activities cannot be measured individually from an alpha spectrum due to overlap of their alpha peaks. Using a high-resolution alpha detector one may distinguish these two nuclides by deconvolution technique separating overlapping peaks with a mathematical fitting process.

Figure XI.2. Canberra alpha detectors (http://www.canberra.com/products/detectors/pdf/passivated_pips_C39313a.pdf).

Table XI.II. Properties of Canberra silicon detectors for alpha spectrometry (http://www.canberra.com/products/detectors/pdf/passivated_pips_C39313a.pdf).

Active area (mm^2)	Diameter (mm)	Alpha resolution (keV)	Typical background (counts per day)
300	20	17	4
450	24	18	18
600	28	22	22
900	34	25	25
1200	39	32	32

Alpha spectrometry

Figure XI.3 shows the components of an alpha spectrometer. The planar sample is placed in front of the detector and close to it. Both detector and sample are placed in a vacuum chamber to prevent absorption of alpha particles in air. The voltage (40-60 V) across the detector is supplied by the bias supply. Pulses created in the detector are amplified first in a preamplifier and then in a linear amplifier. The pulses are transformed into digital form in analog-to-digital-converter (ADC) and directed into multichannel analyser (MCA) for counting pulses and determining their heights.

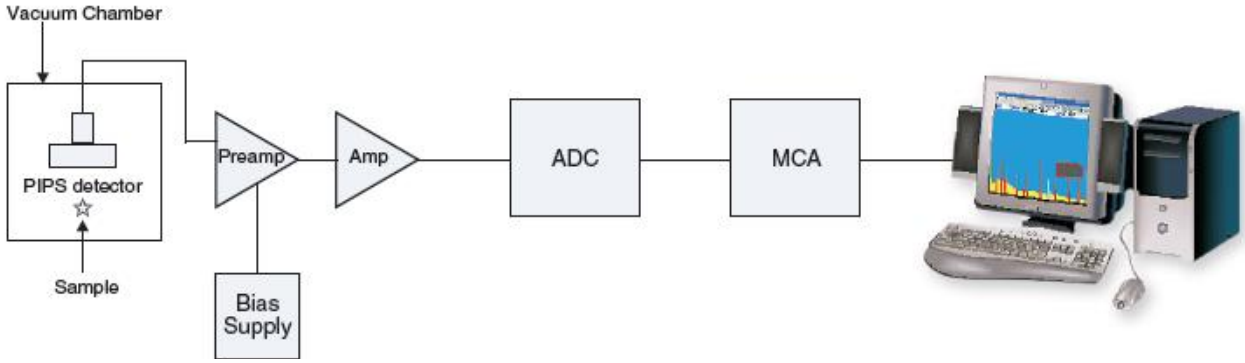

Figure XI.3. Electronics in alpha spectrometry (http://www.ortec-online.com/Products-Solutions/RadiationDetectors/silicon-charged-particle-detectors.aspx).

Prior to counting the alpha-emitting radionuclides, they need to be separated from sample matrix for two reasons. First, alpha particles readily absorb on sample matrices, solid or liquid, and cannot be directly determined from them. In addition, separation is needed from other alpha-emitting radionuclides due to overlapping alpha peaks (see Table XI.I). In nuclear waste samples a typical set of alpha-emitting radionuclides is the isotopes of uranium, plutonium and americium. In environmental samples, such as surface soil and surface waters, this set includes also isotopes of

thorium, ^{226}Ra and ^{210}Po. In geological samples, not affected by radioactive fallouts and nuclear waste, the typical combination includes isotopes of uranium and thorium and ^{226}Ra and ^{210}Po. There are also some other minor components, such as ^{237}Np, but these typically do not interfere with the measurement of the major components. Radiochemical separations used to separate the alpha-emitting radionuclides as pure components are not discussed in this book. A comprehensive presentation of them can be found from another book of the author of this book, J.Lehto and X.Hou, Chemistry and Analysis of Radionuclides, Wiley-VCH, 2010, 400 pages. In the radiochemical separations the chemical separation methods used comprise of precipitation, ion exchange, solvent extraction and extraction chromatography.

Sample preparation for alpha spectrometry

At the end of a radiochemical separation procedure a counting source for alpha spectrometry is prepared. This is done either by electrodeposition of the target element on a steel plate or by microcoprecipitation. The purpose of both methods is to produce a very thin counting source to prevent absorption of alpha radiation in the source. With this respect the electrodeposition method yields a better, thinner, source but in most cases the performance of microcoprecipitation is also satisfactory. In electrodeposition, the solution observed at the end of radiochemical separation and containing the target nuclide is poured into an electrodeposition vessel and mixed with ammonium, sulphate, chloride, oxalate, hydroxide or formate as electrolyte and the solution is made slightly acidic. A metal disk - usually made of polished steel or sometimes platinum - is tightly mounted to the lower part of the electrodeposition vessel. A platinum wire is put in the vessel and a constant current (10-150 mA/cm^2) is set up between the platinum wire and the metal disk so that the platinum wire operates as anode and the metal disk as cathode (Figure XI.4). The current causes a reduction of the metals in the solution and their deposition in metallic form or as hydroxides on the surface of the steel plate. ^{210}Po is spontaneously deposited on a silver disc and in its sample preparation no electric current is needed.

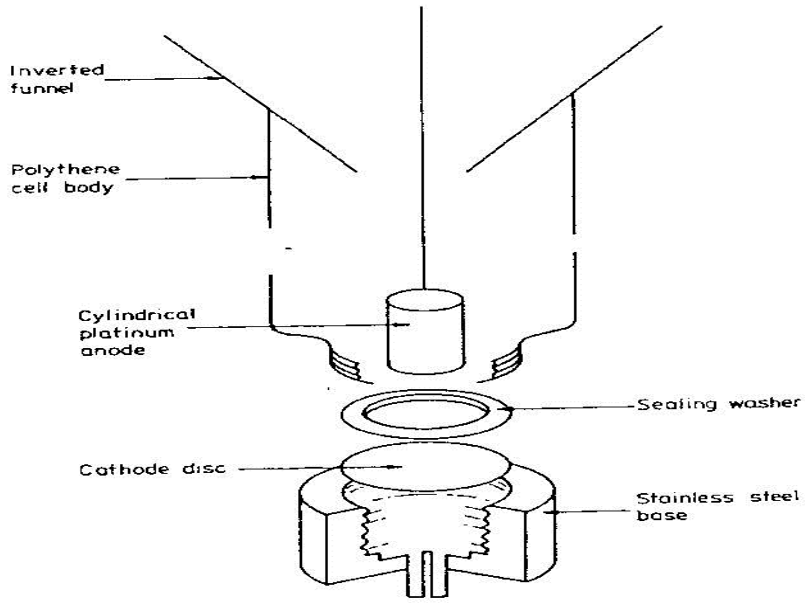

Figure XI.4. Electrodeposition equipment (Holm, E., Source preparations for alpha and beta measurements, Report NKS-40, 2001).

Another way to prepare counting sources is microcoprecipitation typically used for actinides. The coprecipitation is carried out with lanthanide fluorides: 10–50 μg La, Ce or Nd is added to the solution and the fluoride (LaF_3, CeF_3, NdF_3) is precipitated through the addition of HF. Since actinides will only coprecipitate with lanthanide fluoride if they are at their lower oxidation states of +III and +IV the higher oxidation states must be reduced prior to coprecipitation. After precipitation, the precipitate is collected by filtration on a membrane filter, dried and mounted on the measurement plate with glue for alpha counting. The sample to be measured for radium can be prepared by microcoprecipitation with barium sulphate. Because the mass, and so the self-absorption of the sample, is larger, the resolution obtained after microcoprecipitation will be somewhat poorer than after electrodeposition. Microcoprecipitation is a distinctly more rapid technique, however, and the resolution is usually adequate.

The activity of an alpha-emitting radionuclide in an alpha spectrometric measurement following a radiochemical separation is typically determined by adding a tracer to the sample prior to the radiochemical separation. The tracer is another alpha-emitting radionuclide of the target radionuclide element. For all radionuclides given in Table XI.I except ^{226}Ra there is a suitable artificial alpha-emitting tracer. For example, when activity of the naturally occurring radionuclide ^{210}Po is determined in an environmental sample a known activity amount of ^{209}Po (or ^{208}Po) is added to the sample at the start of the radiochemical separation procedure. ^{209}Po is an artificial

radionuclide produced from ^{209}Bi in a cyclotron. Both isotopes of polonium behave identically in the course of the separation procedure and the same fraction of both isotopes is recovered in the counting source. Due to their different alpha energies the two isotopes can be distinguished from alpha spectrum (Figure XI.5). The initial activity of ^{210}Po in the sample can now be simply calculated from the added activity of ^{209}Po and the number of counts, the peak areas. If, for example, 1.0 Bq of ^{209}Po was added and the peak areas were 7000 counts for ^{210}Po and 5000 counts for ^{209}Po the activity of ^{210}Po in the sample was 1 Bq × (7000/5000) = 1.4 Bq.

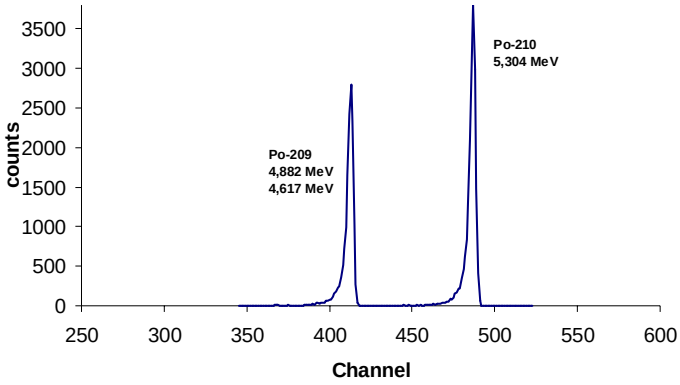

Figure XI.5. Alpha spectrum of naturally occurring ^{210}Po and ^{209}Po tracer.

XII LIQUID SCINTILLATION COUNTING

Content

Liquid scintillation counting is primarily used to measure beta radiation (^{3}H, ^{14}C, ^{32}P). It can, however, also be used for alpha radiation, low energy gamma- or X-rays, as well as measuring conversion- and Auger-electron emitting samples. In addition, the liquid scintillation counters can be utilized in Cherenkov radiation measurement.

The principle of liquid scintillation counting

Liquid scintillation counting is based on the fact that the radioactive sample and a scintillator agent is dissolved into the same solvent. Three components thus comprise the measured sample: a radioactive sample, an organic solvent or solvent mixture, and one or more scintillation agents. The scintillation agent molecules, also called phosphors and fluors, entirely surround the decaying nuclide and thus avoids the harm of self-absorption and offers 4π- counting geometry, in which all emitting particles or rays are detectable.

In the event of the decay of the nucleus the released beta particles collide with the solvent molecules, which are in the majority, and transfer their energy to them. These excited solvent molecules then release energy to other molecules. At some point, the energy is received by the scintillation molecules, which are able to release the excitation energy as light. Using a photomultiplier tube, these light pulses, lasting 3-5 ns, are changed into electrical pulses, their height is measured in an analyzer and registered to the different channels of the multichannel analyzer according to pulse height. The height of the pulse obtained by liquid scintillation counting is proportional to the original energy of the radiation and as the counters are equipped with a multichannel analyzer, they are suitable for energy spectrometry (Figures XII.1-4).

Several commercial scintillation liquid mixtures (scintillation cocktails) for liquid scintillation counting are available, containing both solvents and scintillation agents. Liquid scintillation measurements are generally done in either 20 ml or 6 ml plastic or glass vials, of which polyethylene bottles are the most common.

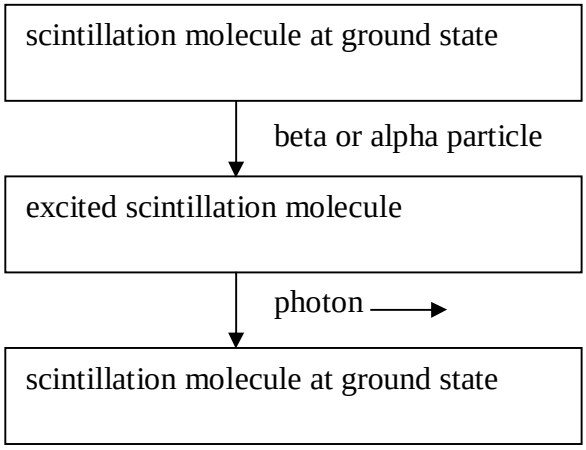

Figure XII.1. Functioning of the scintillation agent.

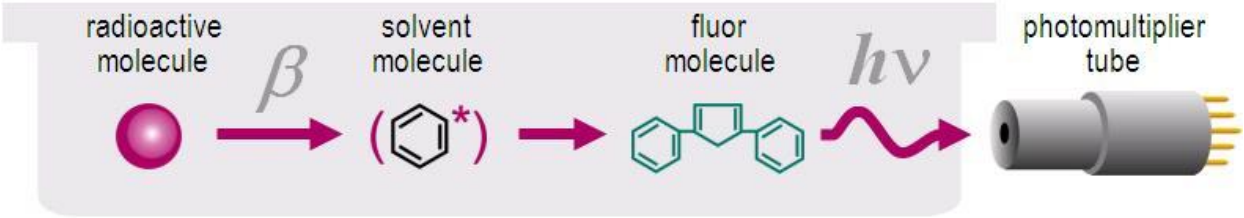

Figure XII.2. Principle of liquid scintillation counting (http://www.perkinelmer.com/ Resources/TechnicalResources).

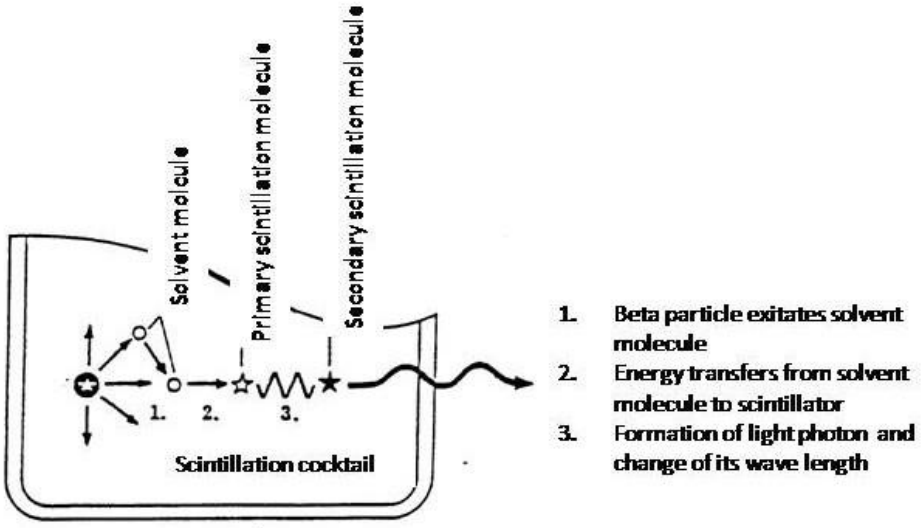

Figure XII.3. The emergence of light pulses in liquid scintillation processes.

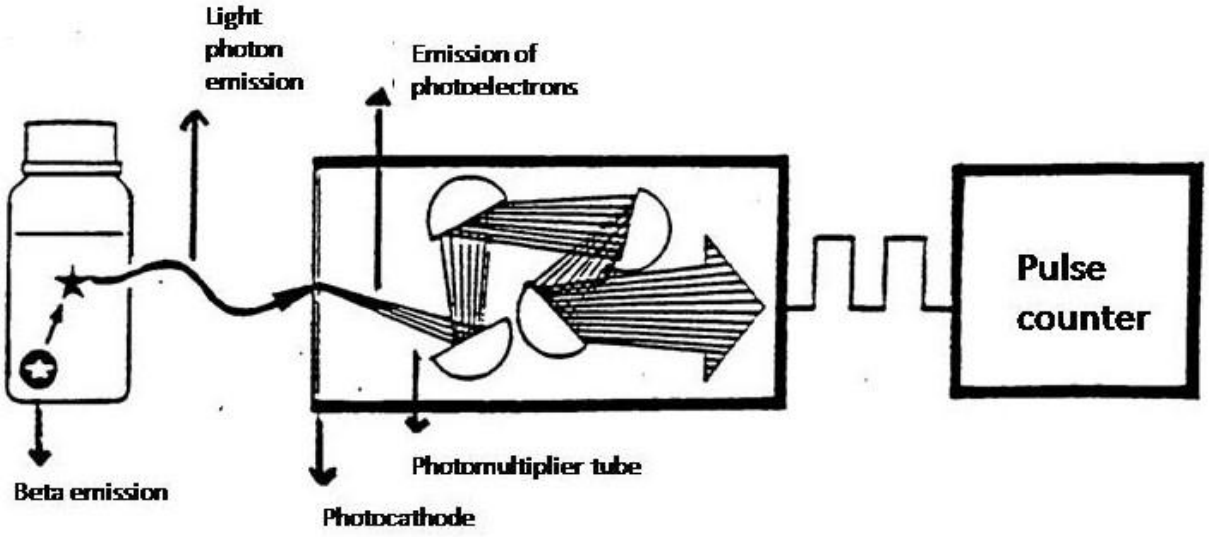

Figure XII.4. Light pulse detection.

Solvents

The solvent component of scintillation cocktail has two functions: it must be able to dissolve the sample and scintillation agent, as well as effectively transfer the energy from radioactive particle or ray to the scintillation agent. The best solvents are the aromatics such as xylene, toluene, benzene, and cumene. Aliphatic solvents, such as 1,4-dioxane and cyclohexane are also used. To improve the dissolution of the sample into the scintillation system, many secondary solvents are also used. The

benefits of the newer liquid scintillation solvents, *e.g.* di-isopropylnaphthalene (DIN) and phenyl–o–xylylethane (PXE), are that they have a lower flammability, volatility and lack of odor, lower toxicity or irritancy, biodegradability, and a better solubility and counting efficiency.

Scintillation agents

Tens of scintillators are recognized for use in liquid scintillation counting. Common ones are p-oligophenyls, or oxazole and oxadiazole compounds. The function of scintillators is to convert as much of the energy received via solvent molecules into light photons. The best scintillation materials have nearly 100% efficiency. Usually the scintillation material alone is not enough, because the sample may absorb light in the emitted wavelength range. In this case, a secondary scintillator is added to the liquid scintillation cocktail, *i.e.* spectrum transfer agents, which after excitation by the light of the primary scintillation emit longer wavelengths. Below are examples of primary scintillation material (PPO) and secondary scintillation material (POPOP).

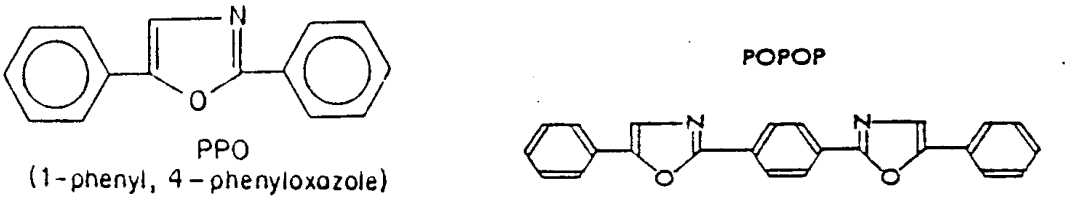

Figure XII.5. Primary scintillation agent PPO (1-phenyl-4- phenyloxazole) and secondary scintillation agent POPOP.

Liquid scintillation counter

The basic element of the liquid scintillation counter is a photomultiplier tube (Figure XII.6), which transforms the light photons into electrons and amplifies them into measurable electrical pulses. At the front end of the photomultiplier tube that the photons hit is a photocathode typically made from Cs_3Sb. When light photons hit the photocathode, it emits electrons. The electrons emitting in the photomultiplier tube are then amplified by dynodes, of which there are 10-14. Between successive dynodes is a voltage applied. The dynodes are also made of Cs_3Sb and when the electrons hit them, the voltage causes the electrons to be amplified due to their growing kinetic energy. The voltage through the tube is 1000-2000V, which causes the electrons to be amplified by a factor of 10^6.

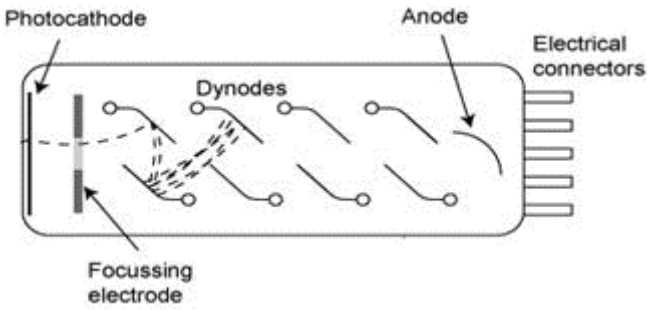

Figure XII.6. Photomultiplier tube (http://mxp.physics.umn.edu/s09/projects/S09_MuonEnergy/details_1.htm).

Liquid scintillation counting is used to detect light pulses with photomultiplier tubes using the coincidence technique (Figure XII.7). The sample is between two photomultiplier tubes, which are situated at an angle of 180° from each other. When the radionuclide decays in the scintillation cocktail, a large amount of light photons are simultaneously (in 10^{-9} s) generated and randomly emitted in every direction. The counter unit only registers pulses coming "simultaneously" (for up to 10^{-7} seconds) from the coincidence unit from both photomultiplier tubes and rejects single pulses coming from only one photomultiplier tube. The coincidence unit of the liquid scintillation counter is an electronic portal, which is open for 10^{-7} s at a time, in other words 100 times the duration of the pulse. With the aid of the coincidence technique the interfering effect of the single pulses is greatly reduced. In this way a lower background is achieved, when the electronic noise of the photomultiplier tubes, pulses from chemiluminescence and phosphorescence, as well as pulses from external radiation are nearly eliminated.

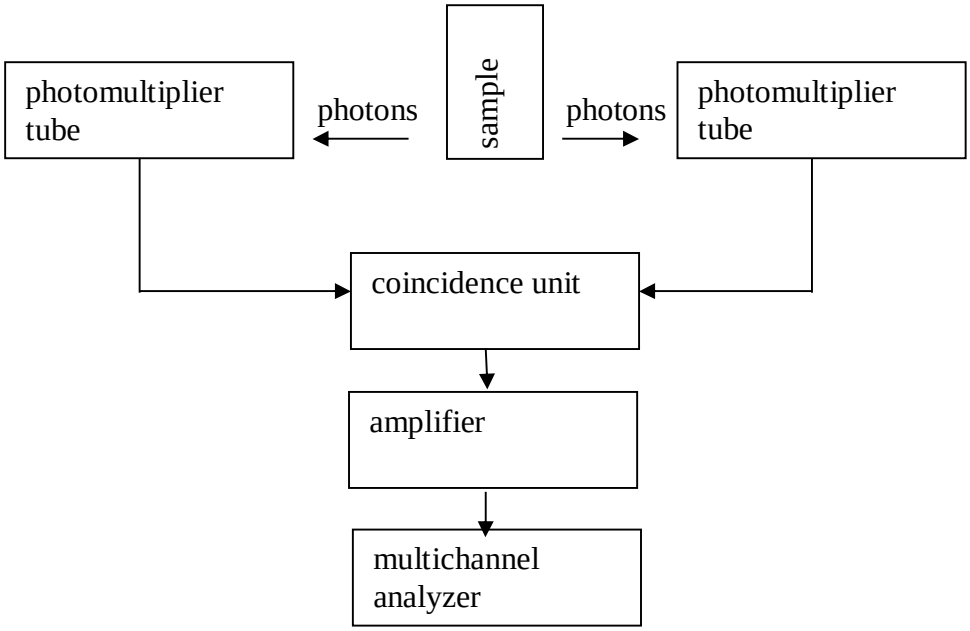

Figure XII.7. Liquid scintillation counter principle.

High count rates are able to be measured by a liquid scintillation counter, because the light pulse lasts only a very short time (10^{-9} s). If, for example, the sample activity is 10^6 Bq (which is so high that it is rarely measured), a decay occurs on an average every 10^{-6} second in a sample. This is 1000 times longer than the duration of a single light pulse and 10 times longer than a coincidence portal is open. Therefore, when measuring even such high activity each pulse can be detected individually without disturbance from the next pulse. From the coincidence unit the pulses go into a multichannel analyzer, which counts the pulses and differentiates them to different channels according to their height. The number of photons generated by liquid scintillation process is proportional to the initial energy of the beta particles. Tritium, for example, with a maximum energy of 18 keV, generates an average of 35 photons and ^{14}C, with a maximum energy of 180 keV, an average 350 photons. As the photomultiplier tube amplifies pulses by a constant factor, the pulses coming into the analyzer are proportional to the energy of the beta particles. Since the energy distribution of particles generated in beta decay is continuous, a continuous spectrum, not a line spectrum, is obtained by the liquid scintillation counter. The measuring of alpha radiation, however, yields a line spectrum. The liquid scintillation counters show the spectrum of beta particle energies on a logarithmic energy scale, because their energies vary greatly. The figure below shows the individually determined liquid scintillation spectra of three nuclides (^3H: E_{max} 18 keV, ^{14}C: E_{max} 180 keV, ^{32}P: E_{max} 1700 keV).

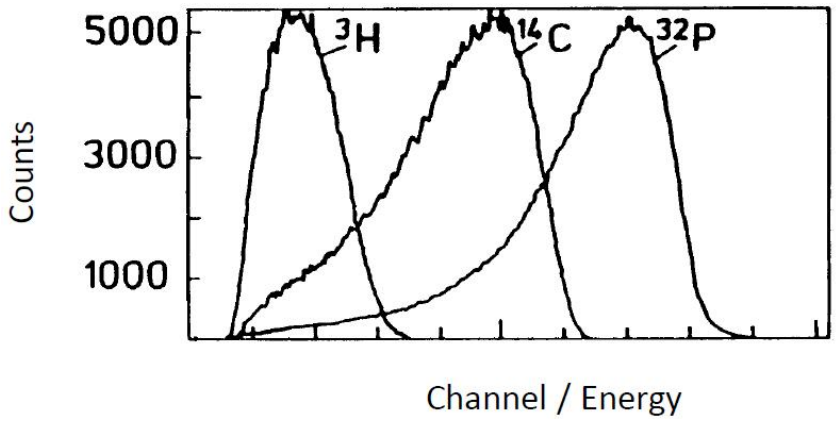

Figure XII.8. The individually determined liquid scintillation spectra of ^3H (E_{max} 18 keV), ^{14}C (E_{max} 180 keV) and ^{32}P (E_{max} 1700 keV).

Since the spectra overlap, the simultaneous measuring of several beta emitters is difficult. The separation of two nuclide spectra is still reasonably simple, if their energies differ sufficiently; however, if a third nuclide is simultaneously being determined it becomes virtually impossible.

Liquid scintillation counters are equipped with an automatic sample changer. The samples are placed in either sample sites of a conveyer or of counter cartridges. One sample at a time is measured in a sealed lightproof counting chamber. The light emissions from the sample are gathered as efficiently as possible to the photocathodes of the photomultiplier tubes, which is why the counting chamber walls are aluminum mirrors or painted with titanium oxide.

Quenching

For determining the activity of radioactive samples, their count rates are often compared to those observed with a standard of known activity. Liquid scintillation counting also uses this approach. This approach, however, requires that both the unknown sample and the standard are measured entirely under the same conditions. In measuring beta radiation by liquid scintillation counting, the measurement conditions are rarely the same, because a varying amount of quenching occurs in the samples. Quenching means that either the beta particle energy is absorbed by the measurement sample (liquid scintillation cocktail) before it causes scintillation agent excitation and further light formation or the light emitted by the scintillation agent is absorbed in the sample, therefore being not registered as electrical pulses in a photomultiplier tube. The most difficult problem in liquid scintillation counting is resolving quenching and its impact. There are three types of quenching, all of which result in the detection of reduced count rates. In physical quenching the beta particle range does not extend to the scintillation agent, in chemical quenching the energy transmission efficiency from beta particle to the solvent and the scintillator is lowered, and in color quenching the photons are absorbed in the colored substances in the sample.

Quenching can be somewhat reduced by adding more scintillator, lowering the temperature, and using a scintillator with the shortest possible fluorescence time (the quenching agent does not have time to intercept the energy). Usually it must be accepted, however, that a sample has some quenching and its effect on the count rate is found out by standardization. Some substances are particularly effective quenching agents even with a concentration of less than 1 ppm. The most common absorbing substance is oxygen, from air, dissolved in scintillation solutions. The strongest absorbing materials are, *e.g.* peroxides, acetone, pyridine, chloroform, carbon tetrachloride, methanol, ethanol, halogens, aldehydes, acids, bases, and heavy metals.

Figure XII.9 shows the effect of quenching on the observed beta spectra. All four samples on both sides have the same activity, but their quenching varies. The shifting of the spectrum to lower channels is due the reduction in intensity of single light pulses. The decrease in the height of the spectrum, in turn, is due to the growing portion of beta particles remaining completely unrecorded. Therefore, even if the activity of the samples is the same, the obtained count rate varies greatly depending on the quenching. Thus, the observed count rates cannot be directly compared to those of the standards to allow direct calculation of the unknown sample activity until quenching is accounted for. This is accomplished by determining counting efficiency individually for each sample, which is the ratio of the observed count rate of the sample to the activity of the sample. Thus when the count rate (R) and the counting efficiency (E) are measured the activity (A) of the sample can be calculated by:

$$A = R/E \qquad \text{[XII.I]}$$

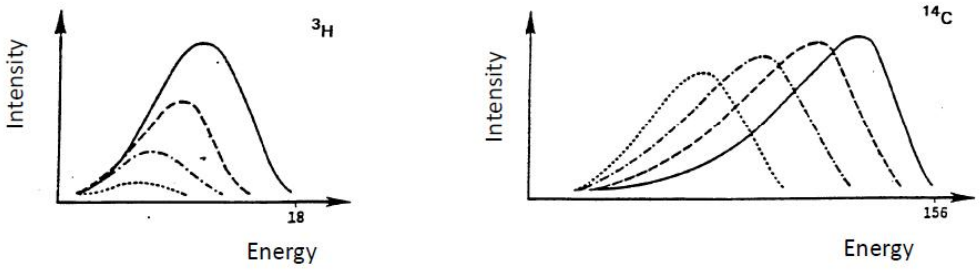

Figure XII.9. The effect of quenching on the beta spectrum in liquid scintillation counting.

Methods for determining counting efficiency

Since quenching varies from one sample to another, the counting efficiency (E) of each sample must be determined, in order to calculate the activity (A, dpm) from the observed the count rate (R, cpm):

$$E(\%) = \frac{R(cpm)}{A(dpm)} \cdot 100\% \qquad \text{[XII.II]}$$

When the count rates are corrected by the counting efficiency to get activity, they may then be compared with each other. The counting efficiency can be determined by many methods, three of which are described here: the use of an internal standard, the external standard channel ratio method, and the external standard end point method.

The use of an internal standard

Using the internal standard is the most accurate, but tedious. The sample is measured twice: first as it is and then by adding a known amount of the same nuclide as was in the sample and measuring again. Count rate growth is measured, and by comparing it to the amount of added activity the counting efficiency can be obtained as follows:

$$E(\%) = \frac{cpm_2 - cpm_1}{dpm} \cdot 100\% \qquad \text{[XII.III]}$$

where cpm_1 = count rate of the sample

cpm_2 = sum count rate of the sample and the added activity

dpm = amount of added activity

E = counting efficiency

The count rate of the unknown sample is then divided by the counting efficiency to get its activity, $A = (cpm_1 \times 100) / E(\%)$.

The external standard ratio method

In the external standard ratio standardization method the device uses an external ^{226}Ra source, which has an activity of about 400 kBq (10 μCi). In standardization step the Ra-source automatically rises next to the sample bottle in the measuring chamber, so that the gamma rays emitting from it also hit the scintillation cocktail. Compton electrons are generated when the gamma rays are absorbed into scintillation cocktail causing a spectrum similar to that of a beta particle emitting sample, only at a higher channel range (Figure XII.10). The pulses move towards lower channels as the quenching increases. The samples are measured twice: when measuring the actual sample the ^{226}Ra source is not in the measuring chamber but is protected, while in standardization it is brought next to the sample bottle. The pulses caused by the radium standard are divided into two channel ranges and the pulse number ratio of these channel ranges is calculated. This external standard ratio (ESR) is proportional to quenching: the more quenched the sample, the more pulses move to the lower channels, in other words, the lower is the external standard ratio. Accordingly, as the sample is quenched the counting efficiency is also reduced.

For the standard curve, which is called the quenching curve, a series of samples are measured (quenching series), all of which have the same activity for a particular nuclide, but the quenching is varied, for example, by adding an increasing amount of $CHCl_3$. The quenching increases with this addition, while the counting efficiency, as well as the ESR, decreases. The counting efficiency (E (%)), *i.e.* the count rate in the channel range covering pulses of an unquenched sample divided by the sample activity is then plotted on the curve as a function of the external standard ratio (ESR) (Fig. XII.11). When an unknown sample is then measured, first the external standard ratio is determined and by using this value the counting efficiency, *e.g.* 70%, is read from standard curve. The sample activity is then calculated by dividing the determined count rate by the counting efficiency (e.g. 0.70). The standard curve is in practice stored in the memory of a liquid scintillation counter and device does the calculation automatically.

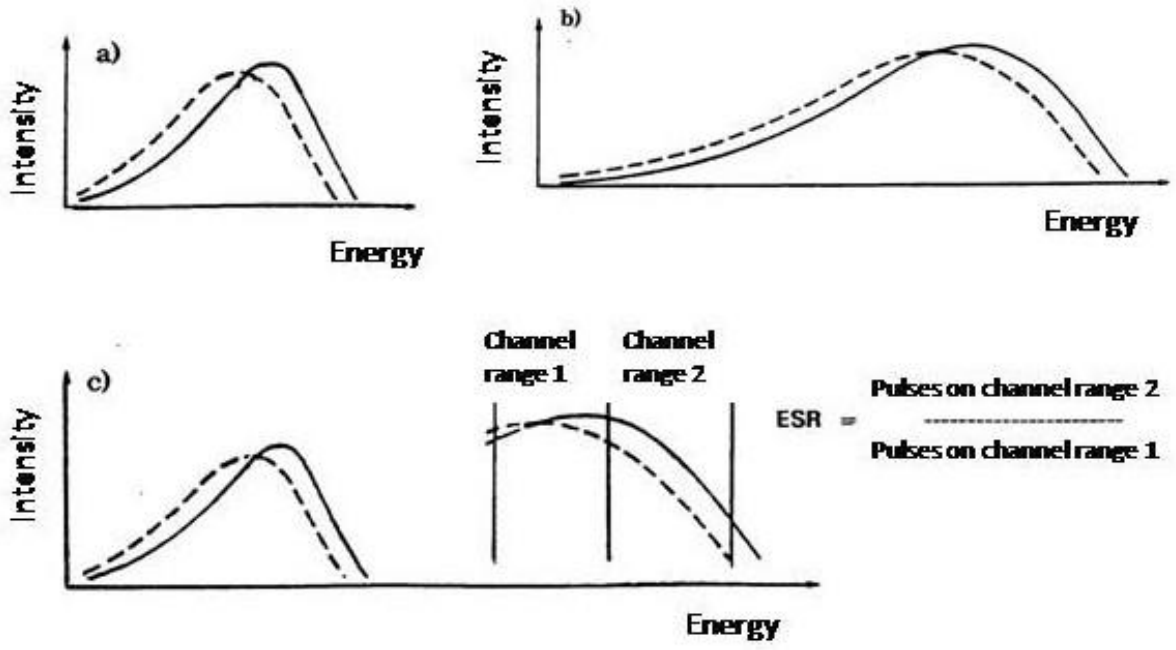

Figure XII.10. a) unquenched sample (-----) and quenched (- - -) spectrum; b) spectra caused by external standard: unquenched (-----) and quenched (- - -) spectrum; c) external standard ratio (ESR) calculation principle.

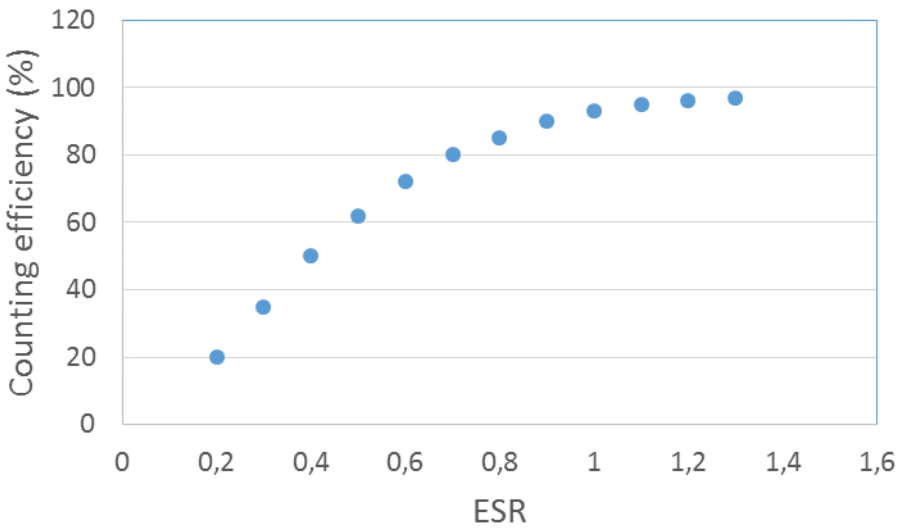

Figure XII.11. Quenching curve (standard curve).

External standard spectrum endpoint method

The measure of quenching in the external standard spectrum endpoint method, is as the name implies, the endpoint of spectrum caused by the external standard: the greater the quenching, the lower the channel on which the spectrum ends. Since it is difficult to exactly define the endpoint of the spectrum, the endpoint is determined by the channel under which 99.5% of all of the pulses occur. Just as in the sample and external standard channel ratio methods, the external standard endpoint, SQP-value, is determined for the quenching series as a function of counting efficiency and the obtained quenching curve is used to calculate the activity of unknown samples.

Cherenkov counting with a liquid scintillation counter

When a charged particle passes through the medium at a speed faster than light, it polarizes the medium molecules. When this polarization is released, the medium molecules emit photon radiation of ultraviolet and visible light spectrum range. This phenomenon, which is called Cherenkov radiation, can be used for beta radiation measurement because it is also identifiable by the photomultiplier tube of a liquid scintillation counter. Beta particle energy must be at least 263 keV for Cherenkov radiation to occur in water. In practice, Cherenkov radiation is only useful for beta radiation measurement when the beta radiation energy is at least 800 keV. For Example, only 2% of counting effectiveness is achieved in Cherenkov counting with ^{137}Cs (average beta energy of 427 keV), while 25% counting effectiveness is achieved with ^{32}P (average beta energy of 695 keV).

Cherenkov radiation measurement has some important advantages compared to liquid scintillation counting. First, larger amounts of the solution can be measured since no liquid scintillation solution needs to be added to the counting vial. Second, no costly liquid scintillation waste is generated in Cherenkov counting.

Alpha measurement with a liquid scintillation counter

The determination of alpha emitters by liquid scintillation counter is a very convenient method. The sample preparation is considerably simpler than when measuring with semiconductor detectors. For measurement with semiconductor detectors the sample must be very thin, *i.e.* "massless", so that the alpha radiation is not absorbed into the sample. In liquid scintillation calculation, this is not generally a problem, because alpha-emitting radionuclides mixed with liquid scintillation cocktail are in immediate contact with the scintillator. Since the energies of alpha particles are high, generally 4-6 MeV, in practice their detection efficiency is nearly 100% and quenching is usually not a problem. In addition, because the liquid scintillation counters have sample changer, its measurement capacity is superior to that of the semiconductor. The disadvantage that liquid scintillation counting has compared to the semiconductor detectors is its significantly worse energy resolution. The best semiconductor detectors will yield a peak width values at half maximum of 10-20 keV, while liquid scintillation counters get, at best, only 200 keV. Therefore, alpha energies that are close to each other are not able to be measured separately with a liquid scintillation counter. Another problem in measuring alpha radiation with a liquid scintillation counter h when measuring environmental samples is the fact that the beta radiation forms a high background that interferes with the measurement. Today, however, there are liquid scintillation counters capable of differentiating between the pulses caused by alpha particles from those caused by beta particles. The electric pulse induced by beta particles is considerably shorter, around a few nanoseconds, than the alpha particle induced pulse that lasts several tens of nanoseconds. Below is a spectrum, in which there are alpha peaks of ^{226}Ra and its daughters, and the beta spectrum of ^{226}Ra daughter nuclides separated by the pulse shape analysis.

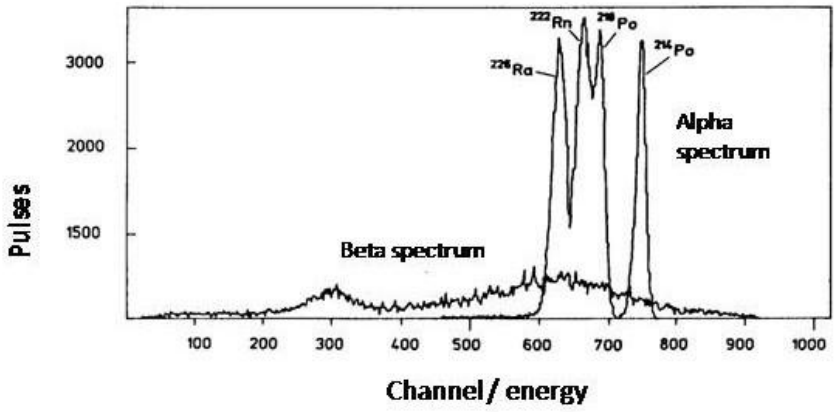

Figure XII.12. The alpha- and beta spectra of ^{226}Ra and its daughters obtained by pulse shape analysis .

Sample preparation for liquid scintillation counting

In addition to the determination of the counting efficiency there is a second critical task in the liquid scintillation counting: preparation of samples. Whenever possible, a homogeneous measurement sample should be obtained in which the radionuclide is evenly dissolved in the liquid scintillation cocktail. If the sample is an organic solvent, it is usually directly soluble in the liquid scintillation cocktail. This, however, is rarely the case. Usually the samples for measurement are aqueous samples. Water is only partially soluble in organic liquid scintillation solvents, but even the best cocktails can reach as high as 50% water concentration. Water samples can also be measured as gels, in which case the water is evenly distributed in the liquid scintillation cocktail. Many insoluble organic substances must be decomposed before measurement. Dissolution can be done with *e.g.* perchloric-hydrogen peroxide oxidation or burning the sample and collecting the CO_2 for measuring if ^{14}C is to be measured. If ^{3}H is to be measured, then H_2O is collected. PerkinElmer offers an automatic system, Sample Oxidizer, where the organic sample is decomposed with a flame and tritium is collected as water into another scintillation vial and radiocarbon to another vial after conversion into a carbamate in Carbosorb column. Liquid scintillation cocktail is then added to the both vials - automatically too (Figure XII.13). Insoluble samples, *e.g.* fine solids and chromatography masses can be measured as heterogenetic samples by adding them and a liquid scintillation cocktail to a gelling substance, like aluminum stearate, forming a gel in which the precipitate is evenly distributed. Radioactive chromatography or electrophoresis strips can be measured directly by immersing them in a liquid scintillation cocktail containing flask. The sample preparation methods are summarized in the Figure XII.14.

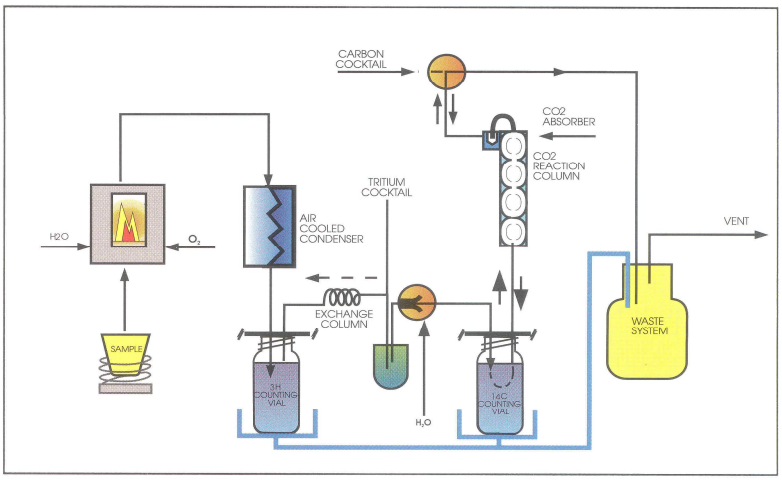

Figure XII.13. Perkin Elmer Sample Oxidizer to prepare ^{3}H and ^{14}C samples for liquid scintillation counting after decomposition of organic samples (http://shop.perkinelmer.com/Content/applicationnotes/app_oxidizercomparisonsampleoxidation.pdf).

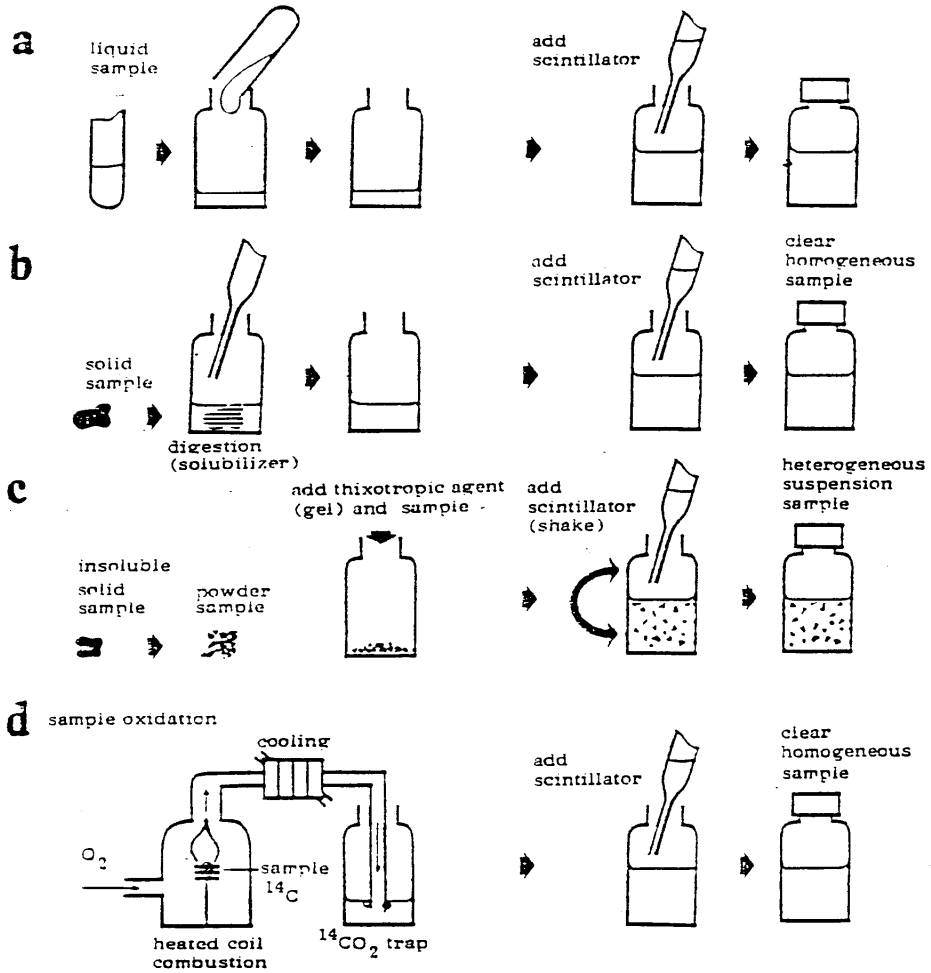

Figure XII.14. Sample preparation methods for liquid scintillation counting.

XIII RADIATION IMAGING

Content

Radiation imaging in used to locate, and in many cases also to quantify, radionuclide or a radionuclide-bearing compound from solid material. There are two basic types of imaging techniques: planar imaging giving information of radionuclide distribution at two dimensions and tomography giving three-dimensional information. The latter technique is only briefly described at the end of the chapter. Imaging techniques are typically used in biological and medical applications to locate target molecules. To enable the location of these molecules they have been labelled with a radionuclide, typically a beta-emitting radionuclide in planar imaging and a gamma-emitting radionuclide in tomography. Radiation emitted by these radionuclides is then detected by autoradiography or using technique based on CCD camera filming in case of planar imaging and by an array of gamma detectors in case of tomography.

Autoradiography can be divided into two categories, film autoradiography and storage phosphor screen autoradiography. The prefix *auto* means that the source of radiation is within the sample unlike in other types of radiographies in which the sample is exposed to an external radiation source, such as X-rays. Autoradiography dates back to late 19^{th} century when Henri Bequerel discovered in 1896 that uranium salts produced an image on photographic plates (Figure XIII.1).

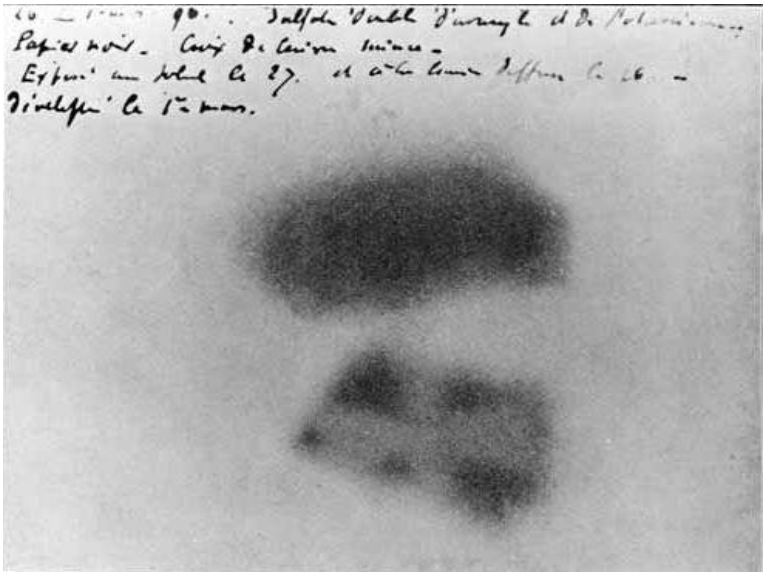

Figure XIII.1. Image of a uranium salt on a photographic plate (autoradiogram) determined by Henri Bequerel in 1896 (http://www.japanfocus.org/-elin_o_hara-slavick/3196/article.html).

Film autoradiography

In film autoradiography a film is apposed to a radionuclide-bearing sample. The sample should be flat and as smooth as possible, for example pressed plant or polished rock surface. The film consists of a 0.2 mm polymeric (polyester or cellulose acetate) support plate coated with an emulsion comprising fine silver halide (AgCl, AgI, AgBr) grains in gelatin. The outer surface facing the sample can have a very thin protective cover. Radiation, typically beta particles but also alpha particles, emitted from the sample pass the surface cover and ionize silver atoms in the emulsion layer, which is typically 10-20 μm thick. The released electrons travel in the emulsion and after losing their kinetic energy reduce Ag^+ ions into metallic silver Ag forming a latent, invisible image of the radionuclide distribution on the sample. These latent metallic silver centers comprise only of a few silver atoms. When the film is developed in a reducing liquid, Ag^+ ions around the latent silver metal centres reduce and the amount of metallic silver in the crystal increases by a factor of 10^8-10^{10} making them visible either by eye (macro autoradiography) or by microscope (micro autoradiography).

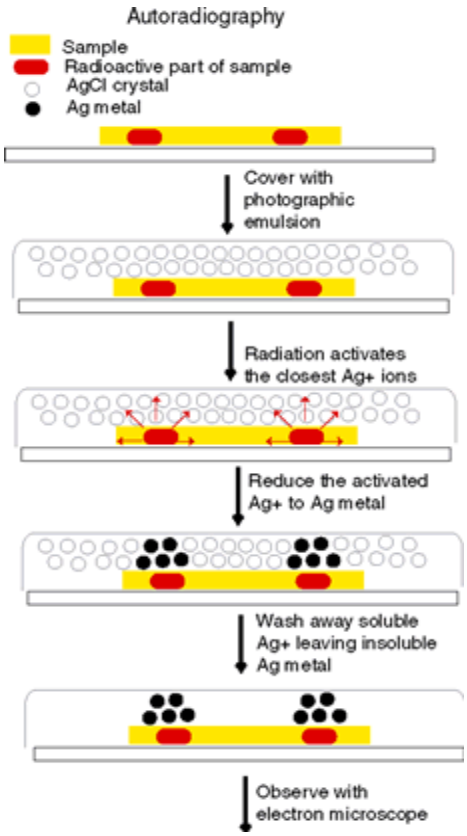

Figure XIII.2. Principles of autoradiography (http://lifeofplant.blogspot.fi/2011/12/autoradiography.html).

The autoradiogram seen on a film gives a qualitative picture of the distribution of the target radionuclide, or the compound/material bearing the radionuclide, in the sample. Depending on the type and thickness of the sample and the type and energy of radiation the image represents the radionuclide distribution either on the surface of the sample or also in its bulk. If, for example, the sample is rock, the density of which is about 2-3 g/cm^3 only radiation originating from the sample surface (alpha particles), or very close to it (beta particles), can be detected on the film due to self-absorption of radiation in the sample at higher sample depths. In the case of imaging a plant sample, having a much lower density, much larger fraction of the radiation comes from the inner part of the sample giving thus also information of radionuclide distribution in its bulk. From the sensitivity point of view autoradiography technique is best suited for tracers utilizing beta emitters of an intermediate energy, such as ^{14}C (E_{max} = 156 keV) and ^{35}S (E_{max} = 167 keV) for which the energy is high enough to avoid self-absorption but low enough to avoid penetration of beta particles through the reactive gel layer.

An important parameter in autoradiography is the resolution, which means the ability of the system to differentiate two individual points in the sample. A typical resolution range is from 5 µm to 50 µm. The resolution is dependent on the following factors, in the order of importance:

1) Distance between the film and the sample. Closer contact to the sample can be obtained by using a fluid silver halide emulsion without the polymeric support, which improves resolution by 5-7 times at maximum.

2) Energy of radiation. The lower the beta energy the better the resolution due to a shorter range of emitted beta particles. The resolution with the low energy beta emitter ^{3}H (E_{max} = 18 keV) is about ten times better than with the high energy beta emitter ^{32}P (E_{max} = 1710 keV). Resolution with the intermediate energy beta emitter ^{14}C (E_{max} = 156 keV) is in between these two.

3) Thickness of the sample, the resolution being the better the thinner the sample is.

Figure XIII.3 shows an autoradiogram of a rock impregnated with polymethylmetacrylate labelled with ^{14}C. The dark areas represent pores (the method is described in detail later in the chapter). In addition to the sample, also standards with known activities of the target nuclide are prepared and their autoradiograms are determined in an identical way as that of the sample. These standards are used to quantify the radionuclide distribution in the sample. The darkness or grey level distribution of the autoradiogram is measured with an optical densitometry measuring the absorption of exposed light at various points of the autoradiogram. The absorption values are converted to optical densities, which are compared point by point to those observed with standard samples and relative activity values can thus be determined at various points at 5-50 µm resolution. The autoradiogram can also be scanned and the grey level values at various points, pixels, are determined with a computer. Exposure times of autoradiographic films vary in a wide range up to weeks, mostly depending on the activity levels. Finding a suitable exposure time requires optimization and experience.

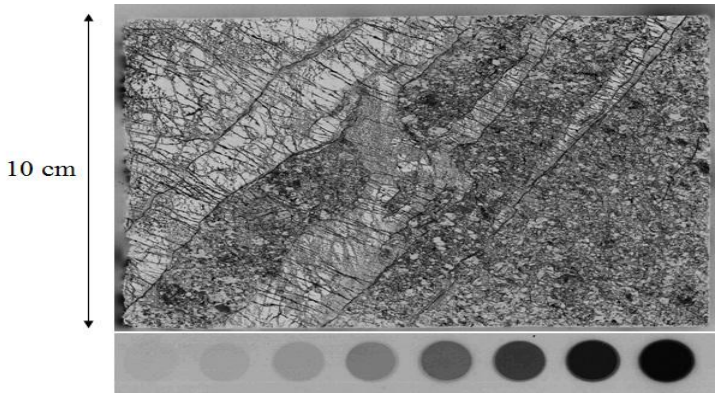

Figure XIII.3. An autoradiogram of the surface of a rock impregnated with polymethylmetacrylate labelled with ^{14}C. Standard series with varying ^{14}C activities are at the bottom.

Storage phosphor screen autoradiography

In storage phosphor screen autoradiography, also known as digital autoradiography, the radiation emitted from the sample excites molecules in a phosphor screen apposed to the sample. The excitations are relaxed by scanning with a laser beam, the light emitted in de-excitation is detected and an image is created in a computer based on detected light intensities at all scanned points. The storage term in the name of the process means that the energy from the emitted radiation hitting phosphor molecules is stored in the phosphor crystal as excitation energy. Phosphor is a general name of compounds, which are able to emit light in de-excitation processes.

The phosphor screen, also known as an imaging plate, consists of a polymer support; polyester for example, over which there is a thin layer (150 μm) of phosphor compound bariumfluorobromide BaFBr doped with trace amounts of divalent Eu^{2+} which replace Ba^{2+} ions in the crystal. The crystal size of BaFBr:Eu^{2+} is very small, at about 5 μm. Since the typical oxidation state of europium is +III, Eu^{2+} is readily ionized to Eu^{3+} when a beta particle from the sample hits the phosphor molecules. The electrons originating from the ionization are trapped in barium vacancies resulting in the excitation of the BaFBr molecules. After exposure, the excitation points are located on points where the radionuclide was present in the sample. To make this “latent” image visible the excitations are relaxed by scanning the image plate with a laser beam and light intensity emitted in the de-excitations at all scanned points (pixels) are detected with a photomultiplier tube. Laser beam moves the trapped electrons to conduction band where they finally combine with Eu^{3+} ions to regain Eu^{2+} ions (Figure XIII.4). This process is called photostimulated luminescence (PSL). Typically the

scanning resolution, pixel size, in digital autoradiography varies from 5 to 500 µm. After scanning the plate, it is erased from excitations by intensive light after which the plate can be reused.

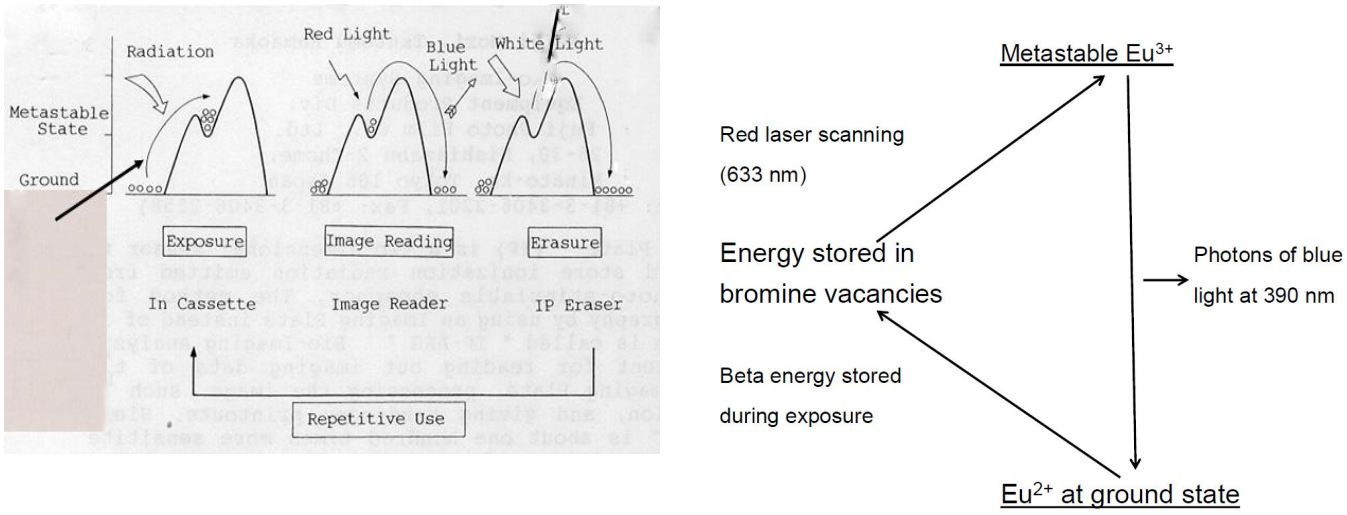

Figure XIII.4. Detection process of beta radiation in a phosphor imaging plate.

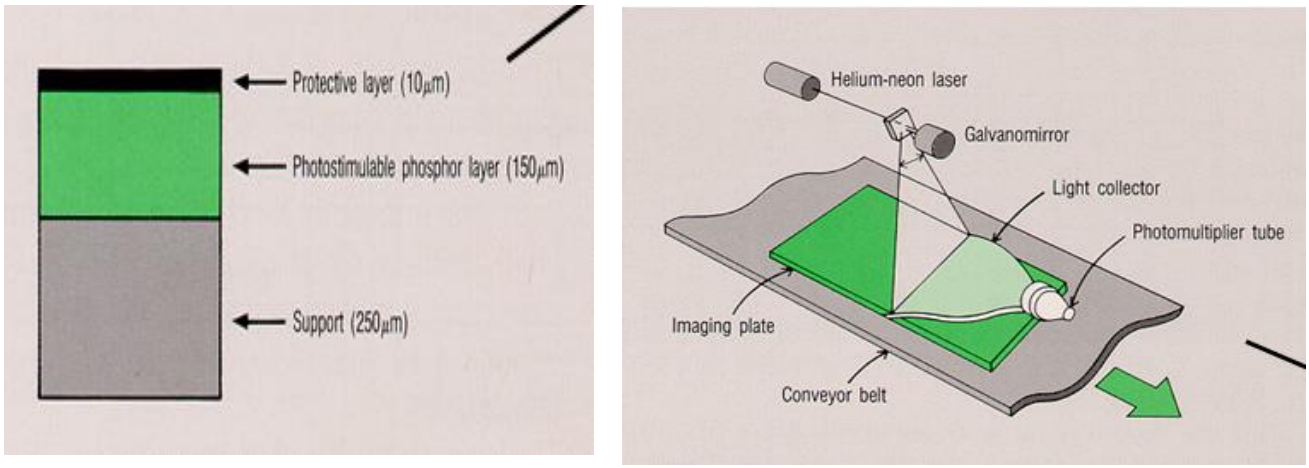

Figure XIII.5. Left: structure of a phosphor screen. Right: scanning of the screen with laser beam and detection of the emitted light with photomultiplier tube.

Storage phosphor screen autoradiography has several advantages over film autoradiography. First, it has clearly higher sensitivity over film autoradiography, 50-100 times for ^{14}C imaging, for example. This has a direct effect on exposure times, which are much shorter in case of phosphor screens. Another advantage is that the phosphor screens can be reused unlike films that are used only once (an advantage of film over the phosphor screen is that the film is a durable record of the results while in case of phosphor screen the data is only in an electronic form). Furthermore, an advantage of phosphor screen over film is that the grey level data can be directly digitized to computer while

in case of film after development the film needs to be digitized for optical density calculation. Comparing the linearity of light intensity (PSL) response with respect to measured activity the phosphor screen is clearly better compared to film. The linear range in case of phosphor screen is four orders of magnitude while in case of film it is only two orders of magnitude.

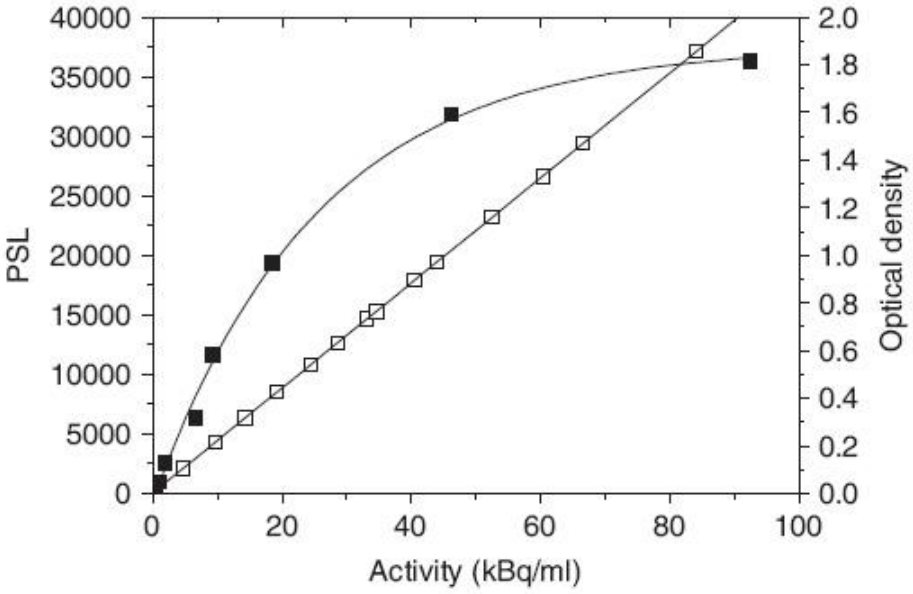

Figure XIII.6. Optical densities and light intensity response (PSL) as a function of detected activity for film (n) and for phosphor screen (*).

CCD camera imaging

Using CCD camera for two-dimensional on-line beta counting is still a more advanced method for imaging beta radiation from planar sources. In the apparatuses based on this technique, such as BetaImager or MicroImager from BiospaceLab, beta particles are transformed into light by scintillation process and the light photons are detected with a CCD camera. At its best modification this technique can offer ten times better spatial resolution compared to phosphor screens. Moreover, it gives real-time information on beta emissions from the studied surface. This also shortens the imaging time since one step compared to phosphor screen and two steps compared to film autoradiography can be avoided.

Radiation imaging by tomography

If a three-dimensional picture of the radionuclide distribution in a sample is needed one could cut thin slices of the sample, determine their autoradiograms and superimpose them to get the three-

dimensional picture. This would, however, be very laborious and not suitable to determine distribution of a short-lived radionuclide, and particularly to distribution in a human body. For this purpose tomographic methods are the choice and they are widely used in the development and clinical use of radiopharmaceuticals. Depending on the type of radionuclide either single photon emission tomography (SPECT) or positron emission tomography (PET) are two choices. In the SPECT mode a radiopharmaceutical labelled with a gamma-emitting radionuclide, most typically ^{99m}Tc, is injected into a body of a test animal or human. In PET mode the label is a positron emitter, most typically ^{18}F. Thereafter the distribution of the radiopharmaceutical in the body is followed with a gamma camera in case of SPECT and with a PET camera in case of PET, both detecting gamma rays outside the body. Gamma camera comprise an array of collimated Na(I) detectors capable to separate gamma rays emitting from various parts of the body. PET camera makes use of two 511 keV gamma rays emitted in opposite directions in the annihilation of positron particles. PET camera consist of an array of Na(I) detectors in a ring. The target is positioned inside the ring and the camera detects pulses in coincidence mode, i.e. when two gamma rays hit detectors on opposite sides of the ring a pulse is registered while in case of only one gamma ray the pulse is rejected. Both SPECT and PET tomographies are powerful tools in medical imaging and they are increasingly used also in the preclinical development.

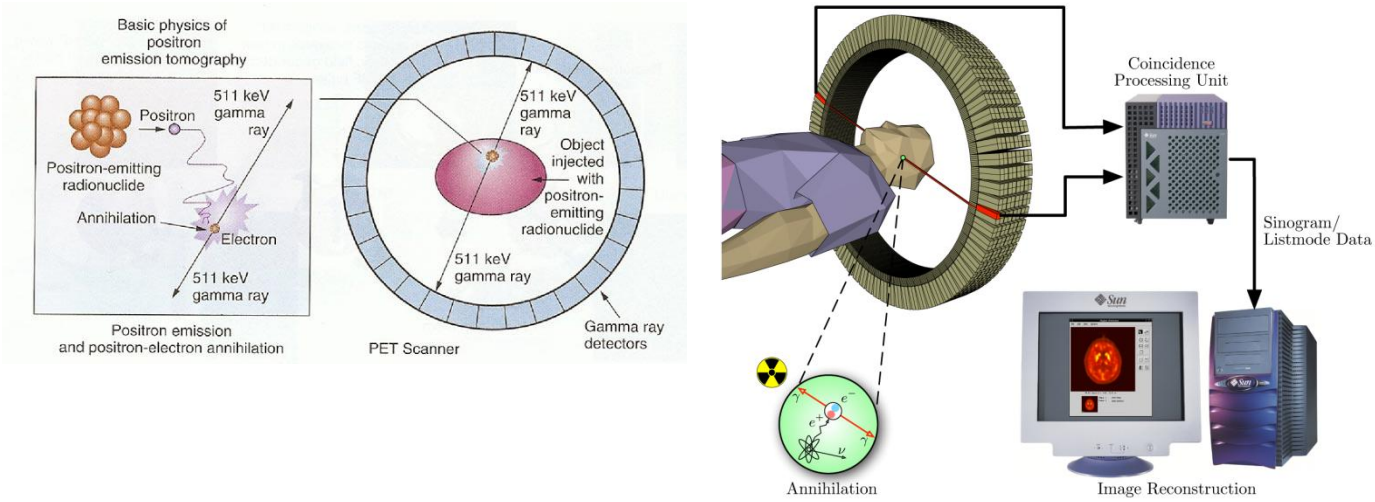

Figure XIII.7. Formation and detection of positron annihilation gamma rays (left) (http://www.cellsighttech.com/technology/pet.html) and scheme of PET camera (right) (http://www.lookfordiagnosis.com/mesh_info.php?term=Positron-Emission+Tomography&lang=1).

Applications of autoradiography

Applications of autoradiography can be divided into two categories: those where the actual study target is the radionuclide and those where radionuclides are tracers to study existence/distribution/ concentration etc. of other substances.

Identification and localization of radionuclide-bearing particles

In environmental radioactivity studies it is a common way to identify and localize particles with higher than typical activities. These particles are present in the environment from fallouts from the nuclear weapons tests in the 1950' to 1970's and from the Chernobyl accident, as well as from releases from nuclear facilities. Particles can be found from air sampling filters and from soils and sediments. Figure XIII.8 shows a film autoradiogram of an air filter taken from a nuclear power plant during maintenance work. The points seen as dark spots in the autoradiogram represent individual particles or their agglomerates removed from the air by filtration (pore size typically about 0.2 μm); the darker the spots are the larger the particles and the higher is their activity. The activity of the largest particle in this autoradiogram was 25 Bq. Based on the information obtained from the autoradiogram larger particles can be localized and further also isolated with the aid of a microscope. The isolated particle can then be characterized with respect to elemental, radionuclide and isotopic composition using a variety of methods, such as scanning electron microscopy, gamma spectrometry, XANES/EXAFS spectroscopy, as well as alpha and mass spectroscopy.

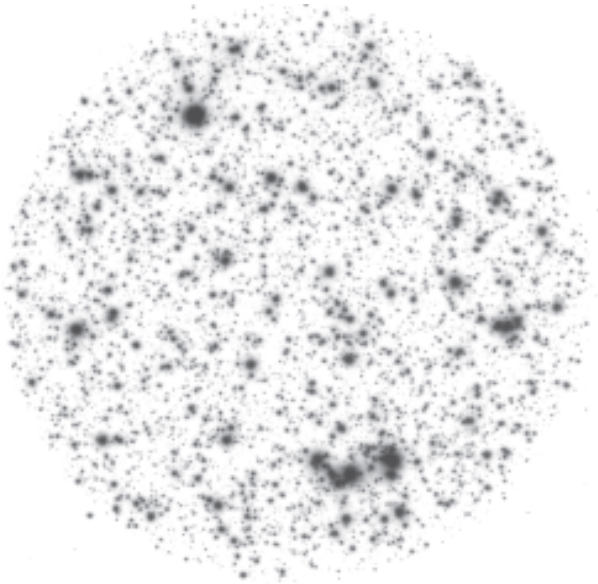

Figure XIII.8. Autoradiogram of an air filter sample taken from a nuclear power plant during maintenance (http://www.stuk.fi/julkaisut_maaraykset/kirjasarja/fi_FI/kirjasarja2/). The diameter of the image is about 10 cm.

Determination of rock porosities

At the Laboratory of Radiochemistry, University of Helsinki, a unique method to determine rock porosities utilizing autoradiography has been developed. In this method a rock piece is heated in vacuum to remove water and air from its pores. Then the piece is impregnated with methylmetacrylate (MMA) monomer solution labelled with ^{14}C. MMA having a lower viscosity than water fills nanometer scale pores in the rock. ^{14}C-MMA within the rock is polymerized by irradiation or chemically to polymethytmetacrylate (^{14}C-PMMA). Now autoradiograms can be produced from the sawn surfaces of the impregnated rock piece, to observe the distribution of ^{14}C in the rock in two dimensions. This distribution corresponds to the distribution of ^{14}C-PMMA in the rock, which in turn corresponds to porosity of the rock (Figure XIII.9). From the grey levels on the autoradiogram, porosities at various parts of the rock can be determined at micrometer scale. By superimposing the mineralogical composition of the rock surface one can conclude in which minerals the porosity can be found. Here, most of the porosity was found in the inter and intragranular space, in the dark minerals which are micas and in altered plagioclase grains.

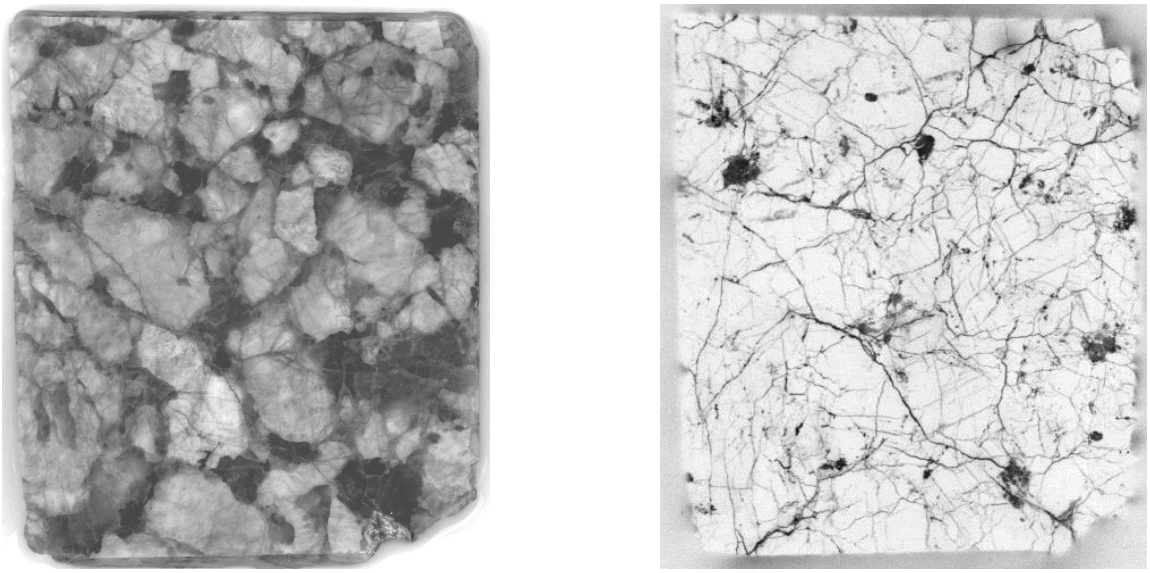

Figure XIII.9. Photograph of a polished rock piece surface (left) and an autoradiogram from the same surface (right) after impregnating the rock with ^{14}C labeled MMA and polymerizing it into ^{14}C-PMMA.

Radionuclide imaging in radiopharmaceutical research

In the development of a radiopharmaceutical the product needs to pass preclinical tests prior to human tests. An essential part of the preclinical tests are imaging studies to reveal distribution of the product into various organs. These imaging studies are carried out by animals, either with living animals or with specific organs/tissues of dead animals. Both autoradiography and PET/SPECT imaging are used in these studies. The autoradiography tests can be divided into *in vivo* and *ex vivo* tests. In the former an organ or tissue is equilibrated with a radiopharmaceutical-bearing solution and in the latter radiopharmaceutical is injected into a living animal. After desired contact time the animal is sacrificed and the distribution of the radiopharmaceutical in the body is determined by measuring radioactivity of various organs separated from the carcass. More detailed distribution can be observed by freezing the organ/tissue or the whole body, by taking thin slices with microtome and by making autoradiograms from the slices. An example of a series of slices taken from a rat's brain incubated with a solution containing a ^{18}F-labelled radiopharmaceutical ^{18}F-CTF-FP is shown in Figure XIII.10. The autoradiograms show the spatial distribution of the ^{18}F radioactivity (red indicates the highest levels, blue the lowest levels), with nonspecific uptake partly subtracted. STR indicates striatum; AMY, amygdala; HIP, hippocampus; LC, locus coeruleus; RAP, raphe nuclei; SN, substantia nigra; CTX, frontal cortex; and CERE, cerebellum.

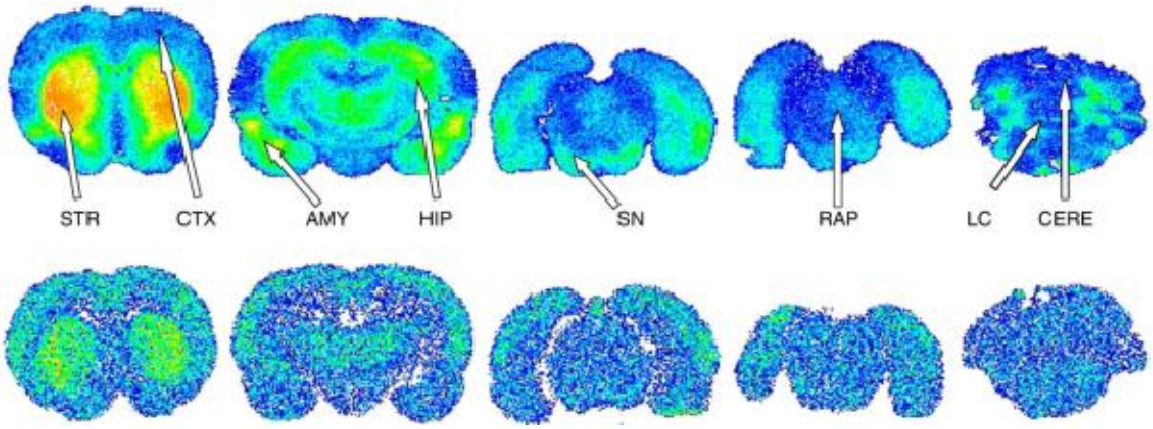

Figure XIII.10. Autoradiograms of *ex vivo* rat brain sections at 15 min after injection of dopamine transporter (DAT) radioligand [^{18}F]*β*-CFT-FP. The upper row depicts a control rat, and the lower row depicts a rat pretreated with the DAT inhibitor GBR12909 (Koivula, T. et al. Nucl. Med. Biol. 35 (2):177-183).

For the quality control of radiopharmaceutical products HPLC (high performance liquid chromatography) and TLC (thin layer chromatography) methods are used. The latter, TLC, utilizes autoradiography. In this method a drop of a radiopharmaceutical product is applied on a TLC plate and the chromatogram is developed with a proper mobile phase. The run separates chemically different products on the plate and their chemical nature can be determined by their position along the transfer track on the plate. Various compounds are separated into individual spots on the plate. Their relative radioactivity contents can be measured either by radioactivity scanning of the plate or by making an autoradiogram, film or phosphor screen, of the plate. Distribution of radioactivity on the TLC plate can then be seen, and quantified, from the darkness and the position of the identified spots.

Solid state nuclear track detectors

Nuclear track methods are based on tracks created by charged particles (from H^+ up) in solid state nuclear track detector (SSNTD) apposed to the sample emitting the particles. SSNTD can be used to locate particles with elevated alpha activity or fissile material and quantify their amounts by the number of detected tracks. SSNTDs are typically made of plastics. Also other detector materials, such as mica and glass, are used but they are not discussed here. The plastic detectors are made of cellulose nitrate, polycarbonate, polethyleneterephthalate and polyallyldiglycol carbonate, of which the latter has the best sensitivity, i.e. it can produce detectable tracks most effectively. Polyallyldiglycol carbonate is also known with a code name CR-39. It is also able to register tracks

from alpha particles, which are not the case with polycarbonate detector. Plastic SSNT detectors are thin foils with thickness varying in the range of 100-1000 µm. The tracks created in the detector are so small, tens of nanometers, that they cannot be seen by eye. They can be detected directly with transmission electron microscopy (TEM) and their number can be counted by eye or computer programs developed for this purpose. Alternatively, the size of the tracks can be enlarged by etching, typically with 2-6M NaOH, which enables detection and counting of the tracks with an optical microscope. Etching is carried at a slightly elevated temperature (50-60 ^{o}C) for about an hour. Furthermore, the tracks can be widened by electrical methods after chemical etching and detected by image analysis techniques. Figure XIII.11 presents a scanned Makrofol film for determination of radon content in the indoor air by counting the number of tracks on the film and magnified image of the tracks by optical microscope.

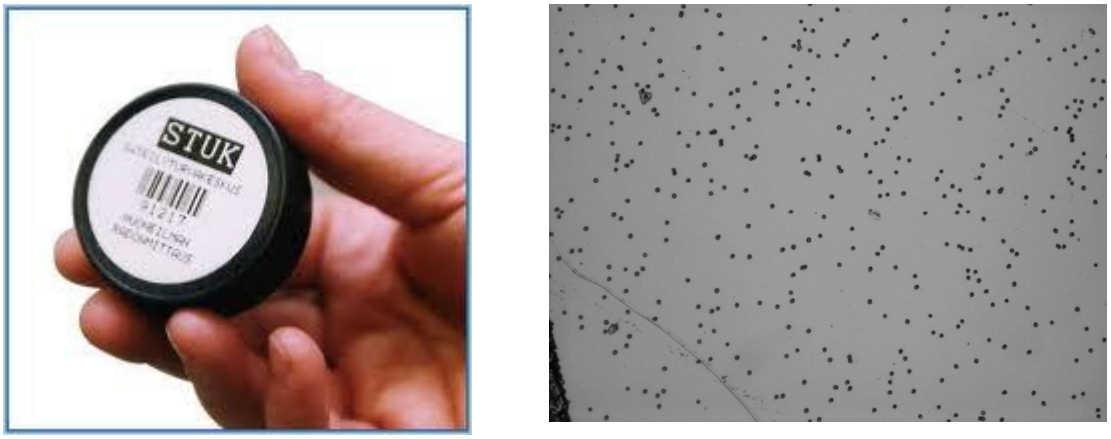

Figure XIII.11. a) Indoor radon monitor having a polycarbonate film detector b) Tracks due alpha particles from radon in polycarbonate film, magnification 40, the photographed area is about 1.3 by 1.0 mm (http://pages.csam.montclair.edu/~kowalski/cf/327squeeze.html).

There are a number applications of SSNTD methods, but here only two, alpha track analysis and fission track analysis, are briefly described. In environmental radioactivity research they are typically used to locate and quantify alpha-emitting radionuclides and fissile material in low concentrations in soil or sediment, for example. Figure XIII.12 shows an image of an alpha-emitting particle in sediment sample. Here, the active particle is mostly embedded among other, non-active material.

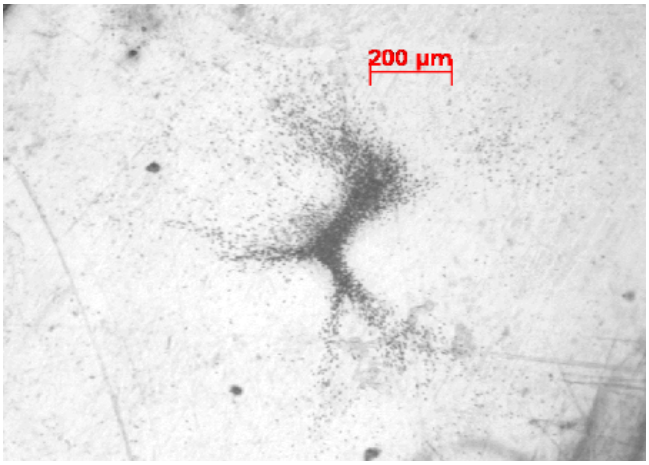

Figure XIII.12. An SSNTD image of an alpha-emitting particle in sediment (J. Jernström, M. Eriksson, J. Osán, G. Tamborini, S. Török, R. Simon, G. Falkenberg, A. Alsecz and M. Betti, Non-destructive characterisation of low radioactive particles from Irish Sea sediment by micro X-ray synchrotron radiation techniques: micro X-ray fluorescence (μ-XRF) and micro X-ray absorption near edge structure (μ-XANES) spectroscopy, J. Anal. At. Spectrom. 2004, 19, 1428-1433).

Presence and amount of fissile materials, particularly of ^{235}U and ^{239}Pu, can be determined by fission track analysis. The sample with the apposed SSNTD is exposed to thermal neutron radiation resulting in fission events in the material. The fission fragments cause tracks in the detector and the amount of fissile material can be determined by taking into account the number of the tracks, neutron flux, exposure time and the reaction cross section. An example of fission tracks seen on a polycarbonate detector is shown in Figure XIII.13.

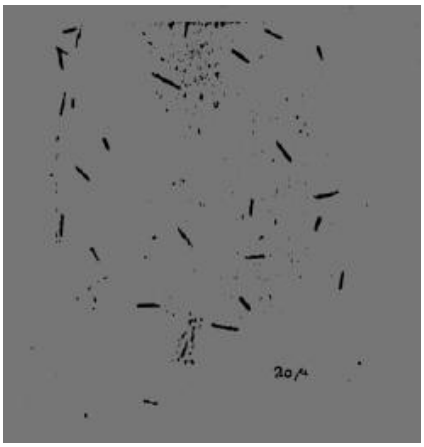

Figure XIII.13. Fission tracks on a polycarbonate SSNTD (http://barc.ernet.in/publications /nl/2005/200506-2.pdf).

XIV STATISTICAL UNCERTAINTIES IN RADIOACTIVITY MEASUREMENTS

Content

Count rate – activity

Systematic and random errors

Poisson and normal distribution

Standard deviation

Uncertainty of cross count rate

Uncertainty of net count rate

Standard deviation of activity

Count rate – activity

When measuring the activity (A_x) of a radioactive source the primary result is the total (gross) count rate (R_g) obtained from the measurement system (detector, amplifier and pulse counter)

$$R_g = \frac{X_g}{t} \qquad \text{[XIV.I]}$$

where X_g = number of collected total pulses and t = measurement time. The unit of count rate is pulses per unit time: counts per second (s^{-1}, cps) or counts per minute (cpm).

The observed gross count rate (R_g) includes, in addition to pulses resulting from the radioactive source (net pulses X_n), also pulses from background (X_{bg}) originating from various sources other than the actual source, such as cosmic radiation, presence of natural or pollution radionuclides and electric noise of the measurement system. These background pulses need to be counted separately in the absence of the radioactive source and the background count rate must be subtracted from the gross count rate to obtain the net count rate (R_n) originating from the radioactive source.

$$R_n = \frac{X_g}{t_g} - \frac{X_{bg}}{t_{bg}} \qquad \text{[XIV.II]}$$

Activity of the source (A_x) is calculated either by comparing the net count rate of the source (R_x) to that obtained by measuring a standard source (R_{st}) with a known activity (A_{st}) in identical conditions as the unknown source

$$A_x = A_{st} \cdot (R_x / R_{st}) \qquad \text{[XIV.III]}$$

or if the counting efficiency (E(%)) of the counting system is known dividing the net count rate with the counting efficiency.

$$A_x = R_x / (E/100)) \qquad \text{[XIV.IV]}$$

What kind of uncertainties are involved here and how they are calculated are discussed below.

Systematic and random errors

In every measurement, including radioactivity measurement, there are two types of errors resulting in an uncertainty in the measurement result:

- Systematic errors arise from erroneous measurement system and they always function into same direction from the right result. If, for example, the activity of the standard is not what it is supposed to be or the settings of the measurement system, such as amplification of pulses, change during the measurement, this causes error to the observed activity. Even if the parallel results were close to each other, i.e. reproducible and precise, the results would not be accurate since they systematically deviate from the real value to certain direction in case of a systematic error.

- Random errors arise from the fact that the measurement system or the phenomenon measured, or both, are intrinsically non-deterministic (stochastic).
  - The measurement systems are always non-ideal and do not always give the same response even though the measured quantity would have a constant value. For example, alpha particles for a certain transition of a radionuclide have always the same energy but we never obtain a perfect line peak spectrum, but the peak has a broadness depending on the system's limited preciseness in transforming alpha particle energies to electric pulses.
  - Some measured phenomena, such as radioactivity, are intrinsically stochastic. We can know

the probability of nuclear transformations, decays, at certain time interval but it is impossible to find out their exact number since they vary in a stochastic manner.

An important feature of a stochastic error is that the reproducibility and preciseness increases with the number of measurements.

Below we discuss in more detail the uncertainties arising from the stochastic nature of radioactive decay.

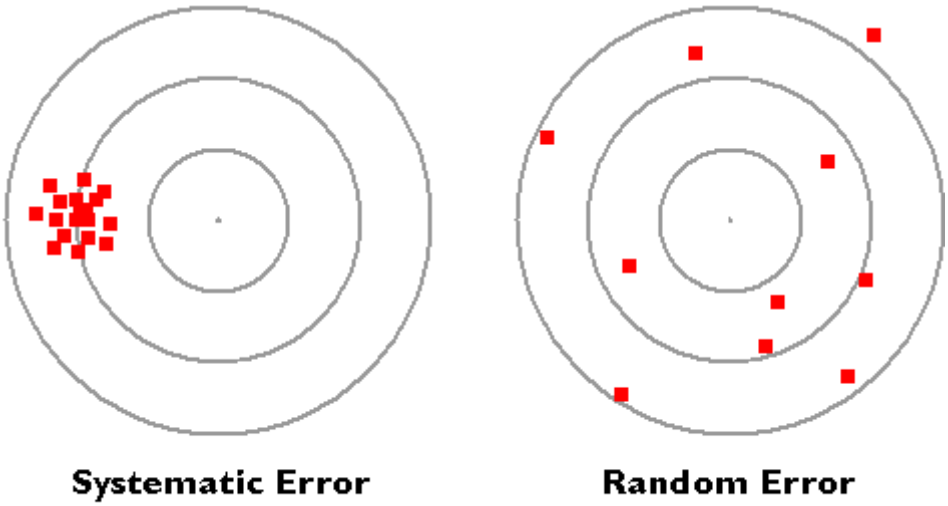

Figure IV.1. Effect of systematic and random error on observed results. Left side: high precision but low accuracy. Right side: low precision but high accuracy.

Poisson and normal distribution

The variation of radioactive decay events and other stochastic processes with low and constant probabilities are mathematically described with Poisson distribution probability function (Equation XIV.V). The variation of radioactive decays (or particle/photon flux) is a fundamental physical characteristic of the radionuclide. If we consider a large enough number of radionuclides the number of decay rate varies with time following the equation:

$$P_x = \frac{m^x}{x!} \cdot e^{-m} \qquad \text{[XIV.V]}$$

where P_x is the probability for x number of events occurring in unit time and m is the most probable number of events. Since the number of decay events can have only integer values the graphical representation of Poisson distribution is a histogram. Poisson distribution is also not symmetrical but is

slightly bended to lower values. To make treatment of results simpler the symmetric normal (Gaussian) distribution is used as an approximation to Poisson distribution. Figure XIV.2 shows the difference of Poisson and normal distributions for the probability to observe decay events in a number of identical time intervals. For a large number (<30) of events (m) Poisson and normal distributions are more or less identical.

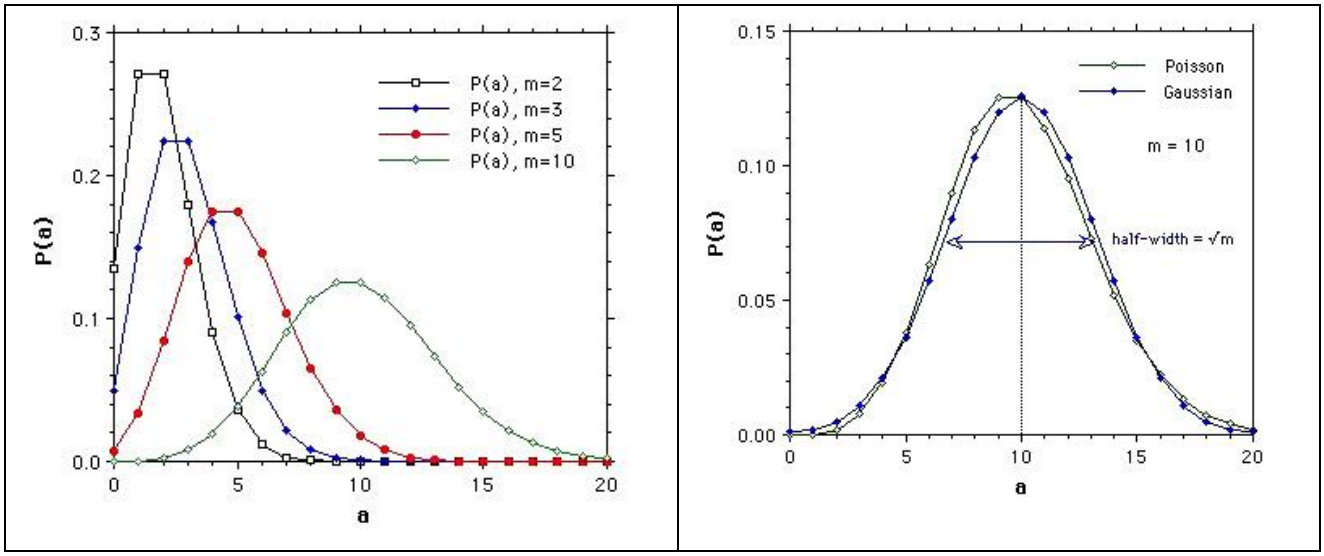

Figure XIV.2. Poisson and normal distribution functions for the probability (P) to observe radioactive decay events (m) in a number of identical time intervals (http://nau.edu/cefns/labs/electron-microprobe/glg-510-class-notes/statistics/).

The mathematical formulation of normal distribution is as follows:

$$P_x = \frac{1}{s\sqrt{2p}} \cdot e^{-\frac{(x-m)^2}{2s^2}} \qquad \text{[XIV.VI]}$$

where P_x is the appearance probability of a stochastic event, m is the real value of the events, s is the standard deviation of events at various time intervals.

Standard deviation

To present the variation for a number of decay events/pulses the quantity used is standard deviation, s. Its mathematical expression is

$$s_x = \sqrt{\frac{\sum (x_i - \bar{x})^2}{n - 1}} \qquad \text{[XIV.VII]}$$

where x_i is the number of pulses observed, $\bar{x}$ is their arithmetic mean value and n is the number of measurements. If for example a radioactive source is measured ten times the number of observed pulses may vary as shown in Table XIV.I. From these results one should calculate both the arithmetic mean and the standard deviation (uncertainty) and present the result as (99.0 ± 8.4) imp s^{-1} or 99.0 imp s^{-1} ± 8.5 %.

Table XIV.I. Variation of pulses in a radioactivity measurement. STDEV = s = standard deviation.

Measurement	Pulses	x - $\bar{x}$
1	99	0
2	102	3
3	89	-10
4	110	11
5	98	-1
6	112	13
7	88	-11
8	91	-8
9	105	6
10	96	-3
Mean	99	
STDEV	8.37	
%	8.45	

For the normal distribution it applies that if several measurements of radioactive decays are carried out and the mean value of pulses (or pulse rate or activity) is $\bar{x}$ a single measurement has a 68.3% probability to be observed in the range $\bar{x} \pm s$, 95.5% probability to be observed in the range $\bar{x} \pm 2s$ and 99.7% to be observed in the range $\bar{x} \pm 3s$. This is illustrated in Figure XIV.3.

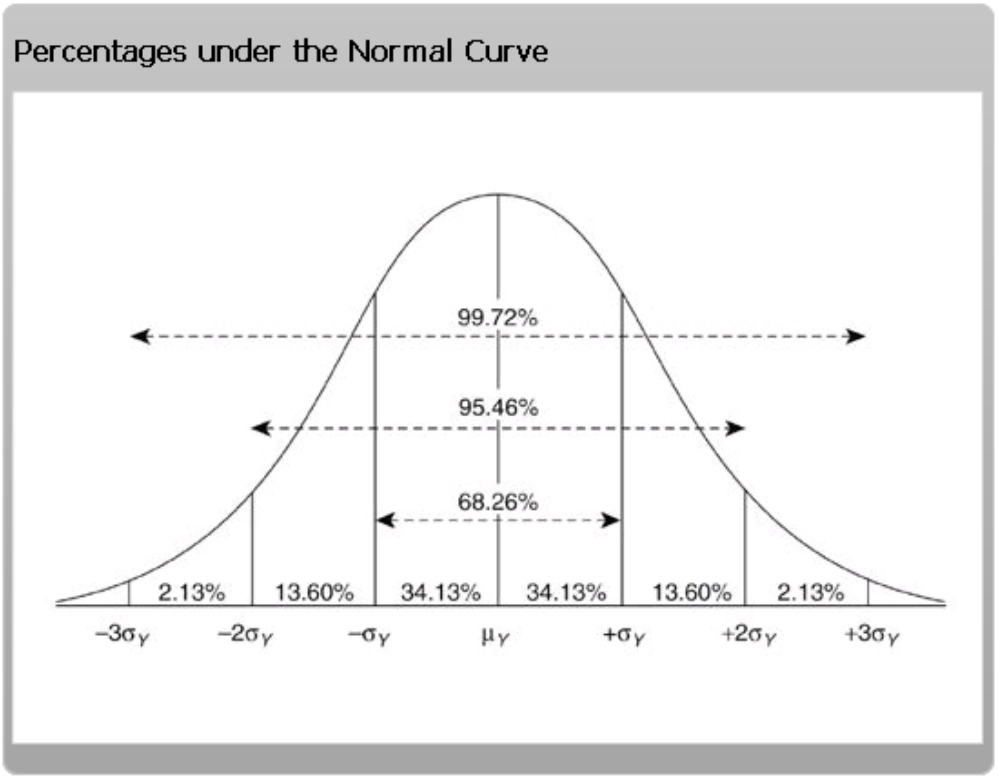

Figure XIV.3. Normal distribution and the probability ranges of standard deviation (https://learn.bu.edu/bbcswebdav/pid-826908-dt-content-rid-2073693_1/courses/13sprgmetcj702_ol/week03/metcj702_W03S01T02_normal.html).

Usually instead of several measurements, only one single measurement is carried out. The uncertainty, i.e. standard deviation (s), of a single measurement is calculated as a square root of the number of observed pulses (X)

$$s = \sqrt{X} \qquad \text{[XIV.VIII]}$$

For the standard deviation derived in this way applies the same rules as presented above: the measured number of pulses has a 68.3% probability to deviate one s value from the "right" value, 95.5% probability to deviate two s values from the "right" value and 99.7% probability to deviate three s values from the "right" value. Right value refers to mean value what would be obtained if several measurements were done. For example, if we observe 100 pulses, the value of s is $\sqrt{100} = 10$ and thus the measured number of pulses has a 68.3% probability to deviate 10% from the "right" value, 95.5% probability to deviate 20% from the "right" value and 99.5% probability to deviate 30% from

the "right" value. If we instead collect 10000 pulses the s gets a value $\sqrt{10000} = 100$ and the measured number of pulses has a 68.3% probability to deviate 1% from the "right" value, 95.5% probability to deviate 2% from the "right" value and 99.5% probability to deviate 3% from the "right" value. Thus increasing the number of observed pulses by a factor of 100 we decreased the uncertainty by a factor of 10. This applies to all measurement: the higher the number of collected pulses the lower is the uncertainty which is illustrated in Table XIV.2.

Table XIV.2. Uncertainties of radioactivity measurements with increasing number of collected pulses.

Pulses (X)	Standard deviation (s)	Relative uncertainty (%)
10	3.16	31.6
100	10	10
1000	31.6	3.2
10000	10000	1
100000	316	0.3

When presenting the results in radioactivity measurement the results should also include the uncertainty. For example in the following ways: 1030 ± 35 (s) Bq or 1030 ± 70 (2s) Bq or1030 ± 105 (3s) Bq.

Uncertainty of gross count rate

The standard deviation of the gross count rate, using 68.3% probability limits, is as follows:

$$s_g = \frac{\sqrt{X}}{t} \qquad \text{[XIV.IX]}$$

and the gross count rate with its uncertainty is thus

$$R_g \pm s_g = \frac{X_g \pm \sqrt{X_g}}{t} \qquad \text{[XIV.X]}$$

The unit of the uncertainty is the same as that of count rate, s^{-1} or imp/s.

Uncertainty of net count rate

When the background is determined with a separate measurement and it is subtracted from the gross count rate it brings further uncertainty to the net count rate. The standard deviations of both the gross count rate and the background count rate are separately calculated using the equation XIV.IX and the standard deviation of the net count rate is calculated with equation XIV.XI which is valid for propagation of any standard deviation of combining two standard deviations from summation or subtraction.

$$s_{R_n} = \sqrt{s_{R_g}^{\ 2} + s_{R_{bg}}^{\ 2}} \qquad \text{[XIV.XI]}$$

which equals with $s_{R_n} = \sqrt{\frac{X_g}{t_g^{\ 2}} + \frac{X_t}{t_{bg}^{\ 2}}}$ [XIV.XII]

Standard deviation of activity

The activity (A) is typically calculated by comparing the net count rate of the unknown sample (R_n) to that of the standard (R_{st}). The standard deviation of the activity (s_A) is then calculated with the equation XIV.XIV which is valid for propagation of any standard deviation of a product or a quotient.

$$\frac{s_A}{A} = \sqrt{\left(\frac{s_{R_n}}{R_n}\right)^2 + \left(\frac{s_{R_{st}}}{R_{st}}\right)^2} \qquad \text{[XIV.XIV]}$$

XV NUCLEAR REACTIONS

Content

Nuclear reaction types and models

The Coulomb barrier

Energetics of nuclear reactions

Cross sections

Nuclear reaction kinetics

Excitation function

Photonuclear reactions

Neutron induced nuclear reactions

Induced fission

A nuclear reaction is an event in which a nucleus is targeted by a projectile (proton, deuteron, alpha particle, *etc.*) or gamma ray causing one of the following interactions with the nucleus:

- Transmutation or the formation of a new nucleus
- Inelastic scattering
- Elastic scattering

Since the specific aim of this communication is production of new nuclei, primarily radionuclides, in nuclear reactions, transmutation lead reactions will be the focus. Scattering is mentioned only briefly. Projectiles can be very heavy, even uranium nuclei, but this communication will concentrate on lighter ones (p, d, α, n).

In nature, nuclear reactions occur in the following sources:

- The cosmic protons and alpha particles of the upper parts of the atmosphere (as well as the neutrons generated by these nuclear reactions) cause nuclear reactions upon hitting with the gas molecules of the atmosphere. The most important of these is the emergence of the ^{14}C from atmospheric nitrogen.
- Fusion reactions occuring in stars.
- A very small number of neutron activation reactions caused by neutrons generated in spontaneous fission of uranium in bedrock and overburden.

The first artificial nuclear reaction was achieved by Ernst Rutherford in 1919, when he targeted nitrogen gas with alpha radiation generated in ^{214}Po decay, which resulted in the following reaction:

$$^{14}N + {}^{4}He \rightarrow {}^{17}O + {}^{1}H \qquad [XV.I]$$

The products of the reaction were oxygen, its ^{17}O isotope and protons. The above reaction equation can also be presented in a shorter form:

$$^{14}N(^{4}He,p)\,^{17}O \text{ or } {}^{14}N(\alpha,p)\,^{17}O \qquad [XV.II]$$

where the left side of the parentheses is the target nucleus and on the right is the result nucleus. Inside the parentheses on the left is a projectile particle/ray and on the right an emitting particle/ray. The bombarded substance is called the target. The neutrons needed for nuclear reactions are primarily obtained by research reactors, but also in neutron generators. The positive projectile particles are produced by particle accelerators that are *e.g.* the van de Graaf accelerator, linear accelerator, cyclotron, and synchrotron.

The first particle accelerator, which could achieve nuclear reactions, was developed in the early 1930s. The first nuclear reaction that created an artificial radionuclide was accomplished in 1934, when Frederik Joliot and Irene Curie used a particle accelerator to bombard aluminum with alpha particles and produced ^{30}P, which is a positron emitter. The reaction was, therefore, $^{27}Al(\alpha,p)^{30}P$.

Nuclear reaction types and models

In most nuclear reactions the target nucleus absorbs the projectile particles (n, p, d, α) and emits other particles in a fairly short period of time (10^{-14}-10^{-18} s). A liquid drop model was developed to describe these types of reactions. The kinetic energy of the projectile particle and its merging with the nucleus generates bonding energy that spreads evenly as the nuclear excitation energy. Much like a liquid droplet, the particles at some point in the nucleus have such an ample energy that it "evaporates" from the nucleus. The liquid drop model is supported, for example, by the fact that the reactions

$$^{12}_{6}C + ^{144}_{60}Nd \rightarrow ^{150}_{66}Dy + 6n \quad \text{and} \quad ^{20}_{10}Ne + ^{136}_{56}Ba \rightarrow ^{150}_{66}Dy + 6n \qquad \text{[XV.III]}$$

have roughly equal probability as a function of the projectile energy (*i.e.* excitation function, which is explained later). In this case, the explanation is that an excited intermediate nucleus or compound nucleus $^{156}_{66}Dy$ is generated in both cases, which breaks down in the same way, regardless of its origin.

The liquid drop model is not able to explain all of the observed reactions, in particular those with high projectile energy. These reactions are, for example, spallation reactions, in which a large number, even many tens of nucleons, are emitted from the nucleus and the resulting nucleus is of a clearly lighter element. Such reactions are also the fragmentation reactions, in which instead of one several lighter nuclei develop. These reactions are depicted by the direct interaction model, according to which the intermediate nucleus does not have time to form, in other words the excitation energy has no time to spread throughout the nucleus and instead breaks down immediately as a direct effect of the projectile particles.

Fission is a reaction in which a heavy nucleus, *e.g.* ^{235}U, decays into two lighter elements. It is also explainable by the liquid drop model. Fusion is the opposite reaction to fission: lighter elements join together to form heavier nuclei.

Scattering is characteristic of neutron interactions with target nuclei. In scattering the projectile particle and emitting particle are identical. If there is no change in the energy of the nucleus during scattering, it is called elastic. In inelastic scattering the nucleus becomes excited and the kinetic energy of the emitting particle reduces.

The Coulomb barrier

When a positively charged particle (proton, deuteron, alpha particle etc.) collides with a nucleus, it is subjected to the positively charged protons of the target nucleus causing a repellent force. In order to penetrate into the nucleus the particle must have enough kinetic energy to overcome this repulsion, in other words cross the Coulomb barrier. The Coulomb barrier is higher, the greater the target substance atomic number is. The Coulomb repulsion in also dependent on the bombarding

particle charge: it is larger for alpha particles that have a charge of +2 than protons, with a charge of +1. According to the Coulomb's law the repulsion force is

$$F_{coul} = k \times e \times Z_1 \times e \times Z_2 / x^2 = k \times e^2 \times Z_1 \times Z_2 / x^2 \qquad [XV.IV]$$

where k is Coulomb's constant (8.99×10^9 N m^2 C^{-2}), *e* is the electron charge, Z_1 is the elemental number of the projectile particle, Z_2 is the corresponding value for the target nucleus, and *x* is their distance. i.e. distance of their center points. So, this is the energy of projectile needed to cross the Coulomb barrier. Figure XV.1 shows the dependence of the Coulomb barrier on the nuclear charge of both the projectile particle and the target nucleus.

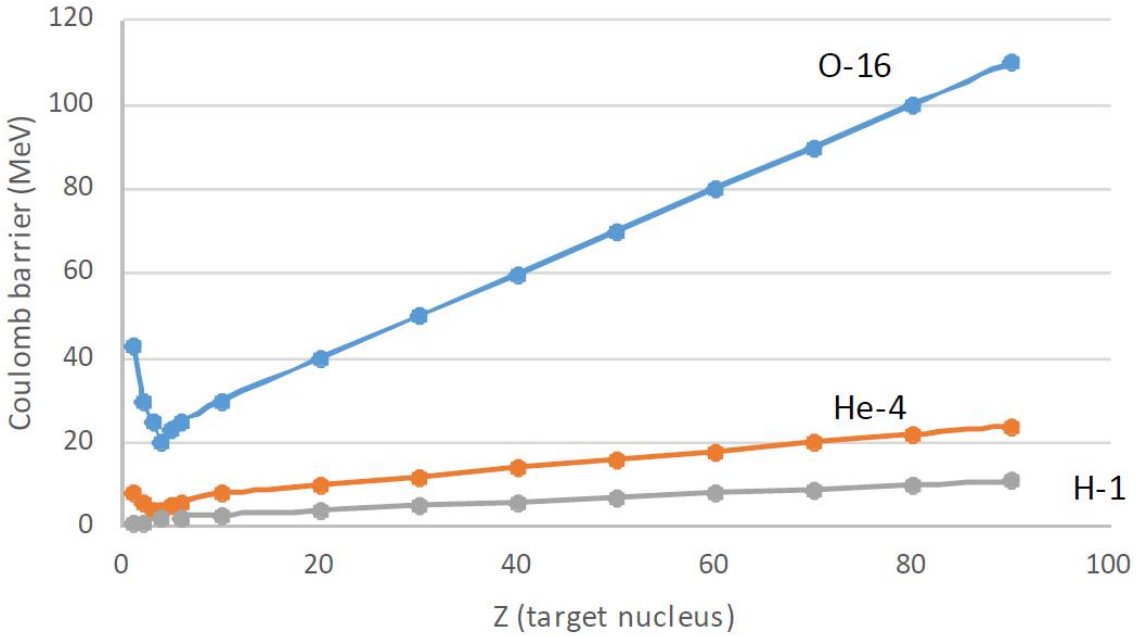

Figure XV.1. The height of the Coulomb barrier for three projectile particles as a function of the target nucleus atomic number.

Energetics of nuclear reactions

As in radioactive decay, the change in energy occurring in nuclear reactions can be calculated from the masses of the initial and resulting nuclei. The change in mass in a nuclear reaction A(x,y)B is thus:

$$\Delta m = m_B + m_y - m_A - m_x \qquad [XV.V]$$

The reaction energy Q (MeV) is -Δm (amu) × 931.5 MeV/amu. If the mass in the reaction decreases, it means that the energy is released, *i.e.* it is an exoergic reaction. On the other hand, if the mass increases, it is an endoergic reaction. For example, in the equation [XV.II] for the reaction $^{14}N(\alpha,p)^{17}O$ the reaction Q is

$$Q = 931.5 \text{ MeV/amu } (16.999131 + 1.007825 - 14.003074 - 4.002603) \text{ amu} =$$
$$931.5 \text{ MeV/amu} \times -0.001279 \text{ amu} = -1.19 \text{ MeV} \qquad \text{[XV.VI]}$$

The total mass increases in this reaction by 0.001279 amu and thus this is an endoergic reaction, *i.e.* the kinetic energy of the projectile particle must import the required energy (1.19 MeV) to the target nucleus. In addition to this energy, the projectile particle must have enough energy to also encompass the kinetic energy of the emitting particle and the recoil energy of the resulting nucleus. The smallest possible projectile particle energy able to cause an endoergic reaction is called the threshold energy (E_{th}) of the reaction. From the energy and momentum conservation laws one can derive threshold energy value by:

$$E_{th} = \frac{m_x + m_A}{m_A}(-Q) \qquad \text{[XV.VII]}$$

The threshold energy of the reaction $^{14}N(\alpha,p)^{17}O$ is thus -(-1.19 MeV)(4+14)/14 = 1.53 MeV, being 0.34 MeV larger than the reaction energy.

To achieve an exoergic reaction, the projectile particle must have enough energy to cross the Coulomb barrier. In exoergic reactions the kinetic energy of the emitting particle is, however, not the same as the reaction energy since also in this case the resulting nucleus gets part of the released energy as recoil energy.

In addition to particle emission the nucleus also often emits gamma rays. For example, in the reaction

$$^{184}_{74}W + a \rightarrow {}^{186}_{76}Os + 2n \qquad \text{[XV.VIII]}$$

the intermediate nucleus $^{188}_{76}Os$ is generated, with an excitation energy of 20 MeV. The release of each neutron reduces the binding energy by 6 MeV and their kinetic energy of 3 MeV, *i.e.* a total of 18 MeV of excitation energy is removed with their emission. The remaining 2 MeV is not enough to overcome the binding energy of a third neutron, but this portion departs the nucleus as gamma radiation.

Cross sections

The cross section describes of the probability of a nuclear reaction occurrence. In other words, it tells us how large a fraction of bombarding particles brings about a nuclear reaction. The cross section is derived in this section.

Let's expose a target with N number of nuclei per unit volume (m^3) and dx in thickness (m) with a coherent particle flux. When the target is so thin that the particle flux density ϕ_o (particles/$m^2 \times s^1$) does not essentially change, the decrease in particle flux density equals with the number of collisions leading to nuclear reactions in a unit of time per unit area (m^2):

$$- df = f_0 \cdot N \cdot \sigma \cdot dx \qquad \text{[XV.IX]}$$

where σ is the probability of events or the cross section. When the target is so thick (x) that the particle flux decreases significantly, its value can be calculated with the equation XV.X, which is obtained by integrating the equation XV.IX. with respect to thickness.

$$f = f_0 \cdot e^{-\sigma \cdot N \cdot x} \qquad \text{[XV.X]}$$

The unit of the cross section derived from the equation XV.VII is unit area. Because this has a very small value, barn (b = 10^{-28} m^2, approximately a unit cross section of a nucleus) is used instead m^2. If we neglect Coulombic interactions and nuclear forces the cross section should approximately be comparable with the size of a nucleus, which in fact applies to many neutron-induced reactions, i.e. cross sections are close to 1 barn. However, due to action of the repulsive and attractive forces from nuclear and Coulombic interactions the cross sections vary several orders of magnitude, both above and below 1 barn.

The decrease in particle flux in the target does not yet explicitly describe the number of a pecific nuclear reaction. Several nuclear reactions can occur simultaneously in the target, for example a reaction can lead to the emission of one neutron and a reaction with emission of two neutrons simultaneously. When all simultaneous reactions are considered, the cross section is called the total cross section while when individual reactions are considered separately it is called a partial cross section in which case the total cross section is the sum of all the partial cross sections of simultaneous nuclear reactions.

Nuclear reaction kinetics

When nucleus B is produced by irradiating a nucleus A in a nuclear reaction, the equation for the growth rate of the resulting nucleus is:

$$\frac{dN_B}{dt} = s \cdot f \cdot N_A \qquad \text{[XV.XI]}$$

where N_A and N_B are the numbers of target and product atoms, respectively. If the product nuclide B is radioactive, it decays at the same time by a factor $-\lambda N_B$, where λ is the decay constant of nuclide B. In this case, the total rate of growth for the product nucleus is

$$\frac{dN_B}{dt} = s \cdot f \cdot N_A - l N_B \qquad \text{[XV.XII]}$$

When the irradiation time is t, the number of product nuclei is calculated at the end of irradiation by the formula XV.XIII, which is obtained by integrating the formula XV.XII in the time interval 0-t assuming that at the start of irradiation $N_B = 0$.

$$N_B = \frac{s \cdot f \cdot N_A}{l}(1 - e^{-lt}) \qquad \text{[XV.XIII]}$$

When producing radionuclides, the activity of the nuclide is of more interest than the number of nuclei. Since $A = \lambda \times N_B$, we can replace N_B with A/λ in the formula XV.XIII to get:

$$A_B = s \cdot f \cdot N_A(1 - e^{-lt}) \qquad \text{[XV.XIV]}$$

The mass *m* is used instead of the target nuclei number N_A and the half-life $t_{½}$ is used instead of the decay constant λ, in which case the formula becomes

$$A_B = \frac{m \cdot I \cdot 6.023 \times 10^{23} \cdot s \cdot f}{M}(1 - e^{-\ln 2 \cdot t / t_{1/2}}) \qquad \text{[XV.XV]}$$

where *m* is the mass of the target element, I the target nuclide's isotopic abundance of the element, $6.023 \cdot 10^{23}$ is the Avogadro's number, and M is the molar mass of the element.

Figure XV.2. shows the relative amount of nuclide produced in the target as a function of irradiation time. Time here is the irradiation time divided by the nuclide's half-life, i.e. it is the number of half-lives. As seen, 50% of the maximum obtainable activity (saturation activity) is produced during one half-life, 75% during two half-lives, and about 99% during ten.

Finally, accounting for the continuing decay of the radionuclide after irradiation, the activity of the produced radionuclide can be calculated at the time point t^* after the end of the irradiation by the formula

$$A_B = \frac{m \cdot I \cdot 6.023 \times 10^{23} \cdot s \cdot f}{M}(1 - 2^{-\frac{t}{t_{1/2}}}) \cdot 2^{-\frac{t^*}{t_{1/2}}} \qquad \text{[XV.XVI]}$$

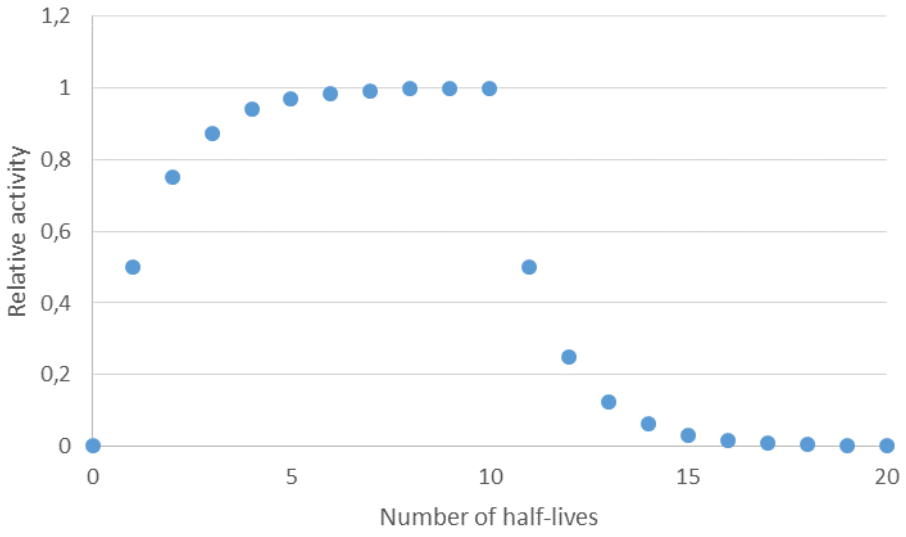

Figure XV.2. The relative amount of a radionuclide in the target as a function of irradiation time up to ten half-lives of the product nuclide and the decay of the product nuclide after irradiation.

Excitation function

The probability of nuclear reactions is also dependent on the projectile particle energy. Presenting the cross sections of all individual reactions as a function of the projectile energy is called an excitation function. The Figure XV.3 demonstrates the excitation function of ^{54}Fe irradiation with alpha particles. As seen, the predominant reactions at low projectile energy lead to emission of a single particle (n and p). As the projectile energy increases also two particle emissions occur and at even higher energies also three particle emissions. The reactions in the figure are:

^{54}Fe(α,p)^{57}Co	^{54}Fe(α,n)^{57}Ni	^{54}Fe(α,pn)^{56}Co
^{54}Fe(α,2n)^{56}Ni	^{54}Fe(α,2pn)^{55}Fe	^{54}Fe(α,p2n)^{55}Co

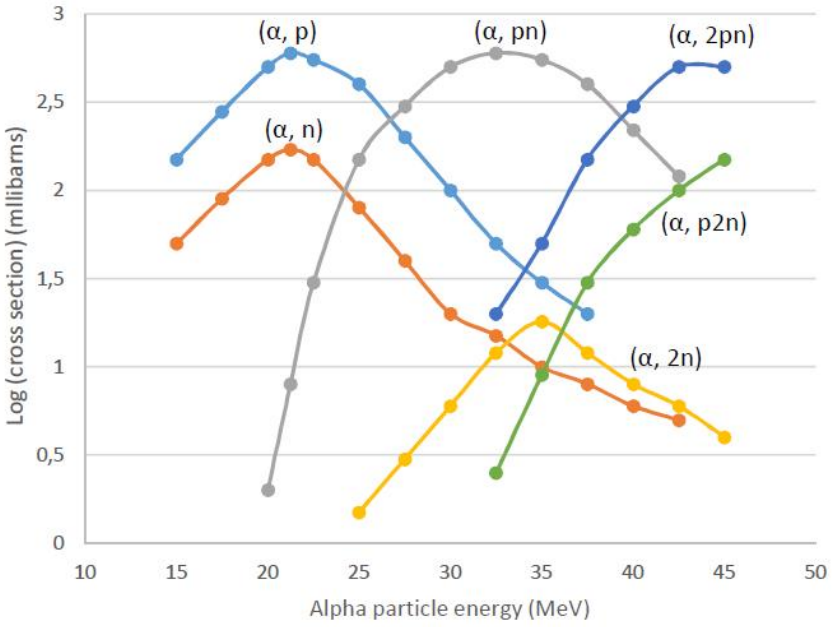

Figure XV.3. The excitation function in irradiation of ^{54}Fe with alpha particles (data from Houck and Miller, Physical Review 123(1961)231.

Photonuclear reactions

Gamma radiation can cause nuclear reactions resulting in particle emissions, *e.g.* (γ,n) and (γ,p). These type of reactions are called photonuclear reaction. These reactions require a certain threshold energy from gamma rays to overcome the binding energies of protons and neutrons. The threshold

energies of protons are higher than those of neutrons, because their removal from the nucleus also requires energy to cross the Coulomb barrier. Threshold energies are usually at least 5 MeV, so most of the gamma rays generated in radioactive decay do not cause nuclear reactions. Some nuclei, such as ^{2}H, ^{9}Be, and ^{13}C, have lower threshold energies, however, and for example the $^{9}Be(\gamma,n)^{8}Be$ reaction can already occur at gamma energies of 1.67 MeV.

Neutron induced nuclear reactions

Since neutrons have no charge they are not affected by the repulsion caused by the positively charged nuclei. Therefore, neutron induced reactions do not have a threshold energy. On the contrary, reactions are achievable even with very little energy. In fact, the reaction probability (cross section) for neutrons with energy less than 1 MeV is higher the lower the energy: the cross section is inversely proportional to the kinetic energy of the neutron (Figure XV.4.).

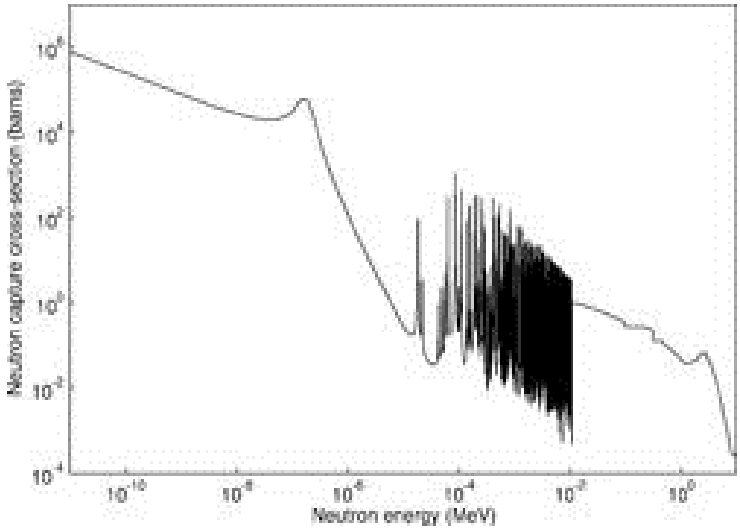

Figure XV.4. The excitation function of nuclear reactions induced by neutrons (neutron capture) in a ^{113}Cd target (http://thorea.wikia.com/wiki/Thermal,_Epithermal_and_Fast_Neutron_Spectra).

For slowest neutrons, called thermal neutrons having energies of 0.005-0.1 eV, the neutron capture cross sections are as high as 10^5 b. The ability of slow neutrons to cause nuclear reactions is due to their high wave length of about 0.1 nm, while the wavelengths of faster neutrons (<0.1 MeV) is a thousand times smaller. Therefore, the probability of slower neutrons hitting the nuclei is greater.

Slow neutrons often cause a capture reaction, that is, the neutrons are absorbed into the nucleus and gamma rays are emitted. These gamma rays get kinetic energy from the binding energy of absorbed neutrons. Typically, the energies of the gamma rays are high, between 5-8 MeV.

As shown in Figure XV. 4 the excitation function of neutrons at intermediate energies has many peaks. These are resonances, in which the excitation energy produced by the projectile particle nuclei are equivalent to the excitation levels of the nucleus. When the projectile energy value rises above 1 MeV the resonance states overlap and the excitation function levels.

Neutrons with a higher projectile energy can also produce reactions leading to alpha and proton emissions. Since their departure from the nucleus requires crossing the Coulomb barrier, these reactions always have a threshold energy.

Neutrons also cause fission reactions, which will be discussed in the next section.

Induced fission

Chapter V dealt with spontaneous fission, and found that the reason for it is that a nucleus is too heavy and that it occurs only in the heaviest nuclei. In many ways, induced nuclear fission is similar to spontaneous fission. In both cases the nucleus disintegrates into two lighter nuclei, but not spontaneously in case of induced fission but through the excitation energy of external particles, typically neutrons, for example

$$^{235}U + n \rightarrow (^{236}U)^{*} \rightarrow {}^{143}Ba + {}^{89}Kr + 3\,^{1}n + 200MeV \qquad [XV.XVI]$$

where $(^{236}U)^{*}$ is the excited intermediate uranium nucleus generated by neutron absorption, which quickly breaks down.

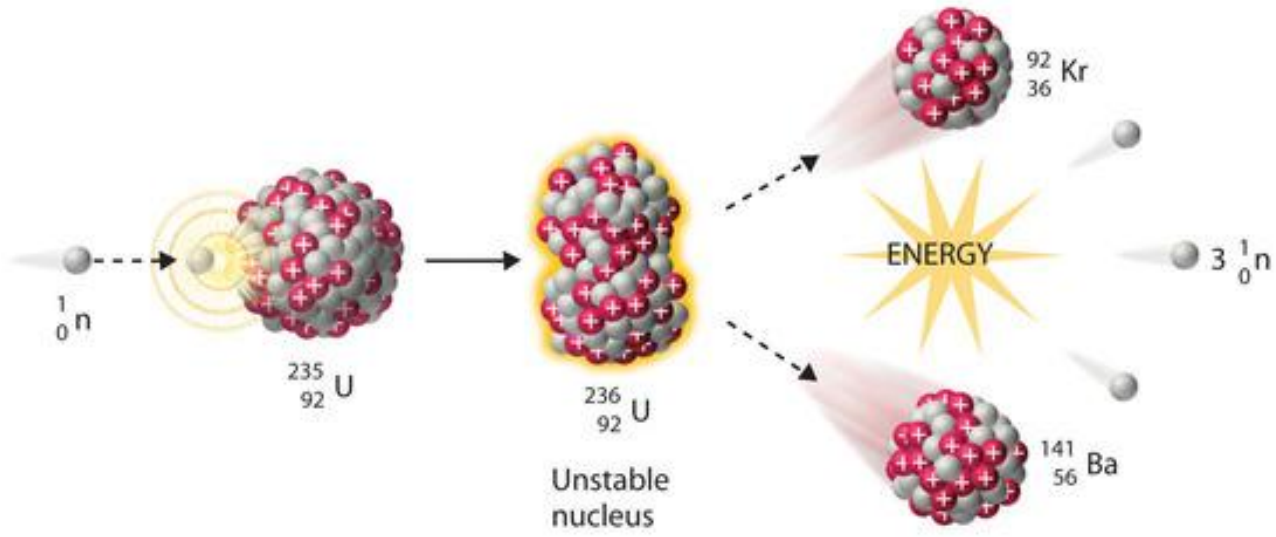

Figure XV.5. Induced fission of a heavy nucleus into two lighter nuclei (http://chemwiki.ucdavis.edu/Physical_Chemistry/Nuclear_Chemistry/Nuclear_Reactions).

Despite fission usually being caused by a neutron, it can be produced by other particles, such as protons, deuterons and alpha particles (and even by the gamma rays) that have enough energy to cross the Coulomb barrier and introduce enough excitation energy via their kinetic energy. The requisite excitation energy of the intermediate nucleus is 4-6 MeV. While spontaneous fission only pertains to heavy nuclei, induced fission can also be achieved with medium heavy nuclei, even lanthanides, as long as the projectile particle energy is high enough, at least 50 MeV.

The fission process can be explained as follows. Two opposing forces exist in the nucleus. The short-range nuclear forces which are smallest when the nucleus is spherical. While the longer range electrical forces, *i.e.* proton repulsion, aims to tear apart and deform the nucleus. Therefore, this is why, for example, the uranium nucleus is slightly elliptical, not perfectly spherical. When a neutron absorbs into the uranium nucleus it causes an increase in the ellipticity and disintegration of the nucleus if the excitation energy is sufficiently large (Figure XV.5).

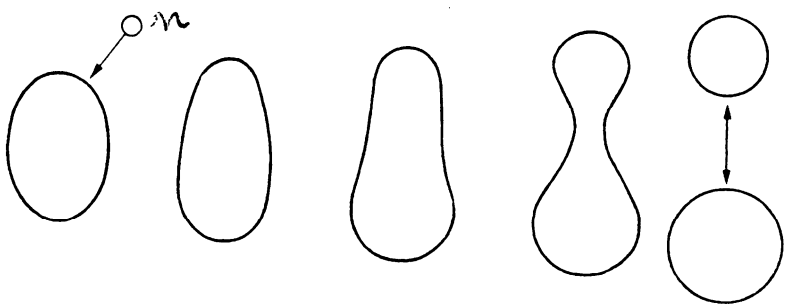

Figure XV.6. Heavy nucleus fission after neutron capture.

Fission releases a large amount of energy, because medium heavy nuclei have a stronger binding energy to nucleons, about 8 MeV/nucleon, than heavy nuclei in which it is about 7 MeV/nucleon (see Figure II.2). For each nucleon an energy of almost 1 MeV is released and in an individual fission event of a heavy nucleus a total of 200 MeV of energy is released, the distribution of which is shown in Table XV.I

Table XV.1. The distribution of the 200 MeV total energy generated by a ^{235}U fission event.

Kinetic energy of fission products	165 MeV
Kinetic energy of neutrons	5 MeV
Gamma energy released immediately at fission	7 MeV
Beta particle energy of fission products	7 MeV
Gamma ray energy of fission products	6 MeV
Energy generated by neutrinos in beta decay	10 MeV

In conventional fission types the fission products generated are mostly of a different size (asymmetric fission). Figure XV.7a shows the distribution of fission products of the thermal neutron induced fission of three nuclides ^{235}U, ^{239}Pu, and ^{241}Pu. Events, in which fission products are of equal size (symmetric fission) are extremely rare, occurring in only 0.05-0.01% of the cases. Distribution of uranium fission products has two peaks, at a mass numbers of 90-100 and of 130-140. The largest fission yields at these mass numbers are about 6-7%. The fission nuclides ^{90}Sr and ^{137}Cs belong to this category: they constitute the major part of the activity of fission products within the next few hundred years. The half-life of both is relatively long, about 30 years. Plutonium also has a fission product peak at the same upper mass number, but the lower mass number peak is transferred to a higher range, 95-105. When going further into heavier fissioning nuclides this lower mass number peak range moves closer to the upper range and the valley between them narrows and becomes shallower, increasing the likelihood of symmetric fission. The probability of symmetric fission also increases when the projectile particle energy grows (Figure XV.7b): in the fission of ^{235}U induced by 14 MeV neutrons already one out of a hundred results in a symmetric fission. When the neutron energy is raised to 100 MeV, the valley between the peaks disappears.

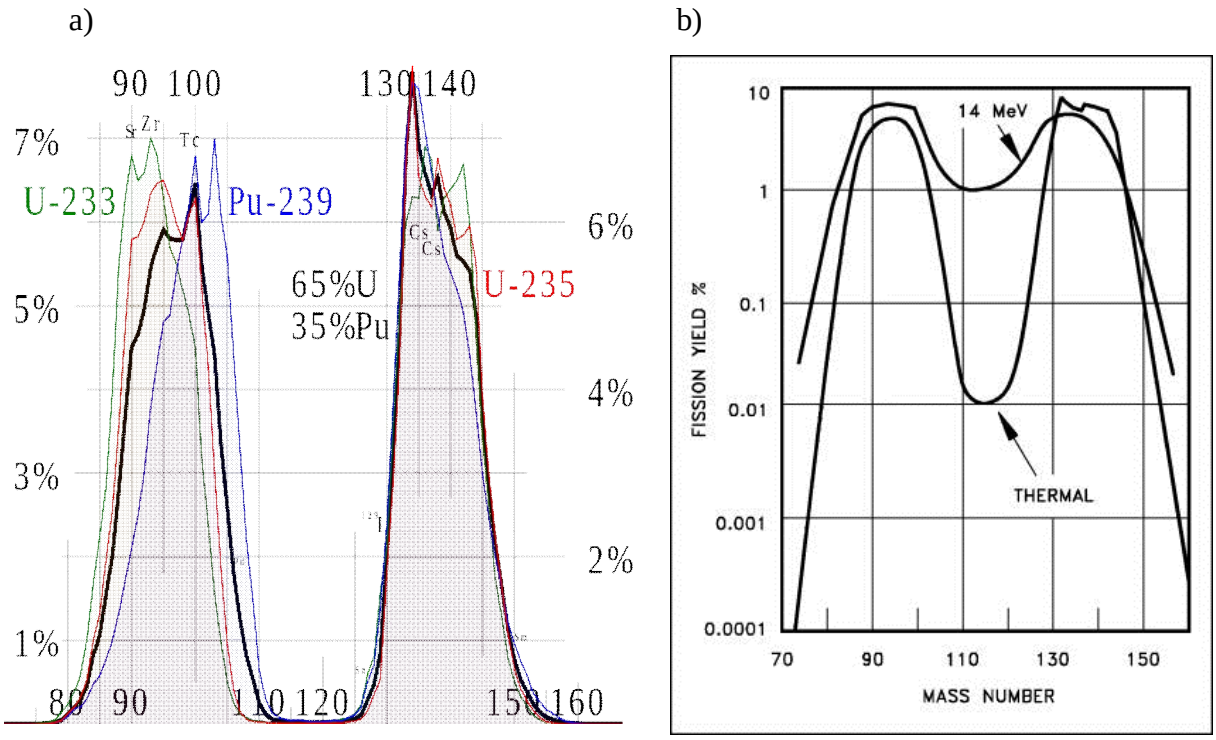

Figure XV.7. Yields of fission products (%) as a function of their mass number: a) thermal neutron induced fission of ^{233}U, ^{235}U, ^{239}Pu and ^{241}Pu (https://en.wikipedia.org/wiki/Fission_product_yield#/media/File:ThermalFissionYield.svg) b): ^{235}U fission with thermal and 14 MeV neutrons (http://www.tpub.com/doenuclearphys/nuclearphysics29.htm).

In a fission event 2-3 neutrons, prompt neutrons, form at disintegration moment. The daughter nuclides formed in fission are always radioactive, because fissioning heavy elements have a greater neutron to proton ratio than lighter elements. Thus, the fissioning nuclides, even after emitting 2-3 neutrons, have too many neutrons and they decay via β-decay to correct the unstable neutron/proton ratio. Decay occurs in several stages forming a decay chain. The neutron to proton ratio of ^{235}U is 1.55 and is roughly the same with the primary fission product nuclides. For example, the stable barium isotopes, however, have a much lower neutron to proton ratio of 1.32-1.46. An example of this type of beta decay chain in which the neutron/proton ratio decreases is:

$$^{137}_{52}Te \xrightarrow{3.5s} {}^{137}_{53}I \xrightarrow{24.5s} {}^{137}_{54}Xe \xrightarrow{3.8\,\text{min}} {}^{137}_{55}Cs \xrightarrow{30a} {}^{137}_{56}Ba(stable)$$

n/p:	1.63	1.58	1.54	1.49	1.45

As shown, when going towards stable nuclides from the primary fission nuclides the half-lives lengthen, reflecting the increase in stability. In some beta decay events, neutrons, called delayed

neutrons, are also emitted. They are only a small fraction of the prompt neutrons, *e.g.* 0.02% in ^{235}U fission.

The nuclides, in which a fission reaction is possible, are called fissionable, *i.e.* eligible for fission. Nuclides able to undergo fission induced by thermal neutron are called fissile. Of these the most important are ^{235}U and ^{239}Pu, which play an important role as nuclear reactor fuel and nuclear weapons material. Of these, ^{235}U is the only naturally occurring fissile material. Neutron bombardment of ^{238}U produce ^{239}Pu by neutron capture and beta decay. A characteristics of uranium, and plutonium, isotopes is that the isotopes (^{233}U, ^{235}U), with an odd mass number are fissile, but ones with an even mass number (^{234}U, ^{238}U) only undergo fission induced by high energy neutrons. This is because when all the protons in the uranium nucleus (Z = 92) are paired, the uranium isotopes with an odd mass number have unpaired neutrons. Binding energy released in the pair formation of the absorbed neutron with the unpaired neutron is enough to induce fission. Instead, with uranium isotopes with an even mass number, not enough binding energy is released to induce fission since the absorbed neutron remains unpaired. In this case, to induce fission, kinetic energy of the fast neutrons is needed. Cross sections of induced fission of ^{235}U and ^{238}U are seen in Figure XV.8.

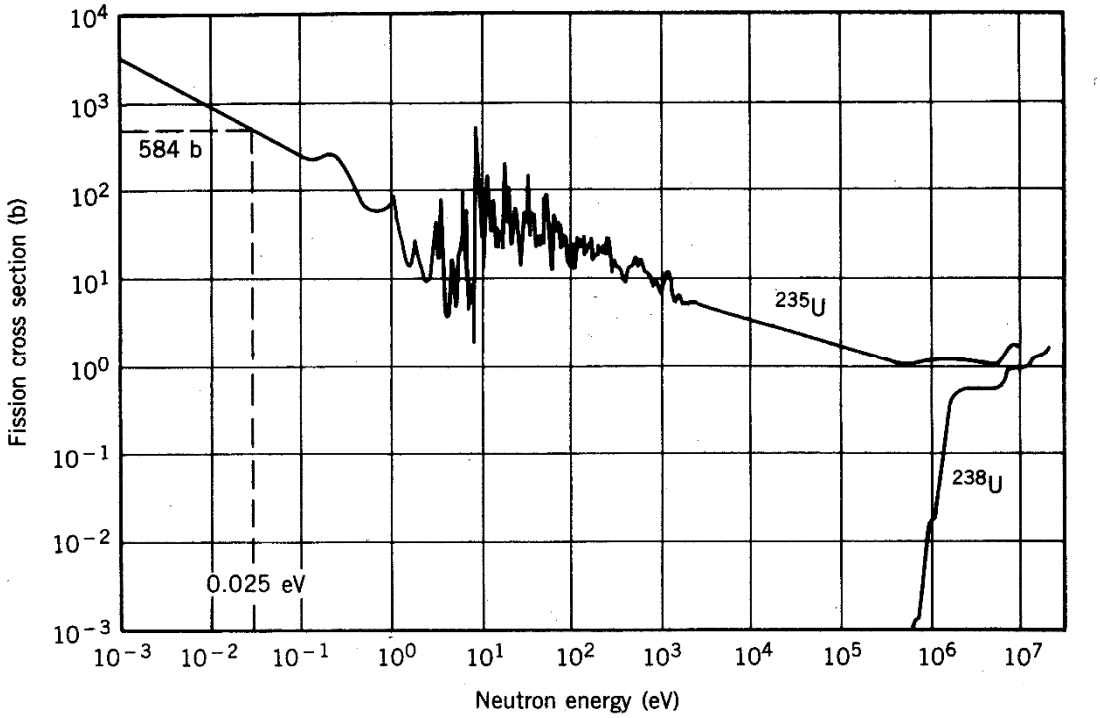

Figure XV.8. Cross section of neutron induced fission of ^{235}U and ^{238}U (D.T.Hughes and R.B. Schwartz, Neutron Cross Sections, Brookhaven National Laboratory Report 325, 2nd Edition, 1958).

In order for fission events to continue spontaneously, become a chain reaction, in fissile material there has to be a sufficient amount of material. If there is too little material the neutrons escape without causing new fission. At least one neutron generated by a fission event must cause at least one new fission in order to create a chain reaction. The chain reaction is controlled, if only one neutron causes one new fission. If more than one neutron induces fission, it is uncontrolled fission, *i.e.* a bomb. The minimum mass of a spherical fissile material at which fission chain reaction occurs is called the critical mass. It is 52 kg for ^{235}U and only 16 kg for ^{239}Pu.

XVI PRODUCTION OF RADIONUCLIDES

Content

Production of radionuclides in cyclotrons

Production of radionuclides in reactors

Radiochemical and radionuclidic purity

Radionuclide generators

This chapter deals with production of radionuclides for utilization in research, medical use and industrial use etc. Production of radionuclides, such as transactinides, for the study of their properties is not discussed here. Radionuclides are produced either in reactors or in particles accelerators, particularly cyclotrons. These two methods are complementary to each other both offering advantages over the other.

Production of radionuclides in cyclotrons

In cyclotrons nuclear reactions are induced by bombarding target atoms by proton-bearing particles, such as protons, deuterons and alpha particles. Depending on the bombarding particle and its energy various product nuclides are obtained (see Figure XVI.3). Most reactions result in change of the atomic number yielding product nuclei having a higher atomic number (or sometimes lower, for example in (d,α) reaction). These nuclei are proton-rich and therefore decay by positron emission or electron capture. Since the product nuclei are of a different element than the target nuclei cyclotrons can produce carrier-free radionuclides. This means that after chemical or physical separation the product nuclide does not contain any (or contains only very minor amounts) of stable isotopes of the same element. This results in the formation of product nuclides with very high specific activity (= activity divided by the mass of the product element). Use of carrier-free radionuclides is in many cases advantageous, for example in labelling of organic molecules, where as many positions in the molecules are aimed to label with a radionuclide and not with a stable isotope of the same element. In carrier-bearing radionuclide products the stable isotopes always "dilute" radionuclides and yield in lower specific activities. An example of cyclotron-produced radionuclides is ^{22}Na which can be produced from magnesium with the reaction ${}^{24}_{12}Mg(d,a){}^{22}_{11}Na$ ($t_{½}$ = 2.6 a). Since the target is made of magnesium it does not, after chemical separation of sodium from magnesium, dilute the product.

Even high activities represent very low chemical amounts, for example 1 MBq of ^{22}Na corresponds to only 2×10^{-10} moles or 4.5 ng of sodium which means that the specific activity is very high at 5×10^{15} Bq/mol or 2×10^{14} Bq/g. In practice completely carrier-free radionuclides are not achieved due to contamination. Furthermore, small amounts of carrier are often added to the system to prevent losses of the radionuclides due to adsorption, for example.

Production of radionuclides in reactors

As cyclotrons produce proton-rich radionuclides reactors produce neutron-rich ones. The reactions needed for radionuclide reactions are typically neutron capture reactions by using thermal neutrons. An example of such reactions is $^{23}_{11}Na(n,g)^{24}_{11}Na$ to produce ^{24}Na ($t_{½}$ = 15 h). As is seen from the reaction formula both the target and the product are of same element, sodium in this case. Thus all radionuclides produced in reactors using (n,γ) neutron capture reaction results in the formation of products containing carrier and therefore the specific activities of such radionuclides are fairly low. ^{24}Na produced by neutron capture reactions has a specific activity of 10^{11} Bq/g Na at maximum, whereas ^{24}Na produced from ^{26}Mg in cyclotron by the (d,α) yields a high specific activity of 10^{13} Bq/g Na. The neutron-rich radionuclide produced in reactors decay by β^- decay to elements having a higher atomic number. In the case the desired radionuclide is a radionuclide produced in the β^- decay of the primary product produced in a neutron capture reactions carrier-free radionuclides can be obtained after chemical separation. Radionuclides can be produced by reactors also by utilizing fission reactions, particularly thermal neutron induced fission of ^{235}U. In this case the number of radionuclides produced is high and the required separations for desired radionuclide/s may be laborious and time-consuming.

Chapter XVI describing nuclear reactions give the equations (XVI.XI-XVI.XVIII) and Figure XVI.2 presenting the kinetics of nuclear reactions used in radionuclide productions. These equations are needed to calculate the required irradiation times to produce a radionuclide with known half-life using a nuclear reactions with known cross-section at given irradiation flux and bombarding energy.

Radiochemical and radionuclidic purity

When a tracer experiment with a certain radionuclide is done it is most often desirable that there are not any other radionuclides present since measurement of single radionuclide is easier as no

radiochemical separations nor spectrometric analysis are needed. When a tracer product contains only one specific radionuclide, it is called radionuclidic pure. Radionuclide purity as a measure means the activity fraction of a specific radionuclide of the total activity. To produce radionuclidic pure tracers by nuclear reactions is not an easy task. The conditions in production reactions, particularly projectile energy and bombardment time, should be kept so that only one product nuclide is observed. This is, however, not typically possible since the cross sections of various reactions overlap in excitation function. For example, if ^{209}Po tracer is produced in cyclotron by bombarding ^{209}Bi with deuterons by the reaction ^{209}Bi(d,2n)^{209}Po the optimum deuteron energy of about 15 MeV, resulting in the highest yield, may not be used due to coproduction of ^{208}Po. Instead somewhat lower deuteron energies should be applied to minimize the fraction of ^{208}Po (Fig. XVII.1).

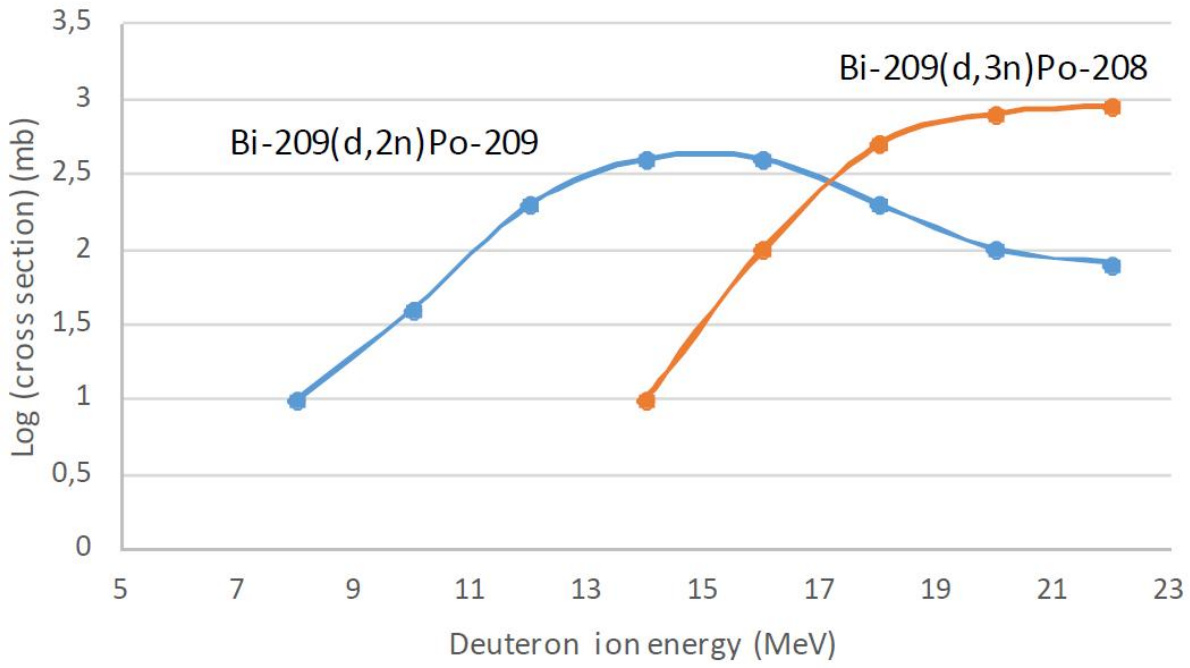

Figure XVII.1. Excitation function of ^{209}Bi(α,xn)-reactions (data from Ramler et al. Physical Review 114(1959)154).

Another critical factor in producing radionuclidic pure tracers is the purity of the target material. Even very low amounts of impurities may result in considerable amounts of undesired radionuclides in the product, especially in case where the impurity atoms have higher cross sections for the used projectiles than the actual target atoms. To avoid formation of undesired radionuclides elementally very pure targets are typically needed. In some cases elementally pure targets are not enough to prevent formation of undesired radionuclides but even isotopically pure targets are needed. For

example, in the production of ^{18}F by the reaction $^{18}O(p,n)^{18}F$ water enriched with respect to ^{18}O is used as the target. The enrichment of ^{18}O in the target water is about 97% while in the natural water it is only 0.2%. Isotopically pure target materials may be very expensive.

In addition to radionuclidic purity another term, radiochemical purity is important, particularly in labelling of organic molecules, for radiopharmaceutical purpose for example. Radiochemically pure compounds are the desired compounds containing the radionuclide or the compounds containing the radionuclide in a desired position. In, for example, ^{18}F-labelled radiopharmaceutical 2-FDG (2-deoxy-2-[^{18}F]fluoro-D-g1ucose) product the radiochemically impure compounds are those where the ^{18}F-label is somewhere else than in 2-deoxy position or other ^{18}F-labelled compounds, such as tetra-acetyl-2-[^{18}F]FDG.

Radionuclide generators

Radionuclide tracers are commercially typically available as liquids containing radionuclides as ions, for example $^{137}CsCl$ and $NH_4H^{32}PO_4$ or as labelled compounds, such as [methyl-^{14}C]methionine and [^{35}S]methionine. A number of radionuclide tracers are available in a mode of generator. In these a radionuclide, produced either in a reactor or a cyclotron, is trapped in column containing a sorbent, such as alumina, capable of sorbing this radionuclide. In the column the sorbed radionuclide decays to its daughter nuclide which is the desired tracer nuclide. The sorbent needs to efficiently trap the parent nuclide but not the daughter which should be eluteable out from the column while the parent nuclide remains. Another requirement is that the half-life of the daughter is shorter than that of the parent; otherwise no radiochemical equilibrium would be attained in the column.

As examples of radionuclide generators the ^{99m}Tc and ^{137m}Ba generators are described. In a Tc generator the parent ^{99}Mo ($t_{½}$ = 66 h), produced in a reactor by neutron activation of stable ^{98}Mo, is trapped in an aluminum oxide column where it decays to a short-lived ^{99m}Tc ($t_{½}$ = 6.0 h). Tc forms an anionic TcO_4^- ion that can be eluted from the column with NaCl solution while ^{99}Mo remains in the column as MoO_4^{2-}. ^{99m}Tc is widely used as a radiopharmaceutical in hospitals in single photon tomography imaging of humans. ^{99m}Tc emits fairly energetic gamma rays (143 keV) which can be readily detected with gamma detectors.

In a ^{137m}Ba ($t_{½}$ = 2.6 min) generator the parent ^{137}Cs ($t_{½}$ = 30 y) is trapped in transition metal hexacyanoferrate column, such as $K_2CoFe(CN)_6$. In the column the parent decays to ^{137m}Ba which can be eluted from the column with NaCl solution. Transition metal hexacyanoferrates are extremely selective for cesium and thus trap it very efficiently. ^{137m}Ba is used in monitoring of industrial processes for example in examining flow profiles on liquids in pipes. ^{137m}Ba emits energetic gamma rays (662 keV) which can be detected from outer surfaces of pipes, for example.

Table XVI.I Most important radionuclide generators.

Mother nuclide	**Decay properties**	**Daughter nuclide**	**Decay properties**	**Application**
^{41}Ti	EC, γ; 47 y	^{44}Sc	β^+, γ; 3.9 h	Teaching
^{68}Ge	EC; 288 d	^{68}Ga	β^+, γ; 1.1 h	Medical
^{87}Y	EC, 3.3 d	^{87m}Sr	γ; 2.8 h	Medical&teaching
^{90}Sr	β^-; 28 y	^{90}Y	β^-; 64 h	Heat/calibration source
^{99}Mo	β^-; 66 h	^{99m}Tc	γ; 6.0 h	Medical
^{113}Sn	EC, γ; 115 d	^{113m}In	γ; 1.7 h	Medical
^{132}Te	β^-, γ; 76 h	^{132}I	β^-, γ; 2.3 h	Medical
^{137}Cs	β^-, γ; 30 y	^{137m}Ba	γ; 2.6 m	Gamma radiography & Radiation sterilization
^{140}Ba	β^-, γ; 13 d	^{140}La	β^-, γ; 40 h	Lanthanum tracer
^{144}Ce	β^-, γ; 284 d	^{144}Pr	β^-; 17 m	Calibration source
^{210}Pb	β^-, γ; 21 y	^{210}Bi	β^-; 5.0 d	Calibration source
^{226}Ra	α, 1600 y	^{222}Rn	α, 3.8 d	Medical
^{238}U	α, 4.5 Gy	^{234}Th	β^-, γ; 24 d	Thorium tracer

XVII ISOTOPE SEPARATIONS

Content

Analytical isotope separations

Industrial isotope separations

1) Chemical isotope exchange
2) Electrolytic separation
3) Electromagnetic separation
4) Gas diffusion method
5) Gas centrifuge method

Isotope separations are difficult, since isotopes are the same element and therefore behave chemically in the same manner. The only difference between the isotopes is the mass, which is due to the variation in the number of neutrons in the nuclei. This mass difference, in a relative way, is the largest in lighter elements. The largest mass differences occur with hydrogen. The mass ratios between ^{1}H, ^{2}H, and ^{3}H are approximately 1:2:3. The relative mass differences for heavier elements, however, are smaller – in general the smaller the heavier the element. For example, the relative mass difference between the uranium isotopes, ^{238}U and ^{235}U, is 1.3%. Due to the mass differences, isotopes have certain physical differences that affect their behavior and this is called the isotope effect. For example, the freezing point of water (H_2O) and deuterium oxide (D_2O) differ by 3.82 degrees and boiling point by 1.43. The optical emission spectrum of hydrogen and deuterium also differ with transitions up to a 0.2 nm. The corresponding transitions for uranium are ten times lower.

Isotope separations are needed for two purposes. First, they are needed to analyze the relative abundances of isotopes, isotope ratios, and second for the preparation of isotopically pure or enriched substances. In analytical separations, the quantity required is very small, but for manufacturing isotopes large amounts, even tons, are required.

Analytical isotope separations

In analytics the most important method of isotope separation is mass spectrometry (Figure XVII.1). In mass spectrometry the sample is first evaporated: *e.g.* the solution containing the analyte is injected on top of the sample wire (filament), the sample is dried and the wire heated, wherein the sample vaporizes. The gaseous molecules are ionized by, for example, by bombarding them with electrons. The generated ions are accelerated by an electric field and separated according to their masses using a magnetic field mass separator or a quadrupole. If the resulting ions have the same charge, the lighter ion will bend more than heavier ions in the magnetic field. In this way, for example, $^{235}U^{16}O^{+}$ (mass number 251) formed in uranium ionization can be separated from $^{238}U^{16}O^{+}$ (mass number 254). The number of ions are calculated with a detector, which can be a photographic plate, in which case system is a mass spectrograph, or an ampere meter.

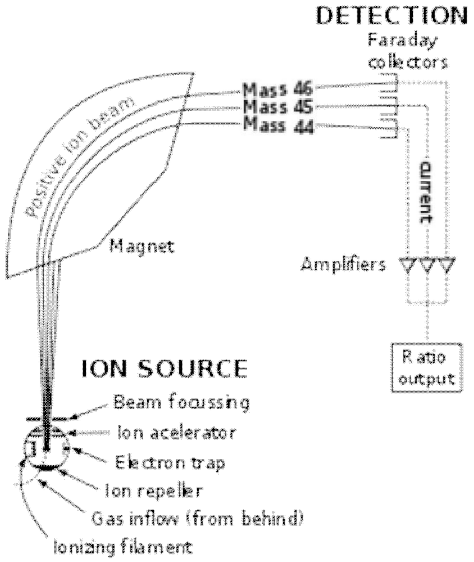

Figure XVII.1. Operating principle of a mass spectrometer (https://www.boundless.com/physics/textbooks/boundless-physics-textbook/magnetism-21/applications-of-magnetism-160/mass-spectrometer-564-6290/images/schematic-of-mass-spectrometer/).

Isotope analysis is also performed using nuclear spectrometry. The relative proportions of the isotopes is determined from the intensity of the particles or rays generated in nuclear decay. The alpha spectrum below is an example of this type of analyses, showing alpha spectrum of uranium after the dissolution of a rock sample and chemical separation of uranium from it. There are three peaks of naturally occurring uranium seen in the spectrum: ^{238}U peak (4.20 MeV), ^{235}U peak (4.68 MeV) and ^{234}U peak (4.77 MeV). The ratio of $^{234}U/^{238}U$ and $^{235}U/^{238}U$ in the sample can be

calculated from the area under the peaks. The spectrum also shows the added ^{232}U-tracer peak (5.32 MeV), with which the chemical yield of the separation process can be determined and from which the absolute amounts of ^{234}U, ^{235}U and ^{238}U in the sample can be calculated. Similar isotope analyses are even easier to perform in gamma spectrometry, because the energies of the isotopes are more readily separated due to better energy resolution.

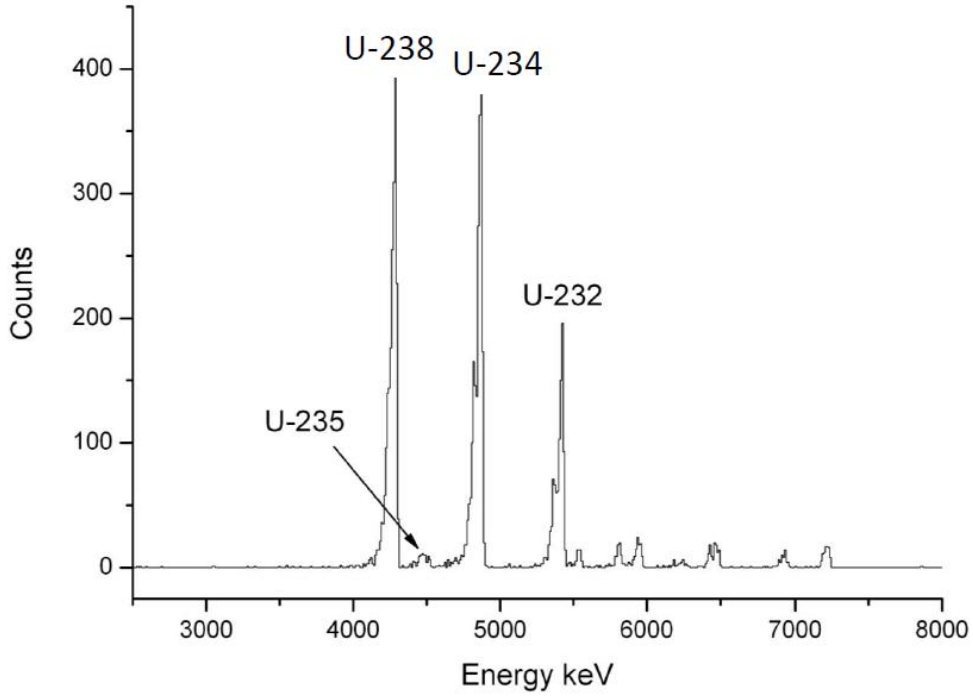

Figure XVII.2. Alpha spectrum of naturally occurring uranium isotopes ^{234}U, ^{235}U and ^{238}U and the ^{232}U tracer used to determine the chemical yield in uranium separation process.

Industrial isotope separations

The main industrial isotope separation processes are related to nuclear power generation, specifically production of nuclear fuel materials. The methods used in the nuclear industry, were originally developed for the production of weapon grade uranium and plutonium. The most important material produced in nuclear power production is naturally the nuclear fuel. Most power-generating nuclear reactors in the world operate based on thermal neutron induced uranium fission. Of the uranium isotopes, only ^{235}U undergo fission induced by thermal neutrons. It accounts for only 0.7% of naturally occurring uranium, however, the rest being isotope ^{238}U (and 0.0055% of ^{234}U). In most reactor types, this fissile uranium fraction is not enough to sustain a chain reaction, rather the portion of ^{235}U should be increased to 3-4%. Since the relative mass difference of the two uranium isotopes is very small, a single separation only provides a relatively small enrichment.

Achieving a sufficient degree of enrichment requires a multi-stage process. Another important isotope material in nuclear industry is D_2O, which is used in certain reactor types as the primary circuit coolant.

1) Chemical isotope exchange

Chemical isotope exchange is used, for example, for deuterium oxide production. The separation process utilizes the following exchange reaction

$$H_2O(l) + HDS(g) \leftrightarrow HDO(l) + H_2S \qquad \text{XVII.I.}$$

The equilibrium of this reaction is dependent on temperature: k(32 ^oC) = 2.32 and k(138 ^oC) = 1.80. The enrichment of deuterium in water molecules is more advantageous at lower temperatures. The separation process uses two columns, one on top of the other, of which the upper column has a lower temperature (30^oC) and the lower column has a higher temperature (130 ^oC). Natural water, with a deuterium proportion of 0.014%, is directed from above into the upper column. At the same time, H_2S gas, with the same proportion of deuterium, is directed into the same column from below. Since low temperatures favor the tritium exchange into water, the aqueous phase is enriched in deuterium. The deuterium-depleted of H_2S leaving from above is now passed to the lower column, where it travels against the current of natural water as it did in the upper column, but at a higher temperature (130^oC). The exchange reaction now favors the deuterium-enriched H_2S phase. The deuterium-enriched H_2S is again directed to the upper column, where the low temperature transfers the deuterium to the water phase and so on. The result is 15% deuterium-enriched water in the upper column and deuterium-depleted water in the lower column. The final fraction of D_2O is nearly 100%, which can be achieved by distillation. Such enrichment plants produce up to 1200 tons of D_2O annually.

2) Electrolytic separation

Electrolytic separation takes advantage of the fact that when the water is decomposed by electrolysis, the proportion of deuterium in the hydrogen gas generated on the cathode is less than in the original water, which is due to the slower dissociation of deuterium in water to D^+ ions compared to H^+ ions. Thus, the deuterium is enriched in the water. The process is no longer in widespread use.

3) Electromagnetic separation

Electromagnetic separation uses the same principle as mass spectrometry, *i.e.* the molecules are ionized and separated by a magnetic field. During the Second World War, the extraction method was used to separate ^{235}U for weapons. The method is currently used only for the manufacturing of isotopically pure isotopes in gram quantities.

4) Gas diffusion method

The gas diffusion method has been used above all in ^{235}U enrichment for use as nuclear fuel and weapon material. The method is based on the fact that lighter molecules move faster than heavier ones in gas phase. For separation, uranium is vaporized as UF_6 and directed to a separation chamber, in which there is a membrane, with a pore size of 10 to 100 nm, separating two sections. Since $^{235}UF_6$ is somewhat lighter than $^{238}UF_6$ it passes more rapidly through the membrane and is enriched in the chamber on the other side of the membrane. Only a small enrichment is achieved in a single separation stage due to the small mass difference, so many successive separations are needed. The enrichment of ^{235}uranium from the original 0.7% to 3% requires 1300 consecutive separations and 80% degree of enrichment requires 3600 separations. Gas diffusion plants have been used in the United States, Russia, France, China, and Argentina.

5) Gas centrifuge method

Gas centrifuges have replaced the gas diffusion plants in ^{235}U enrichment. In a centrifuge the heavier particles or molecules travel towards the walls faster than lighter ones. In ^{235}U enrichment, centrifugation is utilized by leading UF_6 gas into the center of the centrifuge chamber, wherein the $^{238}UF_6$ moves towards the walls somewhat faster than the lighter $^{235}UF_6$ (Figure XVII.3). The centrifugation is continuous, so that ^{235}U-enriched UF_6 is directed out from the middle of the chamber and ^{238}U-enriched UF_6 from the chamber walls. Enrichment is much greater than with gas diffusion, but also in this case a series of successive separation steps are needed. After ten consecutive centrifugations 3% ^{235}U is achieved and after forty-five 80%.

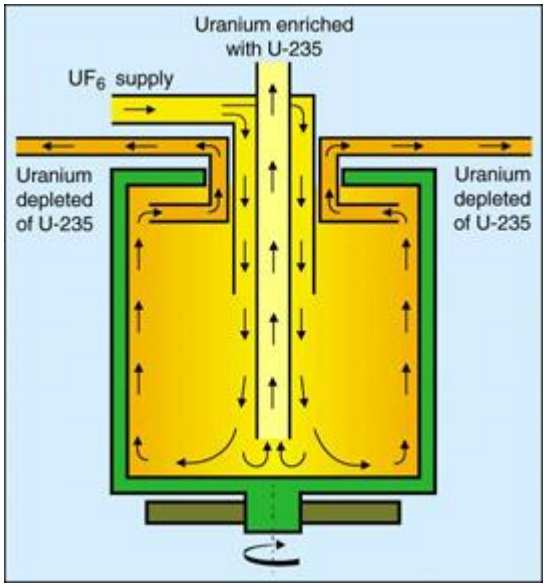

Figure XVII.3. Gas centrifuge process used to enrich ^{235}U (https://www.euronuclear.org/info/encyclopedia/g/gascentrifuge.htm).

XVIII CALCULATION EXERCISES

(produced by Dr. Jukka Kuva)

I ACTIVITY AND UNCERTAINTY CALCULATIONS (CHAPTERS VI AND XIV)

Exercises

1. a) 0.0118% of natural potassium is radioactive ^{40}K isotope the half-life of which is 1.27×10^{9} years. What is the ^{40}K activity in a human body in which the amount of potassium is 125 g? Molar mass of potassium is 39.1 g/mol.

   b) What is the uncertainty of the ^{40}K activity calculated above when the uncertainty of the potassium mass (125 g) is 15%? Use the uncertainty propagation law.

2. a) The activity of a radionuclide decreased to one per mil of the initial value. What is the half-life of the radionuclide?

   b) What is the activity of 8 MBq of ^{90}Sr after 42 years? Half-life is 28.8 years.

3. What is the $^{14}C/C$ ratio in a carbon sample the specific activity of which is 50.1 dpm/g? Half-life of ^{14}C is 5730 years.

4. How many impulses should be recorded from a radioactive sample to observe a standard deviation of the number of impulses lower than 0.5%?

5. The counting efficiency of a whole-body counting system is 1.35% at 935 keV gamma energy. The background count rate at this energy was observed to be 5798 pulses in 60 minutes. A person contaminated with ^{115}Cd was measured for 15 minutes and the number of pulses at 935 keV was 3987. What was the ^{115}Cd activity in the body of this person? ^{115}Cd emits gamma rays of 935 keV energy with 1.90% intensity.

6. Calculate the uncertainty of the human body activity determined in exercise 5. Use uncertainty propagation law. You do not need to take into account uncertainties of intensity, counting efficiency and counting time. Express the result as the activity with its uncertainty.

7. Marie and Pierre Curie used 2 tons of pitchblende (75% U_3O_8) as a starting material to isolate radium. What was the amount of ^{226}Ra (mg) in radioactive equilibrium with the amount of uranium initially present. For simplicity we assume that all uranium was only ^{238}U the molar mass of which is 238.03 g/mol and its half-life is 4.5×10^9 years. The half-life of ^{226}Ra is 1600 years.

8. In the decay chain ^{238}U the end-member is the stable ^{206}Pb. From a rock sample found in Australia the amount ^{206}Pb for each gram of ^{238}U was 0.236 g. What was the age of the rock assuming that it did not contain any lead when it is formed?

Solutions

1a.

^{40}K activity in the body:

$$\boldsymbol{A} = \frac{\ln 2 \cdot m \cdot N_A}{t_{½} \cdot M} = \frac{\ln 2 \cdot 0{,}000118 \cdot 125\text{g} \cdot 6{,}022 \cdot 10^{23} \frac{1}{\text{mol}}}{1{,}27 \cdot 10^{9}\text{a} \cdot 3{,}15 \cdot 10^{7} \frac{\text{s}}{\text{a}} \cdot 39{,}1 \frac{\text{g}}{\text{mol}}} \approx \mathbf{3{,}9\ kBq}$$

1b.

The uncertainty of the ^{40}K activity:

$$\boldsymbol{\delta A} = \sqrt{\left(\frac{\partial A}{\partial m} \cdot \delta m\right)^2} = \left|\frac{\ln 2 \cdot N_A}{t_{½} \cdot M} \cdot \delta m\right|$$

$$= \frac{\ln 2 \cdot 6{,}022 \cdot 10^{23} \frac{1}{\text{mol}}}{1{,}27 \cdot 10^{9}\text{a} \cdot 3{,}15 \cdot 10^{7} \frac{\text{s}}{\text{a}} \cdot 39{,}1 \frac{\text{g}}{\text{mol}}} \cdot 0{,}15 \cdot 0{,}000118 \cdot 125\text{g} \approx 590\ \text{Bq}$$

$$=> \delta A = \mathbf{0{,}6\ kBq}$$

2a.

The half-life of the unknown radionuclide:

$$\frac{A}{A_0} = 1‰ = 0{,}001$$

$$A = A_0 \cdot 2^{-\frac{t}{t_{½}}} \rightarrow \ln\frac{A}{A_0} = -\frac{t \cdot \ln 2}{t_{½}} \rightarrow \boldsymbol{t_{½}} = -\frac{t \cdot \ln 2}{\ln\left(\frac{A}{A_0}\right)} = -\frac{7\text{d} \cdot \ln 2}{\ln 0{,}001} = 0{,}702\ \text{d} = \mathbf{16.8\ h}$$

Based on the observed half-life the nuclide can be identified to ^{125}Xe.

2b.

^{90}Sr activity:

$$\boldsymbol{A} = A_0 \cdot 2^{-\frac{t}{t_{½}}} = 8\,\text{MBq} \cdot 2^{-\frac{42\text{a}}{28{,}8\text{a}}} \approx \mathbf{2{,}91\ MBq}$$

3.

^{14}C/C ratio:

$$A_s^{14} = \frac{\ln 2 \cdot N_A \cdot \rho}{t_{½} \cdot M_C} \rightarrow \boldsymbol{\rho} = \frac{A_s^{14} \cdot t_{½} \cdot M_c}{\ln 2 \cdot N_A} = \frac{\frac{50{,}1}{60}\frac{1}{\text{s}\cdot\text{g}} \cdot 5730\ \text{a} \cdot 3{,}15 \cdot \mathbf{10}^{7}\frac{\text{s}}{\text{a}} \cdot 12\frac{\text{g}}{\text{mol}}}{\ln 2 \cdot 6{,}022 \cdot 10^{23}\frac{1}{\text{mol}}} \approx \mathbf{4{,}33 \cdot 10^{-12}}$$

4.

Number of impulses required:

$$\sigma = \sqrt{x} \leq 0{,}005x \rightarrow \sqrt{x} \geq \frac{1}{0{,}005} \rightarrow \boldsymbol{x} \geq \frac{1}{0{,}000025} = \mathbf{40\,000}$$

5.

^{115}Cd activity in the body of the person:

$$R_n = A\varepsilon x = R_b - R_t \rightarrow \boldsymbol{A} = \frac{R_b - R_t}{\varepsilon x} = \frac{\frac{3987}{15}\frac{1}{\text{min}} \cdot \frac{\mathbf{1}}{60}\frac{\text{min}}{\text{s}} - \frac{5798}{60}\frac{1}{\text{min}}\frac{1}{60}\frac{\text{min}}{\text{s}}}{0{,}0135 \cdot 0{,}019} \approx \mathbf{10{,}99\ kBq}$$

6.

$$\boldsymbol{\delta A} = \sqrt{\left(\frac{\partial A}{\partial R_b} \cdot \delta R_b\right)^2 + \left(\frac{\partial A}{\partial R_t} \cdot \delta R_t\right)^2} = \sqrt{\left(-\frac{\delta R_b}{\varepsilon x}\right)^2 + \left(\frac{\delta R_t}{\varepsilon x}\right)^2}$$

$$= \sqrt{\left(-\frac{\frac{\sqrt{5798}}{60}\frac{1}{\text{min}}\frac{1}{60}\frac{\text{min}}{\text{s}}}{0{,}0135 \cdot 0{,}019}\right)^2 + \left(\frac{\frac{\sqrt{3987}}{15}\frac{1}{\text{min}} \cdot \frac{\mathbf{1}}{60}\frac{\text{min}}{\text{s}}}{0{,}0135 \cdot 0{,}019}\right)^2} \approx 286\text{Bq} \approx \mathbf{300\ Bq}$$

$$\Rightarrow \boldsymbol{A} = \mathbf{(11{,}0 \pm 0{,}3)kBq}$$

7.

The amount of ^{226}Ra:

In radioactive equilibrium: $A_{Ra} = A_U$.

$m(U_3O_8) = 0.75 \times m(\text{pitchblende}) = 1.5$ tons

$M(U_3O_8) = 3 \times 238.03$ g/mol + 8×16.0 g/mol = 842.09 g/mol.

$$A_{238U} = \frac{\ln 2 \cdot m \cdot \rho \cdot X \cdot N_A}{t_{½} \cdot M} = \frac{\ln 2 \cdot 1{,}5 \cdot 10^6 \text{g} \cdot 1 \cdot 3 \cdot 6{,}022 \cdot 10^{23} \frac{1}{\text{mol}}}{4{,}5 \cdot 10^9 \text{a} \cdot 3{,}1536 \cdot 10^7 \frac{\text{s}}{\text{a}} \cdot 842{,}09 \frac{\text{g}}{\text{mol}}} \approx 1{,}571849 \cdot 10^{10} \text{Bq}$$

$$= A_{226Ra}$$

$$\boldsymbol{m_{226Ra}} = \frac{A_{226Ra} \cdot M \cdot t_{½}}{\ln 2 \cdot N_A} = \frac{1{,}5718 \cdot 10^{10} \text{Bq} \cdot 226 \frac{\text{g}}{\text{mol}} \cdot 1600 \text{a} \cdot 3{,}1536 \cdot 10^7 \frac{\text{s}}{\text{a}}}{\ln 2 \cdot 6{,}022 \cdot 10^{23} \frac{1}{\text{mol}}} \approx 0{,}4294 \text{g}$$

$$\approx \mathbf{430 mg}$$

8.

All lead is generated from U, thus the age of the rock is

$$N_{Pb} = N_{0U} - N_U \rightarrow N_U = N_{0U} - N_{Pb} = N_{0U} \cdot 2^{-\frac{t}{t_{½}}} \rightarrow \frac{N_U}{N_U + N_{Pb}} = 2^{-\frac{t}{t_{½}}} \rightarrow \ln\left(\frac{N_U}{N_U + N_{Pb}}\right)$$

$$= -\frac{t}{t_{½}} \cdot \ln 2$$

$$\rightarrow \boldsymbol{t} = -\frac{t_{½} \cdot \ln\left(\frac{N_U}{N_U + N_{Pb}}\right)}{\ln 2} = -\frac{t_{½} \cdot \ln\left(\frac{\frac{m_U}{M_U} \cdot \cancel{N_A}}{\frac{m_U}{M_U} \cdot \cancel{N_A} + \frac{m_{Pb}}{M_{Pb}} \cdot \cancel{N_A}}\right)}{\ln 2}$$

$$= -\frac{4{,}47 \cdot 10^9 \text{a} \cdot \ln\left(\frac{\frac{1 \text{ g}}{238 \frac{\text{g}}{\text{mol}}}}{\frac{1 \text{ g}}{238 \frac{\text{g}}{\text{mol}}} + \frac{0{,}236 \text{ g}}{206 \frac{\text{g}}{\text{mol}}}}\right)}{\ln 2} \approx \mathbf{1{,}55 \text{ Ga}}$$

II COUNT RATE AND DEAD-TIME (CHAPTER VIII)

Exercises:

1. A sample with an activity of 55.0 kBq was measured with a GM counter and number of observed net counts was 280 000. Another sample with an activity of 55.0 Bq, obtained by diluting the first sample by a factor of 1000, was then measured with the same GM counter in identical conditions. In this case the number of pulses was 350. Calculate the counting efficiency of the counting system and dead-time of the GM detector.

2. Calculate the uncertainties of counting efficiency and dead-time observed in exercise 1, using uncertainty propagation law, for a case where the uncertainty of both samples was 2%. Express the results as the counting efficiency and the dead-time with their uncertainties.

3. An unknown radionuclide was measured with a GM counter having a dead-time of 32 μs. The observed net count rate was 280 000 imp/min on March 15^{th} and 123 imp/min on November 10^{th} of the same year. We assume the counting efficiency having been constant. Calculate the half-life of the radionuclide.

Solutions:

1.

At the lower count rate the dead-time has no effect and the counting efficiency can be calculated as:

$$R = Ax\varepsilon \rightarrow \boldsymbol{\varepsilon} = \frac{R_2}{A_2 x} = \frac{350\,\frac{1}{\text{min}} \cdot \frac{1}{60}\frac{\text{min}}{\text{s}}}{55\frac{1}{\text{s}} \cdot 1} \approx \mathbf{10{,}6\%}$$

The dead-time is calculated as:

$$R_{01} = A_1 \cdot \varepsilon = 55\,000\,\frac{1}{\text{s}} \cdot 0{,}1060606\ldots \approx 5833{,}33\ldots\,\frac{1}{\text{s}}$$

$$R_{01} = \frac{R_1}{1 - R_1\tau} \rightarrow \boldsymbol{\tau} = \frac{R_{01} - R_1}{R_{01} \cdot R_1} = \frac{5833\frac{1}{\text{s}} - 280000\frac{1}{\text{min}} \cdot \frac{1}{60}\frac{\text{min}}{\text{s}}}{5833\frac{\mathbf{1}}{\text{s}} \cdot 280000\frac{1}{\text{min}} \cdot \frac{1}{60}\frac{\text{min}}{\text{s}}} \approx 4{,}286 \cdot 10^{-5}\text{s} \approx \mathbf{42{,}9\ \mu s}$$

2.

The uncertainty of the counting efficiency:

$$\boldsymbol{\delta\varepsilon} = \sqrt{\left(\frac{\partial\varepsilon}{\partial A} \cdot \delta A\right)^2 + \left(\frac{\partial\varepsilon}{\partial R} \cdot \delta R\right)^2} = \sqrt{\left(-\frac{R}{A^2 x} \cdot \delta A\right)^2 + \left(\frac{\delta R}{Ax}\right)^2}$$

$$= \sqrt{\left(-\frac{350\,\frac{1}{\text{min}} \cdot \frac{1}{60}\frac{\text{min}}{\text{s}}}{\left(55\frac{\mathbf{1}}{\text{s}}\right)^2 \cdot 1} \cdot 0{,}02 \cdot 55\frac{1}{\text{s}}\right)^2 + \left(\frac{\sqrt{350}\,\frac{1}{\text{min}} \cdot \frac{1}{60}\frac{\text{min}}{\text{s}}}{55\frac{1}{\text{s}} \cdot 1}\right)^2} \approx 0{,}00605 \approx \mathbf{0{,}7\%}$$

$$\Rightarrow \boldsymbol{\varepsilon} = (\mathbf{10{,}6} \pm \mathbf{0{,}7})\%$$

The uncertainty of the dead-time:

$$\boldsymbol{\tau} = \frac{\boldsymbol{A\varepsilon - R}}{A\varepsilon \cdot R} = \frac{1}{R} - \frac{1}{A\varepsilon}$$

$$\boldsymbol{\delta\tau} = \sqrt{\left(\frac{\partial\tau}{\partial A} \cdot \delta A\right)^2 + \left(\frac{\partial\tau}{\partial R} \cdot \delta R\right)^2 + \left(\frac{\partial\tau}{\partial\varepsilon} \cdot \delta\varepsilon\right)^2}$$

$$= \sqrt{\left(\frac{\delta A}{A^2\varepsilon}\right)^2 + \left(-\frac{\delta R}{R^2}\right)^2 + \left(\frac{\delta\varepsilon}{A\varepsilon^2}\right)^2}$$

$$= \sqrt{\left(\frac{0{,}05 \cdot 55000\frac{1}{\mathrm{s}}}{\left(55000\frac{1}{\mathrm{s}}\right)^2 \cdot 0{,}106}\right)^2 + \left(-\frac{\sqrt{280000}\frac{1}{\mathrm{min}} \cdot \frac{1}{60}\frac{\mathrm{min}}{\mathrm{s}}}{\left(280000\frac{1}{\mathrm{min}} \cdot \frac{1}{60}\frac{\mathrm{min}}{\mathrm{s}}\right)^2}\right)^2 + \left(\frac{0{,}008}{55000\frac{1}{\mathrm{s}} \cdot 0{,}106^2}\right)^2}$$

$$\approx 13{,}39\mu\mathrm{s} \approx \mathbf{14\mu s}$$

$$\Rightarrow \boldsymbol{\tau = (43 \pm 14)\mu s}$$

3.

Dead-time correction is needed only for the higher count rate. Below 1 refers to March and 2 to November.

$$A_2 = A_1 \cdot 2^{-\frac{t}{t_{½}}} \rightarrow t_{½} = -\frac{\ln 2 \cdot t}{\ln\left(\frac{A_2}{A_1}\right)} = -\frac{\ln 2 \cdot t}{\ln\left(\frac{\frac{R_{02}}{\epsilon}}{\frac{R_{01}}{\epsilon}}\right)} = -\frac{\ln 2 \cdot t}{\ln\left(\frac{R_2}{\frac{R_1}{1 - R_1\tau}}\right)}$$

$$= -\frac{\ln 2 \cdot 240\mathrm{d}}{\ln\left(\frac{\frac{123\frac{1}{60}\frac{1}{s}}{\frac{2800001}{60}\frac{1}{\mathrm{s}}}}{1 - \frac{2800001}{60}\frac{1}{\mathrm{s}} \cdot 32 \cdot 10^{-6}\mathrm{s}}\right)} = 21{,}0787\ldots\mathrm{d} \approx \mathbf{21\ d}$$

III NUCLEAR REACTIONS, PRODUCTION OF RADIONUCLIDES, SUCCESSIVE RADIOACTIVE DECAY (CHAPTERS VI, XV, XVI)

Exercises:

1. Molybdenum was irradiated with thermal neutrons to produce radioactive ^{99}Mo ($t_{1/2}$ = 2.75 d) isotope from stable ^{98}Mo isotope. ^{99}Mo decays by beta decay to ^{99}Tc ($t_{1/2}$ = 2.13 x 10^5 a) which further decays by beta decay to stable ^{99}Ru. After irradiation molybdenum was separated from the target material; the ^{99}Mo activity in the separated molybdenum was 100 kBq. What were the ^{99}Mo and ^{99}Tc activities after a) 1 h, b) 3d, c) 1a ?

   Use equation: $A_2 = \lambda_2 \frac{\lambda_1}{\lambda_2 - \lambda_1} N_1^0 \left(2^{-\frac{t}{T_1}} - 2^{-\frac{t}{T_2}}\right)$

2. A fish sample of 2.0 g weight was irradiated in a reactor for 2.0 hours with a neutron flux of 5.0×10^{17} $\frac{1}{m^2 s}$ (φ). Twenty days after the irradiation the activity of generated ^{203}Hg activity was measured to be 226 Bq. Calculate the mercury concentration of the fish as mg/kg. The cross section (σ) of the reaction ^{202}Hg(n,γ)^{203}Hg is 380 fm^2, the half-life of ^{203}Hg is 47 days, the isotopic abundance of ^{202}Hg is 29.8% and the atomic weight of mercury is 200.6 $\frac{g}{mol}$.

   Use equation: $A_t = \sigma \phi N_1 \left(1 - 2^{-\frac{t_S}{T}}\right) 2^{-\frac{t}{T}}$

3. To determine the neutron flux of a reactor 10 mg of copper was irradiated for 4.0 hours. 25 hours and 36 minutes after the irradiation was terminated the ^{64}Cu activity was 70 MBq. The cross section of the reaction ^{63}Cu(n,γ)^{64}Cu is 4.51 barn , the isotopic abundance of ^{63}Cu is 69.1%, the atomic weight of copper is 63.5 $\frac{g}{mol}$ and the half-life of ^{64}Cu is 12.8 hours. What is the neutron flux of the reactor.

4. ^{131}Ba ($t_{1/2}$ = 11.5 d) decays by positron emission to ^{131}Cs ($t_{1/2}$ = 9.7 d) and the latter further to stable ^{131}Xe. Barium is separated from a sample containing both nuclides. What are the ^{131}Ba and ^{131}Cs activities in the separated barium fraction after 1, 10 and 100 days when the initial ^{131}Ba activity was 100 kBq. Plot, with excel or other suitable program, the activities of both nuclides for the time period up to 100 days. When the nuclide activities are identical? When the ^{131}Cs activity has its maximum?

Solutions:

1.

Calculation of decay constants:

$$A_1^0 = 100\ \text{kBq}$$
$$\lambda_1 = \frac{\ln 2}{T_1} = \frac{\ln 2}{2{,}75 \cdot 24 \cdot 3600\ \text{s}} \approx 2{,}917 \cdot 10^{-6}\,\frac{1}{\text{s}}$$
$$\lambda_2 = \frac{\ln 2}{T_2} = \frac{\ln 2}{2{,}13 \cdot 10^5 \cdot 365 \cdot 24 \cdot 3600\ \text{s}} \approx 1{,}032 \cdot 10^{-13}\,\frac{1}{\text{s}}$$
$$N_1^0 = \frac{A}{\lambda_1} = \frac{1 \cdot 10^5 \frac{1}{\text{s}}}{2{,}917 \cdot 10^{-6}\,\frac{1}{\text{s}}} \approx 3{,}43 \cdot 10^{10}$$

Inserting these and the half-lives to the equation

$$A_2 = \lambda_2 \frac{\lambda_1}{\lambda_2 - \lambda_1} N_1^0 \left(2^{-\frac{t}{T_1}} - 2^{-\frac{t}{T_2}}\right)$$

yields the following activities for the three time points:

t	$A_1(^{99}\text{Mo})$	$2^{-t/T1}$	$2^{-t/T2}$	$A_2(^{99}\text{Tc})$
1 h	**99.0 kBq**	0.989	1	**36.9 µBq**
3 d	**46.9 kBq**	0.469	1	**1.8 mBq**
1 a	**0 kBq**	0	1	**3.5 mBq**

2.

$$A_t = \sigma\phi N_1 \left(1 - 2^{-\frac{t_S}{T}}\right) 2^{-\frac{t}{T}}$$

and

$$N_1 = \frac{m \cdot \rho_i \cdot N_A}{M}$$

=>

$$\rho = \frac{m_{Hg}}{m} = \frac{N_1 M}{m \rho_i N_A} = \frac{A_t M}{\sigma \cdot \phi \cdot \left(1 - 2^{-\frac{t_S}{T}}\right) \cdot 2^{-\frac{t}{T}} \cdot m \cdot \rho_i \cdot N_A}$$

$$= \frac{226\ \text{Bq} \cdot 200{,}6\ {}^{\text{g}}/_{\text{mol}}}{380 \cdot 10^{-30}\text{m}^2 \cdot 5 \cdot 10^{17}\,{}^{1}/_{\text{m}^2\text{s}} \cdot \left(1 - 2^{-\frac{2\text{h}}{47\ \text{d} \cdot 24\ {}^{\text{h}}/_{\text{d}}}}\right) \cdot 2^{-\frac{20\ \text{d}}{47\ \text{d}}} \cdot 2\text{g} \cdot 0.298 \cdot 6.022 \cdot 10^{23}\,{}^{1}/_{\text{mol}}}$$

$$\approx 7{,}2697 \cdot 10^{-7}\,{}^{\text{g}}/_{\text{g}} \approx \mathbf{0{,}73}\,{}^{\mathbf{mg}}/_{\mathbf{kg}}$$

3.

$$A_t = \sigma\phi N_1\left(1 - 2^{-\frac{t_S}{T}}\right)2^{-\frac{t}{T}}$$

$$\Rightarrow$$

$$\phi = \frac{A_t}{\sigma N_1\left(1 - 2^{-\frac{t_S}{T}}\right)2^{-\frac{t}{T}}} = \frac{A_t M}{\sigma m N_A \rho\left(1 - 2^{-\frac{t_S}{T}}\right)2^{-\frac{t}{T}}}$$

$$= \frac{70 \cdot 10^6\ \text{Bq} \cdot 63{,}5\ {}^{\text{g}}/_{\text{mol}}}{4{,}51 \cdot 10^{-28}\text{m}^2 \cdot 0.01\ \text{g} \cdot 6.022 \cdot 10^{23}\ {}^{1}/_{\text{mol}} \cdot 0.691 \cdot \left(1 - 2^{-\frac{4\ \text{h}}{12.8\ \text{h}}}\right)2^{-\frac{25\ \text{h} + \frac{36}{60}\ \text{h}}{12.8\ \text{h}}}}$$

$$\approx \mathbf{4{,}86 \cdot 10^{16}\frac{1}{\text{m}^2\text{s}}}$$

4.

Calculation of decay constants:

$$A_1^0 = 100\ \text{kBq}$$

$$\lambda_1 = \frac{\ln 2}{T_1} = \frac{\ln 2}{11{,}5 \cdot 24 \cdot 3600\ \text{s}} \approx 6{,}97611 \cdot 10^{-7}\frac{1}{\text{s}}$$

$$\lambda_2 = \frac{\ln 2}{T_2} = \frac{\ln 2}{9{,}7 \cdot 24 \cdot 3600\ \text{s}} \approx 8{,}27066 \cdot 10^{-7}\frac{1}{\text{s}}$$

$$N_1^0 = \frac{A}{\lambda_1} = \frac{1 \cdot 10^5\frac{1}{\text{s}}}{6{,}97611 \cdot 10^{-7}\frac{1}{\text{s}}} \approx 1{,}43346 \cdot 10^{11}$$

Inserting these and the half-lives to the equation

$$A_2 = \lambda_2\frac{\lambda_1}{\lambda_2 - \lambda_1}N_1^0\left(2^{-\frac{t}{T_1}} - 2^{-\frac{t}{T_2}}\right)$$

yields the following activities for the three time points:

t	$A_1(^{131}\text{Ba})$	$2^{-t/T1}$	$2^{-t/T2}$	$A_2(^{131}\text{Cs})$
1 d	94.2 kBq	0.942	0.931	6.69 kBq
10 d	54.7 kBq	0.547	0.489	37.0 kBq
100 d	241 Bq	0.00241	0.000788	1.04 kBq

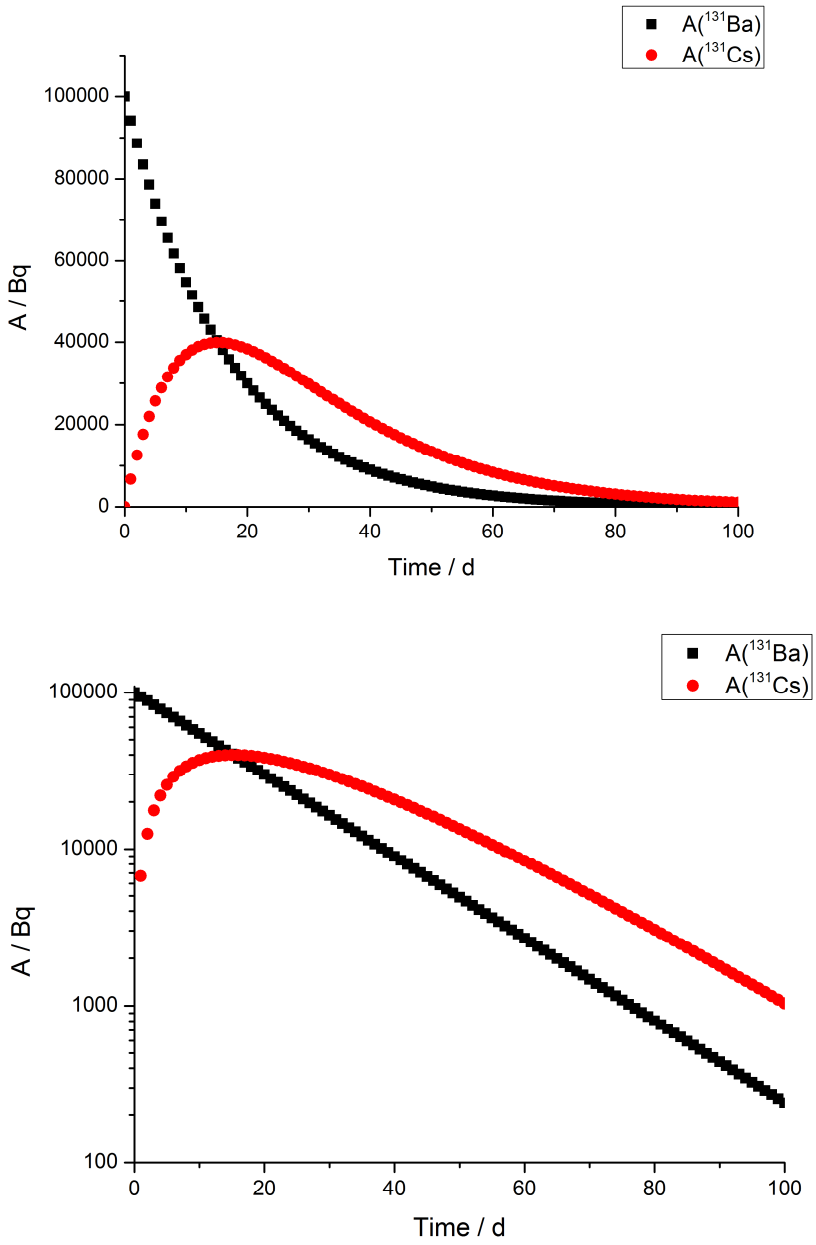

The activities are equal at time point 15 days where the maximum of ^{131}Cs activity also is observed.

IV APPLICATIONS TO SOME OTHER PROBLEMS

Exercises:

1. A medical doctor determines the blood volume of a patient by injecting 0.15 ml of $^{99m}TcO_4$ ($t_{½}$ = 6.01 hours) solution into the patient's blood vessel. The activity concentration of the solution was 30 MBq/ml at the time of injection. After 4 hours a sample of the blood is taken and its activity concentrations is measured to be 610 Bq/ml. Calculate the total blood volume of the patient.

2. Calculate the uncertainty of the blood volume determined in exercise 1. The uncertainty of the injection volume was 0.01 ml and the relative uncertainties of the initial and final ^{99m}Tc activities were 5% (uncertainty of the counting time is very small and is not taken into account). Calculate the uncertainty by using uncertainty propagation law and express the result as the total blood volume with its uncertainty.

3. ^{226}Radium (M = 226.025 g/mol) decays to ^{222}Rn with a half-life of 1600 years. What is the volume of the ^{222}Rn gas generated from 42 kg of Ra (T=25 ^{o}C ja p = 1 atm)?

Solutions:

1.

Activity concentration of ^{99m}Tc in blood at the time of injection:

$$A = A_0 \cdot 2^{-\frac{t}{t_{½}}} \rightarrow A_0 = \frac{A}{2^{-\frac{t}{t_{½}}}} = \frac{610\frac{\text{Bq}}{\text{ml}}}{2^{-\frac{4\text{h}}{6{,}01\text{h}}}} \approx 967{,}5704\frac{\text{Bq}}{\text{ml}}$$

The blood volume (assuming homogenous distribution of ^{99m}Tc in blood):

$$A_{inj} \cdot V_{inj} = A_{blood} \cdot V_{blood} \rightarrow \boldsymbol{V_{blood}} = \frac{A_{inj} \cdot V_{inj}}{A_{blood}} = \frac{30 \cdot 10^6\frac{\text{Bq}}{\text{ml}} \cdot 0{,}15\text{ml}}{967{,}5704\frac{\text{Bq}}{\text{ml}}} \approx \boldsymbol{4{,}65\ \text{l}}$$

2.

$$V_{blood} = \frac{A_{inj} \cdot V_{inj}}{A_{\boldsymbol{blood}}} = \frac{A_{inj} \cdot V_{inj} \cdot 2^{-\frac{t}{t_{½}}}}{A_{\boldsymbol{blood\,sample}}}$$

$$\boldsymbol{\delta V_{blood}} = \sqrt{\left(\frac{\partial V_{blood}}{\partial A_{inj}} \cdot \delta A_{inj}\right)^2 + \left(\frac{\partial V_{blood}}{\partial A_{blood\,sample}} \cdot \delta A_{blood\,sample}\right)^2 + \left(\frac{\partial V_{blood}}{\partial V_{inj}} \cdot \delta V_{inj}\right)^2}$$

$$= \sqrt{\left(\frac{V_{inj} \cdot 2^{-\frac{t}{t_{½}}} \cdot \delta A_{inj}}{A_{blood\,sample}}\right)^2 + \left(-\frac{A_{inj} \cdot V_{inj} \cdot 2^{-\frac{t}{t_{½}}} \cdot \delta A_{\boldsymbol{blood\,sample}}}{\left(A_{blood\,sample}\right)^2}\right)^2 + \left(\frac{A_{inj} \cdot 2^{-\frac{t}{t_{½}}} \cdot \delta V_{inj}}{A_{blood\,sample}}\right)^2}$$

$$= \sqrt{\left(\frac{0{,}15\text{ ml} \cdot 2^{-\frac{4\text{h}}{6{,}01\text{h}}} \cdot 0{,}05 \cdot 30 \cdot 10^6\frac{\text{Bq}}{\text{ml}}}{610\frac{\text{Bq}}{\text{ml}}}\right)^2 + \left(-\frac{30 \cdot 10^6\frac{\text{Bq}}{\text{ml}} \cdot 0{,}15\text{ ml} \cdot 2^{-\frac{4\text{h}}{6{,}01\text{h}}} \cdot 0{,}05 \cdot 610\frac{\text{Bq}}{\text{ml}}}{\left(610\frac{\text{Bq}}{\text{ml}}\right)^2}\right)^2}$$

$$+ \left(\frac{30 \cdot \boldsymbol{10^6}\frac{\text{Bq}}{\text{ml}} \cdot 2^{-\frac{4\text{h}}{6{,}01\text{h}}} \cdot 0{,}01\text{ ml}}{610\frac{\text{Bq}}{\text{ml}}}\right)^2 \approx 451{,}98\text{ ml} \approx \boldsymbol{500\text{ ml}}$$

$$\Rightarrow \boldsymbol{V_{blood}} = \boldsymbol{(4{,}7 \pm 0{,}5)\ \text{l}}$$

3.

first the number of generated ^{222}Rn atoms is calculated:

$$N_{Rn} = N_{0Ra} - N_{Ra} = N_{0Ra} - N_{0Ra} \cdot 2^{-\frac{t}{t_{½}}} = \frac{m_{Ra}}{M_{Ra}} \cdot N_A \cdot \left(1 - 2^{-\frac{t}{t_{½}}}\right)$$
$$= \frac{42000\ \text{g}}{226{,}025\ \frac{\text{g}}{\text{mol}}} \cdot 6{,}022 \cdot 10^{23}\ \frac{1}{\text{mol}} \cdot \left(1 - 2^{-\frac{1\ \text{a}}{1600\ \text{a}}}\right) \approx 4{,}846678 \cdot 10^{22}$$

using the ideal gas law the volume can be calculated:

$$pV = nRT \rightarrow \boldsymbol{V} = \frac{NRT}{N_A p} = \frac{4{,}846678 \cdot 10^{22} \cdot 0{,}08206\ \frac{\text{l} \cdot \text{atm}}{\text{mol} \cdot \text{K}} \cdot 298{,}15\ \text{K}}{6{,}022 \cdot 10^{23}\ \frac{1}{\text{mol}} \cdot 1\ \text{atm}} \approx \mathbf{1{,}97\ l}$$